IAEA-169 VOL. 3

FISSION PRODUCT NUCLEAR DATA (FPND)

VOL.III

PROCEEDINGS OF A PANEL
ON FISSION PRODUCT NUCLEAR DATA
ORGANIZED BY THE
INTERNATIONAL ATOMIC ENERGY AGENCY
AND HELD IN BOLOGNA, 26–30 NOVEMBER 1973

A TECHNICAL REPORT PUBLISHED BY THE
INTERNATIONAL ATOMIC ENERGY AGENCY, VIENNA, 1974

PLEASE BE AWARE THAT
ALL OF THE MISSING PAGES IN THIS DOCUMENT
WERE ORIGINALLY BLANK

Panel on Fission Product Nuclear Data, Part 2:

SELECTED CONTRIBUTIONS TO REVIEW PAPERS.

Table of Contents:

Contribution to
Review Paper No. 2

FISSION PRODUCT NUCLEAR DATA AND ENVIRONMENTAL ASPECTS OF THE NUCLEAR FUEL CYCLE

by M. Laser and E. Merz

Institute for Chemical Technology
Kernforschungsanlage Jülich / Germany

Summary

Among the nuclear data of fission products, important for their environmental aspects, the fission yield of tritium is known with only a relative low degree of accuracy. This data should be redetermined exactly as a function of the neutron energy for ^{233}U, ^{235}U and ^{239}Pu fissions. In addition, other reactions for the formation of tritium should be included.

Beyond this theme the activation product ^{14}C and the formation of actinide elements are of environmental importance. An exact knowledge of the cross sections may be helpful in environmental calculations.

1. Introduction

Small amounts of fission products may be emitted to the environment from the time of their formation in a nuclear reactor up to their final disposal. For the control of these emissions and for the calculations of their impact to mankind precise nuclear data for the fission products, i. e. fission yield, decay schemes, cross sections and so on are necessary. Data for neutron activation products and transuranium elements are also important. They should be included in the following considerations.

2. Release of fission products into the environment

Fission products are released into the biosphere during normal operation of nuclear reactors, reprocessing plants and fission product solidification plants. In the case of malfunction or accident storage facilities, waste transporters and final disposal facilities may also emit fission products.

The gaseous and volatile fission products (tritium, krypton, xenon, iodine) as well as aerosols are discharged into the atmosphere directly or via leakage into the containment or into the service rooms.

The distribution in the atmosphere depends on several factors such as stack height, meteorological conditions, built-up areas and vegetation. These effects may be described mathematically by the Pasquill Atmospheric Diffusion Theory (1).

The liquid effluents are usually diluted by river water. The radioactive isotopes are partly absorbed by minerals, plants, or animals. The behaviour of these radionuclides in surface water is very difficult to predict and to calculate. It depends strongly on the geology and the vegetation.

The impact of radionuclides in the environment on the population may occur by several modes of action:
by submersion, by inhalation and by ingestion.

The relatively complicated interconnection between the fission product inventory of a facility on the one hand and the impact to the people on the other hand is shown in a simplified manner in fig. 1.

Formula for the calculation of the radiation exposures of the population are given by several authors (2, 3). The equations contain among others

- the α- and γ-energy per disintegration,
- the mean β-energy per disintegration,
- the linear energy absorption coefficient of the critical organ for the respective γ-energy,
- the relative biological efficiency,

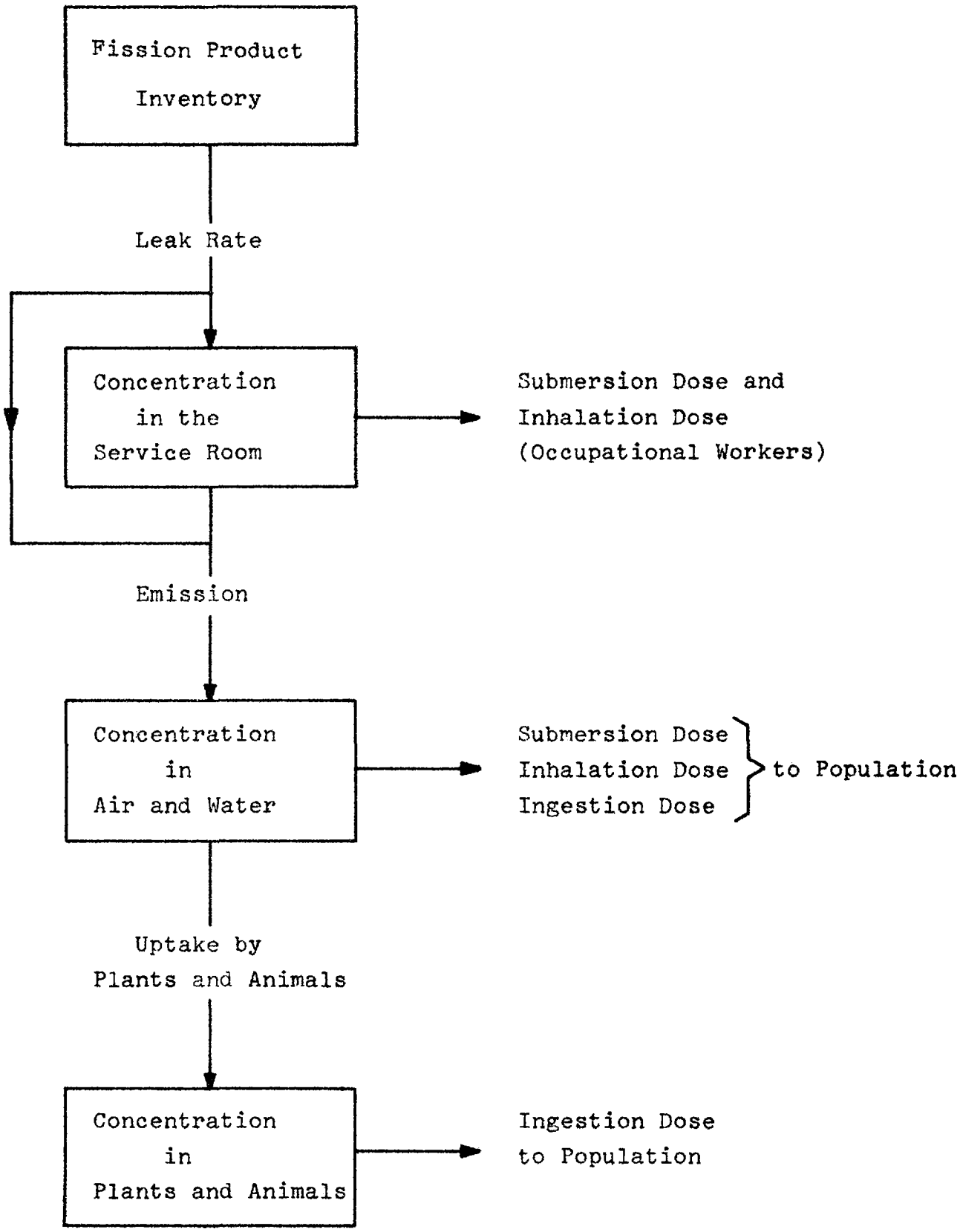

Fig. 1 : Fission Product Impact to Humans

the enrichment of special isotopes in critical organs,

the physical half-life of the isotope

and

the biological half-life of the isotope in the body.

The accuracy of the data used in the calculations are very different. In most cases the nuclear data of the fission products are best known. Biological data like biological half-life, enrichment of isotopes in critical organs or the mass of the critical organ are only mean values valid for a hypothetical "standard man". The margin of error may be in the order of $\pm$ 50 % or higher. The calculations of the dilution and distribution of radioactive isotopes, including the pathways of the isotopes from the contamination of the plants and animals to the ingestion by humans are normally associated with relatively high errors of more than a factor of 2.

In light of these errors one could conclude that the nuclear data for the fission products are known well enough for the use in environmental calculations. Indeed, many environmental scientists use the nuclear data uncritically.

In special cases, however, a better knowledge of the fission product nuclear data may be advantageous. Therefore in the following chapters the different steps of fission product handling and their impact to the environment are described and discussed in detail.

2.1 Fission product inventory in and leakage from nuclear reactors

The fission product inventory of a nuclear reactor can be calculated by computer codes. The results of the computations deviate from each other according to the different input data and assumptions. In several cases, estimations of cross sections as function of the neutron energy were necessary (4). A high degree of accuracy of these data, however, is more important for calculations of burn-up than for environmental calculations.

A small percentage of the fission products, mainly noble gases and iodine leak out of the fuel elements. In light water reactors (LWR) one assumes a "standard defect" of 1 % of the fuel elements for the calculations.

The composition of the liberated noble gas depends strongly on transport mechanism and age of the fission products. Table I shows the noble gas composition as a function of decay time for three theoretical cases (5). In practice, a mixture of the theoretical cases occurs depending on the type and the location of the leak.

In addition to the noble gases, the volatile iodine (^{131}I - ^{135}I) and the short-lived daughters of the volatile fission products ^{88}Rb and ^{138}Cs must be considered. Solid fission products (^{90}Sr, ^{137}Cs, ^{140}Ba) are found in very low concentrations in the primary cooling circuit.

Furthermore gaseous activation products are formed in appreciable amounts (^{3}H, ^{13}N, ^{16}N, ^{17}N, ^{15}O, ^{19}O and ^{41}Ar). For environmental considerations they must be seen in context with the fission products, because they form a homogeneous mixture with the gaseous and volatile fission products. They are especially important for the calculation of the radiation burden of occupational workers. For instance ^{16}N may become the key component for shielding calculations for off-gas treatment facilities.

Unavoidable leaks in the cooling loop, for instance in the heat exchanger, the turbine, the ejector and the demineralizer, permit radioisotopes to leak into the reactor containment shell, the auxiliary equipment and the turbine building. For the surveillance of the air only the total radioactivity is usually measured. The knowledge of the gas composition is important because the maximum permissible concentration depends on the composition. However, the deviation of the real gas composition from a calculated composition is often very high, depending on the unpredictible failure of fuel elements and the complex release pathways. A better knowledge of fission product nuclear data cannot fill this lack.

The reactor off-gas containing the gaseous and volatile

Table I : Composition of Noble Gas Mixtures as Function of the Delay Time (Lindackers [5]).

Delay Time		2 min			30 min			2 h			1 d			3 d			60 d			120 d		
Isotope	Half-life	A	B	C	A	B	C	A	B	C	A	B	C	A	B	C	A	B	C	A	B	C
Kr 91	10 s		0,1																			
Xe 140	16 s		1,8	0,5																		
Kr 90	33 s		18,0	6,9																		
Xe 139	41 s	3,0	21,6	9,6																		
Kr 89	3,2 min	8,2	22,1	21,6	0,1	1,1	0,3															
Xe 137	3,9 min	11,3	25,1	26,7	0,1	3,2	0,9															
Xe 135m	15,3 min	4,6	2,6	5,5	2,0	15,1	8,0	0,1	1,0	0,3												
Xe 138	17 min	14,1	7,0	15,7	7,5	47,5	26,7	0,3	5,4	1,5												
Kr 87	78 min	7,3	0,8	3,8	9,4	13,4	15,7	5,7	26,7	15,2												
Kr 83m	114 min	1,3	0,1	0,6	1,8	1,7	2,5	1,4	4,2	3,1												
Kr 88	2,8 h	10,2	0,5	3,6	14,8	9,9	17,4	13,5	30,1	25,5	0,2	2,1	0,7									
Kr 85m	4,4 h	4,2	0,1	1,2	6,3	2,6	5,8	6,7	9,2	9,7	0,5	4,6	1,9									
Xe 135	9,2 h	17,2	0,2	3,4	27,2	5,5	17,6	32,2	21,6	33,5	14,7	65,7	38,5	0,5	7,7	2,3						
Xe 133m	2,3 d	0,5	-	-	0,8	-	0,2	1,0	0,1	0,4	1,7	1,3	1,8	1,5	3,1	2,1						
Xe 133	5,3 d	18,0	0,002	0,9	29,7	0,4	5,0	39,0	1,9	10,7	82,1	26,2	57,0	96,7	88,9	95,0	-	74,2	-	-	0,2	-
Xe 131m	12,0 d	0,1	-	-	0,2	-	-	0,2	-	-	0,5	0,1	0,2	0,8	0,3	0,4	-	13,8	-	-	3,3	-
Kr 85	10,6 a	0,1	$1 \cdot 10^{-5}$	-	0,1	-	-	0,1	-	-	0,3	-	0,1	0,5	-	0,2	100	12,0	100	100	96,5	100

Typ of Mixture A : Equilibrium Mixture
B . Recoil Mixture
C · Diffusion Mixture

radioactive isotopes as well as a small amount of aerosols passes through several filters and hold-up tanks or beds.

In the United States, power plants are often equipped with hold-up pipes to delay the emission of the radioactive gases by appr. 20 to 30 minutes. Typical examples of off-gas radioactivity, emitted from a boiling water reactor (Dresden I, 210 MWe) and from a pressurized water reactor (Yankee, 185 MWe) are given in table II (6, 7). German power stations use charcoal beds with a delay time of 2.5 and 40 days for krypton and xenon, respectively. The discharged off-gas contains mainly ^{133}Xe, ^{133m}Xe and ^{85}Kr.

Table II : Reactor Off-gas of LWR Reactors

Isotope	BWR Ci/a	PWR Ci/a
Ar 41		0,4
Kr 85m	12 300	0,02
Kr 85	4,4	3
Kr 87	30 747	0,02
Kr 88	24 220	0,03
Xe 133m	473	0,002
Xe 133	15 200	0,1
Xe 135	37 622	0,2
Xe 138	102 713	
H 3	0,3	13
C 14		0,3
Sr 89	0,03	
Sr 90	0,0003	0,0002
I 131	0,03	0,0003
Cs 137	0,0011	$2 \cdot 10^{-7}$
Ba 140	0,014	
Mn 54		0,0001
Co 58	0,0008	
Co 60	0,0008	0,0002

Experience with high temperature reactors (HTR) is very limited. The fuel consists of uranium and/or thorium carbide or oxide, coated with pyrocarbon and in some cases with silicon carbide, and is embedded in a graphite matrix. The pyrocarbon coating seems to be extremely gas tight. However, the fuel element is more or less contaminated with uranium. The fission products found in the primary helium circuit come from this contamination. The radioactivities found in the cooling gas of the AVR reactor (15 MWe) are given in table III(8). After passing charcoal absorbers only small amounts of ^{85}Kr and ^{133}Xe are emitted into the atmosphere. The total gaseous activity emitted during a 17 month period amounted to 20.3 Ci.

Table III: Radiactive Isotopes in the Primary Cooling Gas of the AVR Reactor (HTR 15 MWe)

Isotope	Radioactivity Ci/cm^3 STP
Kr 85m	$2{,}5 \cdot 10^{-9}$
Kr 87	$3{,}4 \cdot 10^{-9}$
Kr 88	$8 \cdot 10^{-9}$
Xe 133	$6 \cdot 10^{-9}$
Xe 135	$4{,}5 \cdot 10^{-9}$

In the reactor containment vessel, small amounts of ^{85}Kr, ^{85m}Kr, ^{133}Xe, ^{135}Xe and ^{88}Rb are measured. In the secondary water and steam loop ^{3}H ($1.8 \cdot 10^{-9}$ Ci/cm^3 H_2O) as well as activation products (^{59}Fe, ^{60}Co, ^{65}Zn, ^{51}Cr, ^{56}Mn, ^{64}Cu) are found.

The liquid effluents of nuclear power stations contain only small amounts of fission products. Individual isotopes are not usually specified. However, tritium is given separately.

In the case of accidental release of fission products the composition of the emission depends on the type of the accident

and on the duration of reactor operation. As shown by Vogt (3), ^{131}I or ^{90}Sr - ^{90}Y are in all cases the most important fission products with thyroid gland or bones, respectively, as critical organ. Other important fission products are:
^{89}Sr, ^{91}Sr, ^{92}Sr, ^{91}Y, ^{92}Y, ^{95}Zr, ^{97}Zr, ^{103}Ru - ^{103m}Rh, ^{105}Rh, ^{129m}Te - ^{129}Te, ^{131m}Te - ^{131}Te, ^{132}Te, ^{132}I, ^{133}I, ^{134}I, ^{135}I, ^{140}Ba - ^{140}La, ^{143}Ce, ^{144}Ce - ^{144}Pr.

Of the fission products, which are of environmental importance for the reactor operation, less is known about tritium than any other isotope. As shown in chapter 3, more attention should be paid to tritium in the future.

2.2 Release of fission products during the transport of depleted fuel elements

Under normal conditions no fission products are emitted during the transport of depleted fuel elements from the reactor to the reprocessing plant. After an accidental release, ^{90}Sr and ^{131}I are the most important isotopes. Other important isotopes may be ^{144}Ce - ^{144}Pr, ^{129m}Te - ^{129}Te, ^{134}Cs and ^{137}Cs.

2.3 Release of fission products from reprocessing plants

After interim storage, the depleted fuel elements are disintegrated and the fuel is dissolved. The gaseous and volatile fission products are liberated to the vessel off-gas or dissolver solution. The most important volatile isotopes are ^{3}H, ^{85}Kr, ^{129}I, ^{131}I and ^{133}Xe. In HTR fuel reprocessing plants, the activation product ^{14}C is of environmental importance.

At the present time the noble gases are quantitatively discharged to the atmosphere. In the future, however, they will be retained by suitable procedures.

Tritium is partly discharged with the off-gas, and is partly retained in the aqueous solution. Today the tritiated water is discharged to a river. The tritium radioactivity in the effluents from big plants, however, would be too high, and

the discharge of tritium into underground strata or into the ocean are being considered.

A high percentage of the iodine is also released to the off-gas, but it can be retained by suitable filter materials.

Table IV shows the calculated annual gaseous emissions from a 50 000 MWe reprocessing plant and the resulting dose rate in the vicinity of the plant, assuming that the gaseous and volatile isotopes are quantitatively emitted (9). It can be concluded from these data, that the emission of gaseous and volatile isotopes from big plants must be limited, if a recommended exposure of 30 mrem/yr is not to be exceeded.

In this context special interest should be paid to the activation product ^{14}C, which is formed mainly in the graphite matrix of HTR fuel elements. The matrix is burnt before dissolution of the fuel. Retention of the ^{14}C, which is emitted as $^{14}CO_2$, seems to be infeasible.

In addition to the gaseous and volatile fission products, small amounts of aerosols containing ^{89}Sr, ^{90}Sr, ^{106}Ru, ^{134}Cs, ^{137}Cs and ^{144}Ce - ^{144}Pr as well as actinide elements are emitted. The dose commitment due to these isotopes may be smaller than that caused by the fall-out from nuclear weapon-tests.

Liquid effluents contain mainly ^{106}Ru, ^{95}Zr - ^{95}Nb, ^{137}Cs and ^{144}Ce - ^{144}Pr. From Windscale, for instance, the critical isotope is ^{106}Ru (10).

The fission product solution is stored temporarily on-site at the reprocessing plant in tanks. Under normal conditions only neglegible amounts of fission products are emitted. If however a tank fails, fission product solution may penetrate into the underground, where soils may act as ion exchanger. The critical isotopes are ^{89}Sr, ^{90}Sr, ^{137}Cs and ^{144}Ce - ^{144}Pr.

2.4 Release of fission products from fission product solidification equipment

Some years after discharge from the reactor the fission product solutions should be solidified on-site at the re-

Table 1 Calculated annual radioactive emissions with gaseous effluents from 50 000 MWe reprocessing plants.

Reactor Type		PWR						HTR						
Burn-up	MWd/t	30.000						100.000						
Throughput	t /yr	1.750						380						
	t /d	5,8						1,25						
Decay Time	d	150						150						
		^{3}H	^{85}Kr	^{129}I	^{131}I	Aerosol β	Aerosol α	^{3}H	^{14}C	^{85}Kr	^{129}I	^{131}I	Aerosol β	Aerosol α
Throughput	Ci/yr	$1,3\cdot10^{6}$	$2,7\cdot10^{7}$	73	$5,4\cdot10^{3}$	$7,6\cdot10^{9}$	$2,4\cdot10^{8}$	$1,6\cdot10^{6}$	$5,0\cdot10^{3}$	$2,5\cdot10^{7}$	50	$1,4\cdot10^{3}$	$3,9\cdot10^{9}$	$2,8\cdot10^{7}$
Fractional Release		0,1	1	0,01	0,01	10^{-8}	10^{-8}	0,1	1	1	0,01	0,01	10^{-8}	10^{-8}
Emission	Ci/yr	$1,3\cdot10^{5}$	$2,7\cdot10^{7}$	0,7	54	76	2,4	$1,6\cdot10^{5}$	$5,0\cdot10^{3}$	$2,5\cdot10^{7}$	0,5	14	39	0,3
Concentration	Ci/m^3	$4,1\cdot10^{-10}$	$8,6\cdot10^{-8}$	$2,2\cdot10^{-15}$	$1,7\cdot10^{-13}$	$2,4\cdot10^{-13}$	$7,5\cdot10^{-15}$	$5,1\cdot10^{-10}$	$1,6\cdot10^{-11}$	$8,0\cdot10^{-8}$	$1,6\cdot10^{-15}$	$4,5\cdot10^{-14}$	$1,2\cdot10^{-13}$	$1\cdot10^{-15}$
Nat. Conc./Fallout	Ci/m^3	$4\cdot10^{-14}$	$1,5\cdot10^{-11}$	$1\cdot10^{-18}$		$0,1\text{-}2\cdot10^{-12}$		$4\cdot10^{-14}$	$1,1\cdot10^{-12}$	$1,5\cdot10^{-11}$	$1\cdot10^{-18}$		$0,1\text{-}2\cdot10^{-12}$	
Inhalation Dose	mrem	1,0		0,5	6	4	40	1,3	0,3		0,3	1,5	4	15
Submersion-β-Dose	mrem	0,03	200					0,03	0,01	185				
Submersion-γ-Dose	mrem		10							9				
Ingestion -Dose	mrem	6		400	1400	16		7	20		230	365	16	
Total	mrem	7	210	400	1400	20	40	8	20	194	230	365	20	15

processing plant. Several processes are under development to produce calcinates, glasses or ceramics. They are produced by high temperature procedures (500 - 1200 °C). Under these conditions several lower volatility elements are volatilized.

Key isotopes may be ^{89}Sr, ^{90}Sr, ^{106}Ru, ^{129}I, ^{134}Cs, ^{137}Cs, ^{144}Ce - ^{144}Pr.

2.5 Interim and final storage of solidified fission products

To date the further treatment of the solidified waste has not been settled. In the USA, engineered storage of the solidified waste for the next 100 years in stainless steel pots under water is being considered.

Emission of radioactive isotopes during this storage period is not expected. Only low activity liquid effluents are possible.

In Germany the solidified fission products will be disposed of in a salt mine for final storage. Under normal operating conditions, neither during the transport nor during final storage will fission products be emitted, with the exception of low activity aerosols resulting from surface contamination.

Even in the case of the maximum credible accident (MCA), when the mine is filled with water, the brine should remain separated from the biosphere. Therefore no radiation exposure is to be expected. If, however, the mine should break down completely, which is very unprobable, the brine may come into contact with the ground water. In this case, the critical isotopes are probably ^{90}Sr, ^{137}Cs and the actinide elements.

2.6 Storage and disposal of noble gases

The noble gases which are emitted into the atmosphere at the present time, must be separated from the off-gas in the future. However only the long living ^{85}Kr is of environmental interest. The separated gases may be compressed into steel cylinders and stored during the next 100 to 150 years.

However, cylinder failure can result in a sudden accidental release. Therefore the disposal of ^{85}Kr into the deep sea has been proposed (9). It can be calculated that the environmental impact is very low. Experiments are continuing.

3. Evaluation

The environmentally most important fission products are schematically summerized in table V. Most of the isotopes are well known. Their path ways from the reactor core, from the reprocessing plant or from other facilities to the human body are very complex and difficult to predict. The errors in such calculations are much higher than the inaccuracies of the fission product nuclear data.

One exception may be tritium. It could turn out to be the most important isotope of all. The fission yield data for this isotope are in part only estimated values. The fission yield value for tritium should be redetermined exactly as a function of the neutron energy for ^{233}U, ^{235}U and ^{239}Pu as targets.

Furthermore, tritium is formed by several other reactions, the most important of which are

$$^{3}He\ (n,p)\ ^{3}H$$
$$^{6}Li\ (n,\alpha)\ ^{3}H$$
$$^{10}B\ (n,2\alpha)\ ^{3}H$$
$$^{10}B\ (n,\alpha)\ ^{7}Li\ (n,n\alpha)\ ^{3}H \quad \text{and}$$
$$^{11}B\ (n,n2\alpha)\ ^{3}H$$

^{3}He is found in natural helium ($\sim 10^{-5}$ %) which is used as cooling gas in HTR's. Lithium is a contaminant of graphite, which is also used extensively in HTR's. And boron is used in control rods. An exact knowledge of the production rate of tritium is essential for good tritium balances in the reactor and in the reprocessing plant.

Table V : Summary of Important Isotopes

Important Isotopes during Normal Operation		Important Isotopes in the Case of Accidental Release
^{3}H ^{83m}Kr ^{85m}Kr ^{87}Kr ^{88}Kr ^{89}Kr ^{131m}Xe ^{133m}Xe ^{133}Xe ^{135m}Xe ^{137}Xe ^{139}Xe ^{88}Rb $^{90}Sr/^{90}Y$ $^{131-135}I$ ^{137}Cs $^{140}Ba/^{140}La$ ^{13}N ^{16}N ^{17}N ^{15}O ^{19}O ^{41}Ar	Reactor	^{89}Sr $^{90}Sr/^{90}Y$ ^{91}Sr ^{92}Sr ^{95}Zr ^{97}Zr $^{103}Ru/^{103m}Rh$ ^{105}Rh $^{129m}Te/^{129}Te$ $^{131m}Te/^{131}Te$ ^{132}Te $^{131-135}I$ $^{140}Ba/^{140}La$ ^{143}Ce $^{144}Ce/^{144}Pr$
	Fuel Element Transport	^{90}Sr $^{129m}Te/^{129}Te$ ^{131}I ^{134}Cs ^{137}Cs
^{3}H ^{14}C ^{85}Kr ^{89}Sr ^{90}Sr $^{95}Zr/^{95}Nb$ ^{106}Ru ^{129}I ^{131}I ^{133}Xe ^{137}Cs $^{144}Ce/^{144}Pr$	Reprocessing Plant	^{90}Sr $^{95}Zr/^{95}Nb$ ^{106}Ru ^{131}I ^{137}Cs $^{144}Ce/^{144}Pr$ Actinides
^{89}Sr ^{90}Sr ^{106}Ru ^{129}I ^{134}Cs ^{137}Cs $^{144}Ce/^{144}Pr$	Fission Product Solidification	^{90}Sr ^{106}Ru ^{137}Cs $^{144}Ce/^{144}Pr$
	Final Disposal	^{90}Sr ^{137}Cs Actinides

Of similar importance for the HTR fuel reprocessing plants is the activation product ^{14}C. The main reactions are

$$^{13}C\ (n,\gamma)\ ^{14}C$$
$$^{14}N\ (n,p)\ ^{14}C \quad \text{and}$$
$$^{17}O\ (n,\alpha)\ ^{14}C.$$

^{14}C is emitted from HTR reprocessing plants as CO_2. It is taken up by assimilation in vegetation which in turn is eaten by animals and humans. Genetic defects may be caused by this long-lived isotope.

Finally, the actinide elements should be mentioned, though a detailed description is beyond the scope of this paper. Due to their long half-lives and their high toxities, they must be stored safely for hundreds of thousand years.

A good knowledge of their production rate should allow one to make better calculations of the effect on mankind in the event of their release to the biosphere.

REFERENCES

(1) F.Pasquill : Atmospheric Diffusion, Nostrand Comp., London 1962

(2) G.Blässer and K.Wirtz : Nukleare Grundlagen für Standort- und Gebäudewahl bei Kernreaktoren; Nukleonik 3, 164-178 and 210-231 (1961)

(3) K.J.Vogt : Umweltkontamination und Strahlenbelastung durch radioaktive Abluft aus kerntechnischen Anlagen; Report Jül-637-ST, 1970

(4) Y.Liu : Zur Behandlung der Spaltprodukte in Abbrandrechnungen unter Berücksichtigung neuer nuklearer Daten angewandt auf Graphitreaktoren; Report Jül-678-RG, 1970

(5) K.H.Lindackers : Einflüsse des atomrechtlichen Genehmigungsverfahrens in der Bundesrepublik Deutschland auf die technische Auslegung und den Betrieb von Kernkraftwerken; Thesis, Aachen 1970

(6) B.Kahn et al. : Radiological Surveillance Studies at a Boiling Water Nuclear Power Reactor Plant, Report BRH/DER-70/1 (1970)

(7) B.Kahn et al. : Radiological Surveillance at pressurized Water Reactors, Trans. Amer. Nucl. Soc. 15, 640 (1972)

(8) J.Engelhard : Abschlußbericht über die Errichtung und den Anfahrbetrieb des AVR-Atomversuchskraftwerkes; Report BMBW-FB K 72-23 (1972)

(9) H.Beaujean, J.Bohnenstingl, M.Laser, E.Merz, H.Schnez : Gaseous Radioactive Emissions from Reprocessing Plants and their possible Reduction; Symposium on Environmental Behaviour of Radionuclides Released in the Nuclear Industry, Aix-en-Provence, 1973. IAEA/SM-172/17.

(10) W.G.Marley : Atomic Energy and the Environment; Symposium on the Management of Radioactive Wastes from Fuel Reprocessing, Paris, 1972

Contribution to
Review Paper No. 3

THE EFFECT OF BURNUP AND FISSION PRODUCT NUCLEAR DATA ON FAST REACTOR STATIC AND DYNAMIC PARAMETERS

D. Ilberg, D. Saphier and S. Yiftah

Soreq Nuclear Research Centre
Yavne, Israel

ABSTRACT

Fast reactor static and dynamic parameters of "clean" and 100,000 MWd/t cores were evaluated. The calculations were performed with five different fission product cross section sets (FPCS). The following results were obtained.

- K_{eff} is reduced by up to 10% after BU of 100,000 MWd/t, however, only small differences were found when using different FPCS.
- The positive sodium void effect is doubled, and up to 50% differences are observed when using different FPCS.
- Minor differences in plutonium isotopic concentration were found after BU of 100,000 MWd/t when using different FPCS in the calculations.
- The effective delayed neutron fraction β_{eff} is changed considerably during the BU process, but only small differences were observed when calculated with different FPCS.
- The prompt neutron lifetime ℓ_{eff} may change by 10%. It is affected by using different FPCS.
- The spatio-temporal behavior of a high BU reactor undergoing a local step perturbation differs by several orders of magnitude from the "clean" reactor and significant differences between transient solutions using different FPCS were obtained.

1. INTRODUCTION

Several authors[1-3] have shown that significant differences exist between a reactor at the beginning of its lifetime and when its fuel has reached considerable burnup (BU). The present goal in fast reactor design is to achieve a BU of 100,000 MWd/t in the fast commercial breeders. At this stage of BU, approximately 10% of the fissile isotopes have been transformed into fission products (FP) while new fissile isotopes were bred, changing the initial fuel composition.

Philbin and Axford[3] have shown that considerable power shift into the blanket occurs during approach to equilibrium. They calculated a 11.2% increase in the sodium void coefficient and a 2% change in the Doppler coefficient.

Wright[4] compared the control rod effect in reducing power excursion in "clean" and 66,000 MWd/t cores. The power excursion was 10% higher in the high BU core.

Yamashita[2] pointed out that there is a tendency towards unfavorable values of the sodium and Doppler coefficients during reactor operation as FP are built up and changes in fuel composition occur, the former becoming positive and the latter less negative.

However, many of the safety and feasibility calculations are still based on clean cores, disregarding the various changes resulting from reactor BU and almost no dynamic calculations including BU fuel are known to the authors. This is partly because until recently, only incomplete data for the Fission Product Cross Sections (FPCS) and yields were available and because complete BU calculations are complicated and costly. Even those calculations accounting for BU use lumped data for the FP as the input to either static or dynamic calculations.

Since detailed Fission Product Nuclear Data (FPND)[5-11] have become avialble recently, it seems timely to test their influence on some of the static and dynamic parameters of fast breeders.

In what follows, detailed BU calculations followed by static and dynamic calculations of one dimensional reactor models were performed. Cores at the beginning of their lifetime were compared with cores undergoing burnup for one and two years without refueling, i.e. with a mean BU of 50,000 and 100,000 MWd/t respectively. The same reactors

were then recalculated using different FPCS. The effect of the differences in the BU level and FPCS on fast reactor transient excursions were compared.

2. METHOD OF CALCULATION

A detailed flowchart of the programs used and the file management procedures is given in Fig. 1.

The present evaluation has the following stages:

1) Preparation of a 25 group cross section library in ABN[12] energy structure for all the isotopes present in the reactor model using the ENDF/B-III file.
2) Preparation of 25 group cross sections for the FP isotopes using 4 different FPCS files.
3) Preparation of simplified one dimensional models for the reactors under investigation.
4) Performing one dimensional BU calculations using the DLEKAH[13] code - see Fig. 1 . This code uses one dimensional diffusion in 25 groups for criticality search, a modified version of the ICON[14] code to calculate the concentration of 380 FP isotopes and the new concentration of the various fissile isotopes at each interval, and a collapse subroutine to obtain four group cross sections serving as the input for the SHOVAV[15] dynamic code.
5) Collapsing the 25 group cross sections into four groups using the appropriate fluxes and isotopic compositions obtained in DLEKAH (see calculation scheme in Fig. 1) for various stages of BU.
6) Calculations of kinetic parameters such as β_{eff} and ℓ_{eff} .
7) Space-time dependent solution of the four group diffusion equation with six groups of delayed neutrons. A local perturbation (control rod withdrawal) is inserted to initiate transient excursions. The calculation is performed with the SHOVAV code.

3. REACTOR MODELS AND NUCLEAR DATA

Three reactor cores were investigated:

a) General Electric - 1968 conceptual design[16] of a 1000 MWe (2260 MWt) fast reactor. The core is enriched with 11% plutonium discharged from thermal reactors. (Enrichment is defined by $(^{239}Pu + ^{241}Pu)/(^{238}U + ^{239}Pu + ^{240}Pu + ^{241}Pu + ^{242}Pu)$) . The composition of the Pu is 60% ^{239}Pu, 25% ^{240}Pu, 12% ^{241}Pu and 3% ^{242}Pu.

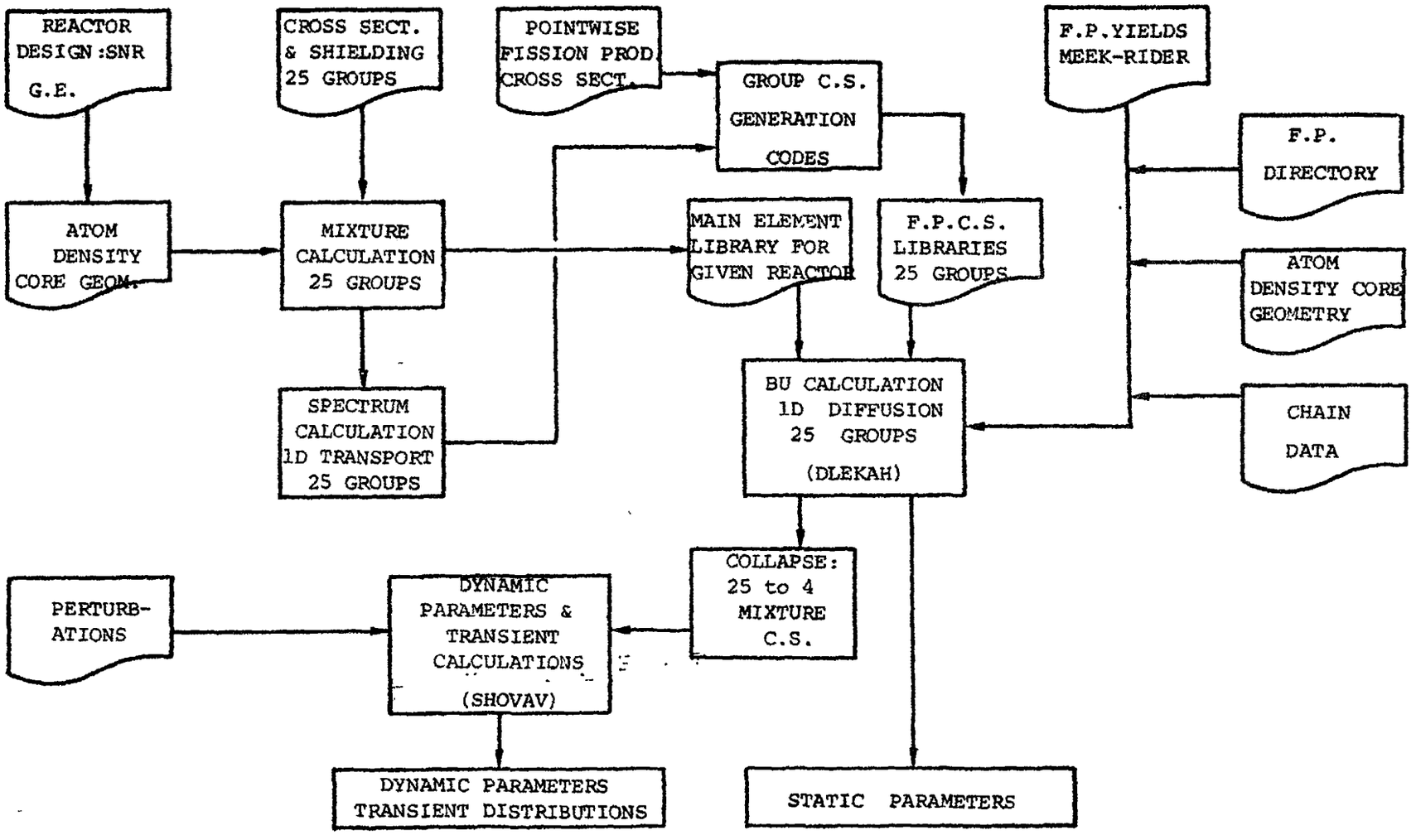

Fig. 1: A schematic flowchart of the computing model for BU static-dynamic calculations

b) Same as above but enriched with ^{239}Pu only.

c) SNR - German prototype reactor [17] (1967), 300 MWe (750 MWt). The core is enriched with 17% plutonium, composed of 75% ^{239}Pu, 22% ^{240}Pu, 2.5% ^{241}Pu and 0.5% ^{242}Pu.

For the isotopes included in the reactor a 25 group cross section set was prepared by Y. Gur [18] from the ENDF/B-III file.

The following FPCS files have been used in this evaluation:

a) Cook's [6] file, which includes cross sections for 192 isotopes in 127 energy groups. A 25 group cross section set for $\sigma_{n\gamma}$, σ_{tr} and a scattering transfer matrix was formed and called COOK-M.

b) Same as (a) but only $\sigma_{n,\gamma}$ was collapsed. This was called COOK-L.

c) The ENDF/B-III file, which includes 58 isotopes. The 25 group cross sections for $\sigma_{n,\gamma}$ and σ_{tr} were computed by Y. Gur [18] in the same way as for the fissile, fertile and structural isotopes mentioned above.

d) The evaluation of BENZI and REFFO [7], which includes 142 isotopes for which pointwise cross sections are given. These were collapsed by a separate program, forming a 25 group library of $\sigma_{n,\gamma}$. This file is designated as BENZI.

e) The 25 group library based on UKNDL, which was prepared by Tone and Hasegawa [19]. The weighting flux was different from the flux used in the above evaluations, but this gave rise only to second order differences in the group cross sections. The file includes $\sigma_{n,\gamma}$ only.

The relevant features of the above files as used in the comparative calculations are shown in Table I. It should be noted that some of the FP isotopes appearing in the original files were omitted in the calculations because of their negligible effect.

In the BU calculations, the independent yields compiled by Meek and Rider [5] were used. Their compilation includes yields for fast fission of ^{235}U, ^{238}U, ^{239}Pu and for thermal fission of ^{241}Pu. For the fast fission of ^{240}Pu, the yields of ^{239}Pu were used. For the fast fission of ^{241}Pu and ^{242}Pu, thermal fission yields of ^{241}Pu were used. These replacements are inevitable because no data were available for all the fissile isotopes, and were made under the assumption that cumulative yields change slowly with energy and only slightly with the mass number.

TABLE 1: Evaluated Fission Product Neutron Cross Section Files

Library	Cross Section	No. of Isotopes In Library	No. of Isotopes Used	Processing for this Study	Designation
COOK [6] 1971	$\sigma_{n\gamma}, \sigma_{el}, \sigma_{in}, \sigma_{tr}$ 127 Groups	192	178	25 group $\sigma_{n\gamma}$ σ_{tr} and scattering transfer matrix	COOK-M
				25 group $\sigma_{n\gamma}$ only	COOK-L
BENZI/REFFO/ PANINI [7] 1969	$\sigma_{n\gamma}$ $(+\sigma_{nn'})$ Pointwise	142 (+18)	113	25 group $\sigma_{n\gamma}$	BENZI
BENZI/ORAZI [8] 1972	$\sigma_{n\gamma}$ Pointwise	80*	8	25 group $\sigma_{n\gamma}$ and adding to the BENZI file	-
ENDF/B-III [9] 1972	$\sigma_{n\gamma}\sigma_{el}, \sigma_{in}, \sigma_{tr}$ Pointwise	58	55	25 group $\sigma_{n\gamma}$ σ_{tr} and scattering transfer matrix	ENDF/B
UKNDL [19] 1968	$\sigma_{n\gamma}$ 25 Groups	78	78	-	UKNDL
RCN [11] 1973	$\sigma_{n\gamma}$	75	0	-	-

*These are 80 new evaluations which were added to the 142 isotopes evaluated by Benzi/Reffo

Keepin's[20] delayed neutron data were used in the dynamic calculations. The delayed neutron spectra were taken from recent measurements of Feig[21].

4. CHANGES IN K_{eff} OWING TO BU AND DIFFERENT FPCS

Burn up and static calculations to find K_{eff} were made for the GE[16] and SNR[17] reactors, using five different FPCS files. The results are summarized in Table II. The reduction in K_{eff} is 5% and 10% for the 50,000 MWd/t and 100,000 MWd/t cores, respectively in the GE core, while in the SNR core the reduction is 8% and 14%. These results are in agreement with those obtained by Yamashita[2]. The greater reduction in SNR is due to the higher enrichment of this core,

TABLE II: K_{eff} of SNR and GE Cores before and after BU Using Different FPCS

FPCS SOURCE	General Electric (1968)			SNR (1967)		
	0 MWd/t	50 000 MWd/t	100 000 MWd/t	0 MWd/t	50 000 MWd/t	100 000 MWd/t
COOK-M	1.021	.9635	.9183	1.040	.9548	.8867
COOK-L		.9729	.9354		.9594	.8949
BENZI		.9723	.9336		.9601	.8963
UKNDL		.9670	.9265		.9540	.8864
ENDF/B-III		.9724	.9360		.9597	.8963
Percent of Change Relative to Zero BU						
COOK-M		- 5.6	-10.1		- 8.1	-14.7
COOK-L		- 4.7	- 8.4		- 7.8	-14.0
BENZI		- 4.8	- 8.6		- 7.7	-13.8
UKNDL		- 5.3	- 9.3		- 8.3	-14.8
ENDF/B-III		- 4.8	- 8.3		- 7.7	-13.8

TABLE III: Na Void Effect of SNR and GE Cores Before and After BU Using Different FPCS

FPCS SOURCE	General Electric (1968)			SNR (1967)		
	0 MWd/t	50 000 MWd/t	100 000 MWd/t	0 MWd/t	50 000 MWd/t	100 000 MWd/t
Percent $\Delta k/k$ of 100 % Na Void in Core						
COOK-M	1.32	1.72	1.98	1.68	2.08	2.26
COOK-L		1.86	2.27		2.20	2.48
BENZI		1.62	1.77		1.88	1.84
UKNDL		2.06	2.56		2.42	2.86
ENDF/B-III		1.73	1.99		2.05	2.20
Percent of Change Relative to Zero BU						
COOK-M		30.3	50.0		23.8	34.5
COOK-L		29.0	72.0		31.0	47.6
BENZI		22.8	34.1		11.9	9.5
UKNDL		56.0	94.0		44.0	71.4
ENDF/B-III		31.1	50.8		22.0	31.0

17% as compared with 11% in the GE core. As a result of using different FPCS, only second order differences were observed in K_{eff}, see Table II. COOK-M and UKNDL files gave the greatest reduction, while COOK-L, ENDF/B or BENZI showed smaller reductions in K_{eff}.

5. The Na VOID EFFECT

The Na void effect was found to be the most sensitive to the various FPCS. The results at zero BU, for 50,000 MWd/t and 100,000 MWd/t cores are given in Table III for the GE and SNR reactors. No appreciable difference exists between the two cores of the GE reactors. It is seen from the table that the positive Na void effect is significantly greater at higher BU. However, there is a discrepancy of 60% between the predictions using BENZI and UKNDL cross sections.

The inclusion of the scattering cross section in the FPCS (COOK-M and ENDF/B files) reduces the sodium void coefficient.

TABLE IV: Changes in fuel isotopic composition, at the middle of the core due to different FPCS sources

REACTOR	BU [mwd/t]	FPCS SOURCE	Fuel isotopic composition [%] U-238	Pu-239	Pu-240	Pu-241	Pu-242	FP
GE	0		84.89	8.90	3.88	1.84	0.49	0
conceptual design of 1000 MWe (1968) Ref. 16	100.000	COOK-M	71.33	9.07	4.48	0.77	0.57	13.71
		COOK-L	71.26	9.03	4.45	0.76	0.57	13.87
		BENZI	71.29	9.00	4.45	0.76	0.57	13.86
		UKNDL	71.41	9.05	4.43	0.76	0.57	13.71
		ENDF/B	71.18	9.05	4.48	0.77	0.57	13.87
GE	0		89.26	10.74	0	0	0	0
1000 MWe pure Pu-239	100 000	COOK-M	74.20	9.86	2.27	0.16	0.015	13.43
		COOK-L	74.10	9.81	2.24	0.16	0.015	13.61
		BENZI	74.15	9.78	2.25	0.16	0.015	13.58
		UKNDL	74.30	9.85	2.20	0.15	0.015	13.42
		ENDF/B	74.04	9.83	2.29	0.16	0.015	13.60
SNR	0		78.83	15.90	4.64	0.53	0.10	0
German prototype design (1967) 300 MWe Ref. 17	100.000	COOK-M	70.49	11.82	5.60	0.60	0.16	11.26
		COOK-L	70.48	11.81	5.58	0.60	0.16	11.31
		BENZI	70.50	11.79	5.59	0.60	0.16	11.30
		UKNDL	70.57	11.86	5.56	0.60	0.16	11.20
		ENDF/B	70.46	11.81	5.60	0.61	0.16	11.30

6. DIFFERENCES IN PLUTONIUM AND FP ISOTOPIC CONCENTRATION

During the lifetime of a fuel rod its isotopic composition is changed considerably; FP are produced and fuel isotopes are consumed and bred. In the core center the consumption process predominates, while in the blanket, the breeding process is dominant. BU calculations were performed with the five libraries and the results obtained are shown in Table IV for the fuel composition at 100,000 MWd/t. It is seen that only minor changes in the concentration result because of the use of different FPCS. This is observed more clearly in Table V, where only the percent of the difference is shown. These results are in agreement with those obtained previously by Tone and Nakagawa [1].

In Table VI the concentrations of the most important FP are listed. In the majority of cases, the influence of the FPCS sources on these concentrations is small, only for ^{151}Sm and ^{107}Pd are the differences observed above 10%.

TABLE V: Percent of change in fuel isotope composition due to calculations performed with different FPCS

REACTOR	BU [MWd/t]	FPCS SOURCE	Percent change in fuel isotopic composition					FP
			U-238	Pu-239	Pu-240	Pu-241	Pu-242	
GE conceptual design of 1000 MWe (1968) Ref. 16	100 000	COOK-M	-15.97	1.91	15.46	-58.15	16.33	100 *
		COOK-L	-16.06	1.46	14.69	-58.70	16.33	101.17
		BENZI	-16.02	1.12	14.69	-58.70	16.33	101.09
		UKNDL	-15.88	1.69	14.18	-58.70	16.33	100
		ENDF/B	-16.15	1.69	15.46	-58.15	16.33	101.17
GE 1000 MWe pure Pu-239	100 000	COOK-M	-16.87	-8.19	100 *	100 *	100 *	100 *
		COOK-L	-16.98	-8.66	98.68	100	100	101.34
		BENZI	-16.93	-8.94	99.12	100	100	101.12
		UKNDL	-16.76	-8.29	96.92	93.75	100	99.93
		ENDF/B	-17.05	-8.47	100.88	100	100	101.27
SNR German prototype design (1967) 300 MWe Ref. 17	100 000	COOK-M	-10.58	-25.66	20.69	13.21	60	100 *
		COOK-L	-10.59	-25.72	20.26	13.21	60	100.44
		BENZI	-10.57	-25.85	20.47	13.21	60	100.36
		UKNDL	-10.48	-25.41	19.83	13.21	60	99.47
		ENDF/B	-10.62	-25.72	20.69	15.09	60	100.36

* Since zero concentrations have been assumed at startup, differences are with respect to results obtained with data of COOK-M.

TABLE VI: Differences in FP concentrations due to different FPND sources after 100,000 MWd/t BU ($x10^{20}$ atoms)

FP Element	COOK-M	COOK-L	BENZI	UKNDL	ENDF/B-III	MAXIMUM DIFFERENCE %
Mo-97	0.598	0.603	0.598	0.590	0.595	2
Tc-99	0.625	0.631	0.596	0.599	0.697 (*)	6
Ru-101	0.667	0.673	0.665	0.654	0.671	3
Ru-102	0.846	0.852	0.849	0.839	0.833	2.5
Rh-103	0.621	0.626	0.640	0.616	0.716 (*)	4
Pd-105	0.527	0.531	0.477	0.471	0.502	6.5
Pd-107	0.350	0.352	0.313	0.310	0.345	13.5
Xe-131	0.429	0.433	0.439	0.436	0.433	1.5
Cs-133	0.735	0.742	0.722	0.714	0.707	5
Nd-143	0.457	0.461	0.476	0.502	0.458	9.5
Pm-147	0.162	0.164	0.177	0.166	0.157	12.5
Sm-149	0.130	0.131	0.131	0.121	0.121	8.5
Sm-151	0.060	0.061	0.076	0.065	0.053	43

(*) For these element $\sigma_{n\gamma}$ was zero (i.e.not given by the library)

7. CHANGES IN β_{eff} and ℓ_{eff} AS A RESULT OF BU AND OF DIFFERENT FPCS

After the termination of the BU calculations, a new criticality search was performed and K_{eff} values as shown in Table II were obtained. The eigenfluxes are normalized and the adjoint flux is also calculated using the SHOVAV[15] code. At this stage the kinetic parameters are evaluated. Table VII shows the effective delayed neutron fraction β_{eff}, and Table VIII gives the effective neutron lifetime ℓ_{eff}.Up to 10% changes in β_{eff} are observed during the BU process as seen in Table VII. This is due to the changes in the ratio

TABLE VII: Effect of BU and FPCS on the Effective Delayed Neutron Fraction β_{eff}

Reactor	FPCS Source	$\beta_{eff} \times 10^3$ for Core Burn Up (MWd/t)		
		0	50,000	100,000
General Electric Conceptual Design (1968) 1000 MWe Ref.16	COOK-M	3.725	3.503	3.365
	COOK-L			3.432
	BENZI			3.439
	UKNDL			3.431
	ENDF/B			3.402
General Electric 1000 MWe Pure Plutonium	COOK-M	3.411	3.323	3.286
	COOK-L			3.340
	BENZI			3.346
	UKNDL			3.340
	ENDF/B			3.303
SNR- German Prototype design (1967), 300 MWe Ref.17	COOK-M	3.029	3.060	3.088
	COOK-L			3.125
	BENZI			3.131
	UKNDL			3.123
	ENDF/B			3.110

TABLE VIII: Effect of BU and FPCS on the Effective Neutron Lifetime - ℓ_{eff} ($\times 10^{-6}$ sec)

Reactor	FPCS Source	Core Burn Up (MWd/t)		
		0	50,000	100,000
General Electric Conceptual Design (1968) 1000 MWe Ref.16	COOK-M	0.2616	0.2601	0.2590
	COOK-L			0.2493
	BENZI			0.2551
	UKNDL			0.2367
	ENDF/B			0.2623
General Electric 1000 MWe Pure Plutonium	COOK-M	0.2754	0.2701	0.2666
	COOK-L			0.2570
	BENZI			0.2642
	UKNDL			0.2439
	ENDF/B			0.2703
SNR German Prototype design (1967) 300 MWe Ref.17	COOK-M	0.3245	0.3395	0.3499
	COOK-L			0.3418
	BENZI			0.3540
	UKNDL			0.3250
	ENDF/B			0.3537

of the number of fission events in ^{238}U to the fissions of Pu isotopes, the latter being poorer delayed neutron emitters than ^{238}U.

The effective neutron lifetime changes approximately by 10% during the BU process, decreasing in the GE reactor and increasing in the SNR reactor. The differences between the various FPCS are also of the order of 10%, the UKNDL giving the lowest value and the ENDF/B-III giving the highest.

8. SPATIO-TEMPORAL BEHAVIOR OF "CLEAN" AND HIGH BU CORES USING DIFFERENT FPCS

After the BU calculations were terminated, a four group cross section set was evaluated to be used with the SHOVAV code. The transient was initiated by inserting a step change in the absorption cross section at the core outer region. This step is equivalent to an abrupt withdrawal of a control rod.

In Fig. 2, the change in the reactor power as a function of time for the GE core with no higher plutonium isotopes is shown for three cases. In each case, the same perturbation was inserted, but the appropriate reactivity was different as explained in Table IX.

TABLE IX: Effect of BU and FPCS on the Reactivity Due to Constant Change in Absorption Cross Section

$$\Delta\Sigma_a \approx \Sigma_a/80$$

Reactor	FPCS Source	Core Burn Up (MWd/t)		
		0	50,000	100,000
G.E. 1000 MWe Conceptual design Ref.16	COOK-M	$1.030	$0.922	$0.913
	COOK-L			0.896
	BENZI			0.908
	UKNDL			0.913
	ENDF/B			0.891
G.E. 1000 MWe Pure Pu-239	COOK-M	1.030	0.815	0.788
	COOK-L			0.766
	BENZI			0.781
	UKNDL			0.786
	ENDF/B			0.765
SNR-German Prototype design 300 MWe Ref.17	COOK-M	1.030	1.096	1.141
	COOK-L			1.145
	BENZI			1.153
	UKNDL			1.156
	ENDF/B			1.144

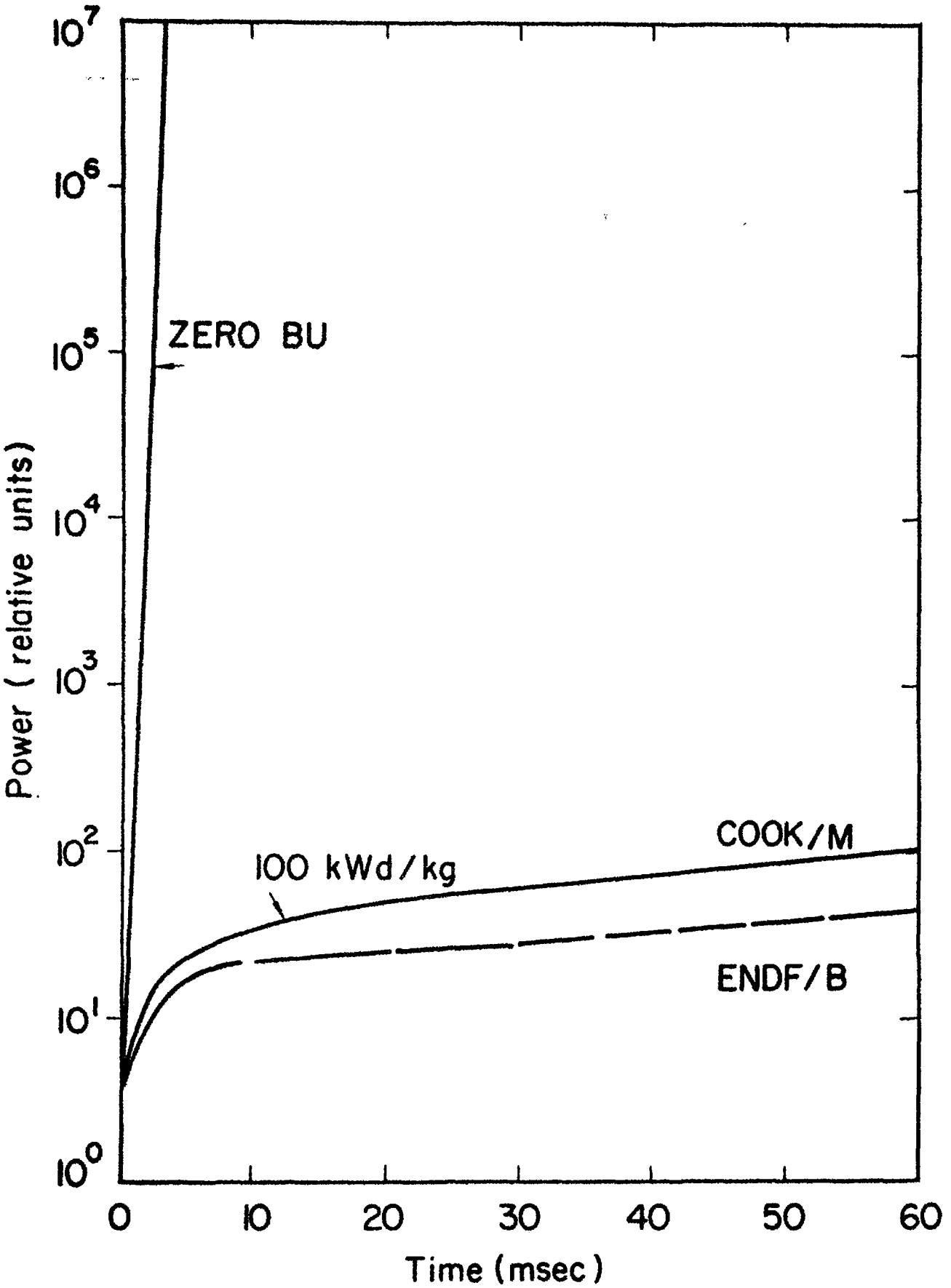

Fig. 2 : Transient power excursion of the GE reactor after the change $\Delta\Sigma_a^1 = 0.0020$, $\Delta\Sigma_a^2 = 0.0003$, $\Delta\Sigma_a^3 = 0.0003$ $\Delta\Sigma_a^4 = 0.0006$ has been inserted.

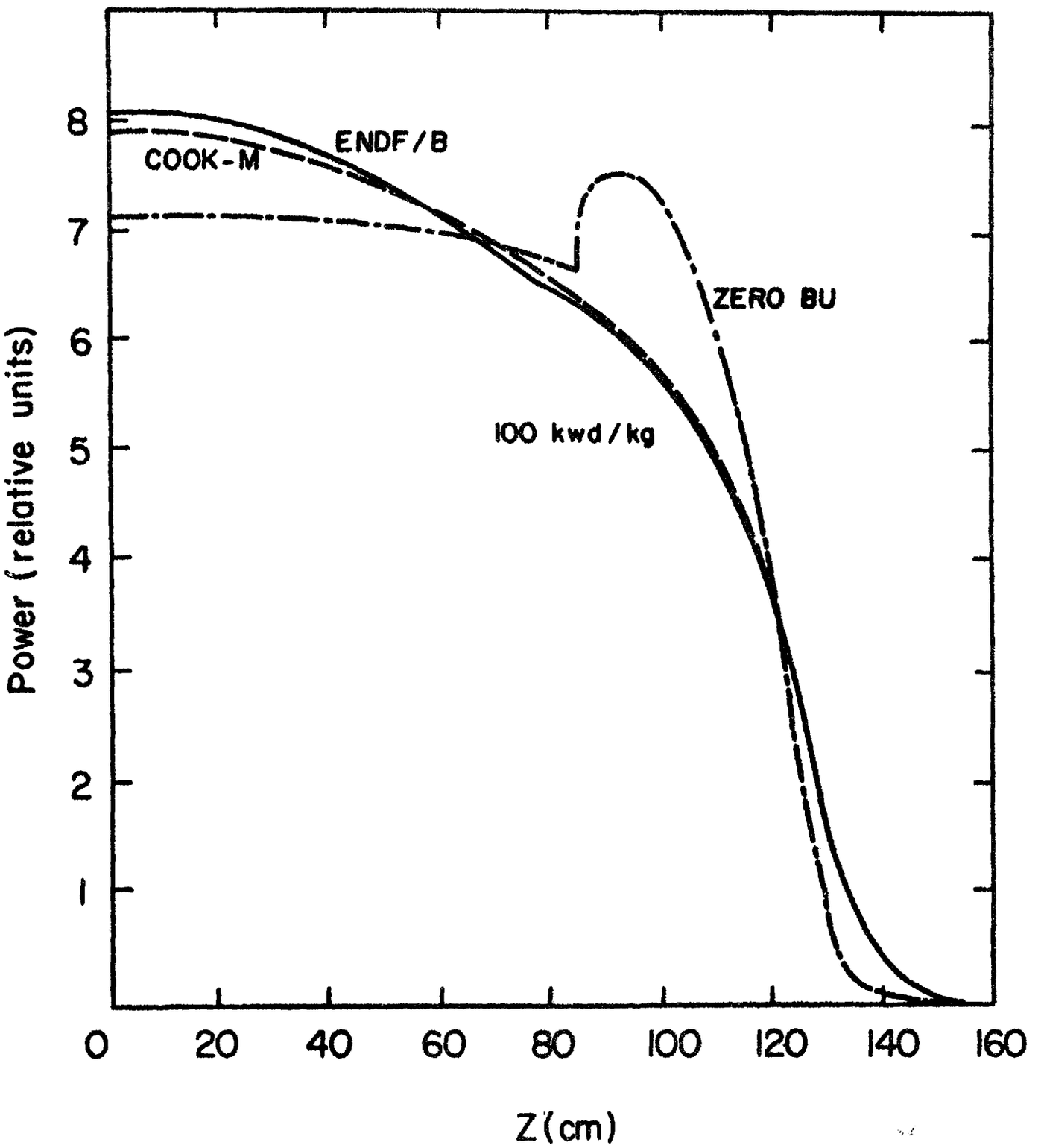

Fig. 3 : Initial power distribution in the "clean" and high BU GE core using two different FPCS for the BU calculations.

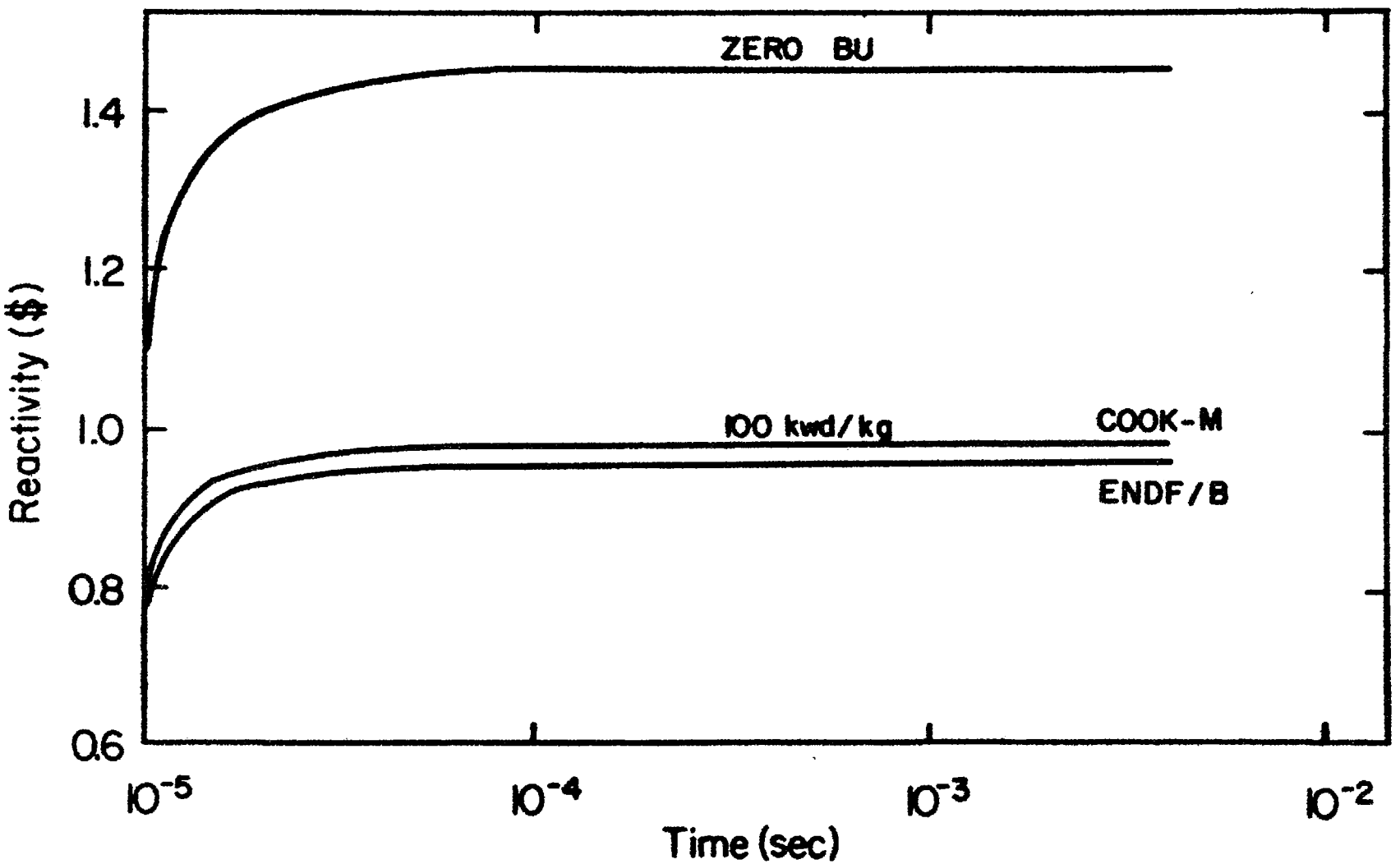

Fig. 4 : Reactivity change as a function of time after a constant step change in the absorption cross section has been inserted.

In the "clean" core the change resulted in a superprompt critical excursion while in the 100,000 MWd/t cores the perturbation was in the delayed critical region. A considerable difference in the power excursions after 60 milliseconds is observed. Using the COOK-M FPCS a 100% higher power excursion is obtained as compared with the results obtained with ENDF/B-III FPCS. There are several reasons for the above differences. First and most important is the initial flux and power distribution. While in the "clean" reactor this distribution is flat giving rise to a considerable flux tilt which increases reactivity; in the 100,000 MWd/t core the power and flux have a more cosine-like distribution as seen in Fig.3. The changes in reactivity as a function of time resulting from different flux shapes of "clean" and high BU cores are shown in Fig. 4. The small difference between ENDF/B and COOK-M curves is due to the fact that these files have only a slight effect on the β_{eff} and the reactor isotopic composition, as shown in Tables V and VII. Hence, the reactivities inserted in dollar units become 0.765 and 0.788 respectively. The other reasons for the differences in the transients are different Σ_f/Σ_c ratios and different spectra. Only a single example is presented here showing the large sensitivity of the dynamic solution to the changes occurring in the core after BU of 100,000 MWd/t and due to the use of different FPCS. The picture may be completely different in other cases (different core size, different core enrichment and Pu composition) i.e. the differences in dynamic behavior may be much larger or much smaller.

9. F.P. RELATIVE IMPORTANCE

After calculations with several FPCS libraries are performed, it becomes apparent that not all the FP are of the same importance. In the DLEKAH code the concentration of 380 FP isotopes was calculated. These concentrations were then multiplied by Cook's[6] FPCS to obtain the macroscopic capture cross sections, which served as a measure of their relative importance. In Table X the various FP are grouped according to their importance. It is seen that 52 isotopes account for 90% of the captures in the FP, and this number seems sufficient for all practical purposes in BU calculations. This explains why only minor differences were found in reactor parameters when using ENDF/B-III data having 55 isotopes, as compared with COOK-M data having 178 isotopes.

TABLE X: Grouping of FP's According to their Cumulative Absorption Effect

Fission Product Group	Number of Elements	Percent of Total Absorption	FP Isotopes in Group (Using Cook Data, and in order* as Obtained in GE Reactor 100 000 MWd/t)
I	13	60	Ru-101, Rh-103, Te- 99, Cs-133, Pd-105, Ru-102, Pd-107, Xe-131 Nd-143, Pm-147, Sm-149, Sm-151 Mo-97
II	13	22	Mo- 95, Cs-135, Nd-145, Mo- 98 Ag-109, Ru-104, Eu-153, Pr-141, Xe-132, Mo-100, Sm-152, Eu-154, Zr-93
III	13	8	Sm-147, Nd-148, Ru-103, Pd-106 La-139, Nd-144, Eu-155, Nd-146, Xe-134, I-127, Pd-104, I-129 Pd-108
IV	13	4.5	Ru-100, Zr- 96, Cs-134, Ce-142 Sm-150, Zr- 91, Ru-106, Kr- 83 Nd-150, Ce-144, Ce-140, Cs-137 Sm-148
V	13	1.9	Cd-111, Rb- 85, Sm-154, Gd-156 Gd-157, In-115, Gd-155, Br- 81 Sb-125, Nb- 95, Pr-143, Zr-94 Zr- 95
Total	65	96.4	
VI	113	3.6	
Total	178	100	

* Order of decreasing magnitude of the isotope's absorption effect

10. CONCLUSION

The above calculations are by no means comprehensive, only two reactors - a 1000 MWe and a 300 MWe reactor were investigated, and only very simple dynamic calculations were performed, excluding the various feedback effects. Nevertheless, it seems that the following conclusions can be drawn:

a) "Clean" and high BU reactors differ considerably mainly
   - in the sodium void effect which increases by almost 100% in certain cases;
   - in β_{eff}, which is changed by up to 10%;
   - in the effective neutron lifetime, which may change by 10%;
   - in the transient power excursion which differs considerably for "clean" and high BU cores, but the extent of this difference depends strongly on the reactor investigated.

b) By using 52 FP isotopes, 90% of the total FP effect of the high BU reactor is accounted for. The differences between the libraries of FPCS used were, therefore, due to their different cross sections and not because of the different numbers of isotopes inserted.

c) The differences between the calculations performed with different FPCS were smaller than those observed between clean and 100,000 MWd/t BU cores using the same data source. The main differences are again, in the sodium void coefficient, up to 50%. Small differences - of a second order - were found in ℓ_{eff}, β_{eff}, and higher plutonium isotopic concentration. However, in the example shown, considerable differences were observed in the reactivity inserted by a control rod withdrawal using COOK-M and ENDF/B-III data.

REFERENCES

1.) T. Tone and M. Nakagawa, "Effect of FP on Physical Quantities Accompanying BU of Large Pu-U Fast Reactors", J. Nucl. Sci. Technol. 6, 6, (June 1969) 295.

2.) S. Yamashita, "Variation in Neutronic Characteristics Accompanying BU in Large Fast Breeders", J. Nucl. Sci. Technol. 6, 10, (October,1969) 573.

3.) J.S. Philbin and R.A. Axford, "BU and Power Shift Effects in Large Fast Breeder Reactors", Nuclear Technology, 15, 3, (Sept. 1972) 327.

4.) J.H. Wright et al, "Conceptual Design and Preliminary Accident Analysis of a Sodium-Cooled Carbide - Fueled Large Modular Fast Reactor", in Proceedings of the Conference on Safety, Fuels and Core Design in Large Fast Power Reactors, ANL-7120 (1965).

5.) M.E. Meek, and B.F. Rider, "Compilation of FP Yields", NEDO-12154 (Jan. 1972).

6.) J.L. Cook, "FP Cross Sections," AAEC/TM549 (June 1970).

7.) V. Benzi, and G. Reffo, "Fast Neutron Radiative Capture Cross Sections of Stable Nuclei with $32 \leq Z \leq 66$", CCDN-NW/10 Newsletter Bulletin 10, ENEA Neutron Data Compilation Centre, (Dec. 1969).

8.) V. Benzi, R. D'Orazi, and G. Reffo, "Fast Neutron Radioactive Capture Cross Sections of Stable Nuclei with Z Between 29 and 70, RT/FI-(72) 6, (Feb. 1972).

9.) R.E. Schenter, and F.A. Schmittroth, "Cross Section Evaluation of 27 FP Isotopes for ENDF/B-III, ENDF-159 (Oct. 1971).

10.) D.S. Norton, "The UKAEA Nuclear Data Library", AEEW-M-824 (Feb. 1968).

11.) G. Launtenbach, to be published as RCN report.

12.) I. I. Bondarenko, "Group Constants for Nuclear Reactor Calculations", Consultant Bureau (1964).

13.) D. Ilberg and D. Saphier, "DLEKAH - A One Dimensional BU Code", to be published.

14.) D. L. Faircloth and M.J. Hoopper, "ICON - A Programme for the Calculation of FP Inventories", AERE-R-6242 (1970).

15.) D. Saphier and S. Yiftah, "SHOVAV - A Program to Solve the Few Group Space-Time Dependent Diffusion Equation with Temperature Feedback," IA-1217 (1971).

16.) "Conceptual Plant Design System Description, and Costs for a 1000 MWe Sodium-Cooled Fast Reactor", GEAP-5678 (1968).

17.) K. Gast et al, "Schneller Natrium Gekuehlter Reactor Na 2" KFK 660 (1967).

18.) Y. Gur, Private communications.

19.) T. Tone and A. Hasegawa, "Multigroup Constants for FP Nuclides: Part III", JAERI - Memo 4251 (1970).

20.) G. R. Keepin, "Physics of Nuclear Kinetics", Addison Wesely (1965).

21.) G. Feig, "Measurements of Delayed Fission Neutron Spectra of U-235, U-238, and Pu-239 with Proton Recoil Proportional Counters", USAEC, CONF-720 901, Book I, TID 4500 (1972).

Contribution to
Review Paper No. 4

PHYSICAL PECULIARITIES OF THE FAST POWER REACTOR FUEL CYCLE

V.V. Orlov, O.D. Bakumenko, E.M. Ikhlov,
M.Ya.Kulakovsky, M.F.Troyanov, A.G.Tzykunov

Inst. Physics and Power Engineerg.,Obninsk,
USSR

Abstract: Main calculated physical characteristics of fast power reactor fuel are presented in the paper: isotopic composition, fission product activity and residual heat release.

Changes of these characteristics with the cooling time of the spent fuel are analyzed, as well as the influence of these values on the problem of fuel transportation and the required degree of fuel decontamination from fission products.

Factors affecting radiation conditions in the process of fabrication of fuel elements and assemblies are considered.

1. Introduction

Reduction of the out-of-pile fuel cycle time is one of the effective ways to increase the rate of growth of the fast reactor nuclear power stations (plants) [1]. If this time is equal to about half a year, fast reactors, even those using oxide fuel, may ensure 6-year doubling time and less, which would allow their faster development and would help to solve the problem of natural uranium demand for nuclear power industry [1, 2].

In order to provide for a short time of the external fuel cycle performance a great number of problems connected with the chain of fuel movement outside a reactor should be considered completely.

1. A discharging system of spent fuel assemblies from a reactor must exclude fuel delay. In this connection a technological system of transportation of a nuclear power plant should make fuel discharge possible without exposure during storage at the reactor site.

2. The means of fuel transportation from a reactor to a reprocessing plant must ensure safe fuel transport in spite of considerable residual heat release and activity. An alternative for fuel transport to a controlled reprocessing plant can be creation of radiochemical facilities at large nuclear power plants, but in such a case the problem of high activity waste storage at atomic power stations arises.

3. A special technique for fuel rod separation and removal of the cladding as well as the technology of the chemical reprocessing should be developed for short cooling times.

4. The fabrication of fuel rods and assemblies of reprocessed fuel as well as the treatment of fuel being introduced into a reactor after fabrication must be performed taking into account the special features mentioned above. In this case there is a considerable difference between cases of complete or incomplete decontamination of fuel from radioactive fission products.

Technological aspects of aqueous and nonaqueous methods of fuel reprocessing for fast reactors are considered in [3, 4].

The paper presents main calculated physical characteristics of fuel for fast power reactors of the BN-600 type: fuel isotopic composition, fission product radioactivity in the discharged fuel, residual heat release, accumulation of stable fission products and inherent activity of the fuel after reprocessing. These changes of the characteristics are analysed depending on the duration of the fuel cooling time as well as the effect of these values on the problem of spent fuel transportation and the requirements of the degree of fuel decontamination.

Factors affecting radiation conditions of fuel rods and assemblies fabrication from reprocessed fuel are studied.

2. Characteristic Features of Fast Power Reactor Fuel

Reprocessing of mixed uranium-plutonium fuel for breeders is the principal task of the external fuel cycle. A mixture of uranium and plutonium dioxides is, probably, to be used for a long time as the main fuel for fast reactors. Utilization of carbides and metallic fuels is considered in perspective. The present paper gives a consideration of an oxide fuel for breeders though it is known that first loadings of the BN-350 and BN-600 reactors would be of enriched uranium dioxide.

High content of fissionable material (10 - 30%) is a peculiarity of fuel for fast reactors in contrast to that of thermal reactors. This fact imposes certain restrictions on nuclear safety during fuel storage and reprocessing.

Fuel power density in fast reactors is considerably higher than in thermal reactors. Thus, in a reactor of the BN-600 type this value is about 150 kwt/kg of an oxide fuel as compared to 40 kwt/kg for a light water cooled power reactor (WWR-1000) [5]. Along with this fact,

accumulation of fission products of a fuel being discharged from a fast reactor is two to three times higher than in the case of a thermal reactor of the water cooled power reactor type. Therefore the specific activity of fission products in fast reactor fuels is 4 - 5 times higher.

One of the main characteristic features of fast breeders in the first stage of their operation in a nuclear power system is utilization of plutonium from thermal reactors. At burn-ups of 30 kg fiss. prod. /ton UO_2 thermal reactors of light water-cooled power reactor type will produce plutonium of a complex isotopic composition with a high content of higher isotopes. The following composition can be given as an example [6, 7]:

Plutonium-239	58%
Plutonium-240	27%
Plutonium-241	12%
Plutonium-242	3%

Changes of such an isotopic composition of plutonium during its use in a reactor of the BN-600 type are given in table I. The same table presents the plutonium isotopic composition that can be obtained as a result of multiple fuel recirculation at make-up with plutonium formed in blankets of fast reactors.

Table I: Isotopic composition of fast breeders plutonium (%)

Maximum burn-up kg fis.prod./t	^{239}Pu	^{240}Pu	^{241}Pu	^{242}Pu
0	58	27	12	3
100	60.7	27.2	8.5	3.6
100*)	61	28	6	5

*) Equilibrium fuel

A complex composition of Pu with a great number of α-emitting and spontaneous fissioning nuclides influences the fuel cycle technology.

3. Accumulation of Fission Products and Activity of Discharged Fuel

Fast power reactors designed for wide use in nuclear power industry achieve a maximum burn-up of about 100 kg fiss.prod./t of fuel. It corresponds to the mean burn-up of ~80 kg fiss.prod./t of the discharged fuel.

Zirconium, molybdenum, cesium, cerium, neodym, praseodymium are the main components of solid fission products.

Gaseous fission products with high activity at short cooling times of a discharged fuel determine schemes and instrumentation for gas activity capture in the process of fuel reprocessing.

Table II gives calculated data for gaseous fission products and iodine activity after discharge from a breeder of the BN-600 type without storage at the reactor site (mean burn-up of about 80 kg fiss.prod./t, maximum burn-up of about 100 kg fiss. prod./t). Iodine, krypton and xenon yields are taken from [8], data for tritium are taken from [9]

Table II: Activity of gaseous fission products per 1 kg of fuel

cooling time (months)	Activity (curie)				
	^{131}I	^{129}I	^{85}Kr	^{133}Xe	T
0	4300	6×10^{-5}	32	11000	0.9
1	320	6×10^{-5}	32	210	0.9
3	1.8	6×10^{-5}	32	0.08	0.9
6	10^{-3}	6×10^{-5}	31	-	0.9
12	-	6×10^{-5}	30	-	0.9

Activity of solid fission products remaining in fuel after Kr, Xe, I and T removal are given in Table III. Fission product yields are taken from [8].

Table III: Activity of solid fission products per 1 kg of fuel

cooling time (months)	Activity		Main contributors to total activity
	Curie	Gram-equivalent Ra	
10 days	8.63×10^4	2.41×10^4	^{140}(Ba+La): 42%; ^{95}(Zr+Nb): 34%; ^{103}Ru: 7%;
1	5.25×10^4	1.29×10^4	^{95}(Zr+Nb): 57%; ^{140}(Ba+La): 27%; ^{103}Ru: 10%;
3	3.2×10^4	6.6×10^3	^{95}(Zr+Nb): 84%; ^{103}Ru: 7%;
6	1.65×10^4	2.58×10^3	^{95}(Zr+Nb): 76%; ^{134}Cs: 6%; ^{137}Cs: 4%;
12	7.5×10^3	7.13×10^2	^{95}(Zr+Nb): 51%; ^{134}Cs: 20%; ^{137}Cs: 13%; ^{144}(Ce+Pr): 10%; ^{106}(Ru+Rh): 6%.

The decay heat of radioactive fission products determined with the same initial data as above is shown in table IV for a fuel assembly of a BN-600 reactor (127 fuel rods of 6.9 mm diameter and 75 cm active length. The fuel assembly contains about 23 kg of dioxide).

Table IV: Residual heat release in a core fuel assembly of a BN-600 reactor

cooling time (months)	1	3	6	12
heat release (kw/assembly)	9	3.5	2.0	1.0

Fuel discharged from a fast breeder will have a neutron activity. The value of this activity depends on the initial composition of the fuel. When using plutonium with a significant amount of higher isotopes, part of the neutron activity of discharged fuel is caused by spontaneous fission and (α,n)-reaction in oxygen.

In this paper it is assumed that plutonium produced in thermal reactors and used for fast reactor fuel fabrication is free from such sources of neutron activity as ^{242}Cm and ^{244}Cm formed in a fast reactor during operation is a main source of neutron activity of discharged fuel.

The duration of fuel storage before loading into a fast reactor influences the rate of ^{242}Cm formation. This is caused by the fact that ^{241}Am is formed by β-decay of ^{241}Pu which is then transformed into ^{242}Cm by neutron capture in the reactor. Fuel storage results in accumulation of ^{241}Am and, therefore, causes an increase of neutron activity of the fuel being discharged.

Table V gives data on neutron activity of fuel discharged from a fast reactor (based on (α,n)-reaction and spontaneous fission of ^{242}Cm) under the assumption that accumulation of americium in the process of storage can be neglected. Contribution of other sources to neutron activity was not taken into account because it was insignificant according to preliminary evaluations.

Table V: Neutron activity of fuel discharged from a fast breeder

cooling time (months)	0	1	3	6	12
Activity neutrons x sec^{-1} x kg^{-1}	3.2×10^{6}	2.8×10^{6}	2.2×10^{6}	1.5×10^{6}	0.7×10^{6}

Note: the ^{241}Am concentration in initial fuel is zero.

When calculating the data for table V it has been assumed that fuel discharge from a reactor is carried out without exposure in an in-pile storage.

If it is assumed that reprocessed fuel has been stored for half a year and accumulated Am-241 **before loading it** into a breeder, the neutron activity increases by about a factor of 2.

Calculated results for fuel γ-activity, and, especially, for neutron activity, depend considerably on the accuracy of available fission product yields and of cross-sections for transplutonium isotope formation. The uncertainty of the γ-activity determination is unlikely to be lower than 30%; the uncertainty in the determination of the intensity of emitted neutrons is evaluated as being a factor 5 /10/. This fact stresses a necessity of serious work on nuclear data service provision for calculations in connection with nuclear fuel cycles.

4. Transportation of Spent Fuel from Fast Power Reactors

Exclusion of an in-pile storage and shortening of the cooling time of spent fuel complicate considerably the fuel handling of the reactor and the problem of fuel transportation from a nuclear power station to a chemical reprocessing plant. First of all, this is caused by considerable residual heat release of the spent fuel assemblies (see table IV).

Considering the fact that in more powerful reactors an increase of fuel assembly dimensions can be expected compared to an assembly of a BN-600 reactor, the residual heat removal will become a serious problem.

The aim should be to ensure heat release without forced cooling, i.e. to provide natural air circulation. For the transportation of spent fuel assemblies after short cooling times containers with sodium filling are considered /11/. The heat is removed by air through a ribbed container surface. In work /11/ the cooling system is studied with the account for an acceptable temperature on a fuel rod surface of about 700° C with maximum temperature of a container surface of 80° C.

Such a container should be designed for emergency situations during transportation. Particular attention should be paid to the presence of failed fuel elements, as in this case fission products escape into container coolant. The requirements for maximum fuel burn-up achievement made it necessary to allow for the fact that each fuel assembly extracted from a reactor may have damaged fuel rods. This should be taken into account when designing transportation containers and systems of fuel handling.

Shortening of the cooling time demands increase of shielding from γ-radiation.

The presence of neutron radiation is also important because special neutron shielding is needed.

5. Fuel Inherent Activity

The inherent fuel activity is the activity other than that due to fission products. When analyzing the inherent fuel activity it is assumed that the fuel in a cycle is in the form of a mixture of uranium and plutonium dioxides. It can also be considered that during the cooling period, the transportation and the production of a new fuel from a reprocessed fuel, γ-activity of uranium-237 accumulated in the fuel in the process of reactor operation decreases to a negligibly low level (for this ~2.5 months will be enough). In this case the following processes will cause fuel inherent activity:

i) Plutonium-241 α-decay and formation of uranium-237. This process causes the activity of about 0.17 curie/kg(UO_2 + PuO_2).

ii) Plutoniu-241 β-decay, formation of Am-241 with γ-activity accumulating with the rate of 3.9 curie/kg(UO_2 + PuO_2) per year.

The nature of inherent activity accumulation with time is shown in table VI.

Table VI: Accumulation of fuel inherent γ-activity

cooling time (months)	Activity per 1 kg			
	^{237}U		^{241}Am	
	curie	g.eq.Ra	curie	g.eq.Ra
1	0.17	0.14	0.38	8.10^{-3}
3	0.17	0.14	0.98	0.023
6	0.17	0.14	1.96	0.047
12	0.17	0.14	3.9	0.094

As it is seen from table VI, prolonged storage of reprocessed fuel results in accumulation of γ-activity in Am-241, that may require additional decontamination from this isotope.

Taking the time of fuel inherent activity accumulation equal to 3 months, one can evaluate the required coefficients of decontamination from fission fragments activity.

It can be seen from tables III and VI that for decontamination of spent plutonium fuel from γ-activity of fission products to the level of inherent activity it is necessary that the coefficients of decontamination at chemical reprocessing for different cooling times should be:

1 month	10^7
3-6 months	10^6

Neutron activity in plutonium fuel caused by spontaneous fission of plutonium and curium isotopes and (α,n)-reaction in oxygen reaches the value of 10^6 - 10^7 n/sec per 1 kg of UO_2 + PuO_2, depending on the amount of ^{241}Am in the fuel being loaded. The main contribution to neutron activity is made by curium, therefore its separation during chemical reprocessing is desirable. In this case only the ^{238}Pu neutron activity is left, its contribution being smaller than that of curium. The value of neutron activity connected with ^{238}Pu depends on the content of this isotope in the loaded fuel. The content of ^{238}Pu in plutonium produced in thermal reactors at high burn-ups is about 1% according to [12]. Using the data on specific activity from [6] a value of the neutron activity can be obtained under the condition of absence of curium in fuel.

This value is equal to about 5.10^4 n/sec per 1 kg of fuel.

6. Radiation Environment at Fuel Elements and Assemblies Fabrication of Reprocessed Fuel

Plutonium fuel inherent activity requires special measures for handling of this fuel.

When obtaining the above decontamination coefficients at the time of chemical reprocessing, the total value of dose rate from fuel elements for reprocessed fuel from a BN-600 reactor within one month storage after chemical reprocessing will be 0.3 mcrem/sec at a distance of 0.5 m from a fuel element, the maximum dose rate for a fuel assembly will be 10 mcrem/sec at the same distance.

Neutron activity of plutonium fuel affects the radiation conditions during handling of this fuel.

Separation of curium during chemical reprocessing will considerably decrease the neutron activity. There exists a principal difference in handling of the reprocessed fuel in case of deep decontamination of fuel from fission products and in treatment of fuel incompletely decontaminated from fission products, from the view point of radiation protection during fabrication of fuel elements and assemblies as well as during repair of the equipment.

In the case of deep decontamination of plutonium fuel from fission products, manual operations connected with adjustment or repairing of equipment, etc. can be allowed. Incompletely decontaminated fuel requires remote fabrication of fuel elements and assemblies.

7. Conclusion

One of the main problems of the development of fast power reactors is to optimize the economy of the external fuel cycle.

There exist many problems and alternative solutions in connection with the external fuel cycle:

- choice of a suitable technology for chemical reprocessing and fabrication of fuel;
- reprocessing of fuel at large nuclear power plants or at a centralized plant; in the latter case the main problem is the transportation of radioactive fuel;
- deep or incomplete decontamination of fuel;
- transportation of fuel with exposure in an in-pile storage or without it and some other problems.

Experience is now too insufficient to choose unambiguously an optimal scheme for the external fuel cycle. Such a scheme will, probably, be developed for the needs of modern nuclear power industry. At the same time, investigations of new approaches would create a basis for further progress in this field.

In the solution of all these problems an important part is the dynamics of the activity decrease and the irradiated fuel heat release at different stages of a fuel cycle. Despite the known uncertainties of initial data, the

information presented in the paper gives a possibility to evaluate the radiation situation at different stages of fuel reprocessing. Although more definite conclusions can be drawn only with the aid of economical studies, these estimations allow a number of important conclusions.

So, in spite of a relatively high "inherent" activity of the fuel, deep decontamination of the fuel from fission products allows a considerable decrease of activity thus reducing significantly the problems of fuel element fabrication.

The problems due to the growth of activity and heat release with shortening of the cooling time of discharged fuel from one year to some months are not too serious and enable a considerable shortening of the fuel handling time.

Experimental studies of isotopic compositions of nuclear fuel at the time of discharge and at all stages of the fuel cycle are of great practical importance.

Considerable attention should be paid to measurements and verification of nuclear data on actinides, of data on isotopic composition of fuel and its activity.

REFERENCES

1. Лейпунский А.И. и др. Пути эффективного использования горючего в атомной энергетике с быстрыми реакторами. "Атомная энергия", 31, вып. 4, 1970, с. 383.

2. Орлов В.В. Пути достижения малых времен удвоения для быстрых натриевых реакторов с окисным топливом. Доклад, представленный на настоящий Симпозиум, 1973.

3. Шевченко В.Б. и др. Доклад на IV Женевской конференции № 435.

4. Верятин У.Д. и др. Доклад на IV Женевской конференции № 448.

5. Денисов В.П. и др. Доклад на IV Женевской конференции № 49/р/693.

6. Nuclear Technology, Vol. 17 (3), 1973, p. 217.

7. Габескирия Б.Я. и др. Исследование накопления трансурановых элементов в горючем реактора ВК-50. "Атомная энергия", т. 34, вып. 3, 1973.

8. Грешилов А.А. и др. Продукты мгновенного деления урана-235, урана-238, плутония-239 в интервале 0 - 1 ч. Справочник Атомиздат, 1969.

9. Reactor and Fuel Technology, Vol. 12, No. 1, Winter, 1968 - 69.

10. Гриблер П. и др. Значение неопределенности ядерных данных для конструкции реакторов. Доклад С-26/102, Хельсинки, 1970.

11. Specialists' meeting on handling and transportation of spent fuel elements for LMFBR's, Rome, 26 - 28 April, 1972.

12. Nuclear Technology, Vol. 18 (1), 1973, p. 5.

Contributions to
Review Paper No. 5

FPND NEEDED FOR NON-DESTRUCTIVE BURNUP DETERMINATION

by K. Debertin, H. Ramthun
Physikalisch-Technische Bundesanstalt, Braunschweig, Germany

ABSTRACT:

There is a need of more accurate fission product nuclear data for the non-destructive burn-up determination by means of γ-ray spectrometry and post-irradiation calorimetry. Mean β-ray energies and γ-ray emission probabilities of medium- and long-lived fission products are primarily required.

The accuracy of non-destructive burn-up determination by means of γ-ray spectrometry depends on the quality of fission product nuclear data. Fission yields and decay constants of the relevant fission products are rather well known whereas absolute γ-ray emission probabilities (also called absolute intensities) of important burn-up monitors such as $^{106}Ru/^{106}Rh$ and $^{144}Ce/^{144}Pr$ have an uncertainty of 3% and more. This may be the dominant error contribution in the commonly practised methods of γ-ray spectrometric burn-up determination and, therefore, more accurate data are required.

The knowledge of the γ-ray emission probabilities is not needed, however, if the method described in reference [1] is used: Spectra of well calibrated standard sources of the single fission products are directly or indirectly compared with the fuel γ-ray spectrum. The calibration procedures for the standards are such that no detailed information on the decay scheme is necessary.

Another non-destructive burn-up determination method [2-4] is based on the calorimetric measurement of the decay heat due to β- and

γ-radiation of the fission products. The accuracy of the burn-up value deduced from the measured heat power mainly depends on the accuracy of

- nuclear data of the fission products (yields, half-lives, mean β-ray energies, branching ratios, conversion coefficients)
- effective absorption and fission cross sections
- the irradiation history
- γ-ray absorption calculations.

For cooling times greater than 30 **days** 95% of the heat power is produced by about 10-15 fission products. (^{89}Sr, ^{91}Y, ^{95}Zr, ^{95}Nb, ^{103}Ru, ^{106}Rh, ^{140}Ba, ^{140}La, ^{141}Ce, ^{144}Ce, ^{144}Pr,...). Mean β-ray energies are normally obtained from semi-empirical formulae with an an estimated accuracy of 1-2%. This procedure could, however, result in an additional systematic error of the burn-up value. Therefore, experimental measurements of the mean β-ray energies (desirable accuracy 1%) are required in order to check the validity of the formulae. As γ-rays are not totally absorbed in the calorimeter also branching and conversion ratios of the mentioned fission products have to be known.

References

/1/ K. Debertin, H. Ramthun,
Bericht FMRB 36/71, Physikalisch-Technische Bundesanstalt, April 1971

/2/ H. Ramthun, K. Debertin, Atomkernenergie 19, 17 (1972)

/3/ K. Debertin, H. Ramthun, Atomkernenergie 21, 119 (1973)

/4/ C. Devillers, G. Lhiaubet, M. Lott, N'Guyen van Dat, F. Dufreche, CEA Bulletin of Scientific and Technical Information 181, 41 (1973)

BURNUP DETERMINATION BY NEUTRON TRANSMISSION

H.G. Priesmeyer

Institut für Reine und Angewandte Kernphysik der Universität Kiel, Reaktorstation Geesthacht, Fed. Rep. of Germany.

Abstract:

A method for non-destructive determination of the residual heavy atom content of irradiated fuel is briefly described. Initial studies for ^{235}U are based on the neutron resonance absorption at 8.78, 11.67 and 12.4 eV. They indicate that this method is applicable to highly irradiated material because of the absence of strong fission product resonances at these energies.

Generally resolvable resonances in the total neutron cross section of a certain material make it possible to determine the amount of that material in the neutron beam, once the resonance parameters are known. One has to do a transmission experiment and to measure $T(E) = \exp(-n\sigma(E))$ in the resonance region. The resonance dips are more or less deep, depending on the resonance cross section, Doppler- and resolution broadening and the number of atoms per cm^2.

In our investigations, which were planned to find unknown resonance parameters in fission product isotopes, we used gross fission product samples and found, that big fission product resonances are very rare and that the remaining ^{235}U resonances were almost unaffected by fission products. So they could be used for ^{235}U content determination.

The method has the following advantages:

1. it gives an absolute measurement of the ^{235}U content;
2. it works even when highly radioactive samples are used;
3. it can be extended to ^{238}U, ^{239}Pu, ^{240}Pu and some fission product isotopes (^{152}Sm, ^{131}Xe).
4. it is principally nondestructive

We have until now tested the method on three samples:

HFR 101: a sample prepared by RCN Petten for their integral measurements, burned down to appr. 60%, originally enriched in ^{235}U to 90% (MTR fuel)

UO_2-Powder: not irradiated, enriched to 2.5 % in ^{235}U.

UO_2-Pellets: from the fuel elements of the KWO nuclear power station, original enrichment 2.8 %, burnup 18500 MWd/to U

The ^{235}U content of the first sample was measured with an accuracy of $\approx$ 4%, whereas for the second sample - fission product resonance influences being absent - the difference between our measurements and the figures given by the manufacturer is $\approx$ 1%.

For the first two samples the ^{235}U contents were known by other measurements. The results of the third sample are "self-consistent" in so far, that for several resonances analysed in ^{235}U and ^{239}Pu the contents differ by less than 4%. They will be counterchecked in the near future by chemical mass spectrometric analysis at Karlsruhe.

To conclude, it can until now be said, that the method will give results with an accuracy of less than 5 %.

THE IMPORTANCE OF FISSION PRODUCT NUCLEAR DATA IN BURNUP DETERMINATION

M. Robin*, R. Hageman**, J. Bouchard*, G. Frejaville*, R. Vidal*
Commissariat à l'Energie Atomique

* Centre d'Etudes Nucléaires de Fontenay-aux-Roses, Department of Reactor Physics and Applied Mathematics, Experimental Physics Section

** Centre d'Etudes Nucléaires de Saclay, Department of Research and Analysis

ABSTRACT

Measuring the content of ^{148}Nd is the most exact method of determining burn-up. A useful supplement to this method is the relative, but non-destructive, measurement of the contents of gamma-emitting nuclides resulting from fission.

A good knowledge of the fission yields is necessary to interpret the results of analysis of the ^{148}Nd content.

This paper gives results recently obtained in France for thermal neutron fission of ^{235}U and ^{239}Pu and for fast neutron fission of ^{235}U, ^{238}U, ^{239}Pu, ^{240}Pu and ^{241}Pu.

I. INTRODUCTION

An analysis of the fuel makes it possible to determine the number of fissions that have taken place in the fuel during irradiation. The energy released can then be deduced by adopting for each fission some appropriate figure, which takes into account the nature of the nuclide, the mean energy of the neutron spectrum, etc.

Determining the burn-up by measuring the number of atoms arising during fission is an attractive method and is widely employed.

Non-destructive methods, in particular gamma spectrometry, have the important advantage of simplicity, but measurement of the content of ^{148}Nd by mass spectrometry is still the most exact method of determining burn-up.

To interpret the analytical results, one needs a good knowledge - for thermal and fast neutron spectra - of the neodymium fission yields for all isotopes which give rise to fission in reactors.

In the case of the Oklo (Gabon) fossil reactor, the problem of determining the characteristics of an irradiated fuel material arises in an entirely new form.

II. NON-DESTRUCTIVE METHODS

II.1. Gamma spectrometry

By means of gamma spectrometry the activity of an isotope resulting from fission can be measured directly in the fuel. In principle the burn-up can then be deduced, at least in a relative sense.

The measuring techniques have been well developed, and with a suitable method of analysis it is possible to isolate the activity of a particular emitter in the spectrum. It is assumed, of course, that the fuel zone "seen" by the measuring instrument is precisely known.

The half-life of the fission product considered must be long enough for the entire irradiation to be taken into account. Some emitters which are subject to migration during irradiation are unsuitable for determining burn-up.

In obtaining a fission rate from the measured activity the following factors must be taken into account:

(a) Radioactive decay during and after irradiation;

(b) The law of transmission of radiation in the fuel;

(c) The detector efficiency;

(d) The branching coefficient near the gamma energy considered;

(e) The mean fission yield.

Gamma spectrometry is often used to compare the burn-ups of similar samples. A number of the above-mentioned points play the same role for all samples and do not therefore need to be taken into account.

Interpreting gamma-spectrometric measurements involves the use of the nuclear constants for the fission products and for the emitters resulting from them. The interpretation will therefore be improved by any refinement of these data, but a big additional effort in this direction does not seem essential.

Among the gamma-spectrometry results, more and more attention is being paid to the activity ratio ($^{134}Cs/^{137}Cs$), which indicates the fluence received, and hence the burn-up. The full interpretation of this quantity involves the capture cross-section of ^{133}Cs in the neutron spectrum existing in the fuel during irradiation. A better knowledge of the cross-section of ^{133}Cs in the thermal, epithermal and fast ranges is required.

II.2. Other techniques

In France, methods employing irradiation by neutron fluxes have not been developed for the determination of burn-up. These techniques are more suitable for checking fissile materials in new fuel elements or in waste.

Neutron emission from the fuel, due to spontaneous fission and (α,n) reactions, increases with burn-up, but the development of an accurate measuring technique based on these phenomena is quite difficult, largely owing to the presence of curium isotopes.

With a calorimeter it is possible to measure the power released by beta and gamma emitters. Results obtained in France with pins irradiated in fast neutron reactors are in good agreement with theory [1]. Calorimetry appears to be a promising non-destructive method for the measurement of total burn-up. This work has been described by Mr. Lott in Revue 15 of the Bologna Conference.

III. SIMULTANEOUS DETERMINATION OF BURN-UP BY MEASURING HEAVY-ISOTOPE CONTENT AND NEODYMIUM CONTENT

In connection with neutron-studies on reactors, considerable attention has been paid in France to the exact analysis of irradiated and non-irradiated fuels [2]. The interpretation of neutron measurements in critical experiments calls for a good knowledge of the composition of the uranium and uranium-plutonium standards employed. Using different physical methods (alpha spectrometry, oscillation, neutron-emission measurements) it has been possible to check the quality of the specimen preparation techniques and the analyses.

For measuring the composition of fuel samples the method of mass-spectrometry has been adopted, which gives the isotopic composition of each element with high precision. The concentrations of the different elements are obtained by double isotopic dilution. All concentrations are given in relative values, referred to one of them (generally ^{238}U).

In the case of irradiated fuel materials we can compare the compositions before and after irradiation, taking into account, by calculation, the slow disappearance of ^{238}U. We can then deduce the number of fissions that have taken place in the fuel.

The content of an isotope resulting from fission can also be measured on the same sample. In France preference has been given to mass 148 as opposed to mass 99 because of the good solubility of neodymium and because of the presence of molybdenum among the constituents of uranium-metal fuel elements.

The technique of double isotopic dilution developed for uranium-plutonium analysis has been used for measuring the content of neodymium-148.

Comparing the number of fissions deduced from the change in the content of heavy atoms and from the content of ^{148}Nd gives the fission yield.

This technique has been used to measure the ^{148}Nd fission yield from ^{235}U in (see Refs [4, 5]):

- The fuel of natural-uranium, graphite-moderated reactors;
- Fast-reactor fuel containing large proportions of ^{235}U;
- ^{235}U samples irradiated in fast-neutron spectra.

The values thus obtained are now being checked on new samples.

The coherence of the results imparts great confidence in the neodymium method used for determining burn-up in all types of fuel.

IV. NUCLEAR CONSTANTS USED FOR DETERMINING BURN-UP

IV.1. Measuring technique

The method used in France for the exact determination of burn-up is to measure the content of neodymium-148 by double isotopic dilution.

This technique has the disadvantage of being destructive and quite tricky to apply; hence it is costly.

However, it has many advantages:

- It gives a good mean value for the sample under study, whatever its nature and geometry;
- Neodymium-148 has well-known advantages as a burn-up indicator;
- The measuring technique, which is the same for all types of fuel, has been progressively improved and simplified;
- The additional cost caused by using the double isotopic dilution method is only a part of the total cost of destructive analysis (sectioning and dissolving of the sample).

The radiochemical method (measurement of the gamma-emitter of another fission product), which can be employed in laboratories not possessing a mass spectrometer, is less accurate. Apart from the disadvantages of radioactive decay and different fission yields, it is difficult to refer the measured activity to a precise mass of fuel. The present limitation of this

method does not seem to reside in the inadequate knowledge of the nuclear constants of the nuclides in question (^{137}Cs, ^{144}Ce, ^{95}Zr, etc.). However, it is quite clear that all basic work relating to these isotopes will be useful.

For measuring the content of neodymium-148, the sample used should be perfectly representative of the fuel zone being studied, and the sampling operation must be performed with the greatest care. The sample is completely dissolved, if necessary using special techniques (plutonium oxide, HTR pellets). The quantity of ^{148}Nd referred to the mass of uranium or plutonium is measured by double isotopic dilution using the same tracers as are used to determine fission yields (cf. section III).

In view of the care taken with the measurements, it is necessary to use precise fission-yield values for the absolute determination of burn-up.

IV.2. Fission yields for thermal neutron spectra

In the majority of thermal reactors most of the fissions come from ^{235}U. Numerous measurements have been performed, and there is a significant lack of agreement among the values published for the ^{148}Nd yield. The discrepancies are greater than the experimental measurement scatter, so that there is reason to suspect systematic errors; the causes of these have not yet been clarified. Further efforts must be made in this connection.

This further work should include intercomparisons among laboratories measuring the ^{148}Nd content of fuel samples, and new determinations of the fission yield.

The role of plutonium-239 increases with irradiation of the fuels considered. Only few measurements of ^{148}Nd fission yield have been made, since they are rather difficult to perform. Instead of determining y_{239} again, it would be more advisable to measure accurately the y_{239}/y_{235} ratio since this is the term involved in comparing widely differing burn-ups. The accuracy of this y_{239}/y_{235} ratio can be rendered almost independent of the accuracy for y_{235}. An experiment of this type is at present being conducted in France.

The remarks on ^{239}Pu apply also to ^{241}Pu, for which only few direct measurements of y_{241} have been carried out.

In thermal-reactor fuel the share of ^{238}U in the total number of fissions is far from negligible (4-8%). The term y_{238}/y_{235}, which differs greatly from unity, is significant in the determination of burn-up. The

published values differ widely from one another. The French programme of measurements in fast neutron spectra includes the determination of y_{238}.

A good knowledge of the ^{148}Nd fission yields from uranium-233 and thorium-232 is needed for the development of certain high-temperature reactor fuels. For high burn-ups it is necessary to take into account the disappearance of neodymium-148 as a result of neutron capture. The correction term is calculated on the basis of the most recent integral cross-section values used in neutron studies on irradiated fuel.

The ^{148}Nd yields at present used to determine the irradiation level of fuel unloaded from a thermal-neutron reactor are:

$$y_{235} = 1.65\%, \quad y_{239} = 1.66\%, \quad y_{241} = 1.87\%, \quad y_{238} = 2.30\%.$$

These values have given very coherent results in the systematic study of the composition of natural-uranium fuel irradiated in gas-graphite reactors [4].

IV.3. Fission yields for fast neutron spectra

Two sets of fission-yield values are at present in use, one of them valid for all types of thermal-neutron reactor (moderated with light water, graphite, heavy water....), the other valid for all-fast neutron spectra including fission spectra.

This distinction will certainly have to be refined for studying the fuel unloaded from large fast-neutron reactors, where the fissions will be produced by neutrons of several keV.

The well-known advantage of neodymium-148 as a fission-rate indicator for thermal-neutron spectra is that the fission yields for ^{235}U and ^{239}Pu are very close. The first experimental results obtained in France [5] show that although this may well be the case for ^{235}U and ^{239}Pu, it is not so for ^{238}U and ^{241}Pu, which make an important contribution to the fissions in the fuel of a reactor such as Phénix, which contains only a small amount of ^{235}U.

Nevertheless, neodymium is being retained as fission indicator because - apart from its numerous other advantages - the measuring techniques involved have been well developed and the results obtained are consistent with the body of the work carried out on irradiated fuels. In view of the low capture-reaction rates in fast-neutron spectra, it is not impossible that some day another neodymium isotope will be used instead of ^{148}Nd.

So far, only a few fission-yield measurements have been made for ^{235}U, ^{238}U and ^{239}Pu. These measurements should be repeated with a view to reducing the discrepancies between the values so far published.

In recycled fuels, heavily laden with higher plutonium isotopes, a considerable proportion of the fissions are due to ^{241}Pu, and the fissions in the even plutonium isotopes (^{238}Pu, ^{240}Pu, ^{242}Pu) and in americium (^{241}Am) cannot be ignored.

The above considerations justify the French programme of measurements described in section V.

V. THE PROGRAMME OF MEASUREMENTS NOW BEING CARRIED OUT

V.1. Thermal neutron spectra

Analyses are being performed on samples of ^{235}U-Al and ^{239}Pu-Al irradiated in the reflector of a thermal reactor. The number of fissions in ^{235}U is measured from the change in isotopic content of the uranium. In the case of ^{239}Pu, the method of isotopic dilution with natural uranium is used to measure the difference in the plutonium contents of two samples (one irradiated, the other not irradiated) which have been previously compared using a physical method (measurement of neutron emission).

In this way it is possible to measure ^{235}U and ^{239}Pu-fission yields with the same technique and the same tracer, which gives good accuracy for the y_{239}/y_{235} ratio used in comparing widely differing burn-ups.

The results obtained on the first experimental facility gave the following values for the ^{148}Nd yield from thermal fissions

^{235}U: $y(\%) = 1.68 \pm 0.03$ (2σ)

^{239}Pu: $y(\%) = 1.71 \pm 0.04$ (2σ)

A fresh irradiation to a higher integrated flux is now being carried out. The above values will thus be checked during the second half of 1974.

When this measurement programme has been completed, the results will be combined with those obtained in analysing other types of fuel with a view to adopting a new set of fission yields for determining burn-up from the content of ^{148}Nd.

V.2. Fast neutron spectra

In the course of studies carried out on fast-neutron reactors, virtually pure isotopes were irradiated with a view to measuring the cross-section ratios of heavy elements. With the results obtained it has been possible to improve the calculation formulae for fast reactors.

The ^{148}Nd fission yield of the isotopes studied can be deduced from the neodymium content.

Three irradiations of this type have already been performed. The methods of measurement and interpretation are given, together with results, in Refs [3-5].

Analyses on samples from a fourth experiment (TACO), which reached a burn-up of 6.5% in Rapsodie-Fortissimo, have been completed.

The tables below summarize the results obtained for the ^{148}Nd yield in fast-neutron fission of ^{235}U, ^{238}U, ^{239}Pu, ^{240}Pu and ^{241}Pu.

Table 1-1
Isotopic composition of fission neodymium

	$^{143}Nd/^{148}Nd$	$^{145}Nd/^{148}Nd$	$^{146}Nd/^{148}Nd$	$^{150}Nd/^{148}Nd$
^{235}U	3.37	2.24	1.74	0.420
^{238}U	2.16	1.79	1.62	0.610
^{239}Pu	2.62	1.80	1.49	0.602
^{240}Pu	2.48	1.72	1.45	0.607
^{241}Pu	2.39	1.70	1.43	0.631

Table 1-2

^{148}Nd yields

	$y \pm \Delta y (2\sigma)$
^{235}U	1.70 ± 0.03
^{238}U	2.30 ± 0.020
^{239}Pu	1.74 ± 0.05
^{240}Pu	2.00 ± 0.20
^{241}Pu	2.05 ± 0.10

The mass spectrometric measurements on these samples have been supplemented by radiochemical measurements, carried out by Mr. Blachot at Grenoble. On the basis of the first results it has been possible to measure the ^{133}Cs and ^{134}Cs fission yields, and the capture cross-section of ^{133}Cs. In the course of the present work the fission yields obtained for these highly irradiated samples will be grouped with those obtained in short-duration irradiations.

Samples of separated isotopes (heavy isotopes and fission products) irradiated in the same Rapsodie-Fortissimo assembly (TACO experiment) are at present being analysed by Dr. Koch of the Institute for transuranic elements at Karlsruhe. The ^{148}Nd fission yields will be compared with the values obtained on French samples. The figures thus obtained in two independent laboratories will be of great value.

With the start-up of the Phénix breeder reactor a new irradiation experiment will be begun on separated isotopes (the PROFIL experiment). The neutron spectrum is much softer than the Rapsodie spectrum and resembles that to be expected in future reactors. The pin contains 46 samples (^{235}U, ^{238}U, ^{238}Pu, ^{239}Pu, ^{240}Pu, ^{241}Pu, ^{242}Pu, ^{241}Am, Li, B, ^{95}Mo, ^{97}Mo, ^{101}Ru, ^{105}Pd, ^{133}Cs, ^{145}Nd, ^{149}Sm).

The purpose of this experiment is to compare the measured reaction rates with those predicted by the fast reactor calculation formula.

From the content of neodymium, measured for each heavy isotope sample, the fission yield of the neodymium isotopes will be determined. The results obtained will be extremely useful for measuring the burn-up of recycled plutonium, containing a very large amount of higher isotopes.

The mass spectrometry measurements will be supplemented by radiochemical measurements, which will give the distribution curve of the fission products as a function of atomic mass for each nuclide.

These experimental results are expected to be available during the first half of 1975.

The migration of fission products constitutes an important problem in the design of all types of power reactor (fast-neutron, high-temperature, light-water, etc.). The experimental programme at present being carried out in France will provide various constants characterizing the migration phenomena of fission products.

VI. THE OKLO FOSSIL REACTOR

In September 1972 the C.E.A. announced the discovery of a fossil nuclear reactor situated in the Oklo uranium deposit in Gabon.

The presence of uranium highly depleted in ^{235}U ($^{235}U/^{238}U < 0.5$) and of characteristic fission products (neodymium, samarium, xenon, krypton, etc.) provides evidence of nuclear reactions which took place almost 2000 million years ago.

This fossil reactor is clearly of great interest from the point of view of fundamental research. Definition of the reaction zones, and determination of the reactor's age and duration of operation, and of the conditions governing the initiation and control of the nuclear chain reaction are the most important problems to be solved here.

A significant point to be stressed in the case of the Oklo fossil reactor is that this is the first time that we have had available a fuel having already reacted very strongly and containing only stable elements corresponding to the ends of the fission chains.

The studies being carried out at present are concerned particularly with the chemical and isotopic analysis of uranium and fission products, which should yield data relating to the operation of the reactor: fluence, spectral index, fission number, conversion factor. The duration of the reaction can be determined from the isotopic composition of the elements produced by neutron capture on elements resulting from fission and having a half-life of the same order of magnitude as that estimated for the reactor.

In order to make use of the measurement results, fundamental data relating to fission yields and neutron capture cross-sections in the thermal and epithermal range are necessary. Such data are needed in particular for Nd, Sm, Tc, Ru, Kr, Xe, I, Cd and Pd. Confirmation of the values of these constants, or new measurements of the constants, are desirable in respect of these elements.

Conversely, once the operating conditions of the fossil reactor have been determined, reactor samples could be used to measure the fission yields of certain elements in this environment, whose particular advantage lies in the fact that it is inactive.

REFERENCES

[1] C. DEVILLERS, G. LHIAUBET, M. LOTT, N'GUYEN VAN DAT, F. DUFRECHE, Calorimetric measurement of the residual power in fuel elements from Rapsodie-Fortissimo (in French), Bulletin d'Informations Scientifiques et Techniques No. 181 (May 1973).

[2] Neutron study of plutonium in thermal neutron reactors (in French), Final Report of C.E.A.-EURATOM contract 002.64.9 TRUF "Recyclage du plutonium".

[3] J. BOUCHARD, J.Y. BARRE, R. BOYER, M. DARROUZET, G. FREJAVILLE, Measurement of integral cross sections of heavy isotopes by irradiation in fast neutron spectra. Conf. BNES - Chemical Nuclear Data - Canterbury (September 1971).

[4] M. ROBIN, J. BOUCHARD, M. DARROUZET, G. FREJAVILLE, M. LUCAS, F. PROST-MARECHAL, Determination of the 148-Nd in the fission of 235-U, 238-U and 239-Pu by thermal and fast neutrons. Conf. BNES Chemical Nuclear Data - Canterbury (September 1971).

[5] J. BOUCHARD, D. CHAVARDES, M. DARROUZET, J. GOURDON, M. ROBIN, Experimental study of burn-up in fast breeder reactors. Conf. ANS - New Developments in Reactor Physics and Shielding - Kiamesha Lake (September 1972).

Measurement of Burnup of Irradiated Fuel by Analysis of Gamma-Ray Spectra

Kanji TASAKA and Nobuo SASAMOTO

Japan Atomic Energy Research Institute
Tokai-mura, Naka-gun, Ibaraki-ken, JAPAN

ABSTRACT

The reliability of fission product nuclear data are examined through the burnup measurement of the irradiated fuel of JRR-4* by analysing the gamma-ray spectra of small samples which were cutted from the MTR-type fuel plate. The fuel assembly is irradiated for about 4 years in the core and the gamma-ray spectra are measured using a Ge(Li) detector after cooling for 522 days.

It is pointed out through the analysis that the improved data of the gamma-ray abundance of each FP nuclide are necessary to get better accuracy of a burnup measurement.

1. Measurement of Gamma-Ray Spectra

Three disk samples (5.3mm diam. x 1.3mm, U-Al Alloy) are made from the MTR type fuel plate, which has been irradiated for about 4 years in the core of JRR-4 reactor. The irradiation history is shown in Fig. 1. The reactor is operated usually 4 times a week, and the power averaged for a month is shown in the figure.

---

* Japan Research Reactor No.4 is a swimming pool type reactor which is constructed for shield research.

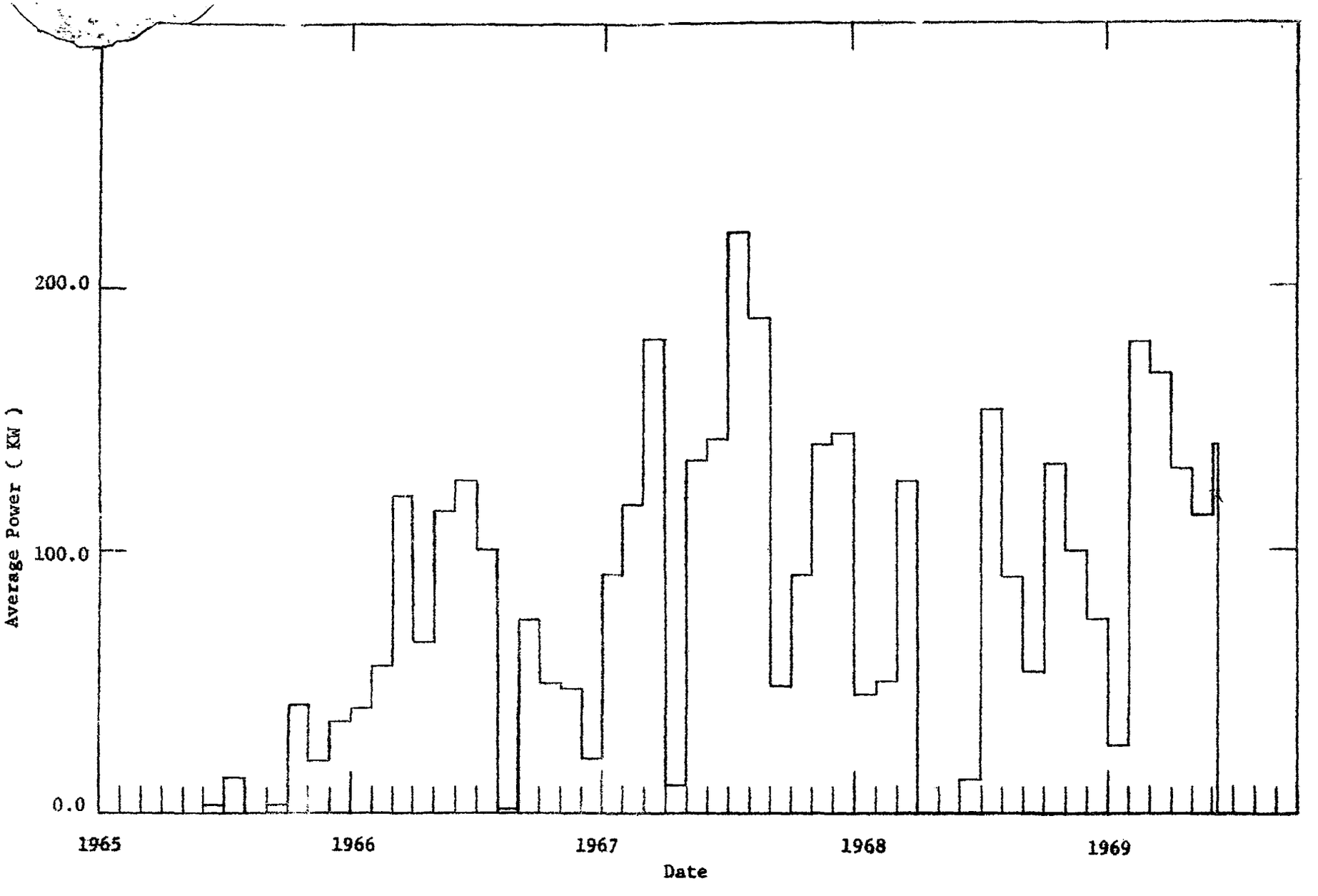

Fig. 1 Irradiation History of JRR-4 Reactor

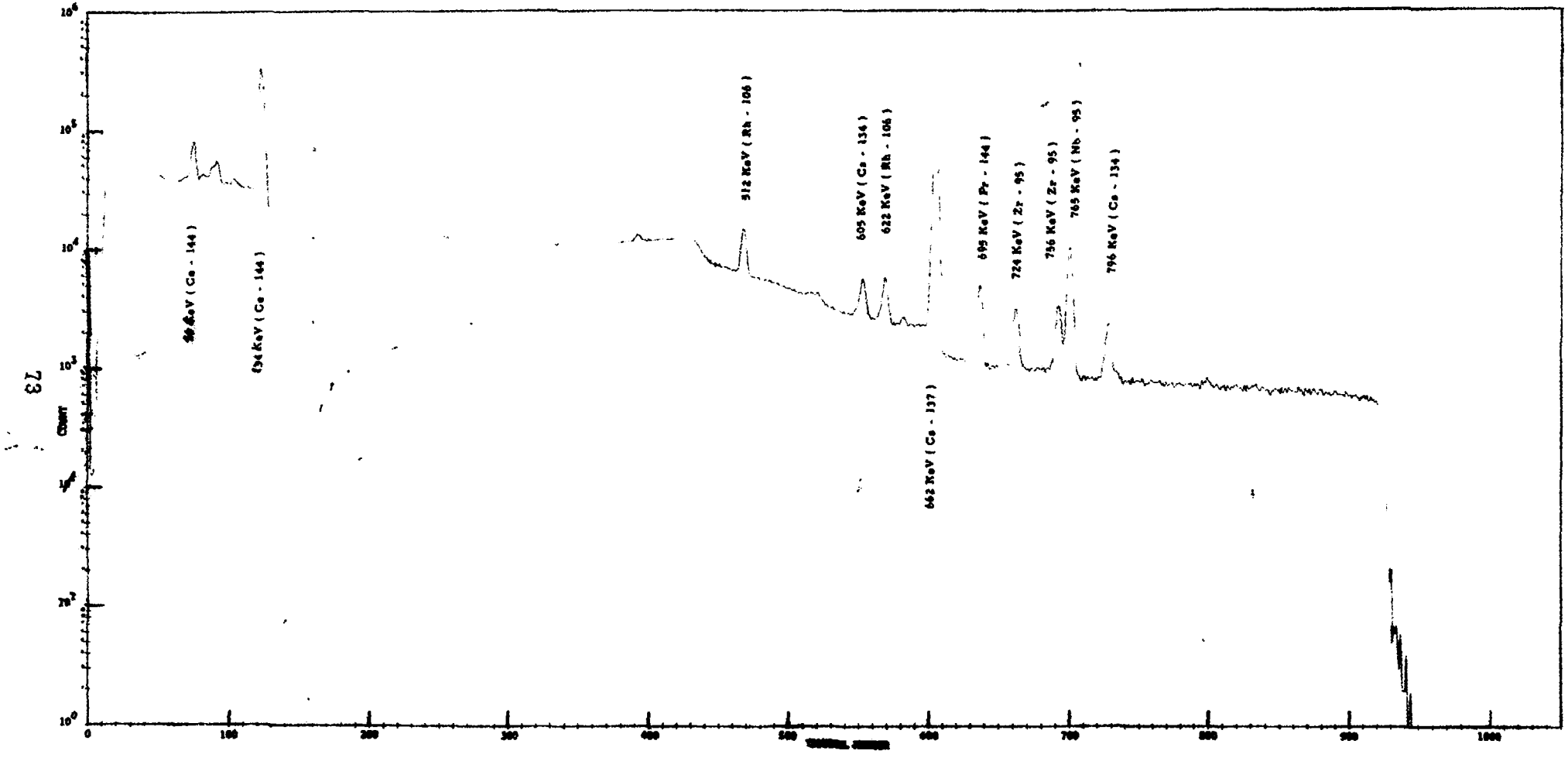

Fig. 2 Gamma-ray spectrum of the sample(002).

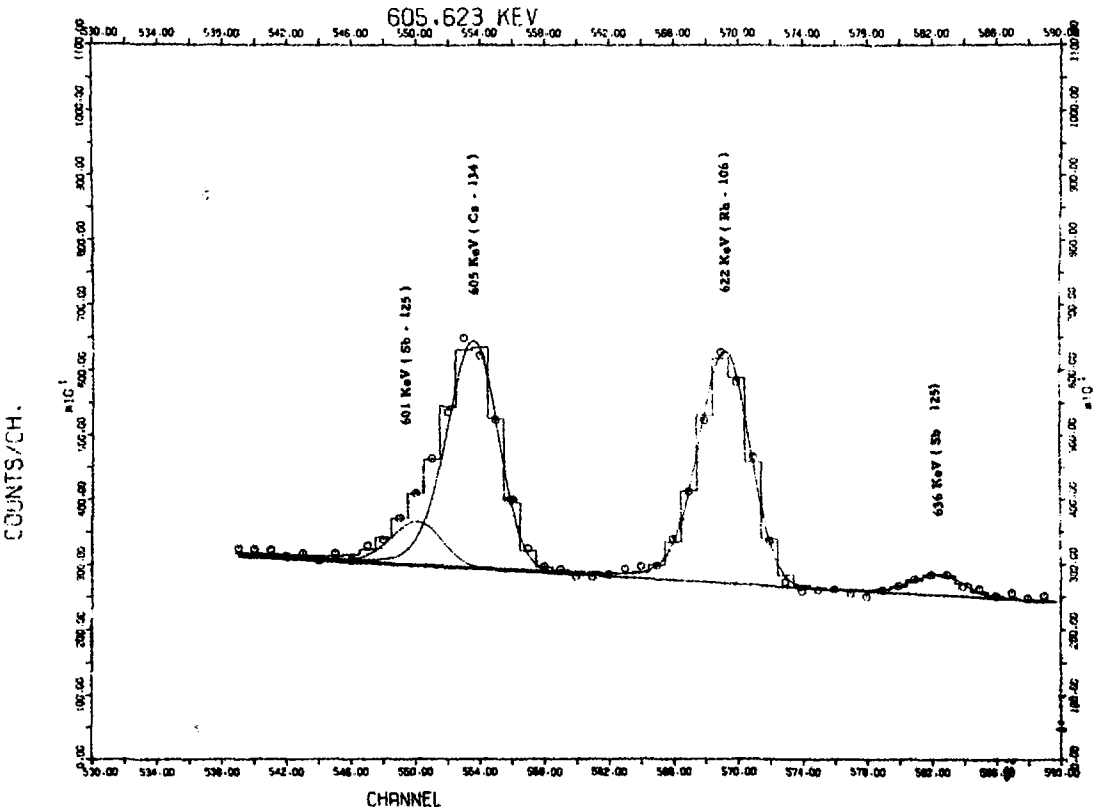

(a)

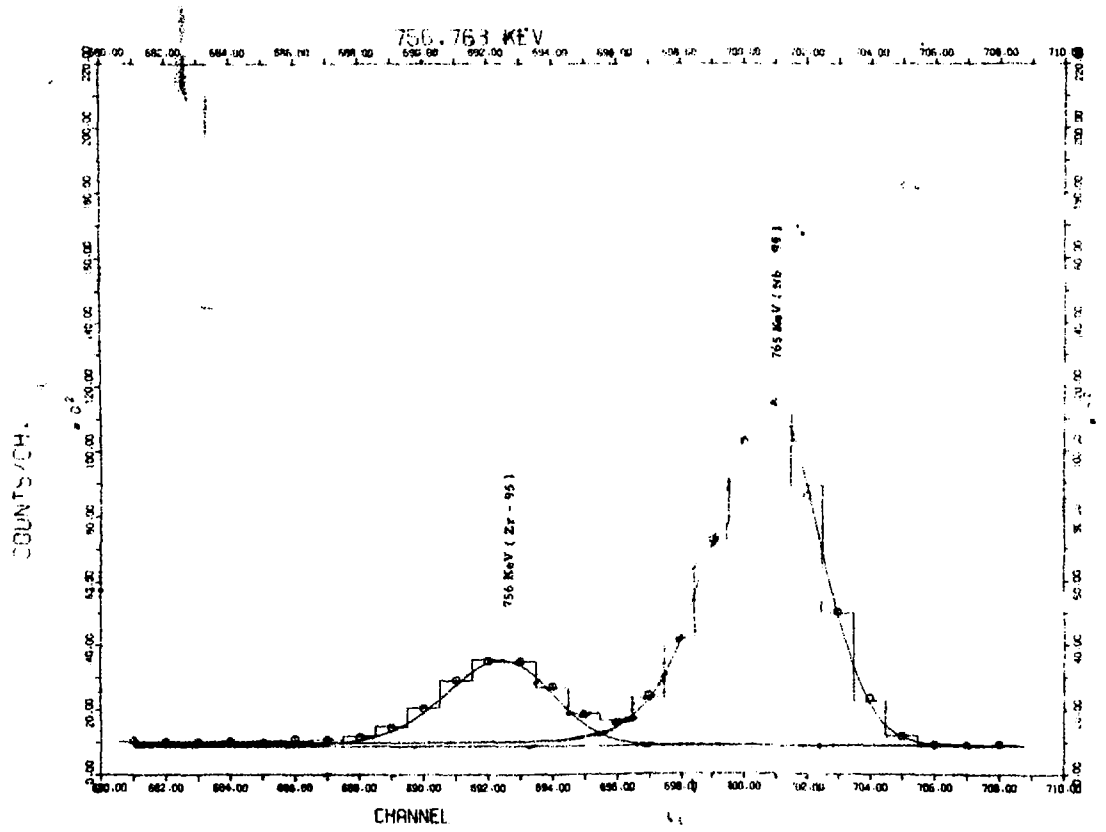

(b)

Fig. 3 Analysis of the gamma-ray spectrum by the standard spectrum method for four peaks (a) and double peaks (b) of the sample (003).

The gamma-ray spectra are measured after cooling for 522 days using a coaxial type Ge(Li) detector ($30cm^3$) and a 1024ch pulse height analyser. The energy resolution of the detector is estimated to be 4.1 keV of FWHM for 662 keV photons of ^{137}Cs. The distance between the detector and the sample is set to be about 1.5 m, and the measuring time of the spectrum is kept constant to be 10^4 sec. The obtained results of gamma-ray spectrum of the sample (002) is shown, for example, in Fig. 2.

It is seen in Fig. 2 that there are ten prominent photopeaks in the gamma-ray spectrum from 100 keV to 1 MeV. Two of them (605 keV and 796 keV) are photopeaks of ^{134}Cs which is made from ^{133}Cs through (n,γ) reaction, and the intensities of these two photopeaks depend on the neutron flux. Then the burnup of the fuel is determined in the present paper analysing the other eight photopeaks in the spectrum.

2. Analysis of Gamma-Ray Spectra

The gamma-ray spectra of the irradiated fuel are analysed by the standard spectrum method[1),(2)]. The part of the results are given, for example, in Fig. 3 for the four peaks and the double peaks of the sample (003). The experimental spectrum is shown by open circles and the fitted one by the staircase line and each peak component is displayed on the linear background continuum. The fitted spectrum is in good agreement with the experiment. The obtained photopeak areas are shown in Table 1.

When the i-th photopeak is emitted by the k-th FP nuclide, its atom number N^k_{mes} is obtained from the peak area S_i of the i-th photopeak as

$$N^k_{mes} = \frac{S_i}{t_m \epsilon_i f_i \lambda^k \psi_i^k} , \qquad (1)$$

Table 1 Peak area of each photopeak in the gamma-ray spectra of the three samples

Energy (keV)	Nuclide	Sample		
		(001)	(002)	(003)
80	^{144}Ce	61621±1462	157605±3630	169803±3860
134	^{144}Ce	434228±1680	1117790±4110	1218840±4070
512	^{106}Rh	14307± 250	35842± 498	39393± 494
605	^{134}Cs	1889± 125	11371± 385	13350± 369
622	^{106}Rh	4806± 137	12765± 286	13526± 242
662	^{137}Cs	143311± 624	357180±2155	398514±2370
695	^{144}Pr	6134± 143	15517± 199	17181± 246
724	^{95}Zr	3439± 110	8828± 223	9382± 137
756	^{95}Zr	3714± 110	9900± 207	10457± 211
765	^{95}Nb	14941± 179	39022± 332	42135± 341
796	^{134}Cs	1105± 52	6241± 211	7620± 272

where

t_m : measuring time ,

ε_i : detection efficiency ,

f_i : gamma-ray attenuation coefficient ,

λ^k : decay constant ,

ψ_i^k : abundance of gamma-ray .

The gamma-ray attenuation coefficient f_i has been calculated for each photopeak energy assuming the thickness of uranium, aluminum and acrylic resins to be 0.0295, 0.168 and 0.237 g/cm^2 respectively. The adopted data of the detection efficiency, the gamma-ray attenuation coefficient and the abundance of gamma-ray are listed for each photopeak in Table 2.

Table 2 Nuclear data for burnup analysis

Gamma Energy (keV)	Nuclide	Abundance $\Psi\gamma$	Gamma Ray Attenuation f	Detection Efficiency ε(x 10^{-5})
80	^{144}Ce	0.0154 [4]	0.9038	—
134	^{144}Ce	0.11 [5]	0.8936	1.105
512	^{106}Rh	0.21 [6]	0.9626	0.182
605	^{134}Cs	0.980[7]	0.9654	0.147
622	^{106}Rh	0.11[6],[8]	0.9659	0.146
662	^{137}Cs	0.851[9]	0.9668	0.132
695	^{144}Pr	0.015[10]	0.9678	0.124
724	^{95}Zr	0.49 [5]	0.9680	0.121
756	^{95}Zr	0.49 [5]	0.9688	0.114
765	^{95}Nb	1.00 [5]	0.9690	0.112
796	^{134}Cs	0.878[7]	0.9696	0.107

Atom number of each FP nuclide is calculated for the cooling time of 522 days after the irradiation for 4 years following the operation history of JRR-4 reactor by the program "FP-S"[3], which calculate atom number of each FP nuclide for arbitrary irradiation history and cooling time by using Bateman's formula and its integral from

repeatedly. The results are shown in Table 3 as the ratio $(N^k/F)_{cal}$ between the atom number of each FP nuclide and the heat generated by fission. The nuclear data used for the calculation are also shown in the table. Then the burnup of the fuel is obtained to be

$$F_{mes} = N^k_{mes} \Big/ \left(\frac{N^k}{F}\right)_{cal} \quad . \tag{2}$$

Table 3 Calculated ratio between atom number and burnup.

Nuclide	Half Life	Decay Const. (1/sec)	Cumulative Yield (%)	(N/F)cal. (atom/W.sec)
^{95}Zr	65 d	1.234×10^{-7}	6.1823	5.263×10^{5}
^{95}Nb	35 d	2.292×10^{-7}	6.3917	6.119×10^{5}
^{106}Ru	367 d	2.186×10^{-8}	0.3979	1.732×10^{7}
^{106}Rh	30 s	2.311×10^{-2}	0.3979	1.647×10^{2}
^{137}Cs	30 y	7.327×10^{-10}	6.1822	1.824×10^{9}
^{144}Ce	284 d	2.825×10^{-8}	5.3845	1.460×10^{8}
^{144}Pr	17.3m	6.678×10^{-4}	5.3845	6.120×10^{3}

The obtained results of burnup of the three samples are shown in Table 4. These results are strongly dependent on the nuclear data in Table 2 and 3. Among them the abundance of gamma-ray is most inaccurate and there are large differences among the experimental data. The present results of burnup measurements changes considerably from peak to peak, which is also considered to result mainly from the inaccuracy of the abundance of each photopeak (cf. Table 4). The values of abundances in Table 5 are recommended in the present paper to make the present results of the burnup

Table 4 Results of burnup measurements

Gamma Ray Energy (keV)	Nuclide	Abundance	Sample		
			(001) (%BU)	(002) (%BU)	(003) (%BU)
134	^{144}Ce	0.11	2.24	5.78	6.31
512	^{106}Rh	0.21	2.37	5.94	6.41
622	^{106}Rh	0.11	1.89	4.99	5.29
662	^{137}Cs	0.851	2.28	5.69	6.34
695	^{144}Pr	0.015	1.92	4.87	5.39
724	^{95}Zr	0.49	2.14	5.50	5.84
756	^{95}Zr	0.49	2.44	6.50	6.88
765	^{95}Nb	1.00	2.28	5.94	6.42

Table 5 Results of burnup measurements by using the recommended abundance of each photopeak.

Gamma Ray Energy (keV)	Nuclide	Recommended Abundance	Sample		
			(001) (%BU)	(002) (%BU)	(003) (%BU)
134	^{144}Ce	0.11	2.24	5.78	6.31
512	^{106}Rh	0.21	2.37	5.94	6.41
622	^{106}Rh	0.092	2.27	5.98	6.36
662	^{137}Cs	0.851	2.28	5.69	6.34
695	^{144}Pr	0.0127	2.27	5.74	6.37
724	^{95}Zr	0.45	2.33	5.98	6.37
756	^{95}Zr	0.53	2.27	6.01	6.36
765	^{95}Nb	1.0	2.28	5.94	6.42

measurement consistent from peak to peak. The results of the burnup measurement by using these abundances are also shown in Table 5. They are considerably in good agreement for every peaks. The maximum deviation of the results amount to 4%, 6% and 1% for the sample (001), (002) and (003) respectively by assuming that the results from the 662 keV photopeak of ^{137}Cs is correct.

3. Discussions

The recommended abundance 0.092 for the 622 keV gamma-ray of ^{106}Rh is approximately equal to the value by Ambiye and Sharma[11] who proposes the abundance ratio ψ (622 keV) / ψ (511 keV) of 0.44 which corresponds to the abundance ψ (622 keV) of 0.093 because ψ (511 keV) is equal to 0.21[6]. Others propose the abundance ratio ψ (622 keV) / ψ (511 keV) of 0.52[12] or 0.53[8], [13], but the data by Ambiye and Sharma is the latest one among them and considered to be most reliable. The present results of burnup measurements also support the value by Ambiye and Sharma.

The recommended abundance 0.0127 for the 696 keV gamma-ray of ^{144}Pr is smaller than 0.015 or 0.016 by Porter and Day[10] and by Graham et al.[14] respectively. The decay constant and the cumulative fission yield of ^{144}Ce are considered to be fairly accurate because the burnup of the sample is accurately determined from the 134 keV photopeak of ^{144}Ce. Then it is natural to consider that the existing value of the abundance of the 696 keV gamma-ray of ^{144}Pr is too large.

The recommended abundances 0.45 and 0.53 respectively for the 724 keV and 756 keV gamma-rays of ^{95}Zr are close to the values of Mittelman[15] who proposes the abundances of 0.43 and 0.54 for the 724 keV and 756 keV gamma-rays respectively through the analysis of the beta-ray spectrum measured by using a magnetic spectrometer. Drabkin et al.[16] proposed the abundances of 0.55 and 0.43 for 724 keV and

756 keV gamma-rays respectively from the spectrum analysis of beta-rays. The present recommended values fall between the results of these two measurements.

The nuclear data of the decay constant, fission yield and gamma-ray abundances of each fission product nuclide, and also the gamma-ray absorption coefficients of fuel and structual materials are necessary for a burnup measurement by the gamma-ray spectrum analysis. Among these nuclear data the gamma-ray abundances are most inaccurate for the long life FP nuclides such as ^{95}Zr-^{95}Nb, ^{106}Ru-^{106}Rh, ^{137}Cs, ^{144}Ce-^{144}Pr etc. which are useful for a burnup measurement. Then it is necessary to improve the data of the gamma-ray abundance for the above mentioned nuclides to get better accuracy of a burnup measurement by the gamma-ray spectrum analysis. It is also important to determine practically the most probable values of these nuclear data through the analysis of the gamma-ray spectrum of fission products of the irradiated fuel.

References

1. K. Tasaka, Method of Standard Spectrum Fitting for the Analysis of Gamma-Ray Spectra from Semiconductor Detectors, J. Nucl. Sci. Technol. 9(7), p.430-432 (1972).

2. K. Tasaka, Standard Spectrum Method for the Analysis of Gamma-Ray Spectra from Semiconductor Detectors, Nucl. Instr. and Meth. 109 (3), p.547-556 (1973).

3. K. Tasaka, N. Sasamoto, FP-S: Program for Calculation of Atom Number for Each Fission Product Nuclide, JAERI-1198 (1971).

4. M.A. Wakat, Catalogue of γ -Rays emitted by Radionuclides, Nuclear Data Tables 8, p.445-666 (1971).

5. C.M. Lederer, et al., Tables of Isotopes Sixth Edition, John Wiley & Sons, (1968).

6. B. Kahn, W.S. Lyon, Phys. Rev. 92, p.902 (1953).

7. D.E. Raeside, et al., Nuclear Physics A93, p.54 (1967).

8. O.J. Segaert, et al., Nuclear Physics 16, p.138 (1960).

9. H.H. Hansen, et al., Z.F. Physik 218, p.25 (1969).

10. F.T. Porter, P.P. Day, Phys. Rev. 114, p.1286 (1959).

11. S.Y. Ambiye, R.P. Sharma, Nucl. Phys. 29, p.657 (1962).

12. R.L. Robinson, et al., Phys. Rev. 119, p.1692 (1960).

13. E.P. Grigor'ev, et al., Bull. Acad. Sci. USSR, Phys. Ser. 22, p.191 (1958).

14. R.L. Graham, et al., Can. J. Phys. 36, p.1084 (1958).

15. P.S. Mittelman, Phys. Rev. 94, p.99 (1954).

16. G.M. Drabkin, et al., Izv. Akad. Nauk SSSR, Ser. Fiz. 19, p.324 (1955).

Problems Encountered in Burnup Determination of Oxide Fuel Specimens with a High Rod Power

H. Wertenbach

Institut für Radiochemie - Projekt Schneller Brüter

Kernforschungszentrum Karlsruhe

Abstract

This work is an indication of the restriction with respect to the accuracy of burnup analysis through migration of the fission products and the heavy atoms and of errors produced in the conversion of atom percent of burnup into MWd/tonne.

It is not considered necessary to achieve errors lower than 1 - 2 % for the fission yields of U-235 and Pu-239 and of 2 - 3 % for Pu-241 both in the thermal and in the fast spectra.

1. Introduction

A method always applicable in the determination of burnup is the fission product monitor-heavy atom technique. Besides the determination of the concentration of the fission product monitor and of the heavy atoms with an accuracy of 0.25 relative percent [1], the fission yield of the monitor is required to compute the burnup.

The thermal fission yields for U-235 and Pu-239 are presently associated with an error of 1 - 2 %. Therefore, the accuracy of the burnup analysis is limited essentially by the errors of the fission yield determination. Consequently, attempts are being made to increase the accuracy of fission yields, above all that of fast fission yields [1].

This work aims at indicating additional factors upon the accuracy of the burnup analysis.

2. Migration of the Fission Products and of Heavy Atoms

It is known that besides the fission products Cs, Ba, etc. also uranium and plutonium undergo migration during irradiation. A uniform, annular enrichment of plutonium in the columnar crystal zone at the edge of the central channel of irradiated UO_2, PuO_2 fuel rods has been regularly observed. In addition to this normal uranium-plutonium demixing process transports have been observed with the capsule test group FR 2-4a studied at the Karlsruhe Nuclear Research Center, which become effective over larger distance in the axial direction within the outer fuel zone and at the edge of the fuel [2] [3].

During irradiation of the capsule test group FR 2-4a in the thermal neutron flux power peaks occurred at the extremities of the rod. This produced a temperature gradient in the axial direction which was linked to a material transport. Broadening of the central channel at the extremities and narrowing in the center of the rods has been observed with many specimens [2].

The radial and axial uranium-plutonium-demixing process was detected by α-autoradiography and measurement with microprobes. Burnup determinations were also performed with the specimens of the FR2 capsule test group 4a. Sections of 8 - 13 mm length were cut from the

central part of the 80 mm long fuel column. Upon dissolution of the specimens the concentrations of Ce-144, Nd-148 and of the heavy atoms were measured as described in KFK 1704 [4].

The results are summarized in Table 1.

For all specimens good agreement becomes evident between the burnup values found via Ce-144 and Nd-148. By contrast, 2 burnup values derived by computation from plutonium depletion deviate considerably.

Considering the isotope composition of plutonium and taking the Pu-242 fraction as a measure of the fluence, specimen 21 should have the highest and specimen 25 the lowest burnup, while the specimens 20 and 27 should be approximately identical.

Table 1. Burnup Determination with Specimens of the FR2 Capsule Test Group 4a

Specimens No.	20	21	25	27
Atoms Pu/atom U	0.0660	0.0560	0.0682	0.0700
Atoms Pu-242/atom Pu	0.0575	0.0726	0.0536	0.0588
Burnup /at.%/ via				
Ce-144	9.76	9.38	9.77	10.31
Nd-148	9.67	9.68	9.64	10.14
Pu-depletion	9.66	10.50	9.48	9.33

There is no doubt that the burnup values have been falsified by migration of the fuel.

In these specimens the rod power was very high. It amounted to about 650 W/cm.

Contrary to the heavy nuclei fission neodymium itself does not seem to migrate in the oxide fuel. Although measurements with the microprobe performed at specimens from the irradiation Mol 7A [5] showed that Nd had accumulated radially by about 12 % at the central channel, plutonium was found to accumulate by some 28 % in the same direction.

Since the fission cross-section of plutonium-239 is higher than that of U-235 -most of the fissions in this irradiation took place at a neutron energy of 10 eV- the higher concentration of Nd in the vicinity of the central channel can be explained by the higher fission rate of plutonium

As a matter of fact, an axial differentiation of plutonium was observed also for these specimens. A 2 % difference was measured with the microprobe between the rod center and the rod extremities [5]. The rod power was 500 W/cm and the maximum value was 560 W/cm.

Results of burnup are also available for specimens examined in the capsule test group 4b [3]. For 8 specimens the burnup was determined via Ce-144, Nd-148 and the depletion in plutonium. The Nd-146/Nd-145 ratio was taken as a measure of the neutron fluence. It was estimated that the errors of the burnup do not exceed 5 percent [6]. The error introduced in the burnup determination with undisturbed specimens is estimated to be $\pm$ 2.5 % [4].

Some results obtained from the FR2 capsule test group 4b will be discussed now.

Three specimens each were taken from some rods of the capsule test rig 49 of this group and subjected to burnup analysis. The results are summarized in Table 2.

It appears from the burnup values that in case of specimen 4 B11-6 there is a considerable difference between the burnup values derived from plutonium depletion and from the fission products. On account of the Nd-146/Nd-145 ratio and due to the position of this specimen in the reactor (between the specimens 4 B11-3 and 4 B12-3) the burnup values obtained via the fission products should be higher by 10 % while the burnup value derived from the depletion in plutonium should be lower by the same amount. This falsification could be easily explained by the assumption that uranium has condensed at the point of the burnup specimen. Also in these specimens the rod power was about 500 W/cm.

Table 2. Burnup Determination at the Capsule Test Rig 49 of the Test Group 4b

Rod No. / Specimen No.	4B10-3	4B10-5	4B10-6	4B12-3
Nd-146/Nd-145	0.9336	0.9430	0.9426	0.9290
Burnup /at.%/ via				
Ce-144	13.16	12.29	13.15	12.60
Nd-148	13.54	13.16	13.58	12.54
Pu-depletion	13.61	13.92	13.95	13.27
Rod No. / Specimen No.	4B11-3	4B11-5	4B11-6	
Nd-146/Nd-145	0.9116	0.9143	0.9148	
Burnup /at.%/ via				
Ce-144	12.34	12.61	11.32	
Nd-148	11.96	12.30	11.26	
Pu-depletion	12.74	12.88	(14.32)	

3. Conversion of Burnup Values from Atom Percent into Megawatt-days/Tonne

Quite often contractors request that the results are converted from atom percent into megawatt-day per metric ton. The conversion factors are available in the literature, both in individual contributions and in compilations.

As an example, the ASTM-Yearbook, Part 30 (1967) Procedure E 244 and E 219-63 T, respectively, indicates that 1 at.% of burnup = $0.7 \pm 0.3 \times b^3$ MWd/tonne while in the ASTM-Yearbook, Part 30 (1970) Procedure E 244-69 1 at.% of burnup is set $9.6 \pm 0.3 \times 10^3$ MWd/tonne.

In 1969 [7] and in 1971 [8] M.F. James compiled and discussed values for the usable energy released in the fission of a number of heavy nuclei. The values recommended by him for the total effective energy per fission of U-235, -238 and Pu-239, -241 are indicated in Table 3 together with the associated errors.

Table 3. Total Effective Energy per Fission

Nuclide	Spectrum	MeV/Fission
U-235	thermal	201,7 ± 0,6
U-238	fission spectrum	205,0 ± 0,9
Pu-239	thermal	210,0 ± 0,9
Pu-241	thermal	212,4 ± 1,0

Based on these values we calculated the conversion factors at.% - MWd/tonne to be 9.50×10^3 for U-235, 9.62×10^3 for U-238, and 9.80×10^3 for Pu-239, the error being approximately ± 3 % [4].

The errors introduced in the conversion factors can be considerably enhanced in the irradiation of highly enriched test elements in small reactors. So, values ranging from 194.4 to 199.6 were found in EBR II instead od 203 MeV/fission and for highly enriched uranium even 190 - 192 MeV/fission [9].

If in the fission yields errors not higher than 1 % are strived for, the usable energy release from the principal fission nuclides should have to be known with approximately the same uncertainty.

4. Conclusions

The statements in Chapters 2 and 3 lead to the conclusion that frequently the accuracy of the burnup analysis -above all for ceramic mixed fuel with a high rating- is not predominantly determined by the error in the fission yields. The migration of fission products and heavy atoms may rather give rise to major errors unless a complete rod is available for analysis. The accuracy is further reduced by the errors contained in the conversion factors. Although fission yields with an error of only ± 1 % are desirable for the fission of U-235 and Pu-239 with fast and thermal neutrons, they might not necessarily be required. Errors of 1 - 2 % for U-235 and Pu-239 and of 2 - 3 % for Pu-241 undergoing thermal and fast fissions could represent adequate values.

Literature

1) W.J. Maeck, R.P. Larsen, J.E. Rein
Burnup Determination for Fast Reactor Fuels
TID - 26209, 4 (1973)

2) W. Dienst, O. Götzmann, H. Kleykamp, G. Ondracek, B. Schulz, H. Zimmermann
Auswertung der Untersuchungsergebnisse an den bestrahlten UO_2-PuO_2-Brennstäben der Versuchsgruppe FR2 - 4a
KFK 1727 (1973)

3) D. Freund
Auslegung, Bestrahlung und Nachuntersuchung der Oxidbrennstabproben im FR2

4) H. Hoffmann, H. Wertenbach
Abbrandbestimmung an den Kernbrennstoffprüflingen aus dem FR2
KFK 1704 (1973)

5) W. Dienst, K. Ehrlich, O. Götzmann, H. Hoffmann, H. Kleykamp, L. Schäfer, B. Schulz, H. Zimmermann
UO_2-PuO_2-Brennstabbündel-Bestrahlung Mol 7A
Auswertung der Untersuchungsergebnisse an den bestrahlten Brennstäben
KFK 1736 (1973)

6) H. Wertenbach, E. Bolz, E. Gantner, K. Matern
Abbrandbestimmung an Proben der FR2-Kapselversuchsgruppe 4b und an Kriechproben
2. Vierteljahresbericht des Projektes Schneller Brüter
KFK 1273/2 EUR 4970 d 115-1 (Sept. 1973)

7) M.F. James. Journal of Nuclear Energy
Vol. 23517-536 (1969)

8) M.F. James. Journal of Nuclear Energy
Vol. 25513-523 (1971)

9) L.B. Miller, A. Gopalakrishnan
Transactions of the American Nuclear Society, 1972 Annual Meeting,
Vol. 15 No. 1, 487-488

Annex

Significant Data on the Specimens Dealt with in this Work [3) 5)]

Specimens	Capsule Test Group 4a	4b	Mol 7A
Fuel	UO_2-PuO_2		UO_2-PuO_2
Composition			
U/Pu /wt.%/	85/15 -	85/20	80/20
Uranium enrichment /wt.%/	0.7		79
Composition of plutonium 239/240 241/242 /wt.%/	90.9/8.21/0.85/0.04		91/8.2/0.74/0.04
Density /% of TD/	84	89	88.4
O/M ratio	1.98		1.98
Length of fuel column /mm/	80		5.00
Diameter of fuel column /mm/	6.25	5.12	5.01
Irradiation	thermal		epithermal (Cd-shielding)
Reactor	FR2		BR2
Burnup /MWd/kg/	85	80	45 max.
Rod power /W/cm/	650	500	560 max.

The Influence of Fission Product Nuclear Data Uncertainties: On a Method of Plutonium Determination from the Burn-up Data in Irradiated Nuclear Fuel

L. Schächter, D. Hacman, O. Mot
Institute of Atomic Physics
Bucharest - ROMANIA

Abstract

A method, regarding the possibility to determine the Plutonium contents in an irradiated nuclear fuel by using the burn-up measuring data is presented.

The method has been applied to fuel irradiated in the Bucharest VVR-S reactor at 10% burn-up after 600 days of cooling time. The Plutonium determination is quoted to be in error by 7%. A study of the influence of the uncertainty, introduced by the FPND, on the final results is carried on.

It was found that a half-life error of 1.5% contributed 1.8% uncertainty to the final results.

A Description of the Method

Starting from a well-known initial number of U^{235} nuclei, the method tries to determine the (U^{235}, Pu^{239}) fissile material concentration in a plutonigen fuel sample, by employing the method of burn-up determination by means of the (1,2,3,4,5) gamma spectrometry.

In order to determine the separate burn-up of U^{235} and Pu^{239}, the fuel sample was measured after an adequate cooling time

and two fission products were chosen, namely Cs^{137} and Ru^{106} and one of them exhibits different fission yields for U^{235} and Pu^{239} (Ru^{106}).

In order to obtain the real number of nuclei of the measured fission products, corrections concerning the irradiation history as well as the selfshielding correction was applied.

When the fuel boundles having the elements displayed in a certain configuration have been determined, a geometric intrinsic factor characterizing the measuring data has been determined.

Figure 1 shows the influence of this factor, which takes into account the reciprocal influence of the fuel rods forming the bundle unit in case of an axial burn-up distribution.

Knowing the number of nuclei of Cs^{137} and Ru^{106}, the number of fissions of U^{235} and Pu^{239} was determined by solving the following system of equations:

$$\begin{aligned} N_{Cs^{137}} &= Y^{5}_{Cs^{137}} F^{5} + Y^{9}_{Cs^{137}} F^{9} \\ N_{Ru^{106}} &= Y^{5}_{Ru^{106}} F^{5} + Y^{9}_{Ru^{106}} F^{9} \end{aligned} \qquad (1)$$

where:

Y^5 .... is the fission yields in U^{235}

Y^9 .... is the fission yields in Pu^{239}

F^5 .... is the number of fissions in U^{235}

F^9 .... is the number of fissions in Pu^{239}

Knowing the initial number of U^{235} fissile nuclei and the number of fissions in U^{235}, F^5, from equation (1), the

number of U^{235} fissile nuclei extant in the fuel after irradiation was determined (N_u^f).

The residual number of Pu^{239} nuclei in the fuel was determined by a measurement of Ba^{140}- La^{140} resulting from a new short exposure in a neutron flux. This new irradiation had to be sufficiently short not to change the content of fissile material and had to be performed after the Ba^{140}-La^{140} produced in the original irradiation had decayed to an unmeasurable amount.

The Ba^{140}- La^{140} pair has been chosen according to the following criteria:

- The Ba^{140}- La^{140} fission yield (Y_{Ba}) is 6.44% for U^{235} and 5.7% for Pu^{239} thermal fission.
- The half-life of Ba^{140} ($T_{1/2}Ba$) is 12.8 days, which requires an irradiation of one day or less in order to avoid corrections for decay during irradiation.
- Its direct descendant, La^{140}, has a half-life of 40 hours and a negligible independent fission yield.

After about 12 days of irradiation the exponential decay of La^{140} follows the half-life of Ba^{140}. La^{140} emits a 1.6 MeV gamma-ray with an absolute intensity of 96%, which appears as sufficiently isolated and marked peak in a gamma spectrum. At this energy selfshielding correction is negligible.

Another important feature of Ba^{140}-La^{140} is, that no change in its yield from thermal to epithermal fission has been observed within experimental error, which means that it is rather independent of neutron energy [6].

Measuring the Ba^{140}-La^{140} peak by means of a high resolution gamma spectrometry device, the number of Ba-La nuclei which resulted from the U^{235} and Pu^{239} fission and which were found in the burnt fuel sample have been determined.

Together with the irradiation, a monitoring of the thermal and epithermal flux was also carried out .

Since the existing number of U^{235} nuclei ($N_u 5$) was known, the number of fissions, F'^5, was determined from the following relation:

$$F'^5 = N_u^5 T_{ir} [\sigma_{f5} \Phi_{th} + RI_5 \Phi_{epi}] \qquad (2)$$

The number of fissions in Pu^{239} (F'^9) was obtained from the equation;

$$N_{Ba\text{-}La} = F'^5 Y^5 + F'^9 Y^9 \qquad (3)$$

were N_{Ba-La} was determined experimentally.

Using a similar relation as for F'^5 (2) but reversely, the number of Pu^{239} nuclei extant in the fuel was obtained.

$$N_{Pu^9} = \frac{F'^9}{T_{ir} \cdot (\sigma_{f9} \cdot \Phi_{th} + RI_9 \cdot \Phi_{epi})} \qquad (4)$$

B. Testing the Method

The method was tested on a plontingen fuel sample with an initial content of $2\ 10^{19}$ U^{235} nuclei.

The sample was irradiated in the VVR-S reactor at the Institute of Atomic Physics in Bucharest at a fluence of

$$\Phi_I = 1.3 \times 10^{20}\ n/cm^2$$

After a cooling time of 600 days the burn-up was measured and the result was:

$$F^5 = 0.2 \times 10^{19} \text{ fissions}$$

Therefore the number of U^{235} nuclei extant in the burn-up fuel was $N_u 5 = 1.8 \times 10^{19}$.

In order to determine the content of Pu^{239} nuclei extant in the burn-up fuel, the sample was irradiated in a thermal channel of the VVR-S reactor for 9 hours at a flux of $\Phi_{th} = 2.02 \times 10^{11}$ n/cm^2 sec, $\Phi_{epi} = 2.74 \times 10^9$ n/cm^2 sec. After a cooling time of 13 days the Ba^{140}-La^{140} peak was measured leading to:

$$N_{Ba-La} = 5.25 \times 10^{12} \text{ accumulated nuclei.}$$

By employing the above mentioned method, the following value was determined:

$$N_{Pu}9 = 1.6 \times 10^{18} \text{ nuclei}$$

Fig. 3,4 presents the γ spectra of the fuel sample tested before and after irradiation.

This method exhibits a ±7% error.

The Influence of the Nuclear Data Uncertainties of the Fission Products used

The authors concentrated their efforts towards reducing the influence of the nuclear data uncertainties of the fission products.

1. The Uncertainty Introduced by the Fission Yields

One possibility of reducing the influence of the uncertainties introduced by the fission yields has been employed by the authors in [5], by inserting Co^{59} into the

irradiated fuel sample which led to a much improved determination of the fluence.

Since the accuracy required for fission yields depends on the irradiation history knowledge, a correction factor can be determined, which estimates the variation of the nuclei number of the fission products during irradiation. In order to determine this factor, the complete period of irradiation is considered as devided into n number of cycles of $T = t' + t''$ duration, where t' represents the irradiation time and t'' - the pause in a cycle. As it is known, the variation with time of the number of nuclei of a fission product x is given by the following relation:

$$\frac{dN_x}{dt} = Y_x N_U \sigma_f \phi - \lambda_x N_x \qquad (5)$$

where from, by integration over the irradiation period, the accumulated number of nuclei of product x is obtained:

$$N_x(t') = Y_x N_U \sigma_f \phi t' \qquad (6)$$

By the end of the first cycle, the number of nuclei is estimated as:

$$N_x^{I} = Y_x N_U \sigma_f \phi t' e^{-\lambda t''} \cong Y_x N_U \sigma_f \phi t' (1-\lambda t'') = A \qquad (7)$$

Similarly, by the end of the second cycle there will be:

$$N_x^{II} = A + A(1-\lambda T) \qquad (8)$$

The same for the third cycle as well:

$$N_x^{III} = A + [A + A(1-\lambda T)](1-\lambda T) = A + [A(1-\lambda T) + A(1-\lambda T)^2] \qquad (9)$$

And furtheron, up to cycle n, as follows:

$$N_x^n = A + A(1-\lambda T) + A(1-\lambda T)^2 + \ldots + A(1-\lambda T)^{n-1} =$$
$$= A\left[1 + (1-\lambda T) + (1-\lambda T)^2 + \ldots + (1-\lambda T)^{n-1}\right] = AS \qquad (10)$$

where S is the sum of a geometrical progression with a ratio of $(1 - \lambda T)$. It results that:

$$N_x^n = A\,\frac{1-(1-\lambda T)^n}{\lambda T} \qquad (11)$$

Therefore, by the end of the n cycles the number of accumulated nuclei of a fission product x will be:

$$N_x^{(1)} = Y_x N_u \sigma_f \phi t' (1-\lambda t'')\,\frac{1-(1-\lambda T)^n}{\lambda T} \qquad (12)$$

If the desintegration during irradiation would not be taken into account, the number of nuclei accumulated during a time nt' would be:

$$N_x^{(2)} = Y_x N_u \sigma_f \phi n t' \qquad (13)$$

The correction factor results from the comparison of the two final relations:

$$F = \frac{n\lambda T}{(1-\lambda t'')\left[1-(1-\lambda T)^n\right]} = \frac{n\lambda T}{(1-\lambda t'')\left[1-\exp(-n\lambda T)\right]} \qquad (14)$$

This correction factor is negligible for fission products with a very long half-life compared to the irradiation time, but becomes important for fission products with a half-life comparable to the irradiation time.

2. The Uncertainty Introduced by the Half-Life

The equation of the La^{140} evolution, the fission product we use in our method, will be as follows:

$$\frac{dN_{La}}{dt} = \lambda_{Ba} N_{Ba} - \lambda_{La} N_{La} \qquad (15)$$

The solution of the equation is:

$$N_{La} = \frac{\lambda_{Ba} N_{Ba_0}}{\lambda_{La} - \lambda_{Ba}} \left(e^{-\lambda_{Ba} t} - e^{-\lambda_{La} t} \right) \qquad (16)$$

If we take into account the known values of λ_{Ba} and λ_{La}

$$\lambda_{La} = 4.8 \times 10^{-6} \text{ sec}^{-1}$$

$$\lambda_{Ba} = 6.27 \times 10^{-7} \text{ sec}^{-1}$$

and the cooling time of 13 days

$$\lambda_{Ba} t = 0{,}693$$

$$\lambda_{La} t = 5.4$$

it comes out that:

$$e^{-\lambda_{Ba} t} = 0.5$$

$$e^{-\lambda_{La} t} = 0.00457$$

The solution in this case, if we neglect $e^{-\lambda_{La} t}$, will be:

$$N_{La} = \frac{\lambda_{Ba} \cdot N_{Ba}}{\lambda_{La} - \lambda_{Ba}} \cdot e^{-\lambda_{Ba} \cdot t} \qquad (17)$$

It can be seen that the decay constant of Ba^{140} is common to the correction factor for the irradiation history, the uncertainty of which ultimately determines the accuracy required for the fission yield, as well as to the equations for the number of La^{140} nuclei formed during the short

irradiation, which are determined in our proposed method. Therefore we consider it of utmost importance that this factor be known as accurately as possible.

In this view, as Behrens [7] also shows, we devide the number of desintegrations in several $\Delta t \ll T_{1/2}$ short periods. In this case, the possibility of a certain number of radioactive desintegrations for each period, will be described by the Poisson distribution, but at the same time, the medium number of desintegration events must vary from one period to the other, according to the radioactive desintegration law.

The point is that, once the law of the variation of the medium activty with time is given, one has to choose the decay constants such that they are in full concordance with the results of the measurements in the periods. Along this line we consider λ and a_0 (the initial activity) to be unknown.

If we write down the number of desintegration events noticed (followed) within the ithperiod, as:

$$m_i = a_0 \Delta_i e^{-\lambda t_i} \qquad (18)$$

and the probability for a certain number of disintegration events to occur during each period (as determined by the Poisson distribution) as:

$$P_{a_0,\lambda(m_i)} = \frac{(a_0 \Delta_i e^{-\lambda t_i})^{m_i}}{m_i!} e^{-a_0 \Delta_i e^{-\lambda t_i}} \qquad (19)$$

then the following expression is finally obtained for λ_0 after a certain number of mathematical operations described in [7]

$$\lambda_o = \frac{\sum_i m_i * t_i * \sum_i m_i * \ln \frac{m_i}{A_i} - \sum_i m_i * \sum_i m_i * t_i * \ln \frac{m_i}{A_i}}{\sum_i m_i * \sum_i m_i * t_i^2 - \left(\sum_i m_i * t_i\right)^2} \qquad (20)$$

and for the dispersion $D\lambda$:

$$D\lambda = \frac{\sum_i m_i}{\sum_i m_i * \sum_i m_i * t_i^2 - \left(\sum_i m_i * t_i\right)^2} \qquad (21)$$

and the relative error in the determination of λ_o will be:

$$\delta\lambda = \frac{\sqrt{D\lambda}}{\lambda_o} = \frac{\sqrt{\sum_i m_i}}{\lambda_o \left(\sum_i m_i * \sum_i m_i * t_i^2 - \left(\sum_i m_i * t_i\right)^2\right)^{1/2}} \qquad (22)$$

Under the experimental conditions of our proposed method and the results we gor for the six periods chosen, the relative error in the determination of λ_{Ba} is:

$$\delta\lambda_{Ba} = 1.46\ \%.$$

The influence of this error results in the following relative error of the final result, the number of La^{140} nuclei:

$$\delta N_{La} = 1.78\ \%.$$

REFERENCES

1. L. Schächter, P.Popa, Rev.Roum.Phys., 14, 10, (1969).
2. L. Schächter, P.Popa, D.Hacman, Rev.Roum.Phys., 15, 7(1970).
3. L. Schächter, P.Popa, D.Hacman, Rev.Roum.Phys., 16, 7(1971).
4. L. Schächter, P.Popa, D.Hacman, Rev.Roum.Phys., 17, 6(1972).
5. L. Schächter, D.Hacman, Q.Motz, Rev.Roum.Phys., 18, 7(1973).
6. P. Popa, M de Coster, P.Van Assche, NSE, 39, 50-55 (1970).
7. D.J.Behrens, AERE Harwell, REP No. T/R 629

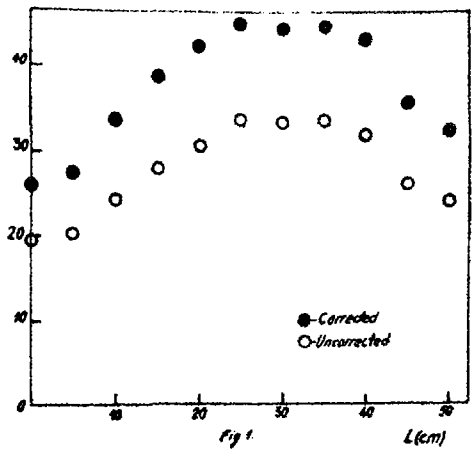

Fig 1.

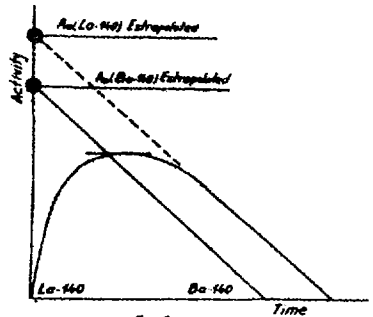

Fig. 2

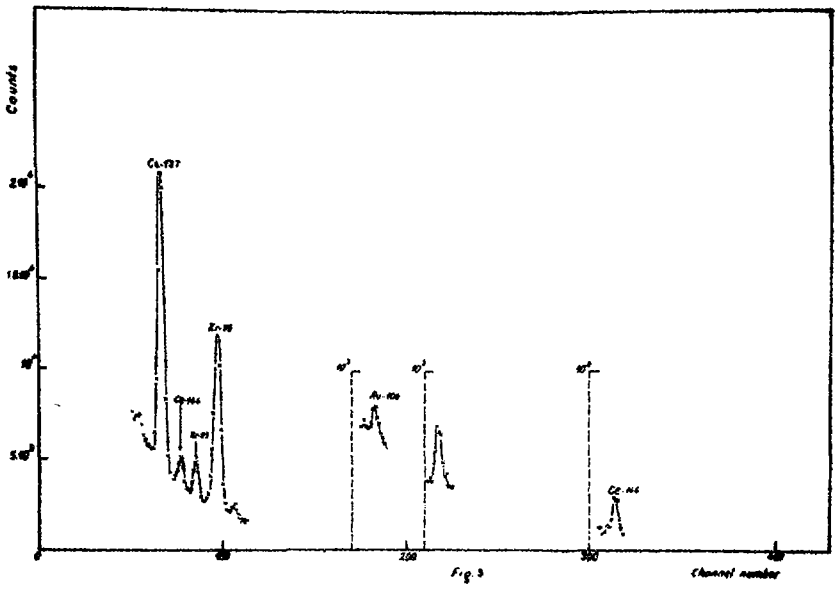

Fig 3

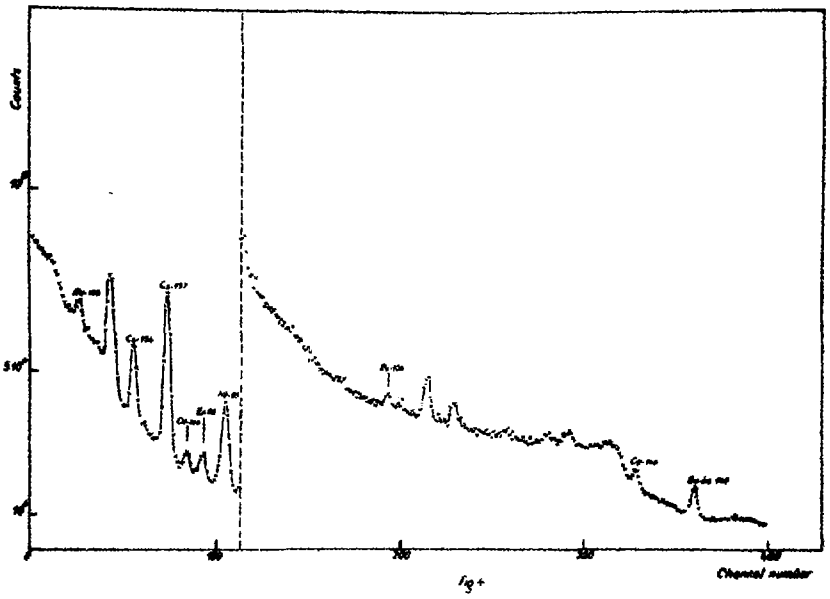

Fig 4

Contributions to
Review Paper No. 6

THE CONTROL OF FISSIONABLE MATERIAL BY MEANS OF DELAYED NEUTRONS

B.P.Maksyutenko and M.Z.Tarasko

Institut of Physics and Power Engineering, Obninsk, USSR

English translation of FEI-370

Abstract:

The authors propose a new method of identifying fissionable materials or determining the percentage of them present in a mixture; the new method, which replaces the normally applied six-group analysis of the delayed neutron decay curve, is based on representation of the decay curve as a continuous distribution of the precursors of the delayed neutrons relative to their half-lives.

The difference between the absolute and relative yields of delayed neutrons in fissionable materials affords a means of identifying them or determining the percentage of them present in a mixture without the use of chemical or isotopic analyses and without destroying the fuel elements.

In this report, the authors consider only the problems associated with measuring relative yields, and in so doing concern themselves with the physical, rather than the technical, aspect of the matter.

The gist of the problem as formulated is, how strictly can two decay curves (for two fissionable materials) be compared mathematically. In view of the statistical scatter of the points, it is difficult to establish any difference criterion for an experimentally observed dependence (counting rate versus time). The criterion can be obtained by formulating the problem in another way, namely by describing the decay curve by means of a set of parameters. Comparison of the parameters (together with the errors attributed to them) will then serve as an identity or difference criterion for the decay curves. At the present time, use is being made of the six-group description of decay curves [1], i.e. the curve showing decrease in neutron activity is decomposed into six exponents. The curves are compared from the contributions (yields) of the

different groups, since the difference is fairly large for various fissionable materials. For these fissionable materials each of the groups has only approximately the same half-life. This is due not only to the experimental errors, but also to the fact that each group is a mixture (the proportions varying with different materials) of several contributors, or in other words, in the given case we are dealing, apart from errors, with poor resolution.

Our approach to the problem differs in that, instead of a limited set of parameters to describe the decay curve, we use in principle, an infinite set of them, or in other words, we try to formulate the problem in terms of a search for an "amplitude" distribution of the components with different half-lives. Being differential in nature, a description of that type enables us to compare the decay curves in greater detail, as compared to one based on a limited set of parameters. Furthermore, it automatically results in smoothing out of the experimental scatter of the points on the curve and is consequently the best method.

Since we are here interested only in the theoretical aspect of the matter, we shall henceforth work only with decay curves calculated theoretically with a computer, and will not use experimental curves containing a statistical scatter of the points. Decay curves of this kind were calculated for the given six-group half-lives and yields [1] for ^{233}U, ^{235}U and ^{239}Pu, during thermal neutron fission. We assumed in the process that the irradiation of the fissionable materials was carried out for an infinite length of time, or in other words that the activation of all the groups was carried to the point of saturation.

Applying the method of the "least directed divergence" [2], we transformed the decay curve (counting rate versus time N(t)) into an "amplitude" distribution for the probability P(T) of the presence of a component with half-life T. Figures 1 and 2 show the distribution P(T), normalized in such a way that the yield from the first group is the same for all the fissionable materials. It can be seen that:

(a) There are only four clear-cut peaks for all distributions, although six groups have been incorporated in the calculation of the decay curves;

(b) The difference in spectral composition is large in all cases, except for the pair ^{235}U-^{239}Pu;

(c) For the pair ^{235}U-^{239}Pu the distributions merge, except in the region of half-lives lasting 7-35 sec.

This analysis permits a clear formulation of the possibility of identifying

fissionable materials when determining their percentage composition in a mixture with other materials. It is obvious that we can distinguish any pair of fissionable materials, except ^{235}U–^{239}Pu, over the whole range of half-lives. In the case of ^{235}U–^{239}Pu, the possibilities are limited to the 7–35 second range, i.e. the interval over which delayed neutrons from the mixture of precursors ^{137}I and ^{88}Br are present.

Let us give some figures. From the decay curves for delayed neutrons from ^{235}U and ^{239}Pu, during fission induced by thermal neutrons, the ratio between the second group (^{137}I and ^{88}Br mixture) and the first group (^{87}Br) yield is:

(a) For decomposition by the method of least squares, 6.65:1 for ^{235}U, and 8.53:1 for ^{239}Pu [1], i.e. they differ by 28%;

(b) The ratio between the distribution peaks (see Fig. 1) for the second group is 1.52, i.e. a difference of 52%.

Thus the processing of the experimental results by the method of "least directed divergence" provides the best opportunity of comparing and establishing the most favourable conditions for identifying or determining the percentage composition of fissionable materials from the relative delayed neutron yields, since:

(a) For different fissionable materials, the same groups have different half-lives on account of varying proportions of contributors, hence a comparison of the yields from groups with a different weighted half-life is, strictly speaking, incorrect; in the new method this shortcoming is corrected;

(b) Comparison of decay curves on the basis of a few selected parameters is also incorrect, because in such a case the curve is decomposed into a different number of parameters (5, 6, 7 and so on), the choice of which is somewhat arbitrary.

The new method enables us to make a comparison over the whole range of half-lives and does not suffer from the limitations referred to.

The authors thank G. Ya. Rumyantsev for his valuable comments and interest in their work.

REFERENCES

[1] KEEPIN, J.R., Fizičeskie osnovy kinetiki jadernyh reaktorov (Physical fundamentals of nuclear reactor kinetics), Atomizdat, Moscow (1967).

[2] TARASKO, M.Z., Preprint FEI-156 (1969).

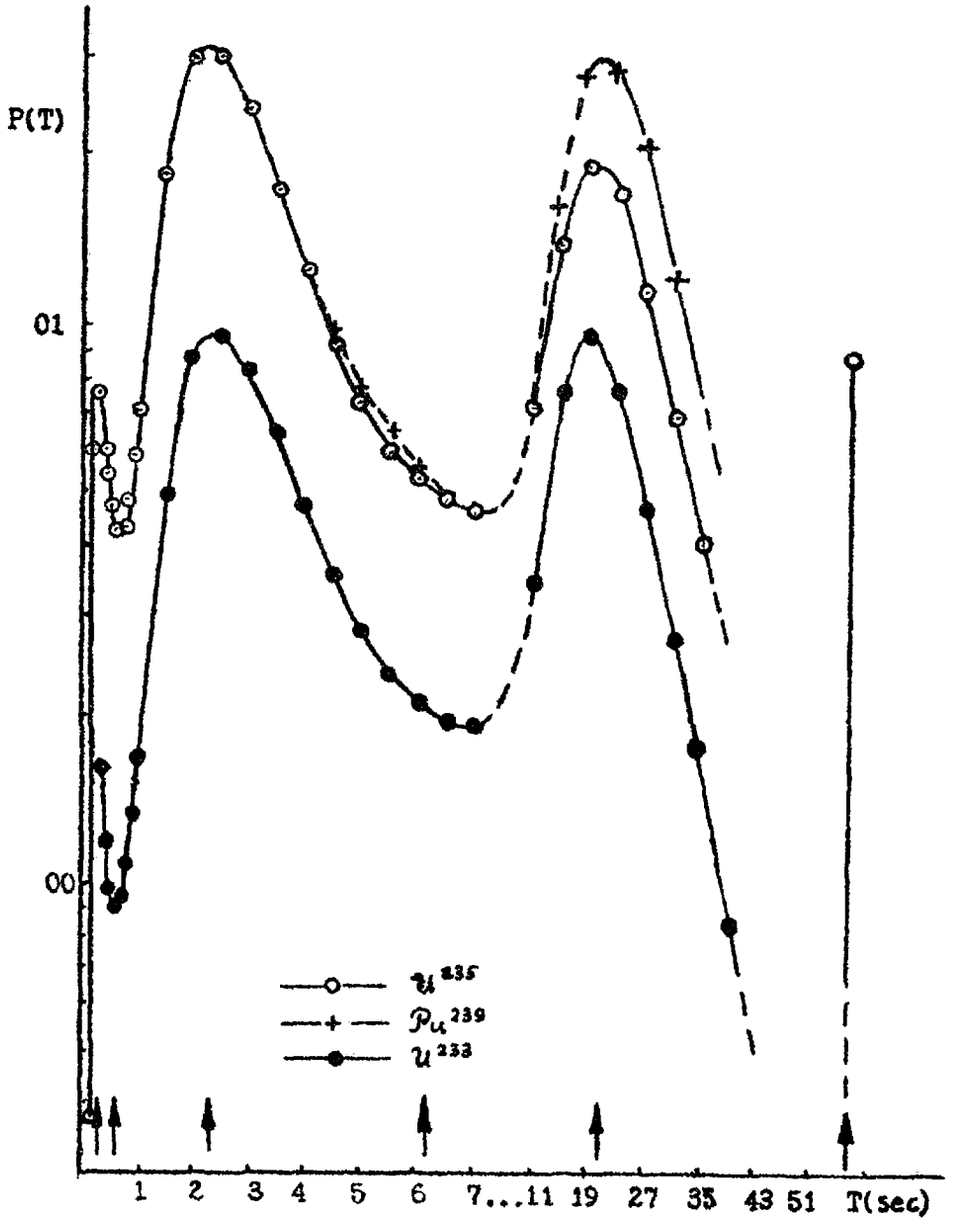

Fig. 1. Spectrum for the probability of delayed neutron yield as a function of half-life (the arrows indicate the half-life incorporated during computation of the decay curve).

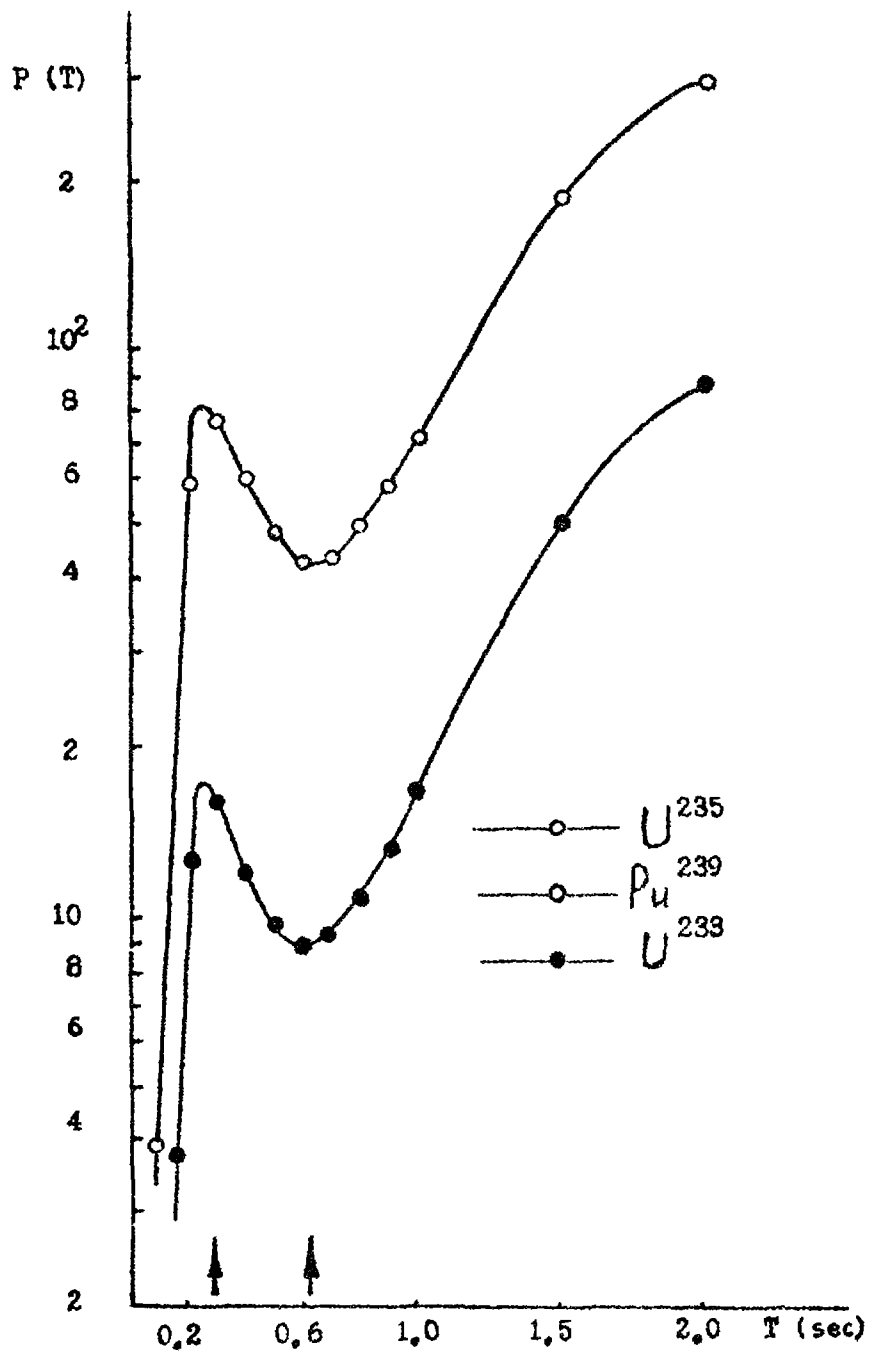

Fig. 2. Spectrum for the probability of delayed neutron yield as a function of half-life (the arrows indicate the half-life incorporated during computation of the decay curve).

FISSION PRODUCT NUCLEAR DATA AND NONDESTRUCTIVE ASSAY SYSTEMS OF NUCLEAR MATERIALS

T. Gozani

Intelcom Rad Tech
San Diego, California

ABSTRACT

A concise list of passive and active nondestructive assay (NDA) techniques for nuclear material is presented. Development, design, and implementation of NDA techniques are shown to be dependent on fission product nuclear data (FPND) to a varying degree. Areas where some additional work would be desirable are identified.

1. INTRODUCTION

This contribution lists some fission product nuclear data (FPND) which could be helpful in the development, design, and the actual application of nondestructive assay (NDA) systems for nuclear materials.

2. PASSIVE AND ACTIVE NDA TECHNIQUES

Nondestructive assay methods are usually divided into two main categories: passive assay and active interrogation. Passive assay involves observation of both gamma rays emitted following alpha decay (as in ^{239}Pu and ^{235}U) which are uniquely characteristic of the individual fission species, and neutrons emitted as a result of (α,n) reactions or spontaneous fissions (e.g., in ^{240}Pu). The latter can be distinguished from the former by using coincidence counting techniques. Passive NDA methods are quite often severely limited by the lack of penetrability for some of the gamma rays and absence of a suitable signature for several fissionable isotopes. Nonetheless, they are extremely attractive due to their inherent simplicity and the fact that they are relatively inexpensive.

A list of the most commonly used passive NDA techniques is given in Table 1. In this table the various methods are very briefly described in terms of the basic detectors used, the main observed radiation, and their status from the point of view of availability and actual experience.

Table 1

PASSIVE NDA TECHNIQUES

Technique	Detector	Observed Radiation	Status
1.1	Typically NaI(Tℓ), Ge(Li)	185 keV (^{235}U) 350-400 keV (^{239}Pu) 750,1000 KeV (^{238}U) } gamma	Commercial
1.2	NaI(Tℓ), Ge(Li)	Fission product gamma ray lines for burnup measurements	Operational
1.3	NaI(Tℓ), Ge(Li)	High-energy fission-product gamma lines as Leached Hull Monitor	Commercial
1.4	Glass scintillator	Alpha activity in solutions	Commercial
1.5	Thermal neutron detector (BF_3, ^3He in moderator)	Total neutron counting from (α,n) and spontaneous fission	Commercial
1.6	High efficiency thermal neutron detector	Slow coincidence counting of neutron from spontaneous fission	Commercial
1.7	Liquid or plastic scintillators (Fission Multiplicity Detector)	Fast coincidence of prompt neutrons and/or gamma ray	Commercial
1.8	Fast neutron detectors —Gas proportional counter (CH_4 or ^4He) —Liquid scintillator with pulse shape discriminator	Fast prompt neutron (from (α,n) or spontaneous fission)	Operational

Active interrogation employs an external source of highly penetrating neutrons or photons to induce characteristic nuclear reactions, usually fissions, in the nuclear material which is constained in the sample under investigation. The induced fissions are measured by detecting particles which are emitted during or following the fission process. The only radiations emitted in such a process which are capable of penetrating the sample container and reaching an outside detector are the prompt and delayed neutrons and gamma rays.

A list of most of the active nondestructive techniques being used and tested or in an advanced state of study is given in Table 2 (see also Ref. 1). In this table the various methods are also very briefly described according to the source they use, the incident (interrogating) radiation, and the observed (induced) radiation. The last column lists the stage of development of the technique.

Most of the techniques listed in Tables 1 and 2 are discussed in the literature, particularly in Refs. 2, 3, and 4. The general physics of the active NDA techniques are discussed in Ref. 1.

3. THE REQUIREMENT IN FPND FOR NDA TECHNIQUES

3.1 GENERAL

A quick survey of the NDA techniques listed in Tables 1 and 2 shows that all of the techniques, except possibly for the burnup determination from fission product gamma lines (Technique 1.2) do not depend directly on the knowledge of FPND. The NDA techniques are usually applied to rather complicated samples in the nuclear industry, ranging from small sintered fuel pellets to the complete fuel assemblies and 55 gallon waste drums. This variety of samples is dictated by the nature of the nuclear industry. The only practical approach to the determination of the amount of fissile materials in such complicated samples is to use standards of similar nature to the measured unknown, rather than attempt to determine the amount in an absolute fashion. Even if all of the nuclear parameters were known to a very high degree of accuracy, variations in the geometrical configuration and the presence of non-fissile matrix materials, among others, will generally not allow an absolute measurement.

The usefulness of FPND lies mainly in providing some guidance in the development and design phases of NDA techniques, and it could be of help in understanding and possibly alleviating problems arising in the utilization of the technique.

3.2 DELAYED GAMMA TECHNIQUES

Gross delayed gamma activities versus time (Refs. 5, 6) provided a highly useful guidance in the development of the nuclear fuel rod scanners (Refs. 7, 8) (Technique 2.12) and the high precision Small Sample Assay System (SSAS) (Ref. 9). However, more work needs to be done in measuring gross delayed gamma yields from relatively early times (a few tenths of a second) out to several tens of minutes after fission. One of the main

Table 2

ACTIVE NONDESTRUCTIVE TECHNIQUES

Number	Source	Incident Radiation	Observed Radiation	Status
2.1	Electron accelerator	5- to 10-MeV gamma bremsstrahlung	prompt neutrons	operational
2.2	Electron accelerator	5- to 10-MeV gamma bremsstrahlung	delayed neutrons	operational
2.3	Electron accelerator	5- to 10-MeV gamma bremsstrahlung	delayed gamma ray (using low or high resolution detectors)	tested
2.4	14-MeV neutron	unmoderated/partially moderated neutrons	delayed neutrons	operational
2.5	14-MeV neutron	unmoderated/partially moderated neutrons	delayed gamma	tested
2.6	3-MeV Van de Graaff	subthreshold neutrons	delayed (and prompt) neutrons	operational
2.7	Electron accelerator	MeV/sub-MeV neutrons	delayed neutrons	tested
2.8	14-MeV neutron generator	low energy lead moderated neutrons	prompt neutrons	operational
2.9	14-MeV neutron generator or electron accelerator	high energy lead moderated neutrons	prompt neutrons (possibly also delayed neutrons and gammas)	tested
2.10	Low E (α,n)	unmoderated/partially moderated neutrons	Fission Multiplicity Detector (prompt neutrons and gammas)	commercial
2.11	^{252}Cf or (α,n)	moderated/unmoderated neutrons	Fission Multiplicity Detector	commercial

Table 2 (Continued)

Number	Source	Incident Radiation	Observed Radiation	Status
2.12	^{252}Cf	moderated Cf-fission neutrons	gross delayed gamma (possible prompt and delayed neutrons)	commercial
2.13	Low E (α,n)	highly/partially moderated neutrons	fast prompt neutrons	tested
2.14	(γ,n)	sub-MeV neutrons	prompt (and delayed) neutrons	tested
2.15	Reactor	thermal neutrons	delayed neutrons	commercial
2.16	Reactor	thermal neutrons	high resolution fission product gamma rays	partially tested
2.17	Reactor	low eV neutrons	prompt neutrons and neutron transmission	tested
2.18	Reactor	thermal and low eV	capture gamma	tested
2.19	Medium E Linac	neutrons (via time-of-flight)	capture gamma	tested
2.20	Zero power reactor	thermal neutrons	reactivity change	tested
2.21	Zero power fast reactor	fast neutrons	reactivity change	under study
2.22	X-ray generator	200-keV x rays	fluorescent x rays	operational
2.23	^{241}Am	low E gamma	fluorescent x rays	operational
		filtered low E (<60 keV) gamma		commercial

motivations for these investigations is to seek a practical way to distinguish between the three main fissile isotopes, namely ^{233}U, ^{235}U, and ^{239}Pu. This may be achieved if significant differences in the gross decay rates and energy distributions exist between these isotopes. A possibility that some useful difference exists in the high energy portion of the spectrum is indicated in the data shown in Ref. 5.

More extensive compilation and evaluation of the existing data and possibly more work is required in generating FPND in the area of high resolution gamma spectroscopy of fission products. Again, the main aim should be not only to determine the amount of a particular fissile isotope in the presence of fertile isotopes (e.g., ^{232}Th and ^{238}U), but to identify individual fissile isotopes when present in a mixture. There have been some attempts in this direction, with varying degrees of success. Studies at Rad Tech (Refs. 10,11) showed little difference between the various fissile isotopes in terms of observed fission product gamma-ray lines, but some useful differences in the line intensities were measured. Additional work in this area for the case of photofission would be desirable. Studies at LASL (Ref. 12) had a similar goal, namely to determine if there are prominent individual high-energy gamma-ray lines in the early-times after-fission ($\sim$1 sec to 30 sec) spectra of $^{235}U(n,f)$ which might be useful for nuclear safeguards applications. Again, it was found that most of the prominent peaks appear in both $^{235}U(n,f)$ and $^{239}Pu(n,f)$ fission product gamma spectra. However, some of the peaks exhibit yields which differ significantly between these two fissile materials.

3.3 DELAYED NEUTRON TECHNIQUES

Many of the techniques listed in Table 2 use delayed neutrons as an indication of fission. The present knowledge of delayed neutron parameters from neutron fission, including energy spectra, is satisfactory from the point of view of the NDA techniques as expressed above. However, no measurement of the energy spectra of delayed neutrons from photofission has been done so far. It thus seems worthwhile to generate some basic data on the energy distribution of delayed neutrons from photofission. Also, more accurate group parameters for delayed neutrons from low energy (6 to 10 MeV) photofission would be desirable.

3.4 BURNUP DETERMINATION FROM FISSION PRODUCT GAMMA RAYS

One of the most commonly used methods to assess the burnup in spent fuel elements is to perform a complete gamma spectroscopy analysis of the

element, usually using a high-resolution Ge(Li) detector (Technique 1.2). Since it is hardly possible to prepare standards for such a measurement, the burnup assessment, based on these spectroscopy measurements, depends heavily on the availability of nuclear and non-nuclear data, such as diffusion properties of fission products within the fuel and cladding material. It is doubtful, however, whether the available FPND, especially yields, half lives, branching ratios, and line intensities, to any appreciable extent, limit the accuracy of burnup determination. However, a complete compilation, error analysis, and sensitivity calculations would be beneficial.

3.5 COINCIDENCE TECHNIQUES

The presence of trace quantities of certain fission products in fresh nuclear fuel will be unavoidable as more and more reprocessed fuel will be used. Thus fission products will inevitably constitute a background to all NDA techniques. The present knowledge of the FPND seems to be sufficient to enable the designer or the user of an NDA technique to estimate the limit of operability and possibly to reduce the error due to the presence of fission product. One exception to this might be the amount of high-energy (>2.2 MeV) gamma rays which induce background in neutron-moderated detectors by the (γ,n) reaction in the deuterium. However, the available information is not sufficient for those NDA methods which are based on the concept of fission multiplicity and use fast coincidence circuits (especially Techniques 1.6, 2.10, and 2.11). In this case it is required to know the existence of positron emission, cascade of gamma rays, the order of multiplicity of the cascade, and the associated gamma energies. Obviously a complete level scheme of the appropriate (relatively long lived) fission products will contain this information. However, the required specific information can also be obtained using simple coincidence techniques, without performing additional comprehensive measurements.

Another set of parameters which are important to systems based on the Fission Multiplicity Detectors (Ref. 13), and should be mentioned in this context, are the average multiplicity for both prompt neutrons and gamma rays (the latter include early delayed gamma rays with half lives up to few tens of nsec). These parameters, although actually not being FPND, are important for the design, efficiency calculation, and, in general, for more efficient utilization of the devices. An interesting example of the latter was attempted a few years ago (Ref. 14). For neutrons, the distribution of multiplicities is moderately well known; for gamma rays the situa-

tion is different. While the multiplicity is reasonably well known (e.g., Ref. 15), the multiplicity distribution and possible multiplicity-energy correlation (Ref. 16) are rather poorly known.

4. CONCLUSIONS

A brief review of the existing NDA techniques and those which are in an advanced stage of testing indicates that the requirements for FPND in this area are quite modest and could possibly be met, to a large extent, by an extensive compilation and evaluation of the available data. Specific areas of recommended additional work are mentioned.

REFERENCES

1. T. Gozani, "Physics of Nuclear Materials Safeguards Techniques," Nucl. Technology, 13, 8-18 (1972).

2. Proc. Symp. Safeguards Research and Development, WASH-1147 USAEC (1969).

3. Proc. Symp. Progress in Safeguards Techniques, IAEA-SM-133, IAEA (1970).

4. Proc. of Institute of Nuclear Materials Management (INMM) Vol. II, No. 1 (1971) through Vol. II, No. 3 (1973).

5. P. C. Fisher and L. B. Engle, "Delayed Gammas from Fast Neutron Fission of ^{232}Th, ^{233}U, ^{238}U, and ^{239}Pu," Phys. Rev. 134, 4B, B796-B823 (1964).

6. R. B. Walton et al., "Delayed Gamma Rays from Photofission of ^{238}U, ^{232}U and ^{232}Th," Phys. Rev. 134, 4B, B824-B830 (1964).

7. H. O. Menlove et al., LASL Report LA-5071-M (1972).

8. D. G. Costello and T. Gozani, "Statistical Consideration in the Design and Utilization of High Speed Fuel Rod Scanner," Proc. of INMM Vol. II, No. 3, 187-204 (1973).

9. T. Gozani et al., "High Precision Small Sample Assay System," ANS Trans. Vol. 17, 2 (1974).

10. "Application of Photoinduced Reactions to Nuclear Materials Safeguards Problems," Project Summary Report, July 1968-June 1969, GA-9614, pages 7-14.

11. T. Gozani et al., "New Developments in Nuclear Material Assay Using Photonuclear Reactions," Safeguards Techniques Vol. II, IAEA-SM-133 (1970).

12. Los Alamos Report LA-4162-MS, 13-15 (1969).

13. T. Gozani and D. G. Costello, "Isotopic Source Assay System for Nuclear Materials," ANS Trans. 13, 2, 746 (1970).

14. T. Gozani and D. G. Costello, "On the Reduction of Prompt Fission Gamma Self Shielding Using the Fission Multiplicity Detector," Intern. Meeting of ND Measurement and Identification Techniques in Nuclear Safeguards, Euratom, Ispra (1971) and ANS Trans. 14, 2, 809 (1971).

15. V. V. Verbinski, H. Weber, and R. E. Sund, "Prompt Gamma Rays from $^{235}U(n,f)$, $^{239}Pu(n,f)$ and Spontaneous Fission of ^{252}Cf," Phys. Rev. C, 7, 3 1173-1185 (1973).

16. T. Gozani, "On the Correlation Between the Multiplicity and Spectrum of Prompt Fission Gamma Rays," 3rd IAEA Symp. on the Physics and Chemistry of Fission, August 1973.

Contributions to
Review Paper No. 10

ON THE CALCULATION OF TOTAL RADIATIVE WIDTHS OF NEUTRON RESONANCES

V. BENZI, G. REFFO, M. VACCARI

Comitato Nazionale Energia Nucleare
Centro di Calcolo
Bologna, Italy

Abstract:

Three different formulae have been proposed to estimate $\overline{\Gamma}_\gamma$ at neutron binding energy, namely: the Brink formula, the Weisskopf-Rohr formula and the Musgrove formula. The three formulae are briefly described in this paper. Results of calculations of $\overline{\Gamma}_\gamma$, using the three formulae, are compared for all fission products, for which experimental data are available

§ 1. INTRODUCTION

The statistical model of nuclear reactions is frequently adopted in order to estimate the fast neutron radiative capture cross-sections of fission product nuclei when experimental data are missing.

The theoretical calculations can be performed provided a number of parameters, like $\overline{\Gamma}_\gamma$, $\overline{D}_{obs}$, etc.., are known. These parameters, in turn, can be obtained from the analysis of the observed resonances at low energy.

When no resonance parameters are available, as frequently occurs in fission product nuclei, an estimate can be obtained on the basis of the systematic behaviour of the required data or by using some semi-empirical recipe.

The aim of this work is to test the validity of three different formulae which have been suggested to obtain an estimate of $\overline{\Gamma}_\gamma$ at neutron binding energy. The test is limited to those nuclei which have the mass number in the region of interest for fission products, with at least two measured $\overline{\Gamma}_\gamma$.

The formulae here considered are: 1. the Brink formula, by several authors indicated as "Axel estimate"; 2. the Weigmann-Rohr formula and 3. the Musgrove formula.

§ 2. THE BRINK FORMULA

If one assumes that the capture radiation is only of the electric dipole type, the total radiation width at binding energy B is given by

$$\Gamma_\gamma(B) = C \int_0^B f(\varepsilon,E)\ \varepsilon^3\ \rho_T(E)\ D_J(B)dE \qquad (1)$$

where $\rho_T(E)$ is the total density of the levels at excitation energy E to which the initial state (spin J) is accessible by emission of E1 radiation, C is a constant and $E=B-\varepsilon$. The function $f(\varepsilon,E)$ is a quantity which depends on both the excitation energy of the initial state and the transition energy ε. The $D_J(B)$ is the spacing of levels with spin J at energy B.

Brink[7] assumes that the quantity $C.f(\varepsilon,E)$ can be derived from the detailed balance principle and from the shape of the photonuclear cross-section, regardless of the fact that in the inverse reaction the initial state of the nucleus is not the ground state.

Considering these hypotheses and taking into account the dipole sum rule, the radiation width $\Gamma_\gamma(\varepsilon,J,\pi)$ for a γ-ray of energy ε is given by

$$\Gamma_\gamma(\varepsilon,J,\pi) = \frac{4}{3\pi}\frac{NZ}{A}\frac{e^2}{\hbar c}\frac{1+0.8x}{Mc^2}\ \frac{\Gamma_R\,\varepsilon^4}{(\varepsilon^2-r_R^2)^2+(\varepsilon\Gamma_R)^2}\ \frac{1}{\rho(B,J,\pi)} \qquad (2)$$

where $\rho(B,J,\pi)$ is the level density at the excitation energy of the initial state having the same spin and parity as the initial state and

x = fraction of exchange force ($x \sim 0.5$)

E_R = energy of the peak of the giant resonance

Γ_R = width of the giant resonance

The total radiation width is given by

$$\Gamma_\gamma(B,J,\pi) = \int_0^B \Gamma_\gamma[(B-E),J,\pi] \sum_{|J-1|}^{J+1} J' \rho(E,J',-\pi)dE \quad . \quad (3)$$

The calculations carried out in this work were performed using the LARA code[12]. In this code, formulae (2) and (3) are slightly modified, in particular

1) As far as formula (2) is concerned, the integrated cross-section as obtained from the Lorentzian fit of photoabsorption experimental data is used instead of the dipole sum rule.

2) Formula (3) is split into two parts in order to take better into account the transitions to the resolved levels.

More explicitly, the formula here adopted is

$$\Gamma_\gamma(B,J,\pi) = \sum_1^K n \frac{2}{3(\pi\hbar c)^2 \rho(B,J,\pi)} \sum_{|J-1|}^{J+1} J' \, \delta_{J',J_n} \, \delta_{\pi,-\pi_n} (B-E_n)^2 \sigma_\gamma(B-E_n)$$

$$+ \frac{1}{3(\pi\hbar c)^2 \rho(B,J)} \int_0^{B-E_c} \sigma_\gamma(\varepsilon)\varepsilon^2 \sum_{|J-1|}^{J+1} J' \, \rho[(B-\varepsilon),J']d\varepsilon \quad , \quad (4)$$

where the δ's take into account the spin and parity selection rules, ρ represents the density of the unresolved levels and E_c is the energy at which the first level of unknown characteristics is assumed to be found.

The composite Gilbert-Cameron[8] formula was used for the analysis of the level spacing of a number of nuclei with at least 10 s-wave measured resonances in order to obtain the level density parameters on which the absolute value of ρ depends.

For the spin cut-off factor σ in the Cameron formula, the estimate of Facchini et al.[9]

$$\sigma^2 = 0.146\ A^{2/3}\ \sqrt{a(B-\Delta)}$$

was adopted.

The results of such an analysis for the parameter "a" are given in Table 1, whereas Fig. 1 shows a plot of "a" vs. the neutron number N of the nucleus. As usual, the plot shows a rather well defined trend of the a-dependence on N, from which a smooth value "a_{syst}" can be guessed.

The photonuclear cross section σ_γ is assumed to have Lorentzian shape for non deformed nuclei and double-Lorentzian shape for the deformed ones.

As far as the photonuclear reaction parameters are concerned, when the required data were not available, the experimental values given for neighbouring nuclei were adopted according to table 1, where the data marked ^ refer to ref. 2, while all the others refer to ref. 3.

§ 3. THE WEIGMANN-ROHR FORMULA

Very recently, Weigmann and Rohr[5] have carried out a systematic analysis of total radiative widths of low-energy neutron resonances for a large number of nuclei, using the following formula

$$\Gamma_\gamma(B) = \xi\ A^{2/3}(B^*)^{5/4}\ e^{-2\sqrt{aB^*}} \int_0^B (B-\varepsilon)^3\ \tilde{\rho}(E^*)dE + s\ A^{2/3}\ g'\ D_{obs}\ S_\ell \qquad (5)$$

The quantity S_ℓ represents the ℓ-wave neutron strength function and $\tilde{\rho}$ the energy dependent part of the level density, for which the Gilbert-Cameron formula is assumed.

The first term of the R.H.S. of the above formula derives from a manipulation of the well known Weisskopf estimate of the radiation width, whereas the second term takes into account the valency nucleon contribution. The ξ is an adjustable parameter, and

$$s = \begin{cases} 3.9 \cdot 10^{-3} & \text{for s-waves, } A \leq 63 \\ 3.82 \cdot 10^{-4} & \text{for p-waves, } 88 \leq A \leq 125 \\ 4.9 \cdot 10^{-2} & \text{for s-waves, } 196 \leq A \leq 204 \\ 0 & \text{otherwise} \end{cases}$$

In addition,

$$E^* = E + \Delta + \eta$$
$$B^* = B + \Delta + \eta \quad ,$$

where Δ and η are excitation energy corrections for shell and pairing effects, which are assumed to be given by the formulae of Kahn-Rosenzweig[10] and Nemirovsky-Adamchuk[11], respectively. The results obtained with these formulae are multiplied by the constants C_Δ and C_η, respectively, which are obtained from a simultaneous best fit of the experimental Γ_γ' s. Thus, formula (5) contains three (adjustable) constants (C_Δ, C_η, ξ), for which the following values are suggested by Weigmann and Rohr:

$$C_\Delta = 0.07$$
$$C_\eta = 0.75$$
$$\xi = 3.72 \cdot 10^{-3}$$

§ 4. THE MUSGROVE FORMULA

The empirical formula suggested by Musgrove[6] is

$$\Gamma_\gamma(B) = K\, a^x \left[D_{obs}(B) \right]^y U^z f(Z)$$

with $U = B - \Delta$.

When Γ_γ and D_{obs} are given in eV and B in MeV, the following numerical values of the parameters have to be adopted

$$K = \begin{cases} 1.13 \times 10^{-3} & \text{for isomeric nuclei} \\ 1.43 \times 10^{-3} & \text{for non isomeric nuclei} \end{cases}$$

$x = 0.02$

$y = 0.21$

$z = 2.08$

In addition,

$$\Delta = \begin{cases} 11/\sqrt{A} & \text{for odd-A nuclei} \\ 22/\sqrt{A} & \text{for even-even nuclei} \\ 0 & \text{for odd-odd nuclei} \end{cases}$$

The quantity $f(Z)$ is an empirical correction factor which depends on the atomic number and ranges between 0.3 and 10 . Such a factor is given for $21 \leq Z \leq 82$ in Ref. 6).

§ 5. RESULTS

The results of our calculations are shown in Table 1. The second column gives the average value D_{obs} of the level spacing as deduced from the analysis of $\ell=0$ neutron resonances. The a-values obtained from D_{obs} are in the fourth column, whereas those suggested by the general trend of a vs. N are shown in the next column.

The parameters E_R , Γ_R and σ_R refer to the photonuclear cross-section. The 15^{th} and 16^{th} columns show the values of $\Gamma_\gamma(B)$ obtained by means of formula (4) for two different choices of the value at level density parameter a , namely the value obtained from D_{obs} and the value suggested by the systematic behaviour as function of N. The $\Gamma_\gamma(B)$ calculated by Weigmann and Rohr are shown in the next column, whereas the last column gives the values obtained using the Musgrove formula and our D_{obs} values.

§ 6. CONCLUSIONS

As one can see from Table 1, in a large number of cases the calculated values are in reasonable agreement with the experimental ones, independently of the formula adopted.

For this reason, it does not seem possible to select the "best" formula among the three considered on the basis of the results here obtained. It should be noted, however, that these conclusions

refer to the case of $\Gamma_\gamma(B)$. If the energy dependence of Γ_γ has to be considered, as in the case of statistical model calculations, the above conclusions are no longer valid. For example, in many cases, the Musgrove formula gives a decreasing trend of Γ_γ vs. E , which does not seem acceptable on a physical basis.

In addition, one should expect that the Weigmann formula fails at high energies because the Weisskopf estimate does not account for the giant resonance phenomenon.

REFERENCES

1) M. Pasquali: Thesis on "Analisi sistematica del parametro "a" della densità dei livelli", carried out at C.d.C, CNEN, Bologna (unpublished).

2) B.I. Goryachev: Atomic Energy Review, vol. 2 n. 3 pag. 71 (1964).

3) E.G. Fuller, H.M. Gerstenberg, H. Vander Molen, T.C. Dum: Photonuclear Reaction Data 1973 - NBS special publication 380.

4) M. Goulassy, S.T. Perkins: UCRL-50400, vol. 13.

5) H. Weigmann, G. Rohr: Proc. "Tripartite Symposium on Nucl. Phys. with Thermal and Resonance Energy Neutrons" to be published as RCN report.

6) A.R. de L. Musgrove: AAEC/E211 - November (1970).

7) D.M. Brink: Thesis, Oxford 1955; See also Handbuch der Physik, vol. XL, pag. 315. Spring-Verlag (1955).

8) A. Gilbert, A.G.W. Cameron: Canadian Journ. of Phys., vol. 43 (1965) pag. 1446.

9) U. Facchini, E. Saetta-Menichella: Energia Nucleare, vol. 15/n.1/ 1968, pag. 54.

10) P.B. Kahn, N. Rosenzweig: Phys. Rev. vol. 187 (1969), pag. 1193.

11) P.E. Nemirovsky, Yu.V. Adamchuk: Nucl. Phys. vol. 39 (1962), pag. 553.

12) G. Reffo, M. Vaccari: to be published as a CNEN report.

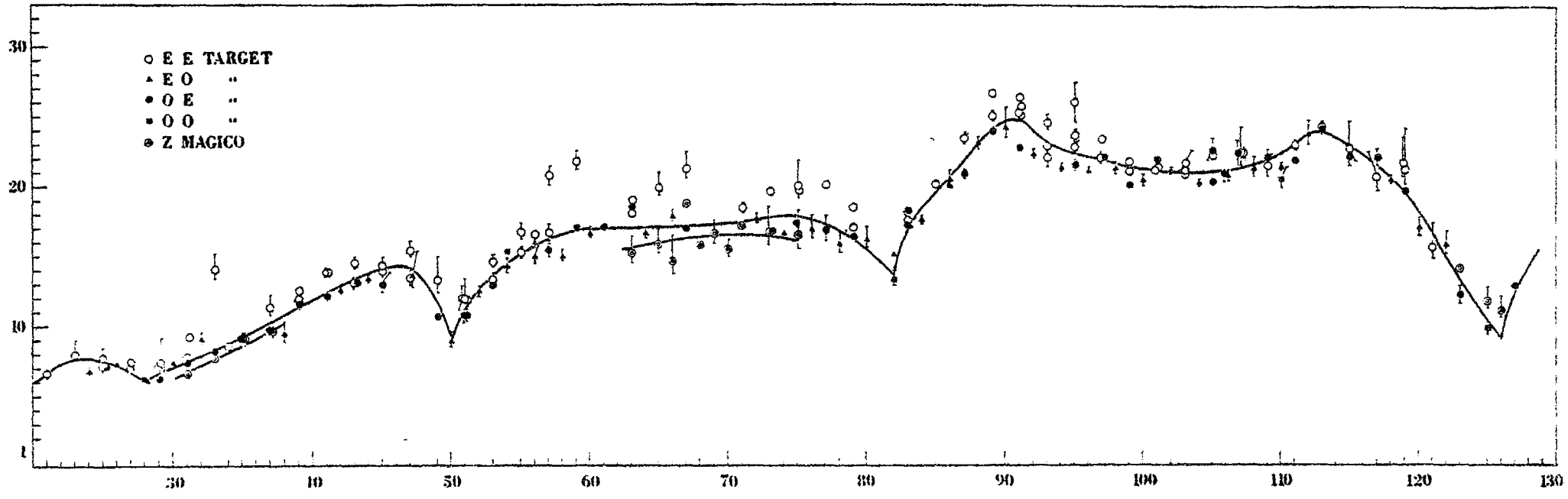

FIG. 1

Plot of the level density parameters a_{exp} vs the neutron number N .
The solid line was obtained fitting the experimental points by eyes.

TABLE I

COMPOUND NUCLEUS	D_{obs} EXPTL eV	Ref	a_{exp} MeV^{-1}	a_{sist} MeV^{-1}	EXPEPIMENTAL E_R MeV	EXPEPIMENTAL Γ_R MeV	EXPEPIMENTAL σ_R barn	ADOPTED E_R MeV	ADOPTED Γ_R MeV	ADOPTED σ_R barn	$\Gamma_{\gamma\ exp}$ mV	N° of Resonances	Ref	$<\Gamma_\gamma>$ From a exp mV	$<\Gamma_\gamma>$ From a sist mV	$<\Gamma_\gamma>$ W - R mV	$<\Gamma_\gamma>$ MSGRV mV
Zn-68	670	5	9.53	10.8				16.3	6.3	0.082	490±80	2	1	646	361	448	538
Zn					16.3*	6.3*	0.082*										
Ga-70	230	1	11.5	11.4				16.5	As for Zn	0.115	270±94	10	1	309	316	328	372
Ga-72	381	4	11.9	12.5				16.5	"	0.115	240±40	9	1	240	203		331
Ga					16.5		0.115										
Ge-71	974	4	13	11.4				17.5	"	0.158	162±25	3	1	211	363	187	214
Ge-73	1550	1	13.75	12.5				17.5	"	0.158	160±25	3	1	158	235	140	144
Ge-74	124	1	12.55	12.9				17.5	"	0.158	197±29	12	1	204	188	209	167
Ge-75	5850	4	12.3	13.4				17.5	"	0.158	195±40	2	1	152	119	159	161
Ge-77	4200	1	13.9	14.1				17.5	"	0.158	120±25	2	1	150	140	121	122
Ge					17.5		0.158										
As-75					17.15*	9.2*	0.092*										
As-76	71.4	1	13.1	13.4				17.15	9.2	0.092	290±55	33	4	298	279	222	460
Se-75	370	1	13.8	12.5				17.15	9.2	0.092	290±50	6	1	218	292	199	417
Se-77	933	4	14	13.4				15.5	5.2	0.118	230±40	5	1	202	258	174	300
Se-78	120	1	13.4	13.8				15.5	5.2	0.118	411±72	16	4	278	238	283	402
Se-79	1000	1	14.34	14				15.5	5.2	0.118	220±45	4	1	160	175	160	283
Se-81	4110	4	13.1	14				15.5	5.2	0.118	220±50	2	1	256	171	130	308
Se					15.5	5.2	0.118										
Br-80	60	5	13.35	14				16	7	0.175	405±56	7	1	488	417	283	345
Br-82				14				16	7	0.175	324±54	3	4		374		
Br					16*	7*	0.175*										
Rb-86	180	1	10.65	11				16.75	4.1	0.192	216±86	2	4	289	264		195
Rb					16.75	4.1	0.192										

TABLE I (continued)

COMPOUND NUCLEUS	D_{obs} EXPTL eV	Ref	a_{exp} MeV^{-1}	a_{sist} MeV^{-1}	EXPERIMENTAL E_R MeV	EXPERIMENTAL Γ_R MeV	EXPERIMENTAL σ_R barn	ADOPTED E_R MeV	ADOPTED Γ_R MeV	ADOPTED σ_R barn	$\Gamma_{\gamma\ exp}$ mV	N° of Resonances	Ref	$\langle\Gamma_\gamma\rangle$ From a exp mV	Γ_γ From a sist mV	$\langle\Gamma_\gamma\rangle$ W - R mV	$\langle\Gamma_\gamma\rangle$ MSGRV mV
Zr-91	5690	4	11	11	16.5	4.23	0.184	16.5	4.23	0.184	290±82	4	4	290	275	181	333
Zr-92	336	4	11.7	12.5	16.3	4.73	0.165	16.3	4.73	0.165	201±59	8	4	195	163	189	231
Zr-93	3560	4	13.2	13.6				16.2	5.2	0.161	252±156	8	1	181	154	123	227
Zr-94					16.2	5.2	0.161										
Zr-95	1810	4	14.42	15.3				16.2	5.2	0.161	327±200	4	1	84	70	150	183
Nb-93					16.5	4.7	0.2										
Nb-94	32.5	5	13.93	13.6				16.5	4.7	0.2	162±27	12	1	134	159	150	89
Nb-95				14.6				16.5	4.7	0.2	187	2	1		127		
Mo-95	430	1	14.64	12.5				16.8	5	0.280	149	1	4	157	204	171	274
Mo-96	51	4	15	14.6				16.8	5	0.280	159±12	6	4	150	161	202	187
Mo-97	1200	5	14.6	15.3				16.8	5	0.280	136±48	4	4	172	140	136	259
Mo-98	50	1	15.94	15.8	16.8	5	0.280	16.8	5	0.280	137±65	5	4	115	118	167	165
Mo-99	940	5	18.42	16.3				16.8	5	0.280	91±17	4	4	45	63	80	152
Mo-101	770	5	19.5	16.8				16.8	5	0.280	103±45	2	4	47	90	60	135
Tc-100	24.4	5	15.6	16.3				16.8	5	0.280	112±32	4	4	130	116	137	142
Ru-100	34	1	14.96	15.8				16.8	5	0.280	160±80	2	1	172	148	229	229
Ru-102	22.3	4	15.6	16.6				16.8	5	0.280	198±53	8	4	154	130	168	212
Rh-103					14.3	3	0.15										
					17.5	3.8	0.24										
Rh-104	33.8	4	16.7	16.7				14.3	3	0.15	161±9	21	4	106	106	165	116
								17.5	3.8	0.24							
Pd-106	14.7	1	16.75	16.9				15.7	5	0.210	155±8	5	4	118	116		135
Pd-108					15.7	5	0.210										
Pd-109				17				15.7	5	0.210	103±19	2	4		101		

TABLE I (continued)

COMPOUND NUCLEUS	D_{obs} EXPTL eV	Ref	a_{exp} MeV^{-1}	a_{sist} MeV^{-1}	EXPERIMENTAL E_R MeV	EXPERIMENTAL Γ_R MeV	EXPERIMENTAL σ_R barn	ADOPTED E_R MeV	ADOPTED Γ_R MeV	ADOPTED σ_R barn	$\Gamma_{\gamma\ exp}$ mV	N° of Resonances	Ref	$<\Gamma_\gamma>$ From a_{exp} mV	$<\Gamma_\gamma>$ From a_{sist} mV	$<\Gamma_\gamma>$ W - R mV	$<\Gamma_\gamma>$ MSGRV mV
Ag-107					15	4.81	0.062										
					16.6	7.01	0.099										
Ag-108	17.5	1	17.1	16.8				15	4.81	0.062	141±14	14	4	145	152	172	152
								16.6	7.01	0.099							
Ag-110	19	4	18.2	17				15	4.81	0.062	133±13	21	4	103	125	141	133
								16.6	7.01	0.099							
In-114	11	1	15.8	17.1				14	3	0.116	71±8	4	4	136	110		98
								16.3	3.8	0.24							
In-115					14	3	0.116										
					16.3	3.8	0.24										
In-116	10	5	17.1	17.2				14	3	0.116	89±28	19	4	94	93	154	83
								16.3	3.8	0.24							
Sn-118	25	5	17.3	16.5	15.6	4.76	0.255	15.6	4.76	0.255	78±28	10	4	131	150	133	115
Sn-124					15.2	4.81	0.283										
Sb-122	10	5	17.4	17.5				15.2	4.81	0.283	95±12	8	4	156	153	120	84
Sb-124	21	5	17	17.8				15.2	4.81	0.283	94±23	4	4	137	121	111	84
Te-124	29.2	4	17.6	17.7				15.2	4.81	0.283	114±47	4	4	151	148	169	97
Te-126	37.8	5	16.8	18				15.2	4.81	0.283	142±5.4	4	1	182	150	151	108
Xe-130				17.5				15.3	5	0.287	118±22	5	4		165		
Xe-132				16.8				15.3	5	0.287	119±22	4	4		176		
Cs-133					15.3	5	0.287										
Cs-134	19.2	1	16.4	16.3				15.3	5	0.287	114±22	5	4	185	185	140	133
Ba-136	26	5	17	15.5				15.3	4.61	0.327	105±9.6	9	4	162	209	166	87
Ba-138				13.5	15.3	4.61	0.327	15.3	4.61	0.327	105±13	2	4		256		

TABLE I (continued)

COMPOUND NUCLEUS	D_{obs} EXPTL eV	Ref	a_{exp} MeV^{-1}	a_{sist} MeV^{-1}	EXPERIMENTAL E_R MeV	EXPERIMENTAL Γ_R MeV	EXPERIMENTAL σ_R barn	ADOPTED E_R MeV	ADOPTED Γ_R MeV	ADOPTED σ_R barn	$\Gamma_{\gamma\ exp}$ mV	N° of Resonances	Ref	$<\Gamma_\gamma>$ From a_{exp} mV	$<\Gamma_\gamma>$ From a_{sist} mV	$<\Gamma_\gamma>$ W-R mV	$<\Gamma_\gamma>$ MSGRV mV
Pr-141					15.16	4.49	0.32										
Pr-142	31.2	1	18.25	17				15.16	4.49	0.32	85±17	10	4	94	115	87	50
Nd-144	32	5	18	18.5	15.1	5.3	0.317	15.1	5.3	0.317	73±7.3	17	4	138	129	91	86
Nd-145	520	1	20.21	19.6	15	6.5	0.297	15	6.5	0.297	78±12	2	1	114	128	64	93
Nd-146	17.7	4	20.4	20.8	14.8	6	0.308	14.8	6	0.308	53±10	17	4	115	108	76	66
Nd-147	310	1	23.54	21.8				14.8	6	0.308	55±8	2	1	49	61	37	67
Nd-148					14.7	7.2	0.263										
Nd-149	258	4	26	23.1				14.7	7.2	0.263	85±35	5	4	42	60		54
Nd-150					12.3	3.3	0.174										
					16	5.2	0.223										
Nd-151	247	4	24.9	24.8				12.3	3.3	0.174	84±19	5	4	31	31		60
								16	5.2	0.223							
Pm-148	4.76	5	21.8	21.8				14.1	4	0.335	68±8	5	4	63	63	65	73
Sm-148	7.4	1	20.51	20.7	14.1	4	0.335	14.1	4	0.335	71±27	4	4	80	78	90	67
Sm-150	2.8	4	23.3	23	13.6	5.5	0.36	13.6	5.5	0.36	64±3.3	4	4	120	125		50
Sm-152					11.6	2.4	0.4										
					14.7	3.4	0.42										
Sm-153	52.5	1	25.4	24.8				11.6	2.4	0.4	57±4	9	10	50	58	49	61
								14.7	3.4	0.42							
Sm-154					11	3	0.204										
					15.3	4	0.320										
Sm-155	125	1	24.6	23.2				11	3	0.204	74±11	3	10	51	63	58	64
								15.3	4	0.320							

TABLE I (continued)

COMPOUND NUCLEUS	D_{obs} EXPTL eV	Ref	a_{exp} MeV^{-1}	a_{sist} MeV^{-1}	EXPEPIMENTAL E_R MeV	EXPEPIMENTAL Γ_R MeV	EXPEPIMENTAL σ_R barn	ADOPTED E_R MeV	ADOPTED Γ_R MeV	ADOPTED σ_R barn	$\Gamma_{\gamma\ exp}$ mV	N° of Resonances	Ref	$<\Gamma_\gamma>$ From a_{exp} mV	$<\Gamma_\gamma>$ From a_{sist} mV	$<\Gamma_\gamma>$ W - R mV	$<\Gamma_\gamma>$ MSGRV mV
Eu-152	1	1	24.1	24.1				12.3	2.8	0.156	92±12	73	4	72	72	62	100
								15.8	5.8	0.222							
Eu-153					12.3	2.8	0.155										
					15.8	5.8	0.222										
Eu-154	1.45	1	22.8	24.8				12.3	2.8	0.156	95±12	48	4	90	71	72	114
								15.8	5.8	0.222							
Gd-152					12	3	0.175										
					15	3.5	0.251										
Gd-153	19	5	24.6	24.1				12	3	0.175	54±7	5	4	42	45	54	103
								15	3.5	0.251							
Gd-155	19	5	24.7	24.8				11.9	2.6	0.180	65±21	3	1	36	36	54	102
								15.2	3.6	0.243							
Gd-156	1.98	4	22.2	23.9	11.9	2.6	0.180	11.9	2.6	0.180	108±28	32	4	78	62	94	101
					15.2	3.6	0.243	15.2	3.6	0.243							
Gd-157	49.3	4	22.8	23.2				11.7	2.6	0.165	82±12	6	1	51	48	72	121
								14.9	3.8	0.249							
Gd-158	5.85	4	21.4	22.6	11.7	2.6	0.165	11.7	2.6	0.165	91±22	23	4	81	69	98	107
					14.9	3.8	0.249	14.9	3.8	0.249							
Gd-159	101	4	22.9	22.4				12.2	2.77	0.215	90±13	6	1	55	60	56	94
								16	5.28	0.233							
Gd-160					12.2	2.77	0.215										
					16	5.28	0.233										
Gd-161	170	4	23.5	21.9				12.2	2.77	0.215	98±15	3	1	45	59	53	87
								16	5.28	0.233							
Tb-159					12.1	3.25	0.205										
					16	4.87	0.240										
Tb-160	3.5	5	21.8	22.4				12.1	3.25	0.805	88±8	13	4	111	103	79	115
								16	4.87	0.240							

TABLE I (continued)

COMPOUND NUCLEUS	D_{obs} EXPTL eV	Ref	a_{exp} MeV^{-1}	a_{sist} MeV^{-1}	EXPERIMENTAL E_R MeV	EXPERIMENTAL Γ_R MeV	EXPERIMENTAL σ_R barn	ADOPTED E_R MeV	ADOPTED Γ_R MeV	ADOPTED σ_R barn	$\Gamma_{\gamma\ exp}$ mV	No of Resonances	Ref	$<\Gamma_\gamma>$ From a_{exp} mV	$<\Gamma_\gamma>$ From a_{sist} mV	$<\Gamma_\gamma>$ W - R mV	$<\Gamma_\gamma>$ MSGRV mV
Dy-157	3.4	1	25.74	24.8				12.1	3.25	0.205	133±25	2	1	64	71		103
								16	4.87	0.240							
Dy-162	2.8	4	21.3	22.2				12.1	3.25	0.205	113±25	6	4	121	109	114	113
								16	4.87	0.240							
Dy-163	72	1	22.04	21.9				12.1	2.7	0.25	155±15	2	1	76	77	82	147
								15.6	4.8	0.287							
Dy-164	8	4	21.7	21.7				12.1	2.7	0.25	109±6	4	4	92	92	116	108
								15.6	4.8	0.287							
Ho-165					12.1	2.7	0.25										
					15.6	4.8	0.287										

ONE GROUP FISSION PRODUCT CAPTURE CROSS-SECTIONS AS USED IN FAST REACTOR CALCULATIONS

C. J. DEAN

United Kingdom Atomic Energy Authority Atomic Energy Establishment
Winfrith Dorchester Dorset

ABSTRACT

In order to give a broad comparison of the various cros-section evaluations available for use in fast reactor calculations a typical fast reactor spectrum has been used to form 1-group cross-sections. This spectrum averaged over the 37 energy groups of the FD5 set is given in Table 2.

One-group capture cross-sections for fission products condensed from the 1971 Lucas Heights data (1), and the Australian and Italian combined evaluation of 1967 (2), (3) over the energy range 10 MeV to 0.0001 eV using this standard fast reactor spectrum are given in Table 1.

REFERENCES

(1) BERTRAM W.K., CLAYTON E., COOKE J.H., FERGUSON H.D., MUSGROVE A.R. & ROSE E.K. (June 1971) AAEC/E214

(2) BENZI V. & BARTOLANI M.V. (Oct. 1966) IAEA Paris Conf. on Nuclear Data for Reactors 1, 537

(3) COOK J.L. (Oct. 1966) IAEA Paris Conf. on Nuclear Data for Reactors 1, 549

Table 1 - 1 GROUP CROSS-SECTIONS IN BARNS

Isotope	Data Files Produced from the Lucas Heights Data of 1971 (1)		The Australian and Italian combined Data Files of 1967 (2) & (3)	
	DFN	Cross-Section	DFN	Cross-Section
Zn72	4001	0.005		
Ga72	4002	0.197		
Ge72	4003	0.021		
Ge73	4004	0.182		
Ge74	4005	0.013		
Ge76	4006	0.013		
Ge77	4007	0.067		
As75	4008	0.428		
As76	4009	0.748		
As77	4010	0.339		
Se76	4011	0.107		
Se77	4012	0.247		
Se78	4013	0.088		
Se79	4014	0.342		
Se80	4015	0.045		
Se82			702	0.011
Br81	4016	0.483	701	1.030
Br82	4017	0.556		
Kr82	4018	0.152		
Kr83	4019	0.396	703	0.871
Kr84	4020	0.059	704	0.357
Kr85	4021	0.129	705	0.144
Kr86	4022	0.005	707	0.004
Rb85	4023	0.145	706	0.178
Rb86	4024	0.305		
Rb87	4025	0.032	708	0.014
Sr86	4026	0.036		
Sr88	4027	0.005	709	0.002
Sr89	4028	0.012	710	0.022
Sr90	4029	0.007	712	0.093
Sr91	4030	0.018		
Y 89	4031	0.010	711	0.012
Y 90	4032	0.038	713	0.152
Y 91	4033	0.048	714	0.015
Y 93	4034	0.031		
Zr90	4035	0.006		
Zr91	4036	0.089	715	0.082
Zr92	4037	0.011	716	0.032
Zr93	4038	0.102	717	0.012
Zr94	4039	0.010	718	0.044
Zr95	4040	0.076		
Zr96	4041	0.046	720	0.058
Zr97	4042	0.048		
Nb95	4043	0.165		

Table 1: (continued)

Mo95	4044	0.293	719	0.319
Mo96	4045	0.080		
Mo97	4046	0.254	721	0.353
Mo98	4047	0.160	722	0.149
Mo99	4048	0.258		
Mo100	4049	0.116	724	0.126
Tc99	4050	0.467	723	0.657
Ru100	4051	0.452		
Ru101	4052	1.526	725	0.796
Ru102	4053	0.277	726	0.350
Ru103	4054	0.463		
Ru104	4055	0.141	728	0.216
Ru105	4056	0.310		
Ru106	4057	0.065		
Rh103	4058	0.541	727	0.833
Rh105	4059	0.234	729	0.009
Pd104	4060	0.410		
Pd105	4061	0.464	730	1.139
Pd106	4062	0.145	731	0.252
Pd107	4063	0.458	732	1.066
Pd108	4064	0.096	733	0.287
Pd109	4065	0.275		
Pd110	4066	0.043		
Pd112	4067	0.061		
Ag109	4068	0.569	734	1.010
Ag111	4069	0.285		
Cd110	4070	0.282		
Cd111	4071	0.221		
Cd112	4072	0.173		
Cd113	4073	0.266	735	0.593
Cd114	4074	0.143		
Cd115	4075	0.344		
Cd116	4076	0.041		
In115	4077	0.483	736	0.717
Sn115	4078	0.152		
Sn116	4079	0.111		
Sn117	4080	0.289		
Sn118	4081	0.111		
Sn119	4082	0.200		
Sn120	4083	0.042		
Sn121	4084	0.245		
Sn122	4085	0.037		
Sn123	4086	0.126		
Sn124	4087	0.027		
Sn125	4088	0.102		
Sn126	4089	0.012		
Sb121	4090	0.392		
Sb122	4091	0.706		
Sb123	4092	0.294		

Table 1: (continued)

Sb124	4093	0.328		
Sb125	4094	0.144	737	0.472
Sb126	4095	0.364		
Sb127	4096	0.111		
Sb128	4097	0.154		
Te122	4098	0.217		
Te123	4099	0.415		
Te124	4100	0.125		
Te125	4101	0.288		
Te126	4102	0.071		
Te127	4103	0.223		
Te128	4104	0.037	739	0.025
Te129	4105	0.087		
Te130	4106	0.008	741	0.030
Te131	4107	0.004		
Te132	4108	0.001		
I 127	4109	0.498	738	0.974
I 129	4110	0.266	740	0.565
I 130	4111	0.588		
I 131	4112	0.168	742	0.450
I 133	4113	0.0004		
I 135	4114	0.002	749	0.004
Xe128	4115	0.349		
Xe130	4116	0.230		
Xe131	4117	0.420	743	0.393
Xe132	4118	0.113	744	0.061
Xe133	4119	0.111	745	0.377
Xe134	4120	0.017	747	0.041
Xe135	4121	0.016	750	0.009
Xe136	4122	0.004	752	0.011
Cs133	4123	0.388	746	0.527
Cs134	4124	0.449	748	1.834
Cs135	4125	0.160	751	0.305
Cs136	4126	0.177		
Cs137	4127	0.017	753	0.002
Ba134	4128	0.381		
Ba136	4129	0.080		
Ba137	4130	0.108		
Ba138	4131	0.007	754	0.003
Ba140	4132	0.194		
La139	4133	0.049	755	0.020
La140	4134	0.186		
Ce140	4135	0.018	756	0.025
Ce141	4136	0.119		
Ce142	4137	0.043	758	0.035
Ce143	4138	0.120		
Ce144	4139	0.076		
Pr141	4140	0.131	757	0.160
Pr142	4141	0.293		
Pr143	4142	0.410		

Table 1: (continued)

Pr145	4143	0.309		
Nd142	4144	0.078		
Nd143	4145	0.421	759	0.003
Nd144	4146	0.131	760	0.121
Nd145	4147	0.352	761	0.573
Nd146	4148	0.092	762	0.155
Nd147	4149	0.515		
Nd148	4150	0.263	764	0.210
Nd150	4151	0.109	768	0.256
Pm147	4152	1.146	763	1.171
Pm148	4153	0.903	766	3.061
Pm149	4154	1.105		
Pm151	4155	1.131		
Sm147	4156	1.212		
Sm148	4157	0.219		
Sm149	4158	1.417	767	2.001
Sm150	4159	0.583	769	0.645
Sm151	4160	2.591	770	3.322
Sm152	4161	0.583	771	0.541
Sm153	4162	1.512		
Sm154	4163	0.268	773	0.249
Sm156	4164	0.402		
Eu153	4165	1.960	772	2.610
Eu154	4166	2.893	774	5.365
Eu155	4167	1.738	775	2.267
Eu156	4168	1.656		
Eu157	4169	1.077		
Gd155	4170	1.312	776	2.198
Gd156	4171	0.407	777	0.765
Gd157	4172	0.655	778	1.428
Gd158	4173	0.294		
Gd159	4174	0.345		
Gd160	4175	0.072		
Tb159	4176	1.534		
Tb160	4177	1.527		
Tb161	4178	0.816		
Dy160	4179	0.740		
Dy161	4180	1.017		
Dy162	4181	0.387		
Dy163	4182	0.571		
Dy164	4183	0.095		
Ho165	4184	1.441		
Tc99M	4185	0.425		
Cd115M	4186	0.360		
Te123M	4187	0.455		
Te125M	4188	0.289		
Te127M	4189	0.252		
Te129M	4190	0.111		
Te131M	4191	0.005		
Pm148M	4192	1.327	765	21.048

Table 2 - STANDARD FD5 FAST REACTOR SPECTRUM

Group	Lower Energy		Flux
1	10.0	MeV	0.018848
2	6.0653		0.366861
3	3.6788		1.783742
4	2.2313		5.036304
5	1.3534		6.983856
6	820.85	KeV	8.315762
7	497.87		15.164340
8	301.97		15.106515
9	183.16		18.969254
10	111.09		19.543854
11	67.380		16.799545
12	40.870		13.466378
13	24.790		9.984438
14	15.034		8.930704
15	9.1190		6.453487
16	5.5310		3.811014
17	3.3546		2.362575
18	2.0347		0.926176
19	1.2341		2.589941
20	748.52	eV	1.734904
21	454.00		0.939303
22	275.36		0.442571
23	167.02		0.154961
24	101.30		0.053409
25	61.440		0.011543
26	37.270		0.001440
27	22.603		0.000232
28	13.710		0.000029
29	8.3150		0.000003
30	5.0440		0.0
31	3.0590		0.0
32	1.8550		0.0
33	1.1250		0.0
34	0.6830		0.0
35	0.41400		0.0
36	0.10000		0.0
37	0.00010		0.0

Compilation of Neutron Capture Cross Section Data for Fission Product Nuclides in the Energy Range from 1 keV to 15 MeV

H. Matsunobu
SUMITOMO Atomic Energy Ind., Ltd.

Abstract

Nuclear data of the fission products play an important role in many fields relating to nuclear energy. In particular, neutron capture cross section of the fission product nuclides is an important quantity in order to determine reactor design and burn up of nuclear fuel. However, the situation of the data for neutron capture cross section is not satisfactory at present.

In this paper, status of the experimental data for neutron capture cross section which were compiled up to date for the important 28 nuclides in the energy range from 1 keV to 15 MeV is explained, and comparisons with the evaluated data are given. Furthermore, measurements of neutron capture cross section are requested for the important nuclides whose the experimental data are not obtained or poor.

1. Introduction

Neutron capture cross section of fission product nuclides plays an important role in the burn up characteristics of reactor. Accordingly, in order to do the accurate burn up calculation, it is necessary to prepare a reliable neutron capture cross section set of FP nuclides. However, the experimental data for FP nuclides are neither enough nor complete at present. Therefore, for FP nuclides whose the neutron capture cross section has not been measured, it is required to produce

the cross sections by theoretical calculation of the basis of some nuclear models. In this case, it is necessary to know the systematic trends for the nuclear parameters and cross sections of the neighboring nuclides whose the experimental data are obtained. In order to grasp this systematic trends, it is desirable to get the experimental data as many as possible.

On the basis of such background, compilation work of the experimental data for neutron capture cross sections of the FP nuclides has been commenced as a part of the nuclear data evaluation works[1] in JNDC (Japanese Nuclear Data Committee) since 1970. As the first step, the experimental data cited in BNL-325 2nd Edition, Supplement No. 2[2] were compiled in the atomic number range $32 \leq Z \leq 66$ in 1970, and a comparison with the evaluated data of Benzi and Reffo [3] was done in the energy range from 1 keV to 10 MeV.

On neutron capture cross sections of the FP nuclides, many measurements have been performed since 1966 in which the above-mentioned Supplement published, and a number of data were accumulated up to date. Therefore, as the second step, the new experimental data for the following important 28 nuclides which play the most effective role in the burn up calculation of fast reactor have been searched in the energy range from 1 keV to 15 MeV.

^{90}Sr, ^{93}Zr, ^{95}Mo, ^{97}Mo, ^{99}Tc, ^{101}Ru, ^{102}Ru, ^{104}Ru, ^{106}Ru, ^{103}Rh, ^{105}Pd, ^{107}Pd, ^{109}Ag, ^{129}I, ^{131}Xe, ^{133}Cs, ^{135}Cs, ^{137}Cs, ^{144}Ce, ^{143}Nd, ^{144}Nd, ^{145}Nd, ^{147}Pm, ^{147}Sm, ^{149}Sm, ^{151}Sm, ^{153}Eu, ^{155}Eu.

The compiled experimental data are compared with the evaluated data of Benzi and Reffo, Musgrove[4], and JNDC data which were obtained in the above-mentioned evaluation works.

As the next step, compilation work of the new experimental data for nuclides except the above-mentioned important 28 nuclides

is in progress at present. These compiled experimental data will be serviceable in estimation of the neutron capture cross sections for the nuclides whose the experimental data do not exist.

2. Neutron Capture Cross Sections for the Important 28 Nuclides

The above-mentioned 28 nuclides were selected on the basis of the fact that the important FP nuclides which give the most dominant effect to the burn up characteristics of reactor, have large values of macroscopic cross section which is defined as microscopic neutron capture cross section times yield ratio. The experimental references on neutron capture cross section for 28 important nuclides were searched using CINDA 72, and the numerical data were collected from the original literatures and NEUDADA. As the result of search, 40 literatures and the numerical data were compiled in the energy range from 1 keV to 15 MeV for the following 11 nuclides.

^{95}Mo, ^{97}Mo, ^{99}Tc, ^{102}Ru, ^{104}Ru, ^{103}Rh, ^{109}Ag, ^{133}Cs, ^{147}Sm, ^{149}Sm, ^{153}Eu.

However, these are not all of the experimental data, because there are some literatures and data that we can not obtain and are not also cited in NEUDADA.

On the remaining 17 nuclides among the important 28 nuclides, the experiments for neutron capture cross section have not been performed up to date. The reason may be that it is difficult to perform the measurement, because the most nuclides among the above-mentioned 17 nuclides are radio-active nuclides. But, it is noted that there are no data in the fast energy range for the most isotopes of Xe which are not radio-active.

On 11 nuclides whose the experimental data exist, there are large differences between numbers of data points for each nuclide.

That is, there is only one data point for ^{147}Sm and ^{149}Sm, on the contrary the experimental data are very rich for ^{103}Rh and ^{133}Cs. The status of the data distribution for 11 nuclides is shown in Table 1.

Table 1 The status of the experimental data for 11 nuclides

Nuclide	No. of References	No. of Data Points	Energy Range of the Experimental Data
^{95}Mo	1	14	below 50 keV
^{97}Mo	1	24	below 60 keV
^{99}Tc	1	30	below 50 keV
^{102}Ru	3	3	2, 24, and 190 keV
^{104}Ru	7	7	2, 24(2 points), 190 keV, 3, 14, and 15 MeV
^{103}Rh	22	many	all range
^{109}Ag	6	37	below 6 MeV
^{133}Cs	9	104	all range
^{147}Sm	1	1	30 keV
^{149}Sm	1	1	30 keV
^{153}Eu	1	20	below 40 keV

The experimental data collected for 11 nuclides are shown in Fig. 1 through 11, and compared with the evaluated data of JNDC and Benzi & Reffo, or Musgrove. Agreement between the evaluated data and the experimental data is generally good for 11 nuclides. However, in detail, there are some discrepancies between the experimental and the evaluated data, between the experimental data, and between the evaluated data, respectively. Especially, for ^{103}Rh, ^{109}Ag, and ^{133}Cs, it is noted that considerable discrepancies exist between the experimental data. On the other hand, it is seen that large discrepancies between the evaluated data of Benzi & Reffo

and JNDC appear in MeV region. That is, the curve of JNDC data are falling down rapidly in MeV region, while the curve of Benzi & Reffo data are rising up above 10 MeV. These discrepancies may be caused by the difference of calculation methods that the contribution for direct process of nuclear reaction is not taken into account in the evaluation of JNDC, while it is taken into account in that of Benzi & Reffo. Judging from the experimental data near 14 MeV for ^{104}Ru, ^{103}Rh, and ^{133}Cs, it should be taken into account of necessity, although this energy range is not so important in reactor calculation.

3. Compilation of the Experimental Data for FP Nuclides except the Important 28 Nuclides

It is necessary to collect the experimental data as many as possible, in order to know the systematic trends of neutron capture cross section for FP nuclides. Accordingly, as the next step, compilation work of the new experimental data measured since 1966 has been performed in the atomic number range $32 \leq Z \leq 66$ for FP nuclides except the important 28 nuclides. This work is not completed at present, because a number of new data are accumulated up to date for many nuclides. At present, the experimental data for 87 nuclides including natural elements have been compiled. However, the number of the experimental data for each nuclide is generally poor except some nuclides. Nuclides which have many data are the following 14 nuclides and 9 elements.

^{75}As, ^{89}Y, ^{90}Zr, ^{93}Nb, Mo, ^{98}Mo, ^{100}Mo, Ag, ^{107}Ag, Cd, In, ^{115}In, Sb, ^{127}I, ^{138}Ba, La, ^{141}Pr, Sm, ^{151}Eu, Gd, ^{158}Gd, ^{159}Tb, Dy,

Next, comparison with the evaluated data of Benzi & Reffo was done for the stable nuclides and the natural elements. As the

results, it was confirmed that agreements are good for nuclides and elements which have many experimental data.

4. Remarks

As mentioned in the previous sections, a number of the experimental data for FP nuclides have been accumulated up to date, but number of the data for each nuclide is not enough except some nuclides. Especially, the data in the energy range above 100 keV are poor for the most nuclides, and the data for radio-active nuclides are also scanty. Furthermore, there are some discrepancies between the experimental data for the nuclides which have many data. These discrepancies are an obstacle to evaluate the data, and the source of them should be clarified in early time.

In view of these facts, it is necessary to have reliable experimental data (neutron capture and inelastic scattering cross sections and resonance parameters) as many as possible in addition to present data, in order to grasp the systematic trends (energy and N-Z dependences) of the data, and to do more accurate calculation and evaluation of neutron capture cross sections.

At least, it is an urgent problem to obtain any experimental data for the important nuclides whose neutron capture cross sections or resonance parameters have not been measured and the data are poor.

References

1. Evaluation of Neutron Cross Sections for 28 Important Fission Product Nuclides: (Communicated by Igarashi S) (1973)
2. BNL 325, 2nd Edition, Supplement No. 2 (1966)
3. Benzi V. and Reffo G. : CCDN-NW/10 (1969)
4. Musgrove A. R. de L. : AAEC/E198 (1969)

5. Kapchigashev S. V. and Popov Yu. P.: JINR-1845 104 (1964)
6. Chou W. : KFK-1270/1 and KFK-EXT4/70-28 (1970)
7. Macklin R. L. et al. : PR 107 504 (1957)
8. Lyon W. S. and Macklin R. L. : PR 114 1619 (1959)
9. Schuman R. P. : WASH 1127 72 (1969)
10. Perkin J. L. et al. : PPS 72 505 (1958)
11. Gray P. R. et al. : NP 75 215 (1966)
12. Chaubey A. K. and Sehgal M. L. : PR 152 1055 (1966)
13. Peto G. et al. : JNE 21 797 (1967)
14. Hummel V. and Hamermesh B. : PR 82 67 (1951)
15. Pasechnik M. V. et al. : 58 GENEVA 15 18 (1958)
16. Diven B. C. et al. : PR 120 556 (1960)
17. Weston L. W. et al. : AP 10 477 (1960)
18. Gibbons J. H. et al. : PR 122 182 (1961)
19. Neiler J. H. : 61 VIENNA 1 95 (1961)
20. Block R. C. et al. : 61 SACLAY TF 203 (1961)
21. Furr : TID-16059 (1962)
22. Popov Yu. P. and Shapiro F. L. : ZET 42 988 (1962)
23. Macklin R. L. et al. : PR 129 2695 (1963)
24. Csikai J. et al. : NP 41 316 (1963)
25. Moxon M. C. and Rae E. R. : NIM 24 445 (1963)
26. Cox S. A. : PR 133 B378 (1964)
27. Pönitz W. P. : NR 19/65 P. 53 (1965)
28. Csikai J. et al. : NP A95 229 (1967)
29. Macklin R. L. and Gibbons J. H. : PR 159 1007 (1967)
30. Fricke M. and Carlson A. : ANS 14 352 (1971)
31. Rigaud F. et al. : NP A173 551 (1971)
32. Hughes D. J. et al. : PR 91 1423 (1953)

33. Kononov V. N. and Stavisskij Yu.Ja.: AE 19 457 (1965)
34. Sriramachendra M. M. et al. : 70 MADURAI 2 29 (1970)
35. Booth R. et al. : PR 112 226 (1958)
36. Borbely I. et al. : KFKI-1467/F (1963)
37. Pönitz W. P. et al. : KRL, SM1 01/9 (1967)
38. Tolstikov V. A. et al. : AE 23 566 (1967)
39. Qaim S. M. : JIN 32 1799 (1970)
40. Brzosko J. S. et al. : APP B2 489 (1971)
41. Rigaud F. et al. : NP A176 545 (1971)
42. Macklin R. L. et al. : Nature 197 370 (1963)
43. Konks V. A. and Fenin Yu. I. : DUB-1845 100 (1964)

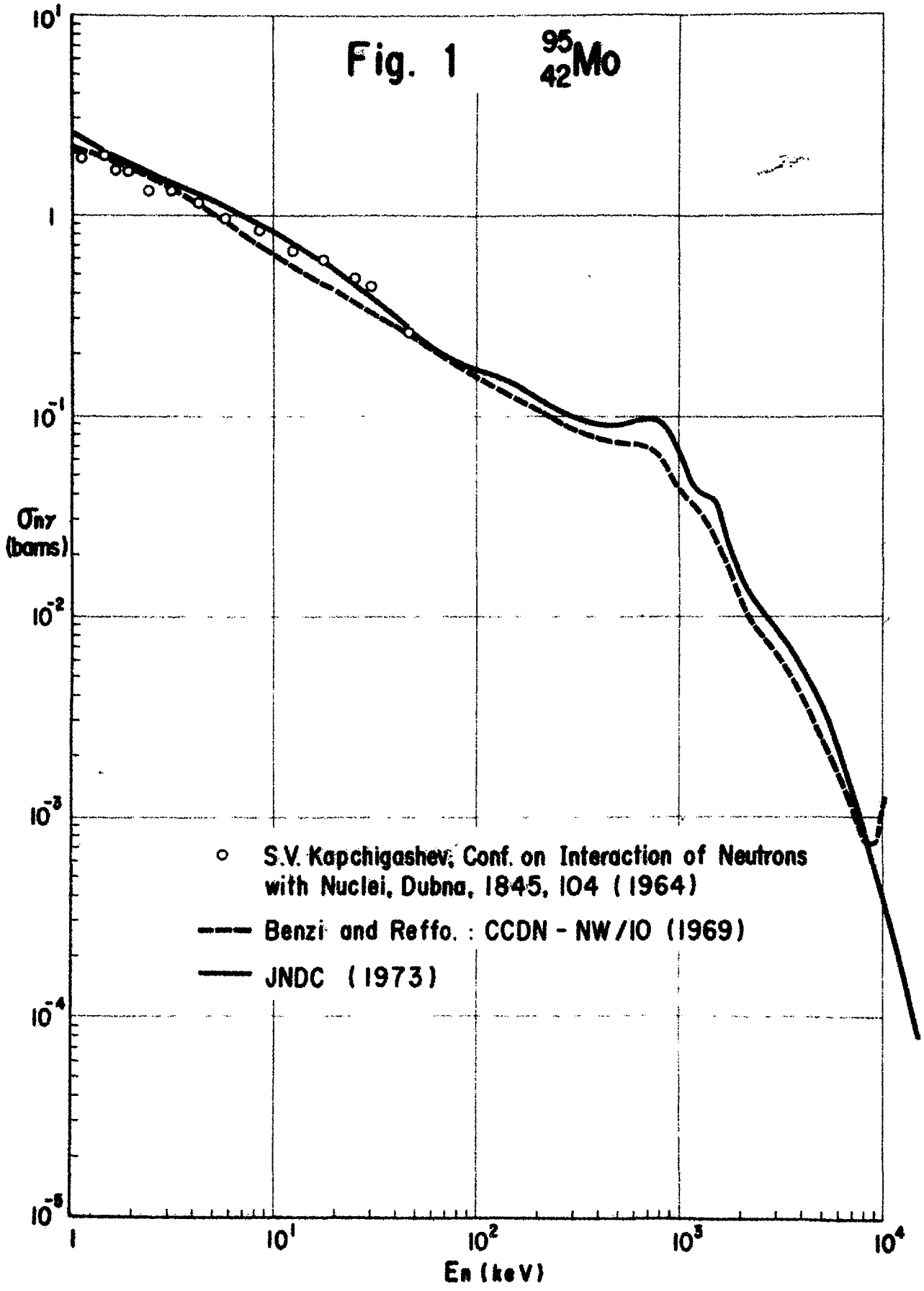
Fig. 1 $^{95}_{42}Mo$
10^{1}
1
10^{-1}
10^{-2}
10^{-3}
10^{-4}
10^{-5}
$\sigma_{n\gamma}$ (barns)
1
10^{1}
10^{2}
10^{3}
10^{4}
En (keV)
S.V. Kapchigashev, Conf. on Interaction of Neutrons with Nuclei, Dubna, 1845, 104 (1964)
Benzi and Reffo. : CCDN - NW/10 (1969)
JNDC (1973)

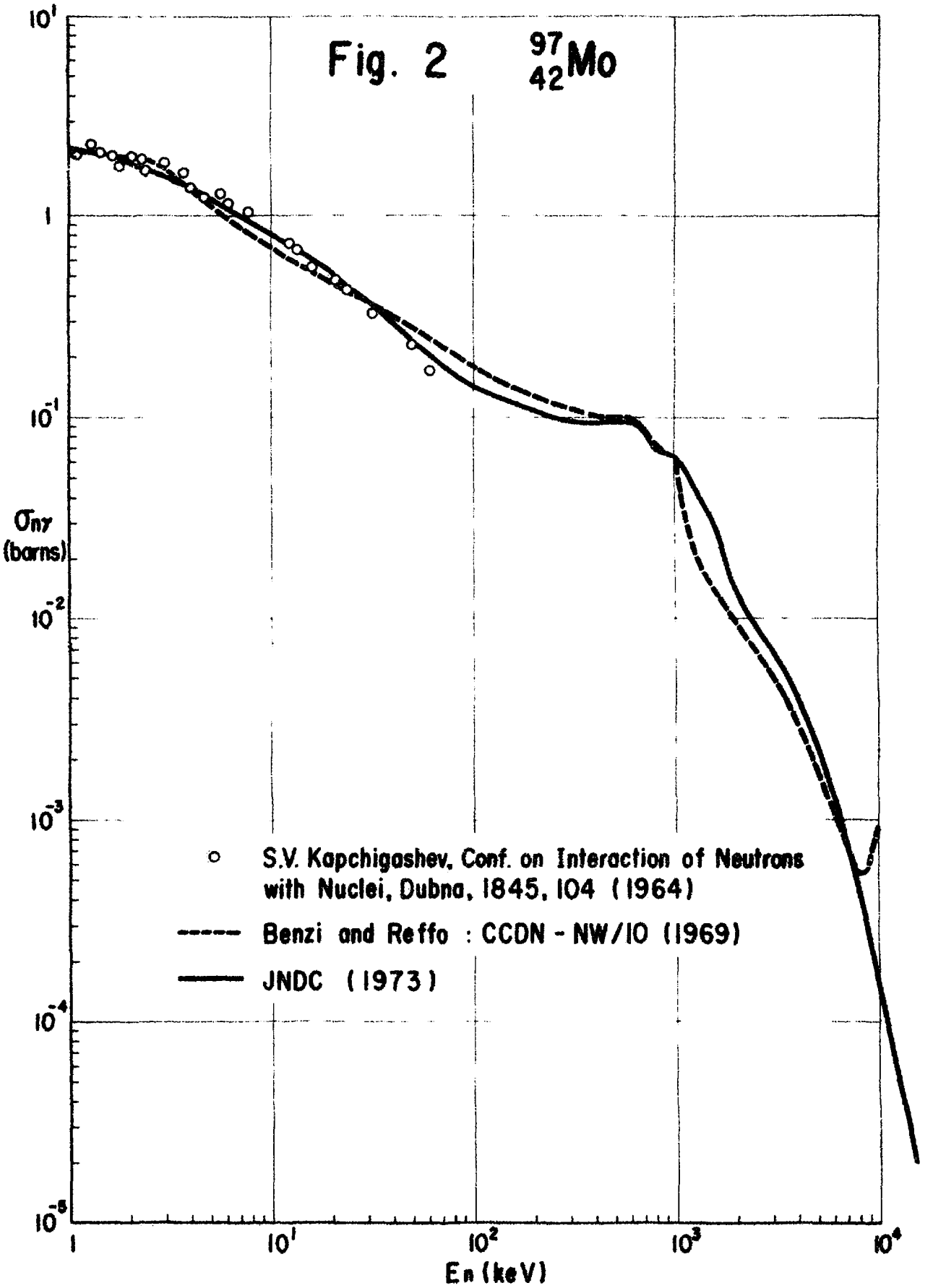
Fig. 2 $^{97}_{42}Mo$
10^{1}
1
10^{-1}
10^{-2}
10^{-3}
10^{-4}
10^{-5}
$\sigma_{n\gamma}$ (barns)
1
10^{1}
10^{2}
10^{3}
10^{4}
En (keV)
S.V. Kapchigashev, Conf. on Interaction of Neutrons with Nuclei, Dubna, 1845, 104 (1964)
Benzi and Reffo : CCDN - NW/10 (1969)
JNDC (1973)

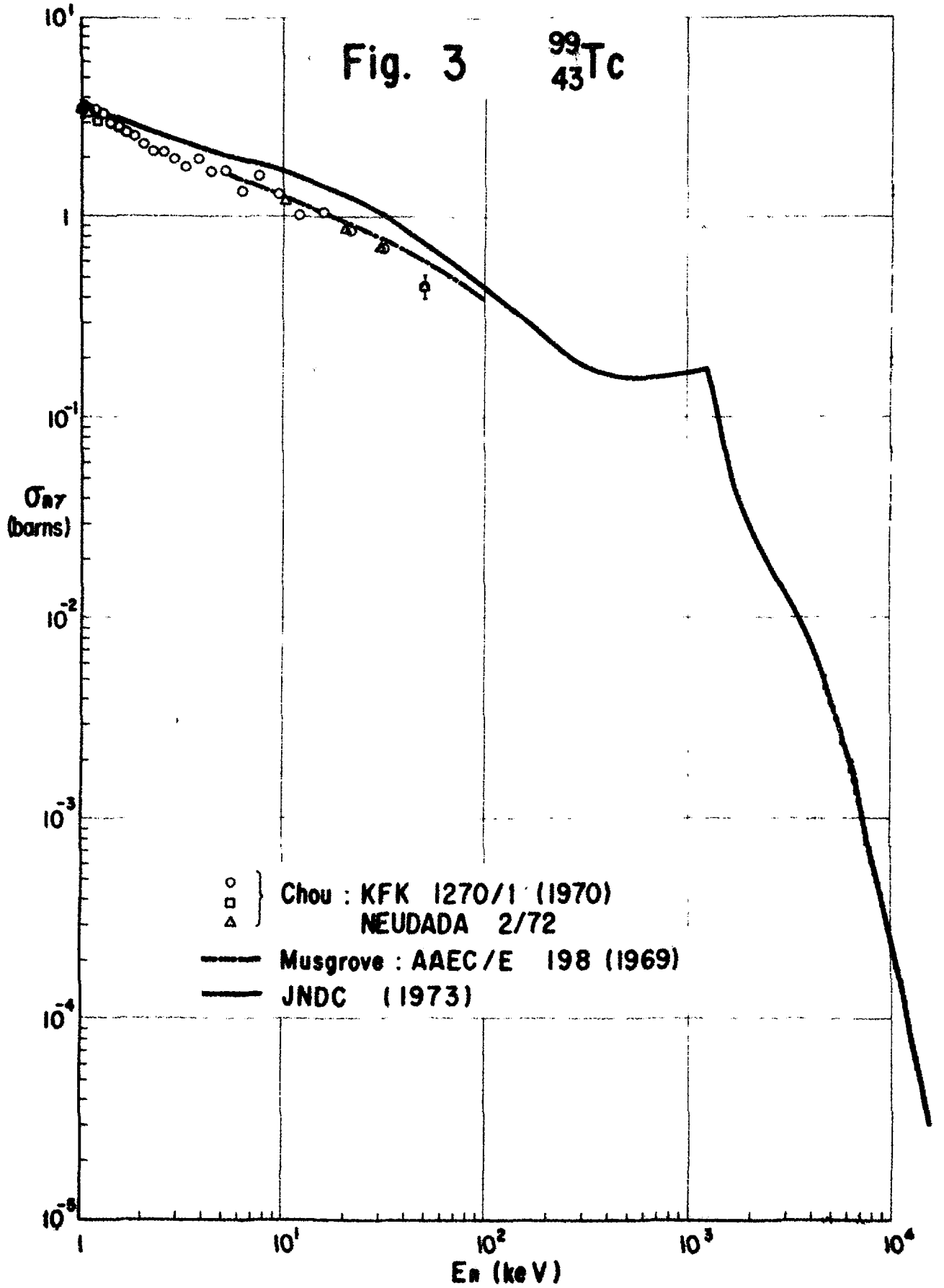
Fig. 3 $^{99}_{43}Tc$
10^{1}
1
10^{-1}
10^{-2}
10^{-3}
10^{-4}
10^{-5}
$\sigma_{n\gamma}$ (barns)
1
10^{1}
10^{2}
10^{3}
10^{4}
E_n (keV)
Chou : KFK 1270/1 (1970)
NEUDADA 2/72
Musgrove : AAEC/E 198 (1969)
JNDC (1973)

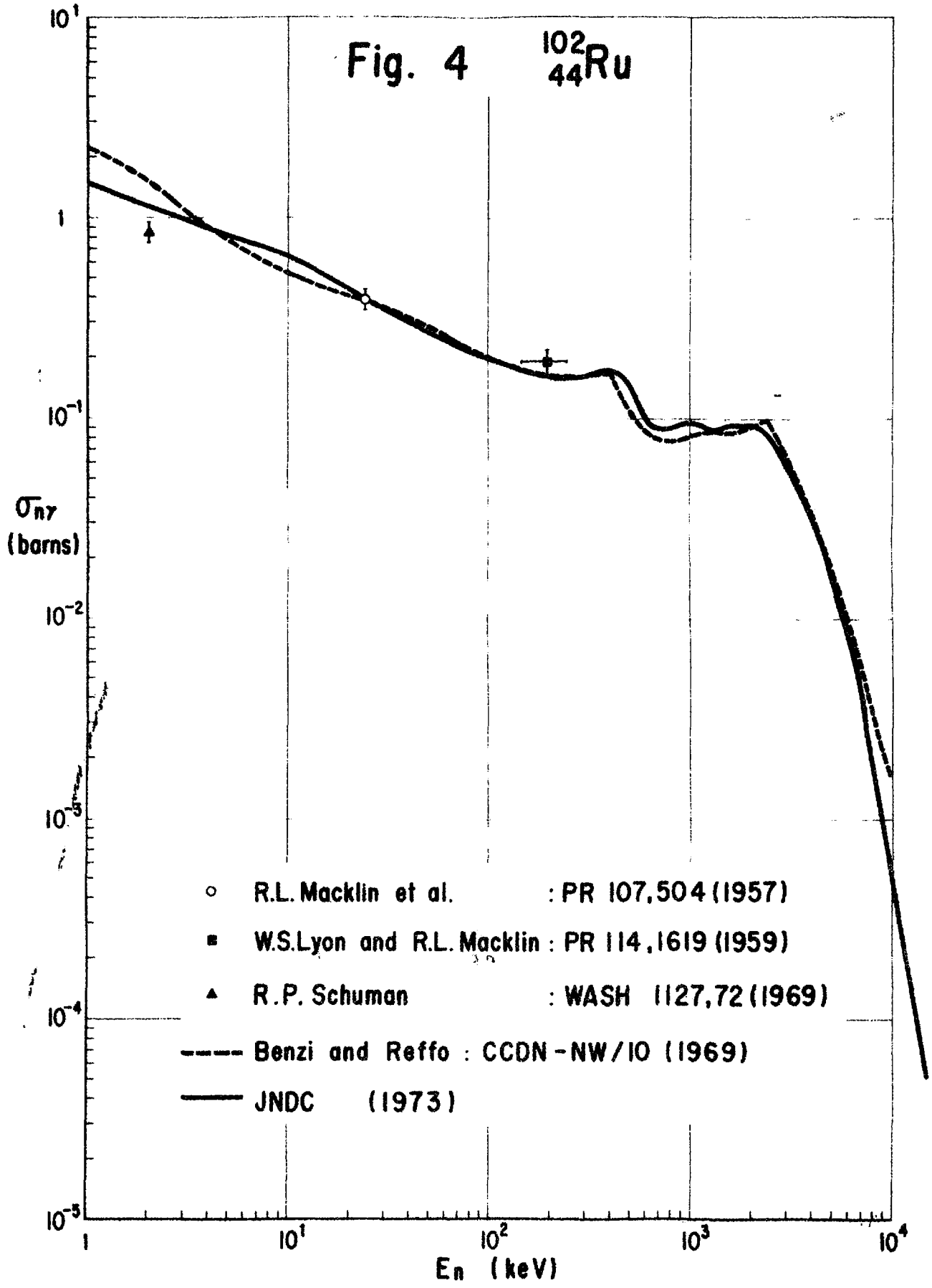
Fig. 4 $^{102}_{44}Ru$
$\sigma_{n\gamma}$ (barns)
En (keV)
R.L. Macklin et al. : PR 107,504 (1957)
W.S.Lyon and R.L. Macklin : PR 114,1619 (1959)
R.P. Schuman : WASH 1127,72 (1969)
Benzi and Reffo : CCDN-NW/10 (1969)
JNDC (1973)

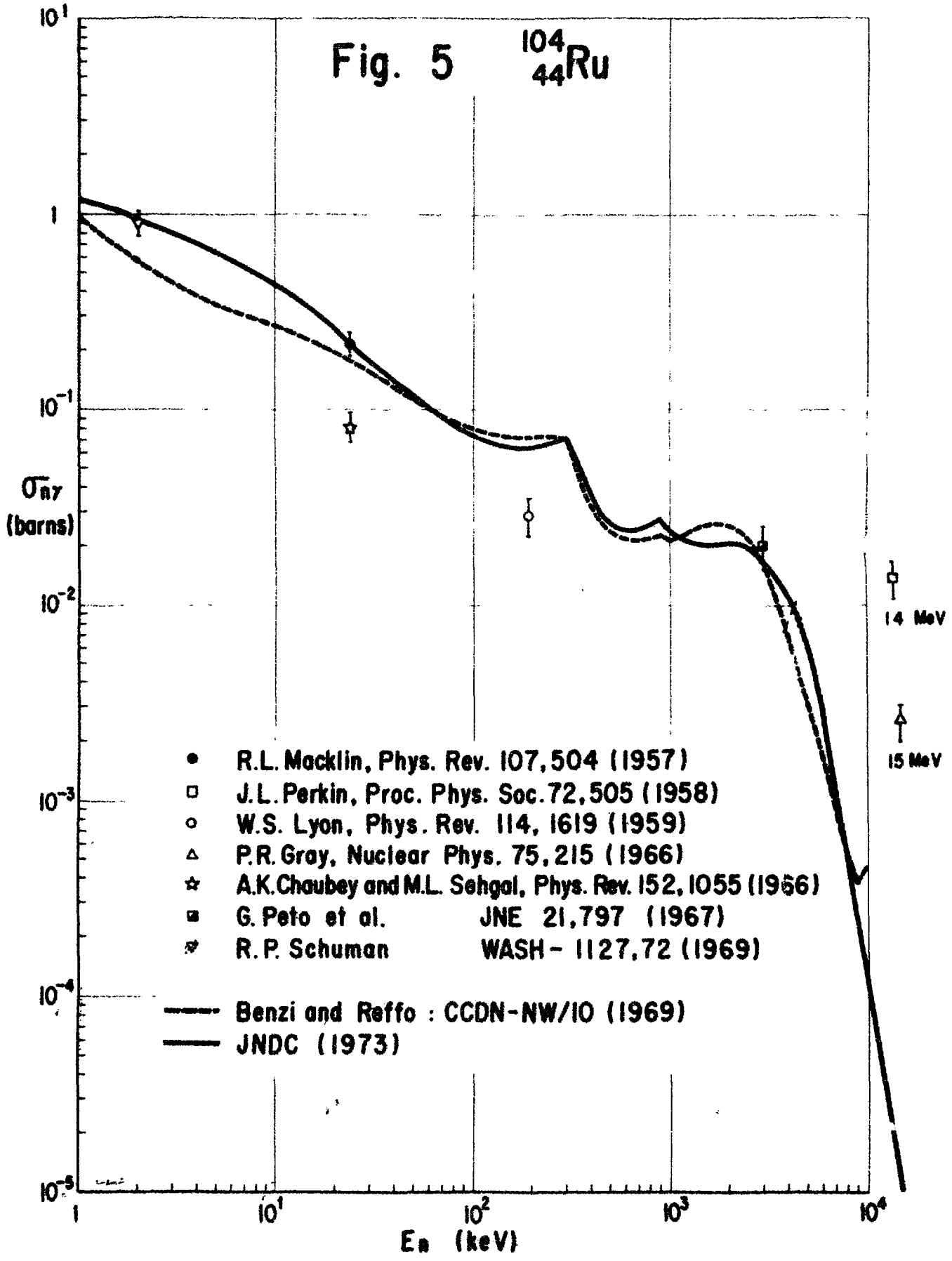
Fig. 5 $^{104}_{44}Ru$
$\sigma_{n\gamma}$ (barns)
E_n (keV)
14 MeV
15 MeV
R.L. Macklin, Phys. Rev. 107,504 (1957)
J.L. Perkin, Proc. Phys. Soc. 72,505 (1958)
W.S. Lyon, Phys. Rev. 114, 1619 (1959)
P.R. Gray, Nuclear Phys. 75,215 (1966)
A.K. Chaubey and M.L. Sehgal, Phys. Rev. 152, 1055 (1966)
G. Peto et al. JNE 21,797 (1967)
R.P. Schuman WASH-1127,72 (1969)
Benzi and Reffo : CCDN-NW/10 (1969)
JNDC (1973)

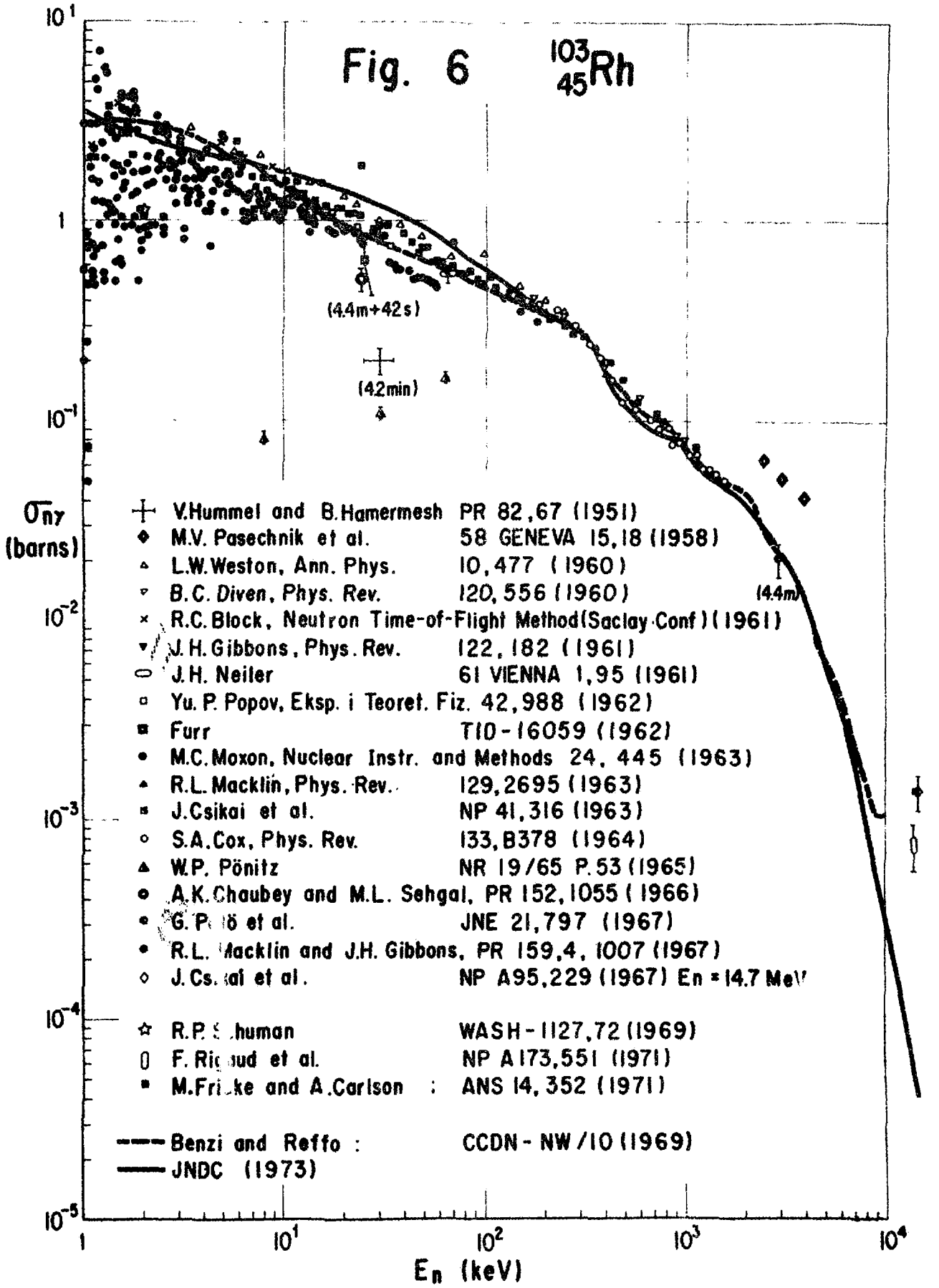
Fig. 6 $^{103}_{45}Rh$
(4.4m+42s)
(42min)
(4.4m)
$\sigma_{n\gamma}$ (barns)
V.Hummel and B.Hamermesh PR 82,67 (1951)
M.V. Pasechnik et al. 58 GENEVA 15,18 (1958)
L.W.Weston, Ann. Phys. 10,477 (1960)
B.C. Diven, Phys. Rev. 120,556 (1960)
R.C.Block, Neutron Time-of-Flight Method(Saclay Conf)(1961)
J.H.Gibbons, Phys.Rev. 122,182 (1961)
J.H. Neiler 61 VIENNA 1,95 (1961)
Yu. P. Popov, Eksp. i Teoret. Fiz. 42,988 (1962)
Furr TID-16059 (1962)
M.C.Moxon, Nuclear Instr. and Methods 24, 445 (1963)
R.L.Macklin, Phys. Rev. 129,2695 (1963)
J.Csikai et al. NP 41,316 (1963)
S.A.Cox, Phys. Rev. 133,B378 (1964)
W.P. Pönitz NR 19/65 P.53 (1965)
A.K.Chaubey and M.L. Sehgal, PR 152,1055 (1966)
G. P. ö et al. JNE 21,797 (1967)
R.L. Macklin and J.H. Gibbons, PR 159,4, 1007 (1967)
J. Cs. ai et al. NP A95,229 (1967) En = 14.7 MeV
R.P. S. human WASH-1127,72 (1969)
F. Ri. ud et al. NP A173,551 (1971)
M.Fri.ke and A.Carlson : ANS 14, 352 (1971)
Benzi and Reffo : CCDN-NW/10 (1969)
JNDC (1973)
10^1
1
10^{-1}
10^{-2}
10^{-3}
10^{-4}
10^{-5}
1
10^1
10^2
10^3
10^4
E_n (keV)

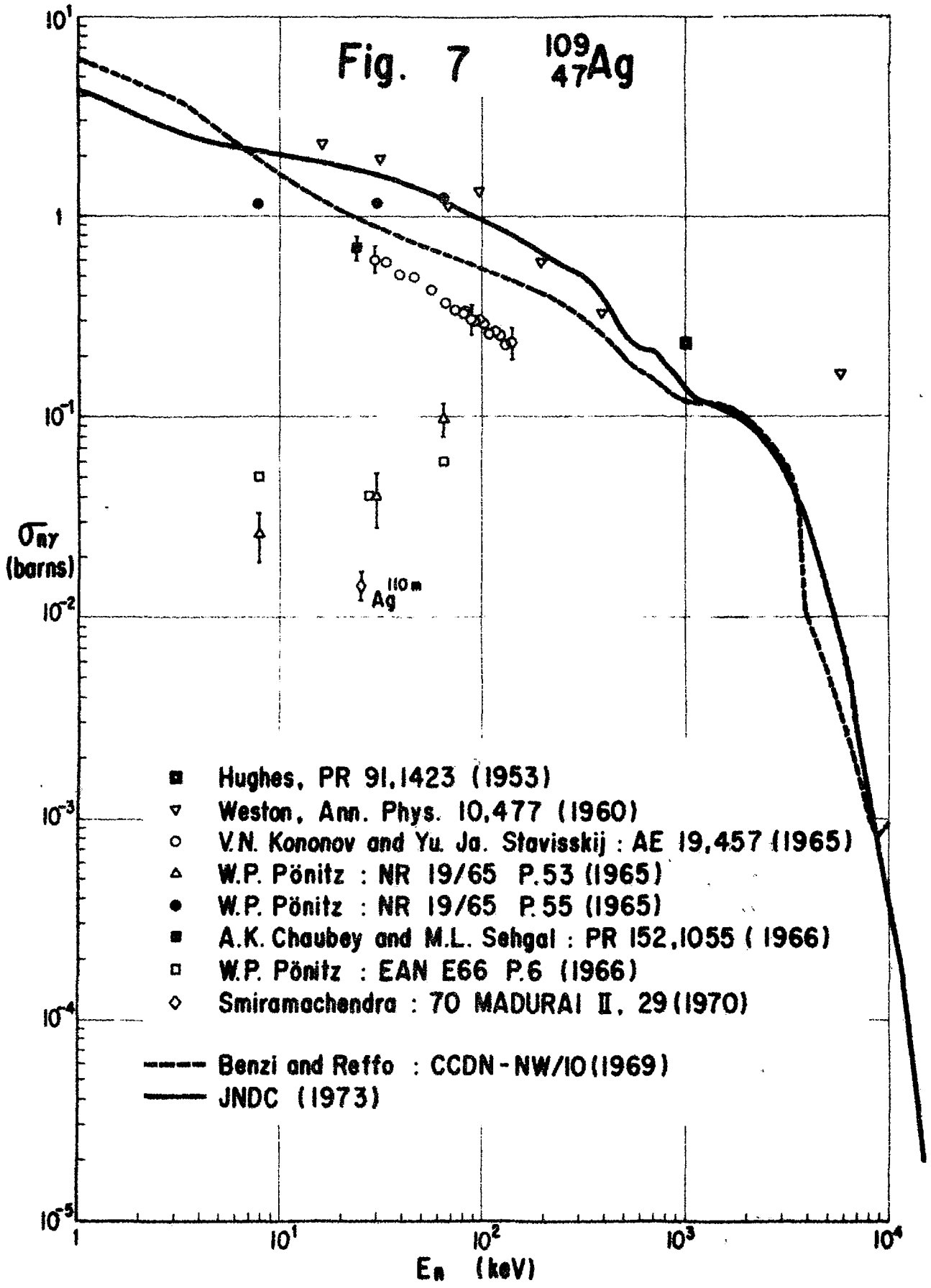
Fig. 7 $^{109}_{47}Ag$
$\sigma_{n\gamma}$ (barns)
E_n (keV)
^{110m}Ag
Hughes, PR 91,1423 (1953)
Weston, Ann. Phys. 10,477 (1960)
V.N. Kononov and Yu. Ja. Stavisskij : AE 19,457 (1965)
W.P. Pönitz : NR 19/65 P.53 (1965)
W.P. Pönitz : NR 19/65 P.55 (1965)
A.K. Chaubey and M.L. Sehgal : PR 152,1055 (1966)
W.P. Pönitz : EAN E66 P.6 (1966)
Smiramachendra : 70 MADURAI II, 29 (1970)
Benzi and Reffo : CCDN-NW/10 (1969)
JNDC (1973)

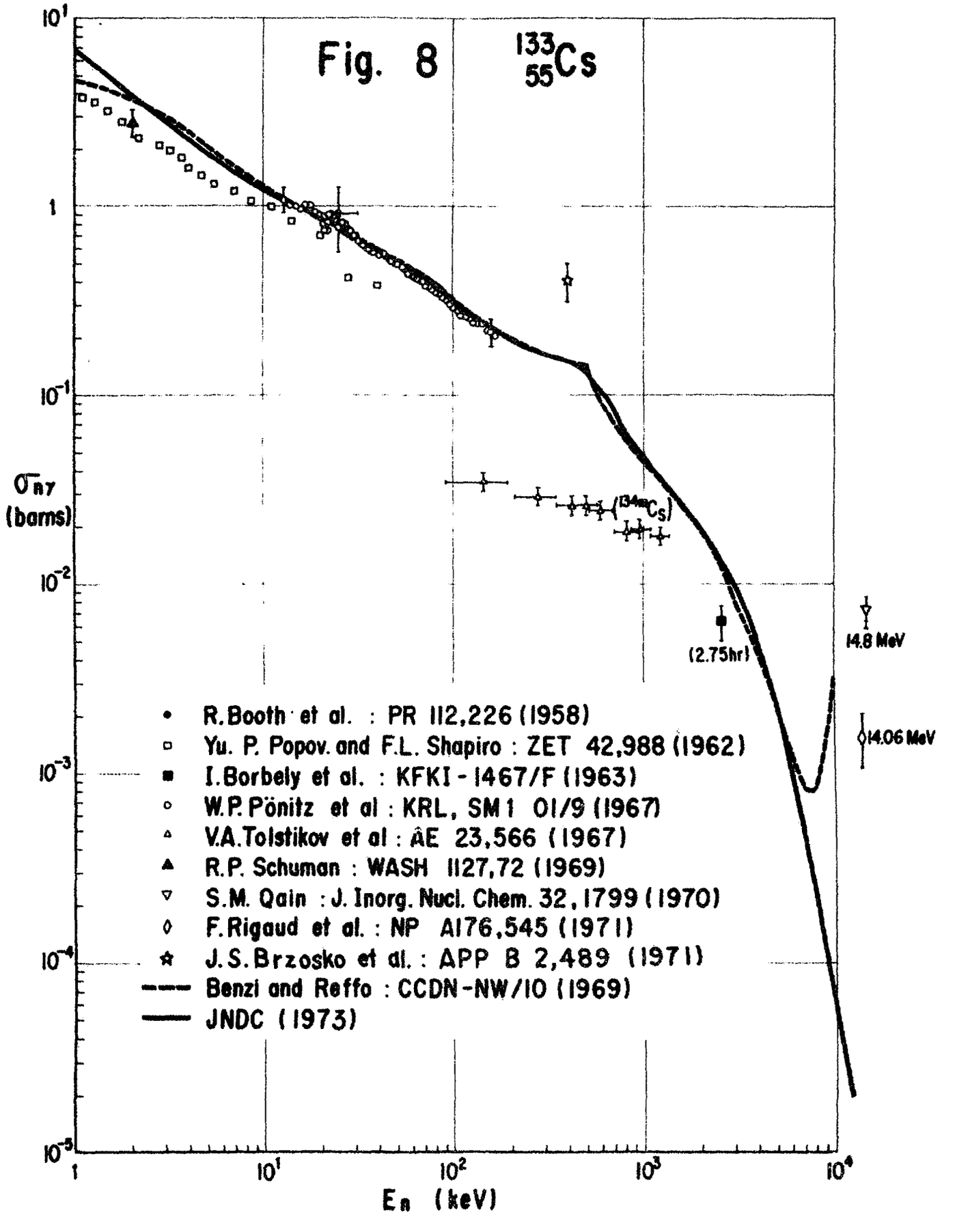
Fig. 8
$^{133}_{55}Cs$
$\sigma_{n\gamma}$ (barns)
E_n (keV)
(2.75hr)
14.8 MeV
14.06 MeV
R.Booth et al. : PR 112,226 (1958)
Yu. P. Popov. and F.L. Shapiro : ZET 42,988 (1962)
I.Borbely et al. : KFKI-1467/F (1963)
W.P.Pönitz et al : KRL, SM1 01/9 (1967)
V.A.Tolstikov et al : AE 23,566 (1967)
R.P. Schuman : WASH 1127,72 (1969)
S.M. Qain : J. Inorg. Nucl. Chem. 32,1799 (1970)
F.Rigaud et al. : NP A176,545 (1971)
J.S.Brzosko et al. : APP B 2,489 (1971)
Benzi and Reffo : CCDN-NW/10 (1969)
JNDC (1973)

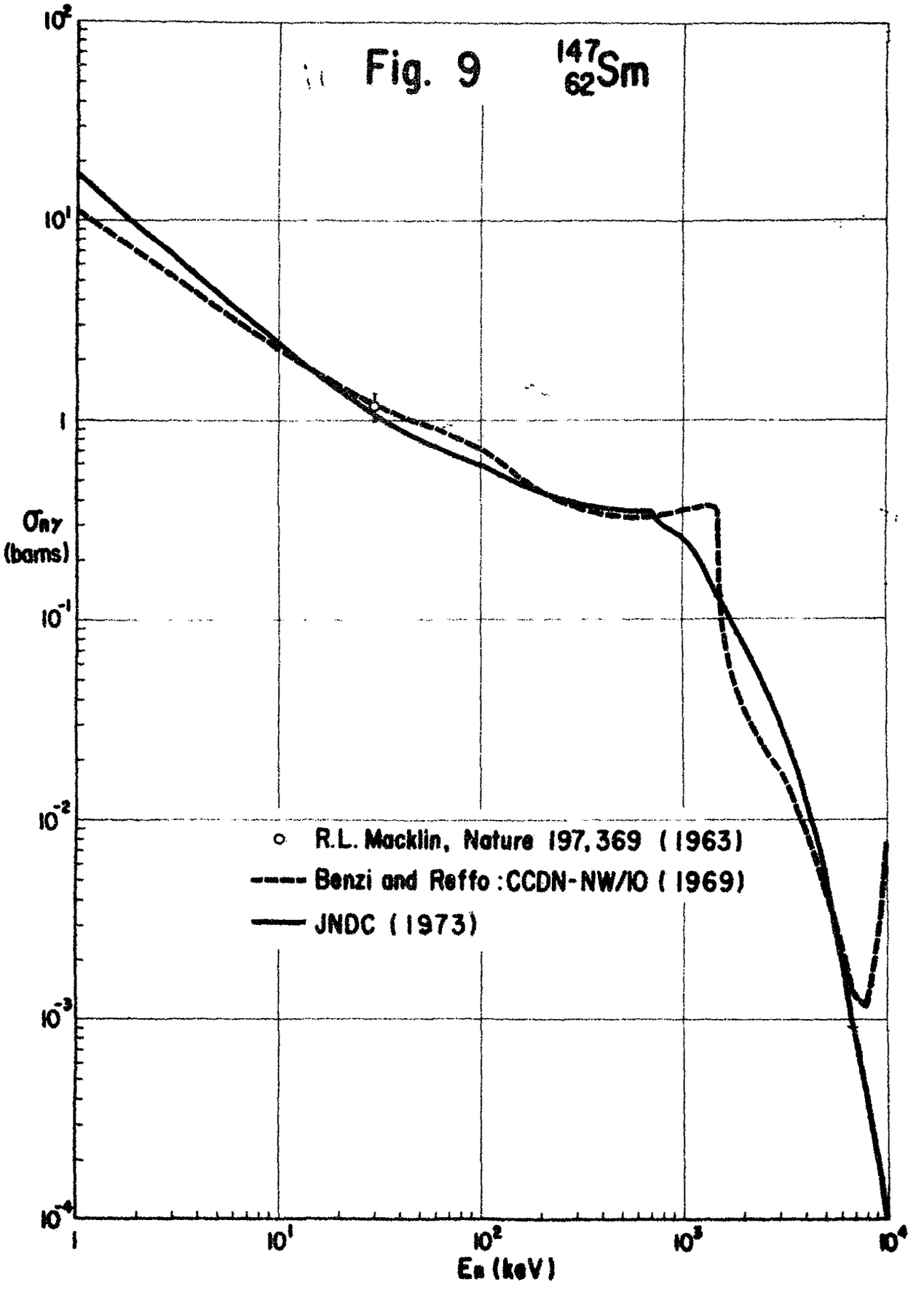
Fig. 9 $^{147}_{62}Sm$
$\sigma_{n\gamma}$ (barns)
10^{2}
10^{1}
1
10^{-1}
10^{-2}
10^{-3}
10^{-4}
1
10^{1}
10^{2}
10^{3}
10^{4}
E_n (keV)
R.L. Macklin, Nature 197, 369 (1963)
Benzi and Reffo : CCDN-NW/10 (1969)
JNDC (1973)

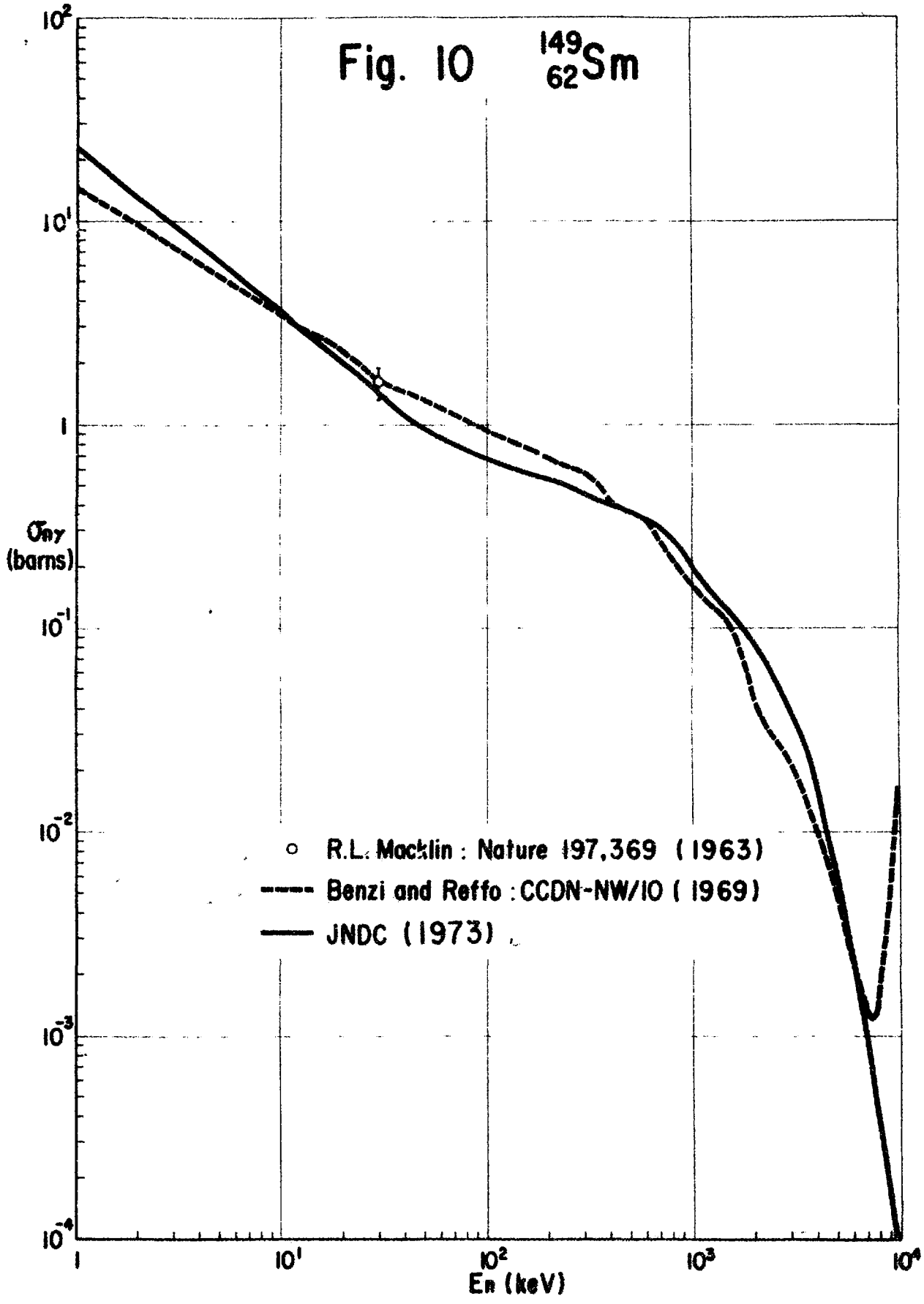
Fig. 10 $^{149}_{62}Sm$
10^2
10^1
1
10^{-1}
10^{-2}
10^{-3}
10^{-4}
$\sigma_{n\gamma}$ (barns)
1
10^1
10^2
10^3
10^4
E_n (keV)
R.L. Macklin : Nature 197,369 (1963)
Benzi and Reffo : CCDN-NW/10 (1969)
JNDC (1973)

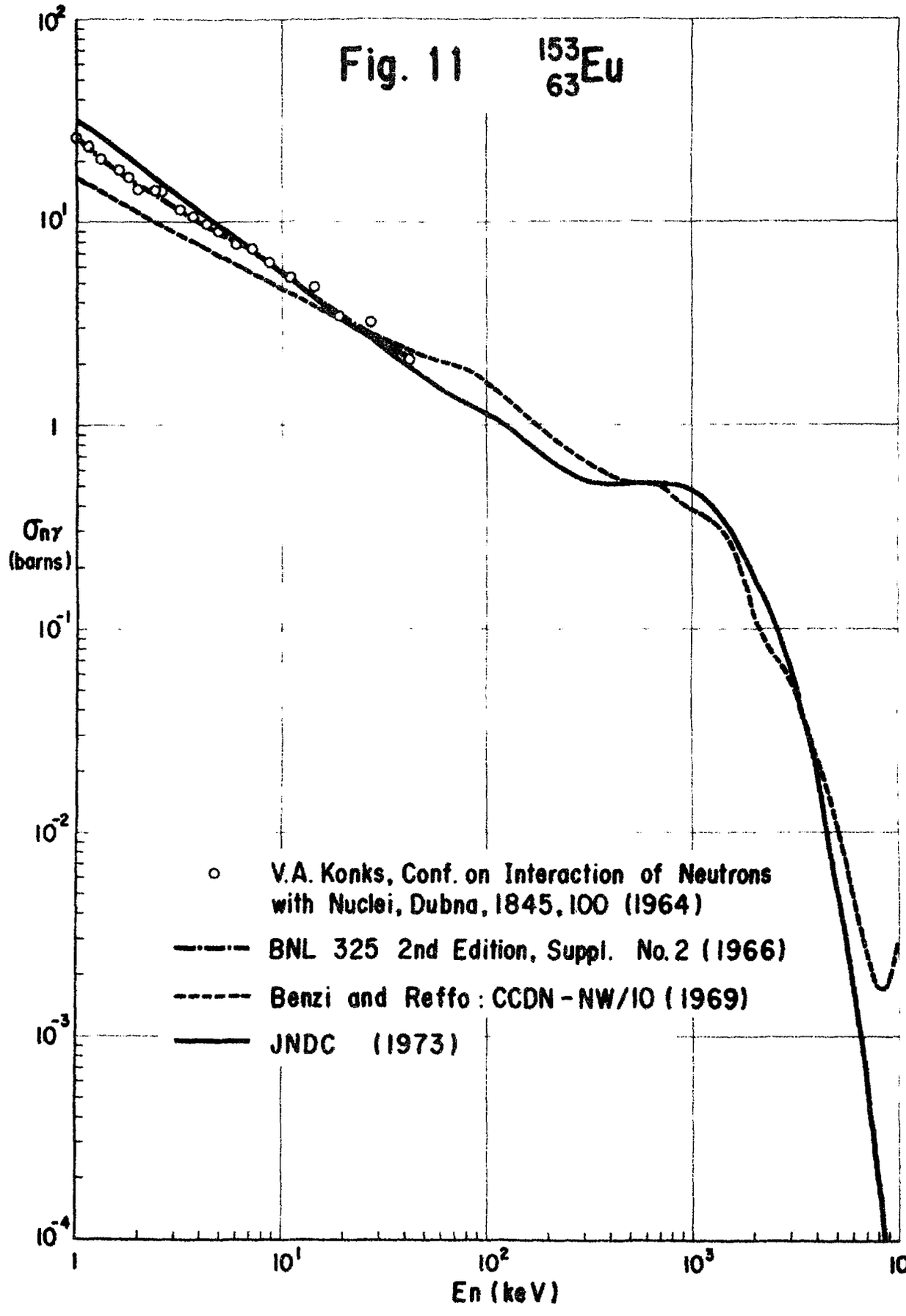
Fig. 11 $^{153}_{63}Eu$
10^2
10^1
1
$\sigma_{n\gamma}$ (barns)
10^{-1}
10^{-2}
10^{-3}
10^{-4}
1
10^1
10^2
10^3
10^4
En (keV)
V.A. Konks, Conf. on Interaction of Neutrons with Nuclei, Dubna, 1845, 100 (1964)
BNL 325 2nd Edition, Suppl. No. 2 (1966)
Benzi and Reffo : CCDN - NW/10 (1969)
JNDC (1973)

THERMAL AVERAGE, RESONANCE INTEGRAL AND FISSION-SPECTRUM AVERAGE NEUTRON CAPTURE CROSS-SECTIONS OF NUCLIDES WITH Z = 30 TO 68

A L POPE & J S STORY

United Kingdom Atomic Energy Authority
Atomic Energy Establishment
Winfrith
Dorchester
Dorset

ABSTRACT

For the fission-product range, Z = 30 to 68, this report gives a comparative table of integral characteristics computed from capture cross-sections in the many evaluated data files presently available in the format of the UK Nuclear Data Library. Similar data relating to the ENDF/B3 data library are included also. The integral characteristics listed are:

(1) Thermal Average Cross-sections

(2) Resonance Integrals, including the 1/V component

(3) Fission Spectrum Averages

Selected means of the experimental data are listed also when available.

1 INTRODUCTION

Nearly 460 files of capture cross-section data for stable and unstable isotopes in the fission-product range (Z = 30 to 68) are presently available in the format of the UK Nuclear Data Library. In 1967 a set of 78 files of fission-product capture cross-sections was assembled for the UKNDL; these are composite files, using in the lower energy range a compilation carried out at Lucas Heights by Cook (1966) and others, and in the higher energy range the data of Benzi & Bortolani (1966) at the Centro di Calcolo in Bologna: these files span the energy range from 0.0001 eV to 10 MeV. In 1969 Benzi & Reffo published 142 files of capture cross-sections from 1 keV to 10 MeV for all stable isotopes with Z = 32 to 66; the Bologna group has subsequently extended this compilation to include all 198 stable isotopes with Z = 29 to 79 (Benzi et al 1971 a), but the present study has been restricted to the atomic number range Z = 30 to 68. The Bologna group has also produced 18 files of fission-product data giving inelastic, (n, 2n) and radiative capture cross-sections (Benzi et al 1971 b). In 1971 the Lucas Heights group (Bertram et al 1971) produced a revised set of fission-product data files, covering the energy range 0.00010263 eV to 15 MeV, for no fewer than 192 nuclides including 82 radioactive nuclides with half-lives down to 24.8 minutes. These files give neutron capture, elastic and inelastic scatter, and transport cross-sections. A few files of UK origin are also available in the UKNDL in the fission-product range.

A number of files of neutron cross-section data in the fission-product range are available in the American ENDF/B3 data library, mainly by Schenter & Schmittroth (1971) and by Livolsi (1971). These files contain data for all

important neutron cross-sections, though only the neutron absorption cross-sections are considered in this paper. We may note also for completeness a recent paper by Schmittroth & Schenter (1973) giving compilations of fast neutron capture cross-sections for 39 fission-product nuclides.

When two or more different files are available for a single nuclide it would be a tedious task to compare them point-by-point, and it is not necessarily the most useful method of comparative assessment in the first instance. In the following table are listed three integral characteristics computed from the capture cross-sections in these various data files, namely the Maxwellian average cross-section in the thermal region (we follow Westcott's convention), the resonance absorption integral, and the fission-spectrum average. Included in the table are values of the thermal average and resonance integral cross-sections drawn mainly from recent summaries of the experimental data.

NOTATION USED IN THE TABLE

The first column of the table lists in order of atomic number Z and atomic weight A the nuclides for which information is given in the table. Included are all stable nuclides or quasi-stable nuclides with Z = 30 to 68; all radioactive fission-products with half-lives greater than 1 day and a few with shorter half-lives, down to 25 minutes; 259 nuclides and isomers in all. The stable and quasi-stable nuclides (with half-lives greater than 10^9 years) are fully underlined, and the very long-lived nuclides with half-lives in the range 10^5 years to 10^9 years have broken underlining. Unstable nuclides have their half-lives in parentheses underneath the isotopic symbol.

For each nuclide the following kinds of information are given, if available:

DFN - Data File Number in UK Nuclear Data Library, or MAT number in ENDF/B3

Thr - Thermal average capture cross-section in Westcott's convention at 20.44°C, (ie Maxwellian average x $2/\sqrt{\pi}$).

RI - Resonance integral including the 1/v component above 0.55 eV.

FSA - Fission Spectrum Average cross-section using the U235 Watt-Cranberg form for the fission spectrum.

Explicit expressions for these three cross-sections may be found in the paper by Pope and Story (1973).

Succeeding column headings identify the origin of the data files as mentioned in the introduction.

AUA + BOL 1967 - the composite files based on the Australian compilations by Cook et al (1966) and those of Benzi & Bortolani (1966) in Bologna.

BOL 1969 - the Bologna compilations by Benzi & Reffo (1969). Because these do not extend below 1 keV the thermal cross-section and resonance integral are omitted.

AUA 1971 - the Australian AEC compilations by Bertram et al (1971)

BOL 1971 - the Bolognese compilations by Benzi et al (1971 a) and (1971 b).

ENDF/B3 - the 1971 edition of the American Evaluated Nuclear Data Files; see for example Ozer & Garber (1973)

UKNDL - some additional data files in the format of the UK Nuclear Data Library; (the files for Ag-107 and Ag-109 and for Eu-151 and Eu-153 were obtained by direct conversion from the corresponding ENDF/B3 files).

Experimental - although we have exercised care in collecting the experimental data and in the selection of recommended values the quantity of information reviewed has precluded any attempt at complete reassessment and renormalisation of every experiment. Resonance integral data are of two kinds, direct integral measurements in a neutron slowing-down spectrum and values derived from resonance parameters. The 'experimental' values of resonance integrals given in the table are recommended values deduced from integral measurements only, if there are any; if there are no integral measurements we have used values calculated from resonance parameters, but these results are given in parentheses.

Exp. Refs - The references given in the table often refer the reader to some earlier compilation where the original sources of the experimental data may be found. It should be confessed however that even when, for example, we have referred to the compilation by Walker (1969) we did not necessarily adopt Walker's choice for the preferred values.

REFERENCES FOR THE TEXT

BENZI V. & BORTOLANI M.V.(Oct. 1966) IAEA Paris Conf. on nuclear data for reactors 1, 537

BENZI V., D'ORAZI R., REFFO G. & VACCARI M. (Nov. 1971 a) CEC(71)9

BENZI V., PANINI G. C., REFFO G. & VACCARI M. (July 1971 b) CEC(71)2

BENZI V. & REFFO G. (Dec. 1969) CCDN-NW/10

BERTRAM W. K., CLAYTON E., COOK J. H., FERGUSON H. D., MUGGROVE A.R. & ROSE E.K. (June 1971) AAEC/E214

COOK J. L. (Oct. 1966) IAEA Paris Conf. on nuclear data for reactors 1, 549

LIVOLSI A. Z. (Nov. 1971) BAW-409

OZER O. & GARBER D. (Ed.) (May 1973) BNL-17541 = ENDF-201

POPE A. L. & STORY J. S. (Apr. 1973) AEEW-M1191

SCHENTER R. E. & SCHMITTROTH F. A. (Oct. 1971) HEDL-TME-71-143

SCHMITTROTH F. & SCHENTER R. E. (Aug. 1973) HEDL-TME-73-63

WALKER W. H. (Dec. 1969) AECL-3037, part 1

Numbered references for the table are given at the end of the report.

Integral capture cross-sections computed from various evaluated data files

Nuclide (Half-life)		AUA + BOL 1967	BOL 1969	AUA 1971	BOL 1971 a, b	ENDF/B3 1971	UKNDL	Experiment	Expt. Ref
Zn-64	DFN				-683-				
(> 8 x 10^{15} y)	Thr				*			0.815 ± .010b	(1)
	RI				*			1.798 ± .028b	(2)
	FSA				13.3 mb				
Zn-66	DFN				-684-				
	Thr				*				
	RI				*				
	FSA				10.9 mb				
Zn-67	DFN				-685-				
	Thr				*				
	RI				*				
	FSA				8.94 mb				
Zn-68	DFN				-686-				
	Thr				*			1.095 ± .15 b	(6)
	RI				*			3.61 ± .51 b	(2)
	FSA				6.87 mb				
Zn-70	DFN				-687-				
(> 10^{15} y)	Thr				*			0.105 ± .008b	(6)
	RI				*				
	FSA				8.42 mb				
Zn-72	DFN			-4001-					
(46.5h)	Thr			55.7 mb					
	RI			63.0 mb					
	FSA			1.83 mb					

Integral cross-sections comparisons, continued

Nuclide (Half-life)		AUA + BOL 1967	BOL 1969	AUA 1971	BOL 1971 a, b	ENDF/B3 1971	UKNDL	Experiment	Expt. Ref
Ga-69	DFN				-688-				
	Thr				*			1.68 ± .07 b	(18)
	RI				*			15.5 ± 1.5 b	(18)
	FSA				18.0 mb				
Ga-71	DFN				-689-				
	Thr				*			4.71 ± .23 b	(18)
	RI				*			31.1 ± 2.9 b	(18)
	FSA				14.8 mb				
Ga-72 (14 h)	DFN			-4002-					
	Thr			4.23 b					
	RI			25.6 b					
	FSA			22.2 mb					
Ge-70	DFN		-603-						
	Thr		*					3.68 ± 0.8 b	(6)
	RI		*						
	FSA		18.8 mb						
Ge-72	DFN		-604-	-4003-					
	Thr		*	0.977 b				0.97 ± .1 b	(3)
	RI		*	0.522 b					
	FSA		12.7 mb	7.61 mb					
Ge-73	DFN		-605-	-4004-					
	Thr		*	13.6 b				14 ± 1 b	(3)
	RI		*	33.9 b					
	FSA		34.7 mb	13.4 mb					

Integral cross-section comparisons, continued

Nuclide (Half-life)		AUA + BOL 1967	BOL 1969	AUA 1971	BOL 1971 a, b	ENDF/B3 1971	UKNDL	Experiment	Expt. Ref
Ge-74	DFN		-606-	-4005-					
	Thr		*	0.432 b				0.36 ± .10 b	(3)
	RI		*	0.345 b				0.55 ± .16 b	(4)
	FSA		6.68 mb	3.56 mb					
Ge-76	DFN		-607-	-4006-					
(> 2 x 10^{16} y)	Thr		*	0.159 b				0.15 ± .01 b	(5)
	RI		*	0.176 b				1.79 ± .12 b	(4)
	FSA		9.97 mb	4.08 mb					
Ge-77	DFN			-4007-					
(11.3 h)	Thr			1.48 b					
	RI			6.98 b					
	FSA			3.58 m					
As-75	DFN		-608-	-4008-					
	Thr		*	4.28 b				4.30 ± .1 b	(1)
	RI		*	60.4 b				63 ± 5 b	(1)
	FSA		38.8 mb	28.4 m					
As-76	DFN			-4009-					
(26.3 h)	Thr			60.5 b					
	RI			215 b					
	FSA			131 mb					
As-77	DFN			-4010-					
(38.7 h)	Thr			12.6 b					
	RI			68.0 b					
	FSA			18.8 mb					

Integral cross-section comparisons, continued

Nuclide (Half-life)		AUA + BOL 1967	BOL 1969	AUA 1971	BOL 1971 a, b	ENDF/B3 1971	UKNDL	Experiment	Expt. Ref
Se-74	DFN		-609-						
	Thr		*					55 ± 5 b	(19)
	RI		*					512 ± 51 b	(23)
	FSA		20.4 mb						
Se-76	DFN		-610-	-4011-					
	Thr		*	84.8 b				85 ± 7 b	(3)
	RI		*	40.5 b					
	FSA		25.6 mb	13.5 mb					
Se-77	DFN		-611-	-4012-					
	Thr		*	41.8 b				42 ± 4 b	(5)
	RI		*	28.1 b				(31.7 ± 2.2) b	(5)
	FSA		47.6 mb	20.1 mb					
Se-78	DFN		-612-	-4013-					
	Thr		*	0.399 b				0.35 ± .05 b	(5)
	RI		*	7.08 b				3.9 ± .6 b	(5)
	FSA		37.2 mb	13.5 mb					
Se-79 (≤ 65000y)	DFN			-4014-					
	Thr			39.1 b					
	RI			54.8 b					
	FSA			19.3 mb					
Se-80	DFN		-613-	-4015-					
	Thr		*	0.573 b				0.59 ± .05 b	(5)
	RI		*	0.986 b				1.60 ± .16 b	(5)
	FSA		5.43 mb	7.30 mb					

Integral cross-section comparisons, continued

Nuclide (Half-life)		AUA + BOL 1967	BOL 1969	AUA 1971	BOL 1971 a, b	ENDF/B3 1971	UKNDL	Experiment	Expt. Ref
Se-82	DFN	-702-	-614-						
($>10^{17}$ y)	Thr	2.03 b	*					45 ± 5 mb	(5)
	RI	1.05 b	*					(0.109 b)	(5)
	FSA	4.35 mb	12.0 mb						
Br-79	DFN		-615-						
	Thr		*					11.3 ± .45 b	(16)
	RI		*					130 ± 11 b	(16)
	FSA		61.0 mb						
Br-81	DFN	-701-	-616-	-4016-					
	Thr	3.25 b	*	2.99 b				2.87 ± .14 b	(16)(22)
	RI	108 b	*	59.5 b				61 ± 6 b	(16)(23)
	FSA	26.3 mb	26.3 mb	39.0 mb					
Br-82	DFN			-4017-					
(35.3 h)	Thr			18.0 b					
	RI			90.1 b					
	FSA			121 mb					
Kr-78	DFN		-617-						
	Thr		*					4.71 ± .68 b	(37)
	RI		*						
	FSA		41.0 mb						
Kr-80	DFN		-618-						
	Thr		*					11.3 ± .4 b	(21)
	RI		*					56.1 ± 2.8 b	(21)
	FSA		40.2 mb						

Integral cross-section comparisons, continued

Nuclide (Half-life)		AUA + BOL 1967	BOL 1969	AUA 1971	BOL 1971 a, b	ENDF/B3 1971	UKNDL	Experiment	Expt. Ref
Kr-82	DFN		-619-	-4018-					
	Thr		*	24.9 b				25 ± 6 b	(5)
	RI		*	191 b				(201 ± 26) b	(5)
	FSA		45.2 mb	30.4 mb					
Kr-83	DFN	-703-	-501D-	-4019-		-1201-	-904-		
	Thr	209 b	*	199 b		187 b	206 b	201 ± 10 b	(5)
	RI	231 b	*	214 b		235 b	253 b	(233 ± 21) b	(5)
	FSA	52.6 mb	61.8 mb	39.1 mb			61.7 mb		
Kr-84	DFN	-704-	-502D-	-4020-					
	Thr	159 mb	*	96.8 mb				117 ± 18 mb	(3)(5)
	RI	22.5 b	*	3.59 b				(8.4) b	(5)
	FSA	5.56 mb	7.05	6.12 mb					
Kr-85 (10.73 y)	DFN	-705-		-4021-					
	Thr	14.5 b		7.91 b				1.66 ± .02 b	(7)
	RI	73.6 b		8.02 b				1.8 ± 1.0 b	(7)
	FSA	2.57 mb		10.6 mb					
Kr-86	DFN	-707-	-505D-	-4022-					
	Thr	58.1 mb	*	995 mb				60 ± 20 mb	(3)
	RI	72.1 mb	*	460 mb					
	FSA	1.91 mb	2.48 mb	1.63 mb					
Rb-85	DFN	-706-	-503D-	-4023-					
	Thr	0.843 b	*	0.419 b				0.399 ± .005b	(5)
	RI	3.85 b	*	3.70 b				6.7 ± 0.2 b	(5)
	FSA	16.3 mb	26.7 mb	20.7 mb					

Integral cross-section comparisons, continued

Nuclide (Half-life)		AUA + BOL 1967	BOL 1969	AUA 1971	BOL 1971 a, b	ENDF/B3 1971	UKNDL	Experiment	Expt. Ref
Rb-86 (18.7 d)	DFN			-4024-					
	Thr			4.90 b					
	RI			43.5 b					
	FSA			64.7 mb					
Rb-87 (4.8×10^{10} y)	DFN	-708-	-506D-	-4025-					
	Thr	0.139 b	*	0.121 b				0.12 ± .025 b	(5)
	RI	0.196 b	*	2.47 b				(2.4 ± .5) b	(5)
	FSA	2.76 mb	3.25 mb	3.15 mb					
Sr-84	DFN		-620-						
	Thr		*					0.88 ± .06 b	(19)
	RI		*					11.7 ± 1.2 b	15)
	FSA		75.8 mb						
Sr-86	DFN		-621-	-4026-					
	Thr		*	0.995 b				0.97 ± .1 b	(5)
	RI		*	0.778 b				3.5 b	(5)
	FSA		20.8 mb	15.5 mb					
Sr-87	DFN		-622-						
	Thr		*					(40) b	(5)
	RI		*					(117) b	(5)
	FSA		11.4 mb						
Sr-88	DFN	-709-	-507A-	-4027-					
	Thr	4.96 mb	*	5.38 mb				~ 3.5 mb	(5)
	RI	15.3 mb	*	46.8 mb				(67) mb	(5)
	FSA	2.31 mb	14.5 mb	2.84 mb					

Integral cross-section comparisons, continued

Nuclide (Half-life)		AUA + BOL 1967	BOL 1969	AUA 1971	BOL 1971 a, b	ENDF/B3 1971	UKNDL	Experiment	Expt. Ref
Sr-89 (50.52d)	DFN	-710-		-4028-					
	Thr	0.406 b		0.415 b				0.43 ± .04 b	(3)
	RI	0.8296 b		0.348 b					
	FSA	1.19 mb		2.23 mb					
Sr-90 (28.3 y)	DFN	-712-		-4029-					
	Thr	0.977 b		0.793 b				0.9 ± .5 b	(3)(5)
	RI	30.2 b		0.393 b					
	FSA	4.92 mb		4.02 mb					
Sr-91 (9.67 h)	DFN			-4030-					
	Thr			0.148 b					
	RI			0.616 b					
	FSA			2.42 mb					
Y-89	DFN	-711-	-508 A-	-4031-	-508D-				
	Thr	1.34 b	*	1.28 b	*			1.28 ± .01 b	(5)
	RI	0.643 b	*	0.657 b	*			1.01 ± .07 b	(18)(5)
	FSA	3.84 mb	5.60 mb	2.63 mb	5.59 mb				
Y-90 (64.0 h)	DFN	-713-		-4032-					
	Thr	7.01 b		3.46 b				< 6.5 b	(5)
	RI	16.4 b		2.54 b					
	FSA	5.71 mb		9.13 mb					
Y-91 (58.8 d)	DFN	-714-		-4033-					
	Thr	1.07 b		1.05 b				1.4 ± .3 b	(5)
	RI	1.31 b		1.92 b					
	FSA	0.898 mb		6.22 mb					

Integral cross-section comparisons, continued

Nuclide (Half-life)		AUA + BOL 1967	BOL 1969	AUA 1971	BOL 1971 a, b	ENDF/B3 1971	UKNDL	Experiment	Expt. Ref
Y-93 (10.3 h)	DFN			-4034-					
	Thr			77.5 mb					
	RI			985 mb					
	FSA			2.49 mb					
Zr-90	DFN		-572A-	-4035-					
	Thr		*	99.0 mb				63 ± 44 mb	(8)
	RI		*	78.8 mb				160 ± 20 mb	(8)
	FSA		9.20 mb	4.99 mb					
Zr-91	DFN	-715-	-510D-	-4036-					
	Thr	1.57 b	*	1.57 b				958 ± 76 mb	(8)
	RI	8.12 b	*	7.78 b				6.7 ± 0.8 b	(8)
	FSA	8.78 mb	14.2 mb	8.57 mb					
Zr-92	DFN	-716-	-511D-	-4037-					
	Thr	250 mb	*	249 mb				158 ± 47 mb	(8)
	RI	619 mb	*	290 mb				(430) mb	(8)
	FSA	9.90 mb	9.17 mb	4.48 mb					
Zr-93 (1.5×10^6 y)	DFN	-717-		-4038-	-512A-				
	Thr	1.09 b		1.99 b	*			< 4 b	(5)
	RI	22.4 b		25.9 b	*			(23) b	(5)
	FSA	4.23 mb		7.56 mb	11.1 mb				
Zr-94	DFN	-718-	-513D-	-4039-					
	Thr	85.8 mb	*	75.0 mb				50.9 ± 2.4 mb	(9)(10)
	RI	610 mb	*	211 mb				296 ± 15 mb	(24)
	FSA	15.0 mb	7.64 mb	2.87 mb					

Integral cross-section comparisons, continued

Nuclide (Half-life)		AUA + BOL 1967	BOL 1969	AUA 1971	BOL 1971 a, b	ENDF/B3 1971	UKNDL	Experiment	Expt. Ref
Zr-95 (63.8d)	DFN			-4040-		-1202-			
	Thr			0.487 b		5.00 b			
	RI			5.41 b		7.98 b			
	FSA			5.57 mb					
Zr-96 (≥3.6 x 10^{17} y)	DFN	-720-	-515D-	-4041-					
	Thr	5.27 mb	*	195 mb				15 ± 5 mb	(9)(10)
	RI	6.34 b	*	5.30 b				4.66 ± .16 b	(24)
	FSA	9.68 mb	8.01 mb	5.77mb					
Zr-97 (17 h)	DFN			-4042-					
	Thr			202 mb					
	RI			1.54 b					
	FSA			3.96 mb					
Nb-93	DFN		-623-			-1164-	-790-		
	Thr		*			1.17 b	1.15 b	1.17 ± .02 b	(3)
	RI		*			9.48 b	11.0 b	15.8 ± 1.7 b	(1)
	FSA		27.6 mb				29.4 mb		
Nb-93m (13.6 y)	DFN								
	Thr			NO	DATA				
	RI								
	FSA								
Nb-94 (2×10^4 y)	DFN								
	Thr							13.9 ± 1.6 b	(1)
	RI							113 ± 14 b	(1)
	FSA								

Integral cross-section comparisons, continued

Nuclide (Half-life)		AUA + BOL 1967	BOL 1969	AUA 1971	BOL 1971 a, b	ENDF/B3 1971	UKNDL	Experiment	Expt. Ref
Nb-95 (35.0 d)	DFN			-4043-		-1203-			
	Thr			1.45 b		4.00 b		< 7 b	(5)
	RI			25.1 b		26.6 b			
	FSA			14.2 mb					
Nb-95m (90 h)	DFN			N O	D A T A				
	Thr								
	RI								
	FSA								
Nb-96 (23.4 h)	DFN			N O	D A T A				
	Thr								
	RI								
	FSA								
Mo-92 ($> 4 \times 10^{18}$ y)	DFN		-573A-						
	Thr		*						
	RI		*						
	FSA		14.2 mb						
Mo-94	DFN		-573A-						
	Thr		*						
	RI		*						
	FSA		17.1 mb						
Mo-95	DFN	-719-	-514D-	-4044-		-1204-			
	Thr	14.0 b	*	14.5 b		14.3 b		14.5 ± .5 b	(3)
	RI	113 b	*	116 b		109 b		106 ± 21 b	(3)
	FSA	54.9 mb	36.5 mb	39.3 mb					

Integral cross-section comparisons, continued

Nuclide (Half-life)		AUA + BOL 1967	BOL 1969	AUA 1971	BOL 1971 a, b	ENDF/B3 1971	UKNDL	Experiment	Expt. Ref
Mo-96	DFN		-575A-	-4045-					
	Thr		*	1.19 b				1.2 ± .6 b	(5)
	RI		*	26.1 b				(26 ± 5) b	(5)
	FSA		25.2 mb	18.1 mb					
Mo-97	DFN	-721-	-516D-	-4046-		-1205-			
	Thr	2.24 b	*	2.19 b		1.91 b		2.2 ± .7 b	(5)
	RI	18.4 b	*	15.0 b		16.1 b		(16 ± 3) b	(5)
	FSA	42.3 mb	41.8 mb	28.9 mb					
Mo-98	DFN	-722-	-517D-	-4047-		-1206-			
	Thr	135 mb	*	143 mb		154 mb		137 ± 3 mb	(5)
	RI	6.82 b	*	6.68 b		6.79 b		6.76 ± .12 b	(5)
	FSA	23.0 mb	27.3 mb	37.3 mb					
Mo-99 (66.3 h)	DGN			-4048-		-1207-			
	Thr			1.73 b		2.00 b			
	RI			24.8 b		25.9 b			
	FSA			21.0 mb					
Mo-100	DFN	-724-	-519D-	-4049-		-1208-			
($\geq 3 \times 10^{17}$ y)	Thr	197 mb	*	225 mb		204 mb		199 ± 5 mb	(5)
	RI	6.37 b	*	6.53 b		3.62 b		4.05 ± .07 b	(5)
	FSA	14.5 mb	14.2 mb	14.5 mb					
Tc-98	DFN								
	Thr							> 2.6 b	(25)
(1.5×10^{6} y)	RI								
	FSA								

Integral cross-section comparisons, continued

Nuclide (Half-life)		AUA + BOL 1967	BOL 1969	AUA 1971	BOL 1971 a, b	ENDF/B3 1971	UKNDL	Experiment	Expt. Ref
Tc-99	DFN	-723-		-4050-	-518A-				
(2.13×10^5 y)	Thr	22.4 b		22.0 b	*			22 ± 3 b	(3)
	RI	205 b		197 b	*			69 ± 20 b	(3)
	FSA	97.9 mb		46.1 mb	92.9 mb				
Tc-99m	DFN			-4185-					
(6.05 h)	Thr			1.62 b					
	RI			26.7 b					
	FSA			46.1 mb					
Ru-96	DFN		-576A-						
	Thr		*					0.21 ± .03 b	(26)
	RI		*					6.67 ± .11 b	(4)
	FSA		91.3 mb						
Ru-98	DFN		-577A-						
	Thr		*					< 8 b	(6)
	RI		*						
	FSA		35.5 mb						
Ru-99	DFN		-578A-						
	Thr		*					10.6 ± .6 b	(6)
	RI		*						
	FSA		54.7 mb						
Ru-100	DFN		-579A-	-4051-					
	Thr		*	5.47 b				5.84 b	(5)
	RI		*	41.2 b				11.4 b	(5)
	FSA		34.1 mb	81.3 mb					

Integral cross-section comparisons, continued

Nuclide (Half-life)		AUA + BOL 1967	BOL 1969	AUA 1971	BOL 1971 a, b	ENDF/B3 1971	UKNDL	Experiment	Expt. Ref
Ru101	DFN	-725-	-520D-	-4052-		-1210-			
	Thr	4.98 b	*	4.83 b		5.21 b		5.23 b	(5)
	RI	213 b	*	86.6 b		79.6 b		79.1 b	(5)
	FSA	53.9 mb	74.5 mb	28.7 mb					
Ru-102	DFN	-726-	-521D-	-4053-		-1211-			
	Thr	1.44 b	*	1.28 b		1.30 b		1.37 ± .12 b	(5) (27)
	RI	180 b	*	10.6 b		6.90 b		4.99 ± .2 b	(5)
	FSA	68.7 mb	86.5 mb	57.9 mb					
Ru-103 (39.5 d)	DFN			-4054-		-1212-			
	Thr			7.67 b		5.00 b			
	RI			65.9 b		9.24 b			
	FSA			58.9 mb					
Ru-104	DFN	-728-	-523D-	-4055-		-1213-			
	Thr	3.50 b	*	0.436 b		0.470 b		0.47 b	(5)
	RI	250 b	*	5.42 b		3.73 b		4.6 b	(5)
	FSA	23.5 mb	24.6 mb	15.5 mb					
Ru-105 (4.44 h)	DFN			-4056-		-1214-			
	Thr			0.188 b		0.300 b		0.30 ± .03 b	(5)
	RI			5.09 b		7.85 b			
	FSA			40.7 mb					
Ru-106 (368 d)	DFN			-4057-		-1215-			
	Thr			137 mb		125 mb		146 ± 40 mb	(5)
	RI			1.27 b		1.41 b		2.09 ± .6 b	(5)
	FSA			11.9 mb					

Integral cross-section comparisons, continued

Nuclide (Half-life)		AUA + BOL 1967	BOL 1969	AUA 1971	BOL 1971 a, b	ENDF/B3 1971	UKNDL	Experiment	Expt. Ref
Rh-103	DFN	-727-	-522D-	-4058-	-522E-				
	Thr	158 b	*	152 b	*			145.5 ± 2.3 b	(3)
	RI	1193 b	*	1006 b	*			1127 ± 71 b	(28)(29)
	FSA	87.4 mb	83.6 mb	81.7 mb	84.4 mb				
Rh-105 (35.6 h)	DFN	-729-		-4059-		-1217-			
	Thr	15088 b		15591 b		17000 b		16100 ± 1200b	(5)
	RI	54676 b		9880 b		7488 b		16700 ± 3000b	(5)
	FSA	0.720 mb		20.6 mb					
Pd-102	DFN		-580A-						
	Thr		*						
	RI		*						
	FSA		75.2 mb						
Pd-104	DFN		-581A-	-4060-					
	Thr		*	373 mb				⩽ 40 b	(3)
	RI		*	22.9 b					
	FSA		63.9 mb	91.9 mb					
Pd-105	DFN	-730-	-524D-	-4061-		-1218-			
	Thr	10.2 b	*	10.8 b		14.0 b		⩽17 b	(3)
	RI	95.8 b	*	74.6 b		86.3 b		(89 ± 8)b	(5)
	FSA	95.8 mb	106 mb	57.3 mb					
Pd-106	DFN	-731-	-525D-	-4062-		-1219-			
	Thr	5.94 b	*	284 mb		293 mb		290 ± 30 mb	(5)
	RI	14.7 b	*	8.37 b		10.1 b		5.73 ± .57 b	(5)
	FSA	42.7 mb	46.9 mb	22.7 mb					

Integral cross-section comparisons, continued

Nuclide (Half-life)		AUA + BOL 1967	BOL 1969	AUA 1971	BOL 1971 a, b	ENDF/B3 1971	UKNDL	Experiment	Expt. Ref
Pd-107	DFN	-732-		-4063-	-526A-	-1220			
	Thr	9.70 b		9.35 b	*	5.00 b		≤ 750 b	(5)
(16.5×10^6 y)	RI	83.5 b		80.3 b	*	79.7 b			
	FSA	91.7 mb		76.4 mb	121 mb				
Pd-108	DFN	-733-	-527D-	-4064-					
	Thr	11.0 b	*	12.0 b				10.0 ± .6 b	(5)
	RI	179 b	*	215 b				(244 ± 60)b	(5)
	FSA	34.7 mb	32.1 mb	12.7 mb					
Pd-109	DFN			-4065-		-1221-			
(13.5 h)	Thr			5.21 b		5.11 b			
	RI			60.8 b		60.2 b			
	FSA			28.7 mb					
Pd-110	DFN		-582A-	-4066-					
	Thr		*	225 mb				270 ± 60 mb	(5)
	RI		*	1.08 b				(6.1 ± 0.6)b	(5)
	FSA		25.7 mb	6.09 mb					
Pd-112	DFN			-4067-					
(20 h)	Thr			286 mb					
	RI			1.98 b					
	FSA			10.9 mb					
Ag-107	DFN		-583A-			-1138-	-973A-		
	Thr		*			36.9 b	36.9 b	37.6 ± 1.2 b	(11)
	RI		*			115 b	115 b	95 ± 4 b	(11)
	FSA		105 mb				114 mb		

Integral cross-section comparisons, continued

Nuclide (Half-life)		AUA + BOL 1967	BOL 1969	AUA 1971	BOL 1971 a, b	ENDF/B3 1971	UKNDL	Experiment	Expt. Ref
Ag-109	DFN	-734-	-528D-	-4068	-528E-	-1139-	-974A-		
	Thr	89.8 b	*	95.2 b	*	92.3 b	93.6 b	92.6 ± 1.8 b	(5)
	RI	1440 b	*	1442 b	*	1457 b	1454 b	1910 ± 200 b	(5)
	FSA	131 mb	129 mb	90.7	130 mb		62.5 mb		
Ag-110 m (252 d)	DFN								
	Thr							82 ± 11 b	(5)
	RI								
	FSA								
Ag-111 (7.45 d)	DFN			-4069					
	Thr			2.81 b				3.2 ± 2.0 b	(5)
	RI			106 b				106 ± 20 b	(5)
	FSA			35.1 mb					
Cd-106	DFN		-624-						
	Thr		*					~1 b	(30)
	RI		>10.1 b						
	FSA		295 mb						
Cd-108	DFN		-625-						
	Thr		*					0.7 ± .2 b	(1)
	RI		>4.58 b						
	FSA		128 mb						
Cd-110	DFN		-626-	-4070-					
	Thr		*	9.94 b				6.3 ± 1.1 b	(1)
	RI		>3.67 b	50.9 b				(38 ± 6) b	(1)
	FSA		102 mb	62.8 mb					

Integral cross-section comparisons, continued

Nuclide (Half-life)		AUA + BOL 1967	BOL 1969	AUA 1971	BOL 1971 a, b	ENDF/B3 1971	UKNDL	Experiment	Expt. Ref
Cd-111	DFN		-529A-	-4071					
	Thr		*	22.8 b				8 ± 2 b	(1)
	RI		> 6.50 b	45.5 b				(57 ± 6) b	(5)
	FSA		54.0 mb	23.2 mb					
Cd-112	DFN		-530-A	-4072-					
	Thr		*	1.98 b				0.3 ± .2 b	
	RI		*	14.1 b				(17 ± 3.6 b)	(5)
	FSA		56.2 mb	34.9 mb					
Cd-113	DFN	-735-	-531A-	-4073-		-1223-	-71 B-		
(9.3 x 10^{15} y)	Thr	26928 b	*	26880 b		26572 b	26601 b	26327 b	(5)
	RI	251 b	*	289 b		386 b	309 b		
	FSA	76.0 mb	81.2 mb	33.2 mb			58.2 mb		
Cd-113 m	DFN								
(14 y)	Thr		N O	D A T A					
	RI								
	FSA								
Cd-114	DFN		-627-	-4074-					
	Thr		*	324 mb				336 ± 16 mb	(6)
	RI		*	16.4 b				26 ± 4 b	(6)
	FSA		76.8 mb	28.8 mb					
Cd-115	DFN			-4075-					
(53.5 h)	Thr			5.38 b					
	RI			79.8 b					
	FSA			80.2 mb					

Integral cross-section comparisons, continued

Nuclide (Half-life)		AUA + BOL 1967	BOL 1969	AUA 1971	BOL 1971 a, b	ENDF/B3 1971	UKNDL	Experiment	Expt. Ref
Cd-115 m (44.6 d)	DFN			-4186-					
	Thr			30.6 b					
	RI			195 b					
	FSA			80.2 mb					
Cd-116 ($\geq 10^{17}$ y)	DFN		-628-	-4076-					
	Thr		*	0.786 b				77 ± 13 mb	(5)
	RI		*	1.27 b				1.3 ± .2 b	(1)
	FSA		19.4 mb	6.34 mb					
In-113	DFN		-629-		-629A-				
	Thr		*		*			11.1 ± 1.3 b	(6)
	RI		*		*			241 ± 29 b	(2)
	FSA		113 mb		196 mb				
In-115 (6×10^{14} y)	DFN	-736-	-532A-	-4077-	-532D-				
	Thr	210 b	*	206 b	*			205.8 ± 1.0 b	(5)
	RI	3379 b	*	3212 b	*			3428 ± 170 b	(5)
	FSA	151 mb	130 mb	101 mb	185 mb				
Sn-112	DFN		-630-						
	Thr		*					0.73 ± .09 b	(1)
	RI		*						
	FSA		73.9 mb						
Sn-114	DFN		-631-						
	Thr		*					.15 to 70 b	(1)
	RI		*					(~4.6) b ≠	(3)
	FSA		66.4 mb						

≠ Excess resonance integral only (excluding 1/v component) because the value of the thermal cross-section is so uncertain

Integral cross-section comparisons, continued

Nuclide (Half-life)		AUA + BOL 1967	BOL 1969	AUA 1971	BOL 1971 a, b	ENDF/B3 1971	UKNDL	Experiment	Expt. Ref
Sn-115	DFN		-632-	-4078-					
	Thr		*	59.8 b				.04 to 130 b	(1)
	RI		*	26.1 b				(~ 1.9) b ≠	(1)
	FSA		25.2 mb	20.1 mb					
Sn-116	DFN		-633-	-4079-					
	Thr		*	255 mb				~ 0.25 b	(1)
	RI		*	17.5 b				(15 ± 1.5) b	(5)
	FSA		47.1 mb	33.9 mb					
Sn-117	DFN		-634-	-4080-					
	Thr		*	1.37 b				.15 to 6.0 b	(1)
	RI		*	16.5 b				(12.4 ± .9) b	(5) ≠
	FSA		46.8 mb	47.9 mb					
Sn-117 m (14.0 d)			N O	D A T A					
Sn-118	DFN		-635-	-4081-					
	Thr		*	0.833 b				~ 0.29 b	(1)
	RI		*	7.39 b				(8.3 ± 1.2) b	(5)
	FSA		24.0 mb	13.6 mb					
Sn-119	DFN		-636-	-4082-					
	Thr		*	1.19 b				.03 to 5.3 b	(1)
	RI		*	5.28 b				(3.5 ± .4) b ≠	(5)
	FSA		29.6 mb	36.0 mb					
Sn-119 ■ (245 d)			N O	D A T A					

≠ Excess resonance integral only (excluding 1/v - component) because the value of the thermal cross section is so uncertain.

Integral cross-section comparisons continued

Nuclide (Half-life)		AUA + BOL 1967	BOL 1969	AUA 1971	BOL 1971 a, b	ENDF/B3 1971	UKNDL	Experiment	Expt. Ref
Sn-120	DFN		-637-	-4083-					
	Thr		*	140 mb				130 ± 55 mb	(1)
	RI		*	1.30 b				(1.6 ± .2)b	(5)
	FSA		15.8 mb	11.9 mb					
Sn-121 (27.0 h)	DFN			-4084-					
	Thr			5.74 b					
	RI			26.2 b					
	FSA			34.8 mb					
Sn-121 m (76 y)	DFN		N O	D A T A					
	Thr								
	RI								
	FSA								
Sn-122	DFN		-638-	-4085-					
	Thr		*	179 mb				158 ± 14 mb	(1)
	RI		*	884 mb				(672 ± 70) mb	(5)
	FSA		13.6 mb	13.0 mb					
Sn-123 (129.3 d)	DFN			-4086-					
	Thr			32.8 mb					
	RI			2.39 b					
	FSA			19.6 mb					
Sn-124 ($> 2 \times 10^{17}$ y)	DFN		-639-	-4087-					
	Thr		*	165 mb				131 ± 14 mb	(1)
	RI		*	11.3 b				(9.1 ± .9)b	(5)
	FSA		8.13 mb	5.62 mb					

Integral cross-section comparisons, continued

Nuclide (Half-life)		AUA + BOL 1967	BOL 1969	AUA 1971	BOL 1971 a, b	ENDF/B3 1971	UKNDL	Experiment	Expt. Ref
Sn-125 (9.64 d)	DFN			-4088-					
	Thr			550 mb					
	RI			13.9 b					
	FSA			9.40 mb					
Sn-126 ($\sim 10^5$ y)	DFN			-4089-					
	Thr			296 mb					
	RI			225 mb					
	FSA			3.66 mb					
Sb-121	DFN		-533A-	-4090-					
	Thr		*	6.19 b				6.13 ± .10 b	(16)
	RI		*	205 b				201 ± 12 b	(16)(32)
	FSA		66.9 mb	62.7 mb					
Sb-122 (2.76 d)	DFN			-4091-					
	Thr			21.3 b					
	RI			159 b					
	FSA			21.3 mb					
Sb-123	DFN		-534D-	-4092-					
	Thr		*	4.17 b				4.38 ± .07 b	(1)
	RI		*	126 b				109 ± 8 b	(2)(16)
	FSA		42.0 mb	36.4 mb					
Sb-124 (60.20 d)	DFN			-4093-					
	Thr			6.27 b				6.5 ± 1.5 b	(5)
	RI			19.1 b					
	FSA			10.3 mb					

Integral cross-section comparisons, continued

Nuclide (Half-life)		AUA + BOL 1967	BOL 1969	AUA 1971	BOL 1971 a, b	ENDF/B3 1971	UKNDL	Experiment	Expt. Ref
Sb-125 (2.74 y)	DFN	-737-		-4094-					
	Thr	1.51 b		967 mb					
	RI	31.9 b		19.0 b					
	FSA	68.5 mb		14.9 mb					
Sb-126 (12.5 d)	DFN			-4095-					
	Thr			5.78 b					
	RI			64.3 b					
	FSA			85.1 mb					
Sb-127 (93 h)	DFN			-4096-					
	Thr			913 mb					
	RI			14.7 b					
	FSA			9.40 mb					
Sb-128 (9.3 h)	DFN			-4097-					
	Thr			1.13 b					
	RI			15.9 b					
	FSA			22.4 mb					
Te-120	DFN		-640-		-640A-				
	Thr		*		*			2.34 ± .30 b	(6)
	RI		*		*				
	FSA		62.0 mb		62.0 mb				
Te-122	DFN		-641-	-4098-	-641A-				
	Thr		*	2.78 b	*			2.8 ± .9 b	(5)
	RI		*	46.8 b	*			(67 ± 20) b	(5)
	FSA		55.8 mb	43.3 mb	63.9 mb				

Integral cross-section comparisons, continued

Nuclide (Half-life)		AUA + BOL 1967	BOL 1969	AUA 1971	BOL 1971 a, b	ENDF/B3 1971	UKNDL	Experiment	Expt. Ref
Te-123	DFN		-642-	-4099-	-642A-				
(1.2×10^{13} y)	Thr		*	416 b	*			406 ± 30 b	(5)
	RI		*	5548 b	*			(5600 ±330)b	(5)
	FSA		76.9 mb	46.5 mb	76.7 mb				
Te-123 m	DFN			-4187					
(120 d)	Thr			42.4 b					
	RI			272 b					
	FSA			46.7 mb					
Te-124	DFN		-643-	-4100-	-643A-				
	Thr		*	6.48 b	*			6.5 ± 1.3 b	(5)
	RI		*	7.81 b	*				
	FSA		28.3 mb	26.8 mb	28.3 mb				
Te-125	DFN		-644-	-4101-	-644A-				
	Thr		*	1.55 b	*			1.55 ± .16 b	(5)
	RI		*	17.5 b	*			(18.5 ± 1.3)b	(5)
	FSA		29.8 mb	36.6 mb	29.8 mb				
Te-125 m	DFN			-4188-					
(58 d)	Thr			11.0b					
	RI			78.7 b					
	FSA			36.7 mb					
Te-126	DFN		-537A-	-4102-	-537D-				
	Thr		*	994 mb	*			940 ± 100 mb	(5)
	RI		*	8.16 b	*			(10.3 ± 2.0)b	(5)
	FSA		16.5 mb	11.2 mb	16.5 mb				

Integral cross-section comparisons, continued

Nuclide (Half-life)		AWA + BOL 1967	BOL 1969	AWA 1971	BOL 1971 a, b	ENDF/B3 1971	UKNDL	Experiment	Expt. Ref
Te-127 (9.30 h)	DFN			-4103-					
	Thr			2.74 b					
	RI			48.2 b					
	FSA			24.5 mb					
Te-127 m (109 d)	DFN			-4189-					
	Thr			9.34 b					
	RI			103 b					
	FSA			24.5 mb					
Te-128	DFN	-739-	-539A-	-4104-	-539D-				
	Thr	291 mb	*	213 mb	*			216 ± 8 mb	(5)
	RI	634 mb	*	1.55 b	*			1.56 ± .09 b	(5)
	FSA	5.91 mb	5.81 mb	3.47 mb	6.88 mb				
Te-129 (68.7 m)	DFN			-4105 -					
	Thr			369 mb					
	RI			7.40 b					
	FSA			11.1 mb					
Te-129 m (34.1 d)	DFN			-4190-					
	Thr			1.11 b					
	RI			20.5 b					
	FSA			11.2 mb					
Te-130 (8×10^{20} y)	DFN	-741-	-541A-	-4106-	-541D-				
	Thr	483 mb	*	259 mb	*			194 ± 20 mb	(5)
	RI	1.43 b	*	178 mb	*			436 ± 48 mb	(5)
	FSA	3.49 mb	3.22 mb	2.31mb	3.22 mb				

Integral cross-section comparisons, continued

Nuclide (Half-life)		AUA + BOL 1967	BOL 1969	AUA 1971	BOL 1971 a, b	ENDF/B3 1971	UKNDL	Experiment	Expt. Ref
Te-131 (24.8 m)	DFN			-4107-					
	Thr			35.6 mb					
	RI			50.0 mb					
	FSA			0.487 mb					
Te-131 m (30 h)	DFN			-4191-					
	Thr			107 mb					
	RI			159 mb					
	FSA			0.495 mb					
Te-132 (78 h)	DFN			-4108-					
	Thr			2.38 mb					
	RI			7.02 mb					
	FSA			0.207 mb					
I-127	DFN	-738-	-538A-	-4109-	-538D-				
	Thr	6.57 b	*	6.16 b	*			6.12 ± .08 b	(5)(16)
	RI	189 b	*	152 b	1			149 ± 4 b	(16)(23)
	FSA	69.8 mb	81.0 mb	73.1 mb	81.7 mb				
I-129 (1.7×10^7 y)	DFN	-740-		-4110-	-540A-				
	Thr	23.2 b		27.9 b	*			28.1 ± 1.3 b	(5)
	RI	44.8 b		25.5 b	*			37 ± 6 b	(3)
	FSA	42.4 mb		47.3 mb	50.3 mb				
I-130 (12.3 h)	DFN			-4111-					
	Thr			16.6 b				19 ± 3 b	(3)
	RI			173 b				(reactor spec	
	FSA			164 mb					

Integral cross-section comparisons, continued

Nuclide (Half-life)		AUA + BOL 1967	BOL 1969	AUA 1971	BOL 1971 a, b	ENDF/B3 1971	UKNDL	Experiment	Expt. Ref
I-131	DFN	-742-		-4112-		-1224-			
(7.969d)	Thr	49.2 b		0.938 b		1.00 b		~ 0.7 b	(5)
	RI	677 b		9.99 b		10.1 b		~ 8 b	(5)
	FSA	16.1 mb		17.2 mb					
I-133	DFN			-4113-					
(20.3 h)	Thr			3.47 mb					
	RI			5.31 mb					
	FSA			.0493 mb					
I-135	DFN	-749-		-4114-		-1225-			
(6.68 h)	Thr	146 mb		21.8 mb		15.0 b			
	RI	158 mb		26.3 mb		6.58 b			
	FSA	0.631 mb		0.260 mb					
Xe-124	DFN		-645-						
	Thr		*					113 ± 20 b	(1)
	RI		*					3100 ± 500 b	(1)
	FSA		90.6 mb						
Xe-126	DFN		-646-						
	Thr		*					2.3 ± 1 b	(1)
	RI		*					39 ± 18 b	(1)
	FSA		58.1 mb						
Xe-128	DFN		-647-	-4115-					
	Thr		*	4.19 b				~ 4 b	(1)
	RI		*	42.4 b				(≲ 112 b)	(5)
	FSA		44.5 mb	70.4 mb					

Integral cross-section comparisons, continued

Nuclide (Half-life)		AUA + BOL 1967	BOL 1969	AUA 1971	BOL 1971 a, b	ENDF/B3 1971	UKNDL	Experiment	Expt. Ref
Xe-129	DFN		-648-						
	Thr		*					17 ± 7 b	(1)
	RI		*					(230 ± 8) b	(5)
	FSA		52.9 mb						
Xe-129 m (8.0 d)				N O	D A T A				
Xe-130	DFN		-649-	-4116-					
	Thr		*	4.24 b				~4 b	(5)
	RI		*	17.2 b				(~5) b	(1)
	FSA		43.3 mb	52.5 mb					
Xe-131	DFN	-743-	-542A-	-4117-	-542D-	-1226-			
	Thr	120 b	*	110 b	*	87.1 b		90 ± 10 b	(1)
	RI	796 b	*	788 b	*	890 b		(870 ± 190)b	(5)
	FSA	28.7 mb	38.7 mb	44.7 mb	39.1 mb				
Xe-131m (11.94 d)				N O	D A T A				
Xe-132	DFN	-744-	-543A-	-4118-	-543D-				
	Thr	193 mb	*	459 mb	*			430 ± 90	(1)
	RI	726 mb	*	2.44 b	*			(~2.8) b	(1)
	FSA	18.8 mb	27.1 mb	27.9 mb	27.2 mb				
Xe-133 (5.29 d)	DFN	-745-		-4119-		-1227-			
	Thr	188 b		189 b		185 b		198 ± 94 b	(3)
	RI	1709 b		49.1 b		49.8 b		(reactor spec)	
	FSA	11.7 mb		8.98 mb					

Integral cross-section comparisons, continued

Nuclide (Half-life)		AUA + BOL 1967	BOL 1969	AUA 1971	BOL 1971 a, b	ENDF/B3 1971	UKNDL	Experiment	Expt. Ref
Xe-133 m (2.26 d)	DFN								
	Thr			N O	D A T A				
	RI								
	FSA								
Xe-134	DFN	-747-	-545A-	-4120-	-545D-				
	Thr	193 mb	*	253 mb	*			221 ± 12 mb	(1)
	RI	478 mb	*	260 mb	*			330 ± 23 mb	(1)
	FSA	14.7 mb	17.4 mb	6.14 mb	17.4 mb				
Xe-135 (9.172 h)	DFN	-750-		-4121-		-1026-	-4F-		
	Thr	3.87 x 10^6 b		3.06 x 10^6 b		3.06 x 10^6 b		(3.09 ± .04) x 10^6 b	(1)
	RI	8659 b		5803 b		7635 b	5893 b		
	FSA	11.3 mb		2.05 mb					
Xe-136	DFN	-752-	-547A-	-4122-	-547D-				
	Thr	146 mb	*	198 mb	*			180 ± 50 mb	(1)
	RI	457 mb	*	115 mb	*				
	FSA	4.99 mb	4.49 mb	2.23 mb	4.53 mb				
Cs-133	DFN	-746-	-544A-	-4123-	-544D-	-1141-			
	Thr	28.6 b	*	29.5 b	*	29.6 b		29.5 ± 1 b	(5)
	RI	386 b	*	377 b	*	380 b		457 ± 15 b	
	FSA	35.8 mb	54.7 mb	37.5 mb	55.3 mb				
Cs-134 (2.07 y)	DFN	-748-		-4124-					
	Thr	132 b		132 b				140 ± 12 b (reactor spec)	(5)
	RI	1136 b		86.1 b					
	FSA	81.5 mb		98.8 mb					

Integral cross-section comparisons, continued

Nuclide (Half-life)		AUA + BOL 1967	BOL 1969	AUA 1971	BOL 1971 a, b	ENDF/B3 1971	UKNDL	Experiment	Expt. Ref
Cs-135 (2.5×10^6 y)	DFN	-751-		-4125-	-546A-	-1229-			
	Thr	8.41 b		8.76 b	*	8.90 b		8.9 ± .5 b	(5)
	RI	52.5 b		61.8 b	*	30.2 b		62 ± 2 b	(5)
	FSA	21.7 mb		10.2 mb	27.1 mb				
Cs-136 (13.7 d)	DFN			-4126-					
	Thr			1.89 b					
	RI			15.5 b					
	FSA			27.7 mb					
Cs-137 (29.93 y)	DFN	-753-		-4127-	-548A-	-1230-			
	Thr	106 mb		103 mb	*	110 mb		91 ± 20 mb	(33)
	RI	67.8 mb		411 mb	*	231 mb			
	FSA	1.03 mb		2.22 mb	4.27 mb				
Ba-130	DFN		-650-						
	Thr		*					11.0 ± 3 b	(6)
	RI		*					270 ± 70 b	(15)
	FSA		81.3 mb						
Ba-132	DFN		-651-						
	Thr		*					8.5 ± 1.0 b	(6)
	RI		*						
	FSA		61.1 mb						
Ba-134	DFN		-652-	-4128-					
	Thr		*	1.93 b				2 ± 2 b	(5)
	RI		*	37.7 b				(11.1 ± 2.4)b	(5)
	FSA		44.4 mb	77.8 mb					

Integral cross-section comparisons, continued

Nuclide (Half-life)		AUA + BOL 1967	BOL 1969	AUA 1971	BOL 1971 a, b	ENDF/B3 1971	UKNDL	Experiment	Expt. Ref
Ba-135	DFN		-653-						
	Thr		*					5.8 ± .8 b	(5)
	RI		*					95 ± 6.5 b	(1)
	FSA		36.8 mb						
Ba-135 m (28.7 h)	DFN			NO	DATA				
	Thr								
	RI								
	FSA								
Ba-136	DFN		-654-	-4129-					
	Thr		*	393 mb				0.4 ± .4 b	(5)
	RI		*	17.1 b				(17.6 ± 1.7) b	(5)
	FSA		19.6 mb	14.3 mb					
Ba-137	DFN		-655-	-4130-					
	Thr		*	5.07 b				5.1 ± .4 b	(5)
	RI		*	4.83 b				4.1 ± .34 b	(5)
	FSA		14.4 mb	14.7 mb					
Ba-138	DFN	-754-	-549A-	-4131-					
	Thr	694 mb	*	349 mb				400 ± 40 mb	(5)
	RI	300 mb	*	210 mb				400 ± 40 mb	(5)
	FSA	25.2 mb	27.4 mb	3.90 mb					
Ba-140 (12.79 d)	DFN			-4132-					
	Thr			1.58 b				1.57 ± .03 b	(5)
	RI			13.6 b				13.6 ± 1.4 b	(5)
	FSA			13.6 mb					

Integral cross-section comparisons, continued

Nuclide (Half-life)		AÜA + BOL 1967	BOL 1969	AÜA 1971	BOL 1971 a, b	ENDF/B3 1971	UKNDL	Experiment	Expt. Ref
La-138 (1.1×10^{11} y)	DFN		-656-						
	Thr		*						
	RI		*						
	FSA		19.7 mb						
La-139	DFN	-755-	-550D-	-4133-	-550E-	-1231-			
	Thr	8.36 b	*	8.97 b	*	9.21 b		9.0 ± .2 b	(5)
	RI	10.4 b	*	15.5 b	*	16.2 b		15 ± 2.3 b	(5)
	FSA	5.61 mb	6.88 mb	5.77 mb	6.49 mb				
La-140 (40.24 h)	DFN			-4134-					
	Thr			2.50 b				2.7 ± .3 b	(5)
	RI			70.6 b				69 ± 4 b	(5)
	FSA			60.4 mb					
Ce-136 (2.9×10^{11} y)	DFN		-657-						
	Thr		*					7.25 ± 1.5 b	(6)
	RI		*						
	FSA		46.8 mb						
Ce-138	DFN		-658-						
	Thr		*					1.1 ± .3 b	(6)
	RI		*						
	FSA		34.4 mb						
Ce-140	DFN	-756-	-551D-	-4135-					
	Thr	642 mb	*	586 mb				580 ± 30 mb	(5)
	RI	677 mb	*	489 mb				487 ± 30 mb	
	FSA	12.8 mb	17.3 mb	10.7 mb					

Integral cross-section comparisons, continued

Nuclide (Half-life)		AUA + BOL 1967	BOL 1969	AUA 1971	BOL 1971 a, b	ENDF/B3 1971	UKNDL	Experiment	Expt. Ref
Ce-141 (32.5 d)	DFN			-4136-		-1232-			
	Thr			28.6 b		29.0 b		29 ± 3 b	(5)
	RI			28.2 b		29.1 b		(reactor spec)	
	FSA			12.8 mb					
Ce-142 (≥5 x 10^{16} y)	DFN	-758-	-553D-	-4137-					
	Thr	965 mb	*	855 mb				900 ± 90 mb	(5)
	RI	1.09 b	*	1.49 b				1.18 ± .09 b	(5)
	FSA	10.8 mb	14.2 mb	8.58 mb					
Ce-143 (33.5 h)	DFN			-4138-					
	Thr			5.57 b				6.0 ± .7 b	(5)
	RI			42.6 b				(reactor spec)	
	FSA			9.76 mb					
Ce-144 (284.4 d)	DFN			-4139-					
	Thr			0.932 b				1.0 ± .1 b	(5)
	RI			2.58 b				2.6 ± .26 b	(5)
	FSA			7.61 mb					
Pr-141 (≥2 x 10^{16} y)	DFN	-757-	-552D-	-4140-	-552E-	-1233-			
	Thr	11.8 b	*	11.0 b	*	11.4 b		11.3 ± .2 b	(5)
	RI	20.8 b	*	17.3 b	*	18.8 b		15.7 ± 1.1b	(1)
	FSA	14.5 mb	18.5 mb	15.5 mb	18.5 mb				
Pr-142 (19.2 h)	DFN			-4141-					
	Thr			17.2 b				20 ± 3 b	(5)
	RI			143 b				(reactor spect)	
	FSA			88.5 b					

Integral cross-section comparisons, continued

Nuclide (Half-life)		AUA + BOL 1967	BOL 1969	AUA 1971	BOL 1971 a, b	ENDF/B3 1971	UKNDL	Experiment	Expt. Ref
Pr-143 (13.6 d)	DFN			-4142-		-1234-			
	Thr			96.3 b		99.5 b		90 ± 10 b	(5)
	RI			471 b		167 b		190 ± 25 b	(5)
	FSA			38.2 mb					
Pr-145 (6 h)	DFN			-4143-					
	Thr			18.3 b					
	RI			445 b					
	FSA			23.7 mb					
Nd-142	DFN		-584A	-4144-					
	Thr		*	18.5 b				18.7 ± .7 b	(5)
	RI		*	8.48 b				8.2 ± .3 b	
	FSA		22.8 mb	29.8 mb					
Nd-143	DFN	-759-	-554D-	-4145-		-1235-			
	Thr	329 b	*	303 b		317 b		322 ± 5 b	(5)
	RI	57.5 b	*	63.9 b		136 b		(197 ± 4) b	(5)
	FSA	4.93 mb	42.3 mb	36.7 mb					
Nd-144 (2.4×10^{15} y)	DFN	-760-	-555D-	-4146-					
	Thr	4.83 b	*	3.38 b				3.8 ± .3 b	(5)
	RI	8.51 b	*	7.57 b				(5.2 ± .8) b	(5)
	FSA	24.4 mb	27.1 mb	32.8 mb					
Nd-145 (>6×10^{16} y)	DFN	-761-	-556D-	-4147-		-1236-			
	Thr	60.9 b	*	44.7 b		41.2 b		45 ± 4 b	(5)
	RI	388 b	*	271 b		298 b		259 ± 35 b	(5)
	FSA	55.9 mb	32.4 mb	25.3 mb					

Integral cross-section comparisons, continued

Nuclide (Half-life)		AUA + BOL 1967	BOL 1969	AUA 1971	BOL 1971 a, b	ENDF/B3 1971	UKNDL	Experiment	Expt. Ref
Nd-146	DFN	-762-	-557D-	-4148-					
	Thr	9.72 b	*	1.31 b				1.33 ± .1 b	(1)
	RI	24.2 b	*	2.32 b				3.0 ± .3 b	(5)(15)
	FSA	27.1 mb	30.1 mb	23.0 mb					
Nd-147 (11.0 d)	DFN			-4149-		-1237-			
	Thr			49.0 b		50.0 b			
	RI			649 b		648 b			
	FSA			49.0 mb					
Nd-148	DFN	-764-	-559D-	-4150-					
	Thr	3.28 b	*	2.34 b				2.52 ± .18 b	(12)
	RI	11.8 b	*	14.0 b				16.8 ± 2.7 b	(12)
	FSA	41.9 mb	29.9 mb	20.0 mb					
Nd-150 ($>10^{16}$ y)	DFN	-768-	-561D-	-4151-					
	Thr	2.89 b	*	1.13 b				1.26 ± .16 b	(5)
	RI	7.61 b	*	2.56 b				~ 14 b	(5)
	FSA	39.9 mb	53.3 mb	25.3 mb					
Pm-147 (2.623 y)	DFN	-763-		-4152-	-558A-	-1238-	-903-		
	Thr	128 b		169 b	*	169 b	188 b	180 ± 9 b	(1)
	RI	1200 b		2175 b	*	2236 b	2237 b	2230 ± 215 b	(5)
	FSA	113 mb		124 mb	83.4 mb		100 mb		
Pm-148 (5.37 d)	DFN	-766-		-4153-		-1239-			
	Thr	1452 b		2884 b		2200 b		3000 ± 2000 b (Hard reactor spectrum)	(5)
	RI	27967 b		25727 b		36438 b			
	FSA	67.6 mb		187 mb					

Integral cross-section comparisons, continued

Nuclide (Half-life)		AUA + BOL 1967	BOL 1969	AUA 1971	BOL 1971 a, b	ENDF/B3 1971	UKNDL	Experiment	Expt. Ref
Pm-148 m (40.6 d)	DFN	-765-		-4192-		-1254-			
	Thr	38668 b		20700 b		24000 b		20500 b	(34)
	RI	35669 b		19250 b		10569 b		3600 ± 2400b	(34)
	FSA	762 mb		188 mb					
Pm-149 (53.1 h)	DFN			-4154-		-1240-			
	Thr			1314 b		1450 b		1450 ± 240 b	(5)
	RI			923 b		807 b		(reactor spec	
	FSA			91.7 mb					
Pm-151 (28 h)	DFN			-4155-		-1241-			
	Thr			171 b		150 b		<700 b	(5)
	RI			1208 b		1201 b		(reactor spec)	
	FSA			120 mb					
Sm-144	DFN		-585A-						
	Thr		*					0.7 b	(6)
	RI		*					(reactor spec)	
	FSA		67.3 mb						
Sm-147 (1.05×10^{11} y)	DFN		-586A-	-4156-		-1242-			
	Thr		*	53.4 b		57.1 b		52 ± 3 b	(5)
	RI		*	566 b		623 b		640 ± 200 b	(5)
	FSA		209 mb	133 mb					
Sm-148 (>2×10^{14} y)	DFN		-587A-	-4157-		-1243-			
	Thr		*	4.41 b		4.73 b		4.72 ± .08 b	(5)
	RI		*	18.4 b		54.2 b		≤ 50 b	(1)
	FSA		65.3 mb	60.2 mb					

Integral cross-section comparisons, continued

Nuclide (Half-life)		AUA + BOL 1967	BOL 1969	AUA 1971	BOL 1971 a, b	ENDF/B3 1971	UKNDL	Experiment	Expt. Ref
Sm-149 ($>10^{15}$ y)	DFN	-767-	-560D-	-4158-		-1027-			
	Thr	68640 b	*	66280 b		67477 b		68600 ± 300b	(5)
	RI	3610 b	*	3594 b		3183 b			
	FSA	131 mb	168 mb	123 mb					
Sm-150	DFN	-769-	-588A-	-4159-		-1244-			
	Thr	96.8 b	*	101 b		100 b		101 ± 5 b	(5)
	RI	871 b	*	328 b		252 b		255 ± 25 b	(5)
	FSA	16.2 mb	85.1 mb	59.6 mb					
Sm-151 ($\approx$87 y)	DFN	-770-		-4160-	-562A-	-1245-			
	Thr	14160 b		13850 b	*	13578 b		13700 ± 1600 b	(5)
	RI	2697 b		2163 b	*	3772 b		(3170 ± 700)b	(5)
	FSA	100 mb		351 mb	157 mb				
Sm-152	DFN	-771-	-563D-	-4161-		-1246-			
	Thr	227 b	*	205 b		204 b		209 ± 4 b	(1)
	RI	2290 b	*	1766 b		3462 b		3060 ± 60 b	(5)
	FSA	88.9 mb	86.0 mb	55.4 mb					
Sm-153 (46.58 h)	DFN			-4162-		-1247-			
	Thr			333 b		9992 b			
	RI			1106 b		5459 b			
	FSA			158 mb					
Sm-154	DFN	-773-	-565D-	-4163-					
	Thr	5.33 b	*	4.69 b				4.9 ± 1.0 b	(5)
	RI	17.1 b	*	38.1 b				(31 ± 6) b	(13)
	FSA	35.6 mb	69.7 mb	47.8 mb					

Integral cross-section comparisons, continued

Nuclide (Half-life)		AUA + BOL 1967	BOL 1969	AUA 1971	BOL 1971 a, b	ENDF/B3 1971	UKNDL	Experiment	Expt. Ref
Sm-156 (9.4 h)	DFN			-4164-					
	Thr			17.1 b					
	RI			332 b					
	FSA			46.8 mb					
Eu-151	DFN		-589A-			-1028-	-921A-		
	Thr		*			8339 b	8336 b	8280 ± 270 b	(3)(5)
	RI		*			3154 b	2390 b	(2485 ± 310)b	≠ (13)
	FSA		360 mb				207 mb		
Eu-153	DFN	-772-	-564D-	-4165-		-1029-	-992A-		
	Thr	459 b	*	435 b		444b	444b	450 ± 70 b	(5)
	RI	1491 b	*	1203 b		1512 b	1500 b	(1620 ± 200)b	≠ (13)
	FSA	287 mb	303 mb	234 mb			152 mb		
Eu-154 (16 y)	DFN	-774-		-4166-		-1248-			
	Thr	1481 b		1480 b		1611 b		1420 ± 280 b	(3)
	RI	4722 b		1157 b		1321 b		(reactor spec)	
	FSA	381 mb		750 mb					
Eu-155 (4.65 y)	DFN	-775-		-4167-		-1249-			
	Thr	19725 b		3674 b		4040 b		4040 ± 125 b	(14)
	RI	1394 b		1213 b		1817 b			
	FSA	261 mb		153 mb					
Eu-156 (15.4 d)	DFN			-4168-		-1250-			
	Thr			472 b		2000 b			
	RI			1238 b		1947 b			
	FSA			319 mb					

≠ Corrected to a cut-off at 0.55 eV

Integral cross-section comparisons, continued

Nuclide (Half-life)		AUA + BOL 1967	BOL 1969	AUA 1971	BOL 1971 a, b	ENDF/B3 1971	UKNDL	Experiment	Expt. Ref
Eu-157 (15.1 h)	DFN			-4169-		-1251-			
	Thr			188 b		2001 b			
	RI			823 b		1651 b			
	FSA			108 mb					
Gd-152 (1.1×10^{14} y)	DFN		-659-						
	Thr		*					1100 ± 100 b	(15)
	RI		*					3000 ± 300 b	(15)
	FSA		160 mb						
Gd-154	DFN		-590A-						
	Thr		*					85 ± 12 b	(35)
	RI		*					260 ± 80 b	(13)(35)
	FSA		242 mb						
Gd-155	DFN	-776-	-591A-	-4170-		-1252-			
	Thr	49770 b	*	51370 b		51527 b		53000 ± 3200 b	(5)
	RI	1594 b	*	1539 b		1555 b			
	FSA	137 mb	158 mb	102 mb					
Gd-156	DFN	-777-	-567D-	-4171-					
	Thr	3.87 b	*	6.11 b				1.5 ± 1.2 b	(35)
	RI	89.3 b	*	121 b				100 ± 30 b	(35)
	FSA	187 mb	117 mb	44.5 mb					
Gd-157	DFN	-778-	-568D-	-4172 -		-1253-			
	Thr	206700 b	*	225800 b		217490 b		218000 ± 1300 b	(1)
	RI	495 b	*	3158 b		1146 b			
	FSA	109 mb	101 mb	56.0 mb					

≠ Corrected to a cut-off at 0.55 eV

Integral cross-section comparisons, continued

Nuclide (Half-life)		AUA + BOL 1967	BOL 1969	AUA 1971	BOL 1971 a, b	ENDF/B3 1971	UKNDL	Experiment	Expt. Ref
Gd-158	DFN		-569D-	-4173-					
	Thr		*	2.66 b				2.78 ± 0.42 b	(5)
	RI		*	97.8 b				66.7 ± 16 b	(15)
	FSA		87.3 mb	36.1 mb					
Gd-159 (18.0 h)	DFN			-4174-					
	Thr			16.2 b					
	RI			186 b					
	FSA			29.2 mb					
Gd-160	DFN		-592A-	-4175-					
	Thr		*	720 mb				768 ± 115 mb	(36)
	RI		*	1.42 b				(6.9 ± 1.0) b	(13)
	FSA		59.1 mb	25.0 mb					
Tb-159 (>5 x 10^{16} y)	DFN		-570A-	-4176-					
	Thr		*	21.6 b				23.2 ± .5 b	(11)
	RI		*	376 b				406 ± 19 b	(1)
	FSA		208 mb	202 mb					
Tb-160 (72.1 d)	DFN			-4177-					
	Thr			479 b				600 ± 100 b	(5)
	RI			1017 b				(reactor spec)	
	FSA			322 mb					

Integral cross-section comparisons, continued

Nuclide (Half-life)		AUA + BOL 1967	BOL 1969	AUA 1971	BOL 1971 a, b	ENDF/B3 1971	UKNDL	Experiment	Expt. Ref
Tb-161 (6.9 d)	DFN			-4178-					
	Thr			95.5 b					
	RI			654 b					
	FSA			83.6 mb					
Dy-156 ($>10^{18}$ y)	DFN		-660-						
	Thr		*					33 ± 3 b	(38)
	RI		*					960 ± 80 b	(38)
	FSA		242 mb						
Dy-158	DFN		-661-						
	Thr		*					47 ± 6 b	(1)
	RI		*					130 ± 20 b	(1)
	FSA		228 mb						
Dy-160	DFN		-662-	-4179-					
	Thr		*	56.6 b				61 ± 5 b	(1)
	RI		*	1159 b				1000 ± 78 b	(1)
	FSA		143 mb	83.7 mb					
Dy-161	DFN		-571A-	-4180-					
	Thr		*	561 b				623 ± 13 b	(1)
	RI		*	1345 b				1490 ± 100 b	(1)
	FSA		213 mb	111 mb					
Dy-162	DFN		-663-	-4181-					
	Thr		*	205 b				165 ± 7 b	(1)
	RI		*	2543 b				2360 ± 1100 b	
	FSA		66.2 mb	47.4 mb					(1)

Integral cross-section comparisons, continued

Nuclide (Half-life)		AUA + BOL 1967	BOL 1969	AUA 1971	BOL 1971 a, b	ENDF/B3 1971	UKNDL	Experiment	Expt. Ref
Dy-163	DFN		-664-	-4182-					
	Thr		*	131 b				126 ± 6 b	(1)
	RI		*	1642 b				1690 ± 300 b	(1)
	FSA		98.2 mb	33.9 mb					
Dy-164	DFN		-665-	-4183-		-1031-			
	Thr		*	2688 b		2489 b		2620 ± 30 b	(1)
	RI		*	749 b		328 b		570 ± 80 b	(1)
	FSA		45.8 mb	16.4 mb					
Dy-166 (81.6 h)	DFN			N O	D A T A				
	Thr								
	RI								
	FSA								
Ho-165 (7.6×10^{16} y)	DFN			-4184-	-690-				
	Thr			62.5 b	*			64.3 ± 1.0 b	(1)
	RI			677 b	*			681 ± 20 b	(1)
	FSA			315 mb	133 mb				
Ho-166 (26.9 h)	DFN			N O	D A T A				
	Thr								
	RI								
	FSA								
Ho-166m (~1200 y)	DFN			N O	D A T A				
	Thr								
	RI								
	FSA								

Integral cross-section comparisons, continued

Nuclide (Half-life)		AUA + BOL 1967	BOL 1969	AUA 1971	BOL 1971 a, b	ENDF/B3 1971	UKNDL	Experiment	Expt. Ref
Er-162	DFN				-691-				
	Thr				*			160 ± 30 b	(19)
	RI				*				
	FSA				428 mb				
Er-164	DFN				-692-				
	Thr				*			1.65 ± .17 b	(6)
	RI				*				
	FSA				211 mb				
Er-166	DFN				-693-				
	Thr				*			30 ± 5 b	(19)
	RI				*			90 ± 25 b	(1)
	FSA				127 mb				
Er-167	DFN				-694-				
	Thr				*			699 ± 20 b	(36)
	RI				*			(3177 ± 325)b	(13)
	FSA				124 mb				
Er-168	DFN				-695-				
	Thr				*			1.9 ± .2 b	(19)
	RI				*			(35.5 ± 7.0)b	(13)
	FSA				68.7 mb				
Er-169 (9.3 d)	DFN								
	Thr								
	RI			N O	D A T A				
	FSA								

Integral cross-sections continued

Nuclide (Half-life)		AUA + BOL 1967	BOL 1969	AUA 1971	BOL 1971 a, b	ENDF/B3 1971	UKNDL	Experiment	Expt. Ref
Er-170	DFN Thr RI FSA				-696- * * 34.3 mb			4.9 ± .6 b 32.2 b	(1) (37)

REFERENCES

1 POPE A. L. & STORY J. S. (1973); evaluations for this report.

2 RICABARRA M. D., TURJANSKI R. & RICABARRA G. H. (Oct. 1969) Can. J. Phys. 47, 2031

3 STORY J.S. & SJOSTRAND N-G. (Apr. 1961) AEEW-M122

4 RICABARRA G. H., TURJANSKI R. & RICABARRA M. D. (Jun. 1970) Helsinki 2, 589

5 WALKER W. H. (Dec. 1969, Jan. 1972) AECL-3037, Part 1

6 BNL-325 (Feb. 1966, May 1966, Aug. 1966)

7 BEMIS C. E., DRUSCHEL R. E., HALPERIN J. & WALTON J. R. (Mar. 1972) NSE 47, 371

8 POPE A. L. & STORY J. S. (July 1969) AEEW-M921

9 RICABARRA M. D., TURJANSKI R. & RICABARRA G. H. (Oct. 1970) Can. J. Phys. 48, 2362

10 FULMER R. H., STRICOS D. P. & RUANE T. F. (Nov. 1971) NSE 46, 314.

11 RYVES T. B., & ZIEBA K. J. (Aug. 1973) EANDC(UK)-151L, 53

12 STORY J. S. (Jan. 1972) WNDG-96, unpublished

13 RAHN F., CAMARDA H. S., HACKEN G., HAVENS W. W., LYON H. I., SLAGOWITZ M., WYNCHANK S. (June 1972) Nucl. Sci. Eng. 48, 219

14 WALKER W. S. & MOWATT R. S. (Oct. 1970) Can. J. Phys. 48, 1933

15 STEINNES E. (Sept. 1972) J. Inorg. Nucl. Chem. 34, 2699

16 RYVES T. B. (May 1969) EANDC(UK)-110 AL, 45

17 PEARLSTEIN S. & MILLIGAN R. F. (Oct. 1961) Nucl. Sci. Eng. 26, 281

18 RYVES T. B. (Mar. 1971) J. Nucl. Energy 25, 129

19 GOLDMAN D. T., ALINE P., SHER R. & STEHN J. R. (Aug. 1968) unpublished

20 CHING-SHEN SU (Aug. 1967) Diss. Abstracts B28. 720

21 BRADLEY J. G. & JOHNSON W. H. (Jan. 1972) Nucl. Sci. Eng. 47, 151

22 EMERY J. F. (May 1965) J. Inorg. Nucl. Chem. 27, 903

23 RICABARRA M. D., TRUJANSKI R., RICABARRA G. H. & BIGHAM C. B. (Nov. 1968) Can. J. Phys. 46, 2473

24 SANTRY D. C. & WERNER R. D. (Nov. 1972) EANDC (Can)-46L, 1

25 ANDERS E. (Apr 1958) Phys. Rev. 110, 427

26 KATCOFF S. & WILLIAMS D. C. (Oct. 1958) J. Inorg. Nucl. Chem. 7, 194

27 ISHIKAWA H. (Oct. 1969) J. Nucl. Sci. Tech. 6, 587

28 WALKER W. H. & COPLEY L. A. (Sept. 1966) Can. J. Phys. 44, 1985

29 LESAGE L. & SHER R. (Feb. 1966) ANS San Diego meeting

30 WAY K & HAINES G. (Feb. 1948) AECD-2138

31 KEISCH B. (Jan 1963) Phys. Rev. 129, 769

32 ORVINI E., GAGGERO G., LESCA L., BRESESTI A. M. & BRESESTI M. (July 1968) J. Inorg. Nucl. Chem. 30, 1353

33 STUPEGIA D. C. (May 1960) J. Nucl. Energy A12, 16; weighted mean of the six results presented

34 KIROUAC G. J., EILAND H. M., CONRAD C. A., SLOVACEK R. E. & SEEMANN K. W. (Nov. 1973) Nucl. Sci. Eng. 52, 310

35 HIRSSBERGER E. (Sept. 1969) SGAE G-14/1969

36 MANGAL S. K. & GILL P. S. (Mar. 1963) Nucl. Phys. 41, 372

37 KONDAIAH E., RANAKUMAR N. & FINK R. W. (Nov. 1968) Nucl. Phys. A120, 329

38 ALSTAD J., PAPPAS A.C & SYVERSON T. (May 1972) INDC(NOR)-1/G,2.

Contribution to
Review Paper No. 11a

AN INVESTIGATION ON THE GAUSSIAN WIDTH PARAMETER IN $^{235}U(n_{th},f)$

A. Zukeran
Power Reactor and Nuclear Fuel Development Corporation
9-13, 1-chome Akasaka, Minato-ku, Tokyo, Japan

Abstract

The most stable charge Z_A has been obtained from the Garvey's mass table [1], and the most probable charge Z_p in $^{235}U(n_{th},f)$ has been estimated using the Z_A-values under the ECD postulate [2]. Dependence of the estimated most probable charge Z_p on the mass number A has been compared with that of semi-empirical Z_p-values obtained from the observed fractional yields [3] using the assumed Gaussian width parameter σ. The fairly well agreement between them has been confirmed.

Contrarily to investigate on the Gaussian width parameter σ assumed above, the σ-value has been obtained from the same observed fractional yield using the estimated Z_p-value mentioned above. The resultant σ-values as functions of mass number A have been investigated from the point of view of dependencies on the neutron number n and proton number p respectively. It is found that some possible systematics may exist in the dependencies of σ-values on the n and p.

To examine the validity of dependencies of Z_p and σ-values only on the mass number A, the following attempt has been made. If Z_p and σ-values depend only on the mass number A, there should be a common point (Z_p,σ) to all isotopes of the isobar on the Z_p-σ correlation curve, i.e. the calculated fractional yields based on the Gaussian distribution [4] should be exactly equal to the observed ones of those isotopes. The result of investigation on the correlation between Z_p and σ shows that such a common point scarcely exists. It seems to be possible interpretation that Z_p and σ wouldn't be the functions of mass number A as a single variable but the functions of the proton and neutron numbers respectively. Further investigations, however, are still required, e.g. on the validity of simple Gaussian distribution function used for present work.

1. INTRODUCTION

A preliminary evaluation [5] was made for the fission product yields of ^{235}U, ^{239}Pu and ^{241}Pu thermal neutron induced fissions and of ^{238}U and ^{239}Pu fast neutron induced fissions. The charge ditributions in that work were based on the constant Gaussian width parameter σ= 0.58 [6] and the most probable charge obtained from the Garvey's mass table [1] as described in this

paper. Remarkable discrepancies between the observed [3] and estimated fractional yields arose as the consequence of that work even in the thermal neutron induced fission of ^{235}U. The discrepancies, for instance, for ^{133}Sb, ^{95}Y, ^{94}Y, ^{131}Te, ^{139}Ba and ^{150}Pm were significantly large; e.g. the calculation to experiment ratios (C/E's) of those fractional independent yields ranged from 0.37 to 9.2. Therefore it was fully realized that the Gaussian width parameter including the most probable charge Z_p should be extensively investigated, although the further evaluations of experimental data themselves were still required.

The present work has been devoted to the following points; 1) to obtain the Gaussian width parameters based on the conventional Gaussian distribution from the observed fractional independent and/or cumulative yields using the calculated most probable charges, 2) to investigate on the possibility of some systematics existing between the Gaussian width parameter and the mass number, and 3) to examine the validity of the dependence of Gaussian width parameter only on the mass number.

2. THE MOST STABLE CHARGE Z_A

Garvey et al [1] compiled the new mass table based on 1271 measured masses and mass relations. The most general fundamental dependence on proton number Z, neutron number N and mass number A, whose masses satisfy those mass relations, was obtained by a least-squares fit to the body of known masses. The magnitude of the average deviation between predicted and measured masses in this table is 0.089 MeV which is the smallest one among the mass tables [1, 7, 8] considered. Considering a lot of measured masses used for the compilation and also the acceptable deviation, it will be the most suitable one for the purpose of estimating the most stable charge Z_A.

The total binding energy B(N,Z) of a nucleus with $N \geq 10, Z \geq 6$, $A \geq 16$ and $N \geq Z$ in the Garvey's mass table is defined by;

$$B(N,Z) = B_0 + g_1(N) + g_2(Z) + g_3(A) \qquad (2.1)$$

$$B_0 = 110.7824 \text{ MeV}$$

where $g_1(N)$, $g_2(Z)$ and $g_3(A)$ functions and the other related quantities such as mass excess and neutron binding energy are also shown in their mass table. The most stable charge is obtained by means of numerical derivation on the smooth

curve fitted to the masses of isobars. The most stable charge Z_A is the solution of the following equation;

$$(\partial M(A-Z,Z)/\partial Z)_A = (M_H - M_n) - (\partial B(A-Z,Z)/\partial Z)_A = 0$$

$$M_H = 7.28899 \quad \text{MeV [9]}$$

$$M_n = 8.0714 \quad \text{MeV}$$

The trend of the most stable charges obtained from Garvey's mass table is shown by the solid line in Fig. 2.1. The minimum requirement should be that the location of the estimated most stable nucleus has to be close to the location of the observed one when the most stable nucleus for odd mass number is considered, or between the locations of two observed ones when the most stable nucleus for even mass number is considered, and also that the estimated trend shows reasonable shell effects. The present results satisfy both requirements as shown in the Fig. 2.1.

The comparison of the present work with the Fiedler and Herrmann's [10] obtained from the mass table compiled by Konig et al [11] is shown in Fig. 2.2. The estimated curve agrees fairly well with their's within about 0.3 charge unit on the overall range of mass number and also has some fine structures, e.g. the stair-like behavior from 92 to 114 of mass number. This behavior seems to be due to the mass relations used by Garvey et al for compiling the mass table. Similar ones are found over 143. Furthermore, the valley around 121 becomes deeper than that of Fiedler and Herrmann [10].

3. CHARGE DISTRIBUTION IN $^{235}U(n_{th},f)$

3.1 CHARGE DISTRIBUTION FUNCTION

The Gaussian width parameter σ, which is a basic parameter in the Wahl's method, is obtained by fitting the Gaussian charge distribution function to several observed fractional yields [3]. In early work by Wahl, the same Gaussian distribution with constant value of σ was used. However in the latter work it was pointed out by Wahl [12] and Amiel and Feldstein [13] that the same Gaussian distribution does not satisfactorily fit to the observed independent yields, i,e. the importance of even-odd effect were emphasized. One of attempts to take it into account has been made by Musgrove [14] for this panel. However, for present work the following simple distribution function has been used because the auther has been interested in the capability of the conventional Gaussian distribution when the Gaussian width parameter is varied in the wide range.

The fractional independent yield $y_i(Z)$ and fractional cumulative yield $Y_c(Z)$ of an isotope with atomic number Z and mass number A can be approximately expressed in terms of β-decay chain length $(Z-Z_p)$ and the Gaussian width parameter σ;

$$P(Z) = \frac{1}{\sqrt{c\pi}} \mathrm{Exp}\left[- \frac{(Z - Z_p)^2}{c} \right] \tag{3.1}$$

$$y_i(Z) = \frac{1}{\sigma\sqrt{2\pi}} \int_{Z-0.5}^{Z+0.5} \mathrm{Exp}\left[- \frac{(n - Z_p)^2}{2\sigma^2} \right] dn \tag{3.2}$$

$$Y_c(Z) = \frac{1}{\sigma\sqrt{2\pi}} \int_{\infty}^{Z+0.5} \mathrm{Exp}\left[- \frac{(n - Z_p)^2}{2\sigma^2} \right] dn \tag{3.3}$$

$$c \approx 2(\sigma^2 + 1/12)$$

where P(Z) and σ mean the Gaussian charge dispersion and the Gaussian width parameter respectively.

3.2 THE MOST PROBABLE CHARGE Z_p

The most probable charge Z_p based on the equal charge displacement (ECD) postulate [2] can be obtained from the most stable charge Z_A. A well-known relationship [10] between Z_p and Z_A are as follows;

$$Z_{pl} = Z_{Al} - 1/2(Z_{Al} + Z_{A_F} - Al - \nu_T - Z_F) \tag{3.4a}$$

$$Z_{ph} = Z_{Ah} - 1/2(Z_{Ah} + Z_{A_F} - Ah - \nu_T - Z_F) \tag{3.4b}$$

$$\nu_T = \nu_l + \nu_h$$
$$A_F = A_l + A_h + \nu_T \tag{3.4c}$$

where suffix l, h and F mean the light and heavy fragments, and the fissioning nucleus, and A and ν mean the mass number and the number of emitted neutron per fission respectively.

The empirical Z_p-values of ^{235}U thermal neutron induced fission have been obtained from the observed fractional independent and/or cumulative

yields compiled by Wahl [3] using the charge distribution function defined by equ. (3.2) and (3.3) under the assumption that Gaussian width parameter σ does not depend on the mass number. The number of emitted neutron per fission ν_T, ν_l and ν_h recommended by Wahl have been used.

As shown in Fig. 3.1, there are larger scatter in the empirical Z_p-values. The Z_p-values near closed and semi-closed nuclei except ^{132}Sn and ^{123}Sn significantly scatter. Although ^{96}Nb and ^{97}Nb are far from the closed nuclei, they show the similar behaviors as the closed ones since their complementary fragments have the proton number of 51. Eight heavy nuclei ^{140}Cs, ^{141}Cs, ^{142}La, ^{143}Ba, ^{144}Ba, ^{146}Pm, ^{148}Pm and ^{150}Pm show systematically larger deviations from the estimated Z_p-values although they are also relatively far from the closed nuclei with neutron number of 82. Among them the discrepancies of ^{140}Cs, ^{146}Pm and ^{148}Pm were pointed out by Wahl [3]. One of possible sources of their discrepancies seems to be due to some systematic errors of observed fractional yields. Except the scatted cases near the closed nuclei and the eight heavy ones mentioned above, we consider that the estimated Z_p-values fairly well agree with the empirical values. We have also found the following differences in comparison of the present results with others.

(1) the relatively larger valley exists in the estimated trend around the mass number 122.
(2) the deviations of estimated Z_p-values from Z_p^{UCD}'s are generally smaller than those of the empirical values over the mass number 140, and the differences between the estimated and empirical Z_p-values increase as the mass number increases.

The existence of the valley is consistent with the empirical values of ^{117}Pd, ^{123}Sn and ^{125}Sn except ^{112}Ag, ^{126}Sb, ^{127}Sb etc. The estimated trends by several authers like Pappas et al [6] show monotonously decreasing function of mass number. Although we have examined some possibilities of rejecting the existence of the valley, no one could be found. This problem may be left pending until more experimental data become available.

Z_p-values obtained by three authers are shown in Table 3.1. As shown in the Table, their deviations from the mean value are relatively large around the valley, the peaks and near the centre of wings of mass distribution, and the minimum deviations appear in the mass number 131(105) and 143(94) whose magnitudes are about ±0.2 and ±0.3 percents respectively. The deviations of the present work in the heavy fragments gradually increase from -0.7 to +0.4 percents

as the mass number increases, and the same tendency appears in the light fragments. The status of the other's are nearly the same to our's although their directions of deviations are different from each other.

It will be important to examine the dependence of the scatter of empirical Z_p-values on the σ's. The empirical Z_p-values obtained from the same observed fractional yields [3] by varing the magnitude of the Gaussian width parameter are shown in Fig. 3.1 to 3.3. However, the scatter of empirical Z_p-values is hardly improved. For instance, the Z_p-values of ^{140}Cs, ^{144}Ba, ^{146}Pm and ^{148}Pm, which have shown uniformly larger deviations ($Z_p - Z_p^{UCD}$), show only slight change against about 15% change of σ-value. Average most probable charges $\overline{Z}_p$'s are also shown in Fig. 3.1 to 3.3 by dashed lines as a temporally standard to indicate the movement of empirical values. Average Z_p-values together with the other averages denoted by $\overline{Z}_{pl}$ and $\overline{Z}_{ph}$ for light and heavy fragments respectively are shown in Table 3.2. When the σ's increases from 0.55 to 0.62, the $\overline{Z}_{pl}(\sigma)$ decreases from 0.350 to 0.225, but contrarily $\overline{Z}_{ph}(\sigma)$ increases from 0.425 to 0.521. Averages of $Z_{pl}(\sigma)$ and $Z_{ph}(\sigma)$ denoted by Z_p in the 5th column are 0.300 and 0.483 respectively. Comparing the present result with Wahl's, $\overline{Z}_p$ of 0.438 for heavy fragments fairly well agrees with his result of 0.45 for mass number 141 to 144. As it is clear from the normalized $\overline{Z}_{pl,h}$ representation as shown in Table 3.1, $\overline{Z}_{pl}$ is more sensitive to σ than $\overline{Z}_{ph}$. Since the function $\overline{Z}_{pl}(\sigma)$ is decreasing and $\overline{Z}_{ph}(\sigma)$ increasing respectively, the empirical most probable charge as a whole move towards the average value $\overline{Z}_p$ of 0.40 as shown by dashed line in Fig. 3.1 to 3.3.

3.3 GAUSSIAN WIDTH PARAMETER IN $^{235}U(n_{th},f)$

3.3.1 FITTING OF GAUSSIAN WIDTH PARAMETER

In the preceding discussion on the empirical Z_p-values as a function of Gaussian width parameter, it was assumed that the Gaussian width parameter would'nt depend on the mass number. As the consequence, the empirical Z_p - values significantly scatted around the calculated trend as shown in Fig. 3.1. It seems to be one of possible sources of the scatter that the constant value of Gaussian width parameter has been used. Therefore as the next attempt the Gaussian width parameters depending on the mass number are obtained from the same measured fractional yields [3] using the most probable charge Z_p obtained in Section 3.2. Such an attempt was done by Chouch [4] but in our case the emphasis has been placed on the derivation of some systematics from those σ-values.

The resultant Gaussian width parameter is shown in Fig. 3.4 as a function of mass number A, and it is also shown in Fig. 3.7 together with the others. The present σ-values of light fragments are uniformly smaller than Crouch's below 86, in the range from 92 to 95 and above 96. The difference at the mass number 133 is significantly large. To examine if there are some systematics between σ and proton number as well as neutron number, again the same empirical σ-values shown in Fig. 3.4 are plotted against the proton number and the neutron number as shown in Fig. 3.5 and 3.6 respectively. The fine structures of σ-values seem to be enhanced near the magic numbers of proton and neutron.

The σ_p and/or σ_n of the following nuclei remarkably differ from the others;

$$^{91}Kr(\sigma_p),\ ^{91}Y(\sigma_n),\ ^{95}Y(\sigma_p),\ ^{131}Sn(\sigma_p,\sigma_n),\ ^{133}Sb(\sigma_n),\ ^{133}Sn(\sigma_n),$$
$$^{134}Sb(\sigma_p,\sigma_n),\ ^{140}Xe(\sigma_p),\ ^{140}Cs(\sigma_p,\sigma_n),\ ^{143}Ba(\sigma_p,\sigma_n),\ ^{144}Ba(\sigma_p,\sigma_n),$$

where σ_p and/or σ_n shown in the parentheses mean the large differences occur in those σ-values as shown in Fig. 3.5 and 3.6 respectively.

The solid lines shown in Fig. 3.5 and 3.6 have been obtained from the empirical Gaussian width parameters by means of weighting the inverse squares of experimental errors except extream cases specified by chemical symbols. The σ_n-value of 1.1 at the neutron number 50 has been determined by considering the trend around the neutron number 50, and σ's at neutron magic 82 is ^{132}Sn's respectively. The trend in the range from 61 to 75 of neutron number has been estimated by interpolating a few observed data under the assumption of the complementary relations; namely that the trends in the complementary domains would have similar behaviors since the fragments with neutron number 62 and 82 are nearly complementary, and also the 50 and 72 nearly complementary with each other. The σ_p- and σ_n-values obtained from the smooth curves are shown in Table 3.2.

As an application of the smooth curves shown in Fig. 3.5 and 3.6, we can use them to estimate the Gaussian width parameters of arbitrary nuclei as the combination of σ_p and σ_n. Some ways to express σ_A in terms of σ_p and σ_n may be possible but the following ones are typical;

$$\sigma_A = 1/2(\sigma_p + \sigma_n) \quad \text{.....} \quad \text{Method-1}$$

$$\sigma_A = \frac{p\sigma_p + n\sigma_n}{p + n} \qquad \text{..... Method-2}$$

$$\sigma_A = \frac{2\sigma_p\sigma_n}{\sqrt{\sigma_p^2 + \sigma_n^2}} \qquad \text{..... Method-3}$$

where p and n mean the proton(atomic) number and neutron number respectively. The method-1 is the simple average of σ_p- and σ_n-values. This is the most suitable procedure because the σ_p- and σ_n-values are essentially the same Gaussian width parameters as the original σ_A before separation to σ_p and σ_n. Therefore the method-1 is recommended for the comparison of present work with others like Crouch's. However, when we wish to extend such a method to predict the unknown Gaussian width parameters, we have to establish some appropriate extrapolation methods such as method-2 or -3. Method-2 is the weighted mean of σ_p-and σ_n-values but it has no physical significance. Method-3 is the "equivalent" Gaussian width parameter σ_A when the Gaussian charge dispersion P(Z) is the product of two independent Gaussian charge dispersions in terms of the width parameters σ_p and σ_n respectively. The overall comparison between Crouch's and our's is shown in Fig.

3.3.2 SIMULTANOUS FITTING OF Z_p AND σ

In section 3.3.1, the Z_p-values have been obtained from the observed fractional yields using the assumed Gaussian width parameters. On the other hand, the Gaussian width parameter can be contrarily obtained from the same observed fractional yields even when the Z_p-values are given. In both cases, the experimental errors of yields are drawn in either of two variables Z_p or σ. Therefore, we have attempted to fit Z_p and σ to the observed fractional yields simultanously, and the emphasis in this section has been placed on the examination of the validity of the mass number dependence of Z_p and σ.

Let us assume that both Z_p and σ depend only on the mass number A, and also that the fractional yields can be estimated by eq.(3.2) and (3.3). If these assumptions were valid, there should be a pair of Z_p and σ-values which could simultanously satisfy the observed fractional yields of all isotopes with the same mass number A.

Trends as functions of Z_p-values are shown in Fig. 3.7 as a part of whole Z_p-σ correlation map. The intersecting point of a few correlation curves shown by the solid lines is just the point which satisfy the assumption..

We have searched for these intersectiong points on the Z_p-σ plane(Fig. 3.8) obtained from the observed fractional yields of ^{235}U(nth,f) compiled by Wahl[3]

The results are shown in Table 3.3. There are some isotopes whose correlation curves do'nt intersect with any. The case for mass number 141 is the only case whose three correlation curves of ^{141}Xe, ^{141}La and ^{141}Cs intersect with each other, and the remainders are of two-crossing cases. Three correlation curves for ^{141}Xe, ^{141}La and ^{141}Cs intersect with each other at the point of Z_p=54.85 and σ=0.85.

The Gaussian width parameters obtained in this section (Z_p-σ fitting) are shown by square (⊡) in Fig. 3.7 in comparison with the others. Discrepancies between the present results and the preceding ones obtained by use of calculated Z_p-values based on the Garvey's mass table are remarkably large near mass numbers 84, 134, 136 and 139. Z_p and σ-values of mass number 84 significantly deviate from the average values; Z_p-Z_p^{UCD}=0.44 and σ=0.60. It seems due to the small fractional yields of ^{84}As as pointed out by Wahl [3].

In order to examine the overall reliabilities of observed fractional yields from the viewpoint of satisfactory fit in three different procedures used in this section, major fission products largely differed from the others are shown in Table 3.5. As it is clear from this Table, these fission products show more than two unsatisfactory fittings in most cases. Total number of quetion-marks shown in the last column will be a measure of discrepancies in the fitting.

4. CONCLUDING REMARKS

(1) The most stable charge Z_A has been obtained from Garvey's mass table [1] and compared with Fiedler and Herrmann's. Both Z_A's agree within 0.3 charge unit on the overall range of mass number but the present result in the deviation (Z_A-0.40A) has non-linearity and "stair-like" fine structure on the mass number from 92 to 114, where Fiedler and Herrmann's linearly decreases. This stair-like behavior as mass number seems to be due to the mass relations used by Garvey.

(2) The most probable charge Z_p based on the ECD postulate has been estimated from the Z_A-values and compared with the empirical values obtained from the Wahl's compilation [3] using the constant Gaussian width parameter. The calculated Z_p trend, (Z_p-Z_p^{UCD}) vs A, has a relatively deeper valley around mass number 122. As shown in Fig. 3.1, the existence of it is consistent with ^{117}Pd ^{123}Sn and ^{125}Sn but inconsistent with ^{112}Ag, ^{126}Sb and ^{127}Sb. To establish the

existence , the more availability of experimental data is extensively required.

The investigation on the dependencies of empirical Z_p-values on the constant Gaussian width parameter σ has been made since the empirical Z_p-values scatter around the calculated values. However, the scatter of Z_p-values was hardly improved, and consequently it suggested that the constancy of Gaussian width parameter for overall mass number might be invalid. If the even-odd effect is taken into account for the distribution function, the scatter may be improved [6] since the present one has no even-odd effect.

(3) Gaussian width parameter σ depending on mass number has been obtained from the same observed fractional yields using the calculated Z_p-values and compared with Crouch's [4]. The present result is generally smaller than Crouch's below mass number 88 and from 92 to 95 for light fragments, but greater than Crouch's for overall heavy fragments with four exceptions; mass numbers 134, 139, 140 and 144.

(4) In order to investigate the fine structure and systematics of the Gaussian width parameters obtained from the observed fractional yields [3], the Gaussian width parameters have been separated into two terms depending on proton (atomic) number p and neutron number n respectively. The shell effects is enhanced in these term-presentations and the systematics becomes more clear. Two components as smooth curves σ_p vs p and σ_n vs n have been evaluated by means of inverse-square weighting and by assuming the complementary relations. The Gaussian width parameters for unobserved nuclei, especially nuclei in the symmetric fission region, can be estimated by using these two curves. As an attempt for predicting the Gaussian width parameters depending on mass number, simple average method $\sigma_A = 1/2(\sigma_p + \sigma_n)$ has been used and the resultant σ_A has been compared with Crouch's and the others obtained in this paper.

(5) Z_p-σ correlation curves, which satisfy the observed fractional yields, have been prepared in order to examine the validity of mass number dependencies of the most probable charge Z_p and Gaussian width parameter σ. If Z_p and σ are functions of only mass number A, there should be a pair of Z_p and σ which can simultaneously satisfy the observed fractional yields of all isotopes with mass number A. The case for mass number 141 was only one whose three correlation curves of ^{141}Xe, ^{141}La and ^{141}Cs intersected with each other at the point (Z_p=54.84, σ=0.58), and the remainders 28 cases were of two-crossing cases. Some cases such as mass numbers 91, 95, 97, 132, 133, 134, 139 and 143 gave

several different points (Z_p,σ), for instance, (Z_p=52.59,σ =0.41), (Z_p=53.59, σ =1.35) and (Z_p=51.70,σ =0.59) for ^{134}Cs, ^{134}Sb and ^{134}I, and (Z_p=54.55,σ = 0.53) and (Z_p=54.35,σ =0.85) for ^{139}Cs, ^{139}Ba and ^{139}Xe respectively. This result shows that the Z_p and σ may be not the single variable functions of mass number, i.e. it is one of possible cases that they are functions of proton (atomic) number and neutron number and consequently of mass number. Further investigations, however, is seriously required since the present Gaussian distribution function excludes the even-odd effect, and also more careful evaluation of experimental data themselves should be made.

ACKNOWLEDGMENT

The auther wish to thank Dr's M. Yamamoto, S. Iijima and S. Igarashi for their advices and encouragements as members of JNDC (Japan Nuclear Data Committee), and also acknowledge Miss M. Inai for her help in the CRC computation.

REFERENCE

[1] Garvey,G.T., et al., Rev. Mod. Phys., 41 (1969) 4, Part II.

[2] Pappas, A.C., Massachusetts Institute of Technology, Laboratory of Nuclear Science Technical Report No. 63, (1953)

[3] Wahl, A.C., Norris, A.E., Rouse, R.A., and William, J.C., Second IAEA Symposium on Physics and Chemistry of Fission, Vienna (1969), IAEA-SM-122/116

[4] Crouch, E.A.C., AERE-R6056 (1969)

[5] To be published.

[6] Denshlag, H.O.,et al., Second IAEA symposium on Physics and Chemistry of Fission, Vienna (1969), IAEA-SM-122/26.

[7] Kümmel,H., Mattauch, J.H.E., Thiele, W. and Wapstra, A.H., Springer-Verlag, Wien-New York,(1964).

[8] "Weizsäcker-Brthe liquid-drop model", Weizsäcker, C.F. von, Z. Physik, 96 (1935) 431.

[9] Myers, W.D. and Swiatecki, W.J., " Nuclear Masses and Deformations", N.P. 81 (1966).

[10] Fiedler, J. and Herrmann, G., Z. Naturforsh., 18a (1963), 553.

[11] König, L.A., Kümmel, H., Thiele, W. and Wapstra, A., AERE-M-1078, P. 35-36, (1962), unpublished.

[12] Wahl, A.E., etal., Phys. Rev. 126 (1962) 1112.

[13] Amiel, S. and Feldstein, H., Rochester Conference (1973).

[14] Musgrove, A.R. de., IAEA Panel on Fission Product Nuclear Data, Bologna, Nov., (1973)

[15] Pappas, A.C. and Alstad, J., Second IAEA Symposium on Physics and Chemistry of Fission, Vienna (1969), IAEA-SM-122/206, Review Paper.

[16] Rider, B.F., private communication.

Table 3.1 Comparison of Evaluated Most Probable Charge Z_p

Mass No. A	Evaluated Z_p-values			Mean and Std. $\bar{Z}_p$	$Z_p(X)/\bar{Z}_p$		
	Ours	Crouch [4]	Wahl [3]		Ours	Crouch	Wahl
77	30.71	30.31	30.71	30.58±0.19	1.0044	0.9913	1.0043
78	31.11	30.70	31.12	30.98±0.20	1.0042	0.9910	1.0045
80	31.87	31.48	31.94	31.76±0.20	1.0035	0.9912	1.0057
82	32.51	32.26	32.75	32.51±0.20	1.0000	0.9923	1.0074
83	32.81	32.71	33.16	32.89±0.19	0.9976	0.9945	1.0082
84	33.15	33.15	33.57	33.29±0.20	0.9958	0.9958	1.0084
86	33.83	34.03	34.40	34.09±0.24	0.9924	0.9982	1.0091
87	34.28	34.46	34.82	34.52±0.22	0.9930	0.9983	1.0087
89	35.22	35.37	35.66	35,42±0.18	0.9944	0.9986	1.0068
90	35.70	35.85	36.06	35.87±0.15	0.9950	0.9990	1.0050
91	36.21	36.32	36.46	36.33±0.10	0.9970	0.9997	1.0036
92	36.72	36.86	36.86	36.81±0.07	0.9995	1.0013	1.0014
93	37.26	37.38	37.27	37.30±0.05	0.9988	1.0021	0.9991
94	37.79	37.96	37.67	37.81±0.12	0.9996	1.0041	0.9964
95	38.33	38.44	38.08	38.28±0.15	1.0012	1.0041	0.9947
96	38.84	38.82	38.47	38.71±0.17	1.0033	1.0028	0.9934
97	39.24	39.18	38.87	39.10±0.16	1.0037	1.0021	0.9942
98	39.62	39.50	39.26	39.46±0.15	1.0041	1.0010	0.9949
99	40.01	39.84	39.65	39.83±0.15	1.0044	1.0002	0.9954
102	41.01	40.93	40.75	40.90±0.11	1.0028	1.0008	0.9964
103	41.32	41.21	41.11	41.21±0.09	1.0027	1.0000	0.9976
105	42.02	41.88	41.88	41.93±0.07	1.0022	0.9989	0.9989
106	42.41	42.21	42.29	42.30±0.08	1.0026	0.9979	0.9998
112	44.85	44.71	44.70	44.75±0.07	1.0022	0.9990	0.9988
115	45.76	46.20	45.66	45.87±0.23	0.9995	1.0071	0.9953
117	46.24	47.04	46.34	46.54±0.36	0.9936	1.0107	0.9957
121	47.42	48.24	47.60	47.75±0.35	0.9930	1.0102	0.9968
123	48.06	48.75	48.27	48.36±0.29	0.9938	1.0081	0.9981
125	48.40	49.04	48.84	48.62±0.29	0.9954	1.0086	0.9960
125	48.69	49.29	48.71	48.90±0.28	0.9958	1.0080	0.9962
126	48.94	49.51	49.01	49.15±0.25	0.9957	1.0073	0.9971
127	49.21	49.73	49.32	49.42±0.22	0.9958	1.0063	0.9980
128	49.53	49.94	49.66	49.71±0.17	0.9964	1.0046	0.9990
129	49.87	50.18	50.02	50.02±0.13	0.9969	1.0031	0.9999
130	50.22	50.44	50.39	50.35±0.09	0.9974	1.0018	1.0008

Table 3.1 (continued)

Mass No.	Evaluated Z_p-values			Mean and Std.	$Z_p(X)/\bar{Z}_p$		
A	Ours	Crouch [4]	Wahl [3]	$\bar{Z}_p$	Ours	Crouch	Wahl
131	50.60	50.75	50.80	50.72±0.08	0.9977	1.0007	1.0016
132	5s.96	51.09	51.21	51.09±0.10	0.9975	1.0000	1.0024
133	51.34	51.52	51.65	51.50±0.13	0.9968	1.0003	1.0028
134	51.77	51.93	52.12	51.94±0.14	0.9967	0.9998	1.0035
135	52.20	52.34	52.56	52.37±0.15	0.9967	0.9995	1.0037
136	52.60	52.70	52.98	52.76±0.16	0.9970	0.99989	1.0042
138	53.49	53.10	53.79	53.46±0.28	1.0006	0.9933	1.0062
139	54.02	53.88	54.19	54.03±0.13	0.9998	0.9972	1.0030
140	54.55	54.40	54.59	54.51±0.08	1.0007	0.9979	1.0014
141	55.09	54.91	54.99	55.00±0.07	1.0017	0.9984	0.9999
142	55.60	55.46	55.39	55.48±0.09	1.0021	0.9996	0.9983
143	56.12	55.95	55.78	55.95±0.14	1.0030	1.0000	0.9970
144	56.59	56.45	56.18	56.41±0.17	1.0033	1.0008	0.9960
146	57.53	57.39	57.00	57.31±0.22	1.0039	1.0015	0.9946
147	58.01	57.83	57.46	57.77±0.23	1.0042	1.0011	0.9947
150	59.09	59.13	58.70	58.97±0.19	1.0019	1.0027	0.9954
160	61.67	63.62	62.47	62.59±0.80	0.9853	1.0165	0.9981

Table 3.2 Average Values of Z_p as functions of Gaussian Width Parameter σ

	Charge dispersion σ			Average Z_p [c]
	0.55	0.58	0.62	
$\overline{Z}_{pl}(\sigma)$ [a]	0.350	0.326	0.225	0.300
$\overline{Z}_{ph}(\sigma)$	0.425	0.469	0.521	0.438
$\overline{Z}_{p}(\sigma)$ [b]	0.393	0.408	0.396	0.399
$\overline{Z}_{pl}(\sigma)/\overline{Z}_{pl}$ (0.55)	1.000	0.931	0.643	
$\overline{Z}_{ph}(\sigma)/\overline{Z}_{ph}$ (0.55)	1.000	1.105	1.227	
$\overline{Z}_{p}(\sigma)/\overline{Z}_{p}$ (0.55)	1.000	1.038	1.008	

a) $\overline{Z}_{pl}(\sigma)$ means the average of empirical Z_p values for assumed Gaussian width parameter σ, where 1 reffers to light fragment and absolute value of Z_p is used.

b) $\overline{Z}_{p}(\sigma)$ is the average of light and heavy fragment's Z_p values.

c) it means the average of thee $\overline{Z}_{p}(\sigma)$ values.

Table 3.3 Gaussian Width Parameters σ_n and σ_p as Functions of Neutron and Proton Numbers respectively

n*	σ_n#	n	σ_n	p	σ_p	p	σ_p
45	0.60	68	0.54	30		53	0.66
46	0.58	69	0.60	31		54	0.70
47	0.57	70	0.60	32	0.60	55	0.62
48	0.59	71	0.54	33	0.58	56	0.58
49	0.64	72	0.47	34	0.57	57	0.57
50	1.10	73	0.45	35	0.58	58	0.56
51	0.94	74	0.55	36	0.62	59	0.55
52	0.77	75	0.74	37	0.65	60	0.54
53	0.67	76	0.83	38	0.64	61	0.53
54	0.60	77	0.65	39	0.58	62	0.525
55	0.53	78	0.64	40	0.45	63	0.52
56	0.46	79	0.59	41	0.43	64	0.51
57	0.41	80	0.58	42	0.45	65	0.50
58	0.50	81	0.62	43	0.56		
59	0.61	82	1.12	44	0.66		
60	0.69	83	0.76	45	0.68		
61	0.71	84	0.65	46	0.58		
62	0.69	85	0.60	47	0.43		
63	0.63	86	0.64	48	0.46		
64	0.53	87	0.70	49	0.70		
65	0.44	88	0.70	50	1.40		
66	0.44	89	0.68	51	0.80		
67	0.48	90	0.68	52	0.71		

* n and p mean the neutron and proton numbers respectively.

σ_n and σ_p mean the Gaussian width parameters as a function of neutron number and as a function of proton number respectively.

Table 3.4 Comparison of Z_p and σ values obtained by different procedures.

Mass No. A	G.W. Pra.*) (Z_p-σ fit)	Most Probable Charge Cal§)	Most Probable Charge (Z_p-σ fit) σ=0.62†	$\Delta Z_p(x)/Z_p^{cal}$ (%) (Z_p-σ fit)	$\Delta Z_p(x)/Z_p^{cal}$ (%) σ=0.62	Crossing¶)
84	0.47	33.15	33.83	32.63	2.0	-1.7	(Rb,As)
89	0.76	35.22	35.25	35.44	0.90	0.6	(Kr,Rb)
90	0.74	35.70	35.80	35.81	0.3	0.3	(Rb,Y),Kr
91	2.0	36.21	34.10	36.73	-6.2	1.5	(Sr,Y),Kr,Rb
	0.68		36.90	36.71	2.1	1.5	Sr,(Y,Kr),Rb
92	0.58	36.72	36.75	36.72	0.8	0.0	(Y,Kr),Rb
93	0.56	37.26	37.30	37.28	0.2	0.1	(Y,Kr),Rb
94	0.52	37.79	37.60	37.69	-0.6	-0.3	(Y,Kr),Rb
95	0.51	38.33	38.00	38.13	-0.8	-0.5	(Zr,Kr),Rb,Y
	0.61		38.30	38.10	-0.1	-0.6	Zr,(Kr,Rb),Y
96	0.52	38.84	38.5	36.71	-0.9	-5.5	(Rb,Nb)
97	0.62	39.24	39.15	37.04	-0.2	-5.6	(Rb,Kr),Nb
	0.54		38.80	38.92	-1.1	-0.8	Rb,(Kr,Nb)
131	0.71	50.60	50.40	50.72	-0.4	0.0	(I,Te),Sn
132	0.66	50.96	50.95	51.00	0.0	0.0	(Ce,Te),I
	0.61		50.85	50.92	-0.2	-0.1	Cs,(Te,I)
133	0.43	51.34	52.20	49.65	1.7	-3.3	(Xe,Sb),I,Sn
	1.08		53.30	49.91	-3.8	-2.8	Xe,(Sn,I),Sb
134	0.41	51.77	52.59	51.98	1.6	0.4	(Cs,Sb),I
	1.35		53.92	52.21	4.2	0.9	Cs,(Sb,I)
	0.59		51.70	51.52	-0.1	-0.5	(I,Cs),Sb
139	0.53	54.02	54.55	54.08	1.0	0.0	(Cs,Ba),Xe
	0.85		54.35	54.01	-0.6	0.0	Cs,(Ba,Xe)
140	0.54	54.55	54.90	54.49	0.6	0.0	(Ba,La),Xe,Cs
141	0.58	55.09	54.85	54.88	-0.4	-0.4	(Xe,La,Cs),Ce,Ba
142	0.49	55.60	55.08	55.33	-0.9	-0.5	(La,Xe)
143	0.60	56.12	55.90	55.95	-0.4	-0.3	(Ce,Xe),Ba
	0.52		55.55	55.88	-1.0	-0.4	Ce,(Xe,Ba)
144	0.67	54.50	56.60	54.94	3.9	0.8	(Cs,Xe),Ba

*) Gaussian width parameter σ was derived from two variable, Z_p and σ, fitting.

§) The most probable charge Z_p was obtained from the Garvey's mass table.

†) The most probable charge Z_p was derived from the observed fractional yields assuming the Gaussian width parameter σ=0.62.

¶) Fission products whose correlation curves in the two variable fitting intersect with each other are shown in the parentheses.

Table 3.5 Major Fission Products largely differed from the others in three different fitting procedures.[a)]

F.P.	Z_p-fitting(b)	σ-fitting(c)		Z_p-σ fitting (d)			
	Z_p	σ_p	σ_n	σ	$\Delta Z_p/Z_p^{cal}$ (%)	Crossing	
^{91}Kr		?(e)		2.0?	-6.2 ?	(Sr,Y),Kr,Rb	3?
Y	?		?	0.68	2.1 ?	Sr,(Y,Kr),Rb	3?
^{95}Y		?		0.51	-0.8 ?	(Zr,Kr),Rb,Y	2?
131Sn	?	?	?	0.71?	-0.4	(I,Te),Sn	4?
^{133}Sb	?		?	0.43?	1.7 ?	(Xe,Sb),I,Sn	4?
Sn	?		?	1.08?	-3.8 ?	Xe,(Sn,I),Sb	3?
^{134}Sb	?	?	?	0.41?	1.6 ?	(Cs,Sb),I	5?
^{140}Xe		?		0.54	0.6 ?	(Ba,La),Xe,Cs	2?
^{141}Cs(f)				0.58	-0.4	(Xe,La,Cs),Ce,Ba	
^{142}La				0.49?	-0.9 ?	(La,Xe)	2?
^{143}Ba	?	?	?	0.60	-0.4	(Ce,Xe),Ba	3?
^{144}Ba	?	?	?	0.52	-1.0 ?	Ce,(Xe,Ba)	4?

(a) Fission products which showed larger scatters in these fitting procedures. This table is prepared in order to check the overall discrepancies among three different procedures.

(b) Z_p-values obtained from the observed fractional yields assuming σ=0.62.

(c) The mass number dependent Gaussian width parameter σ_A are decomposed to the proton (atomic) number dependent term σ_p and neutron number dependent term σ_n.

(d) Z_p and σ are obtained by simultaneously fitting. Some fission products whose correlation curves intersect with each other are shown in the parentheses.

(e) "?" means that the isotope shows the larger deviation from the others in this fitting procedure.

(f) This is an example of the best case.

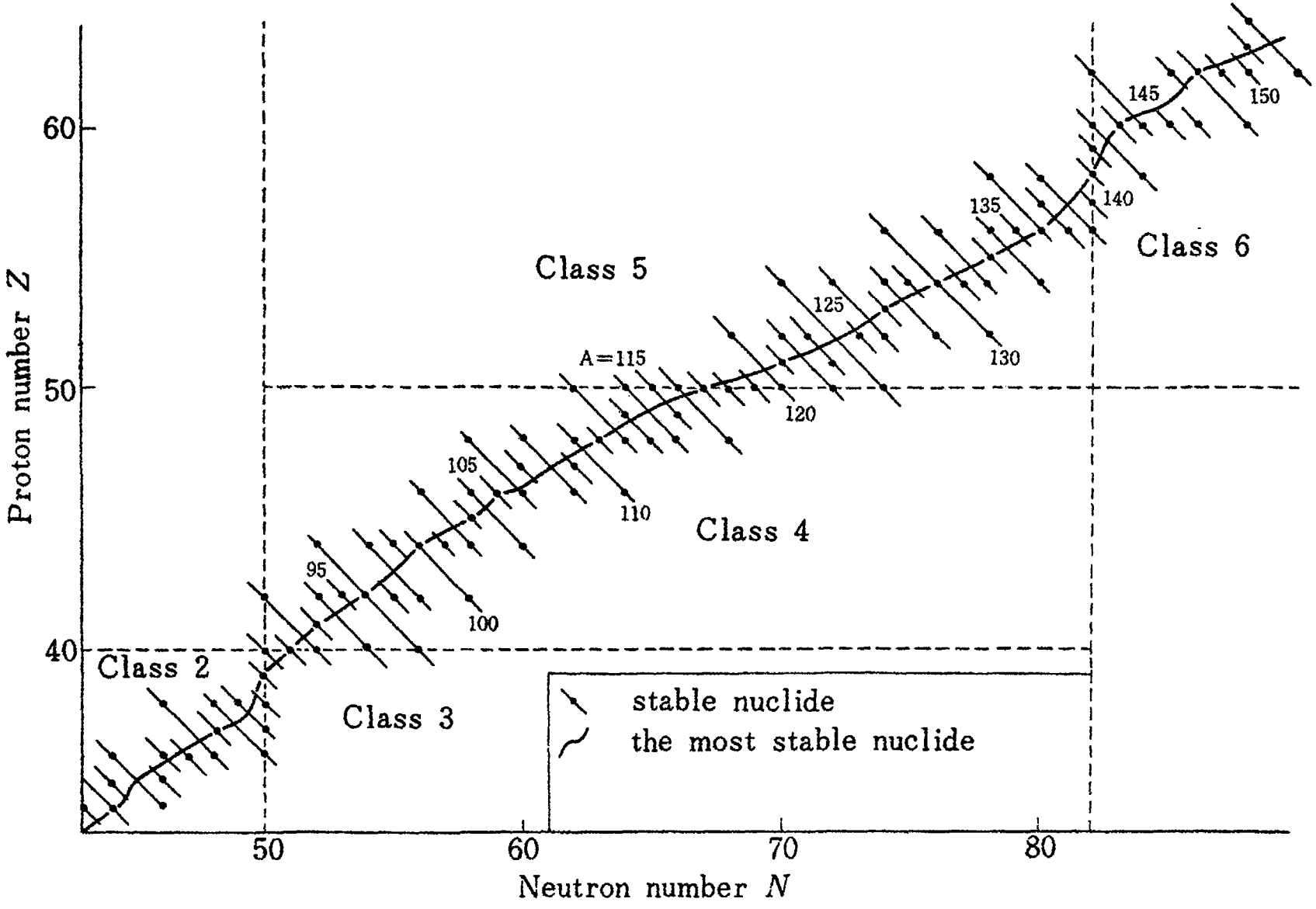

Fig. 2.1 The observed stable nuclei and the calculated most stable nuclei. The solid line shows the trend of the most stable nuclei derived from the mass table compiled by Garvey et al [1] and the closed circles on the straight lines show the observed stable nuclei with mass number A. Classes shown by the dotted lines mean the Levy's shell classes, where co-classes for complementary fragments are excluded.

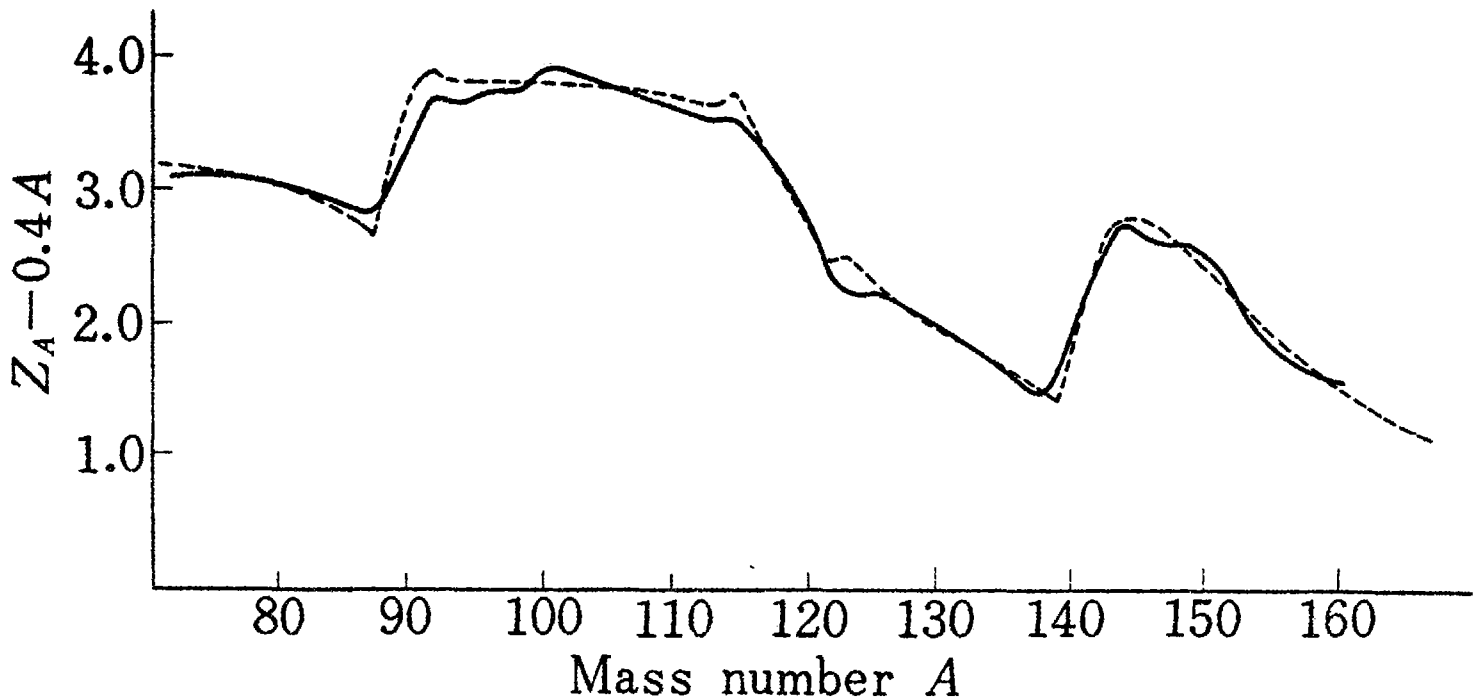

Fig. 2.2 The most stable charge Z_A as a function of mass number A. Two theoretical curves are shown for comparison. The solid curve is ours derived from Garvey's mass table [1] which is essentially the same as the result shown in Fig. 2.1 and the dotted line is the result obtained by Fiedler and Herrmann [10].

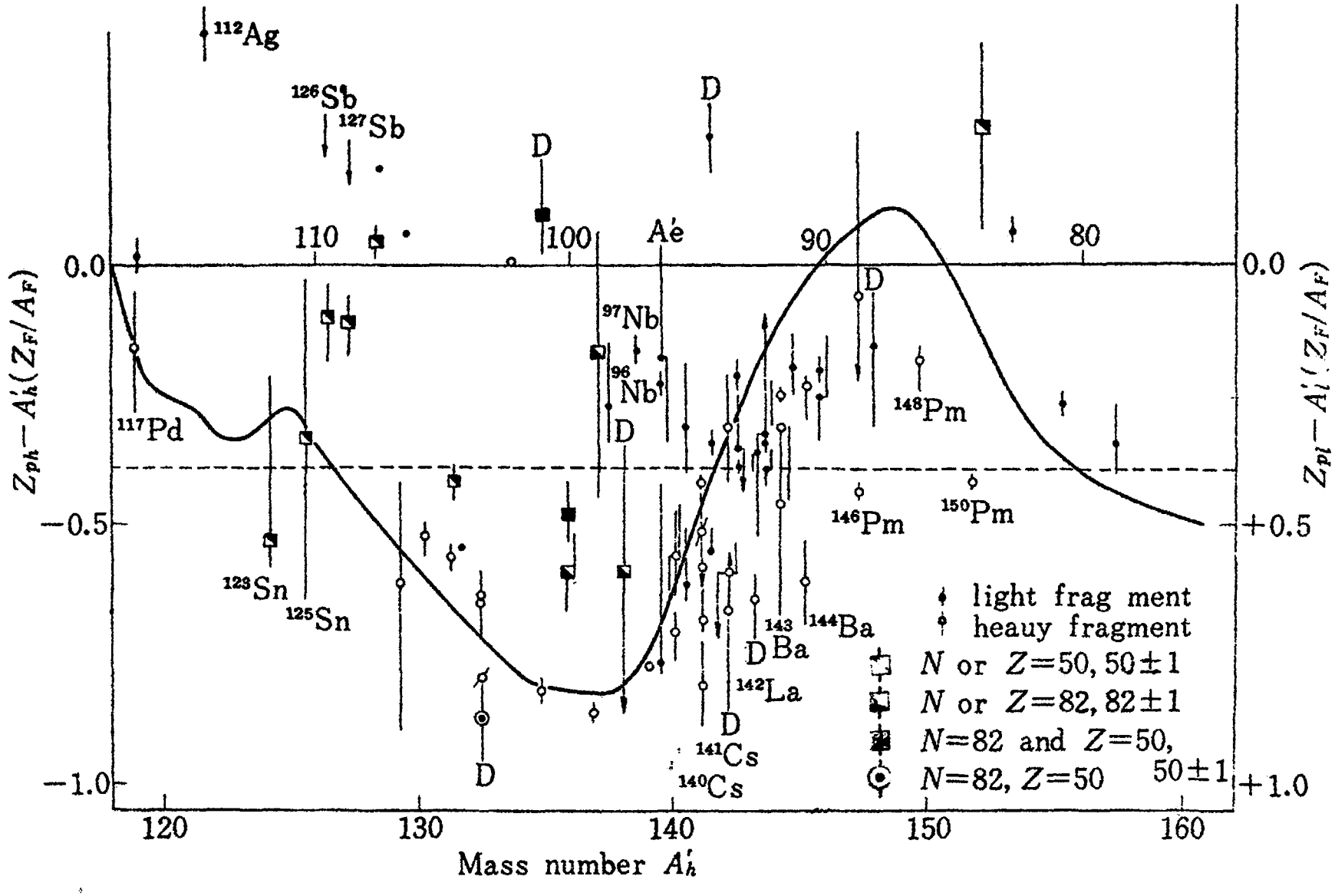

Fig. 3.1 Deviation of the most probable charge Z_p from the unchanged charge distribution Z_p^{UCD} (σ=0.62). A_h' and A_l' mean the mass numbers of heavy and light fragments before emission of neutrons where the number of emitted neutrons per fission recommended by Wahl [3] is used. The solid line reffers to the most probable charge Z_p obtained from the most stable charge Z_A basing on the ECD postulate [2]. The empirical Z_p-values were obtained from the observed fractional yields compiled by Wahl [3] assuming Gaussian width parameter σ=0.62. Dotted line is for reference to show the average of empirical Z_p-values. Several nuclei near shell edges are distinguished by special marks and also some delayed neutron precurcer by letter D respectively.

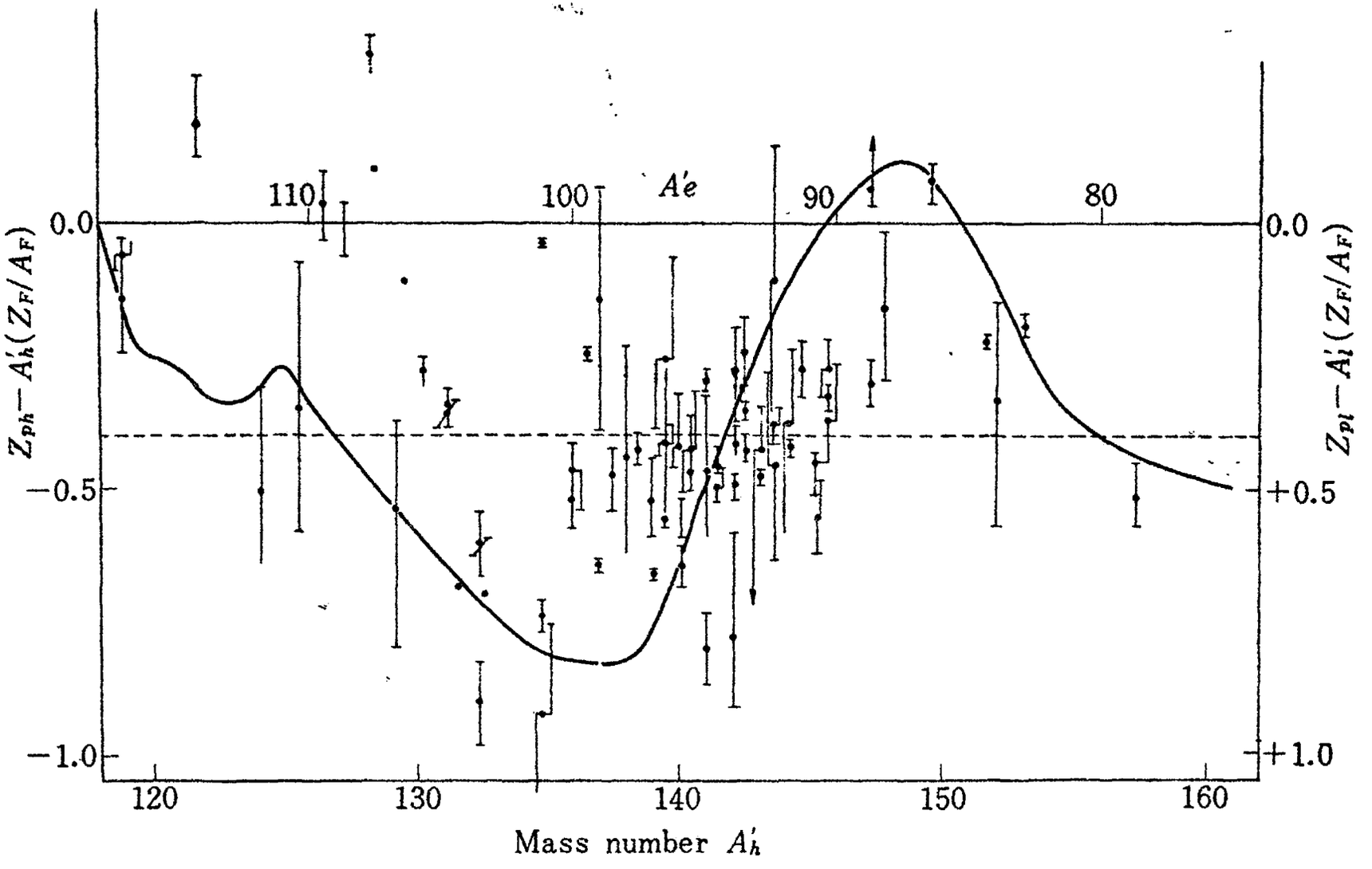

Fig. 3.2 Deviation of the most probable charge Z_p from unchanged charge distribution Z_p^{UCD} (σ=0.58). Fig. 3.2 and 3.3 together with Fig. 3.1 are provided for studying the dependence of the empirical Z_p-values on the Gaussian width parameter σ. In this case the σ-value is assumed to be 0.58 charge unit and the special marks used in the Fig. 3.1 are removed. Dependence of average Z_p-values shown by dotted line is summarized in Table 3.2.

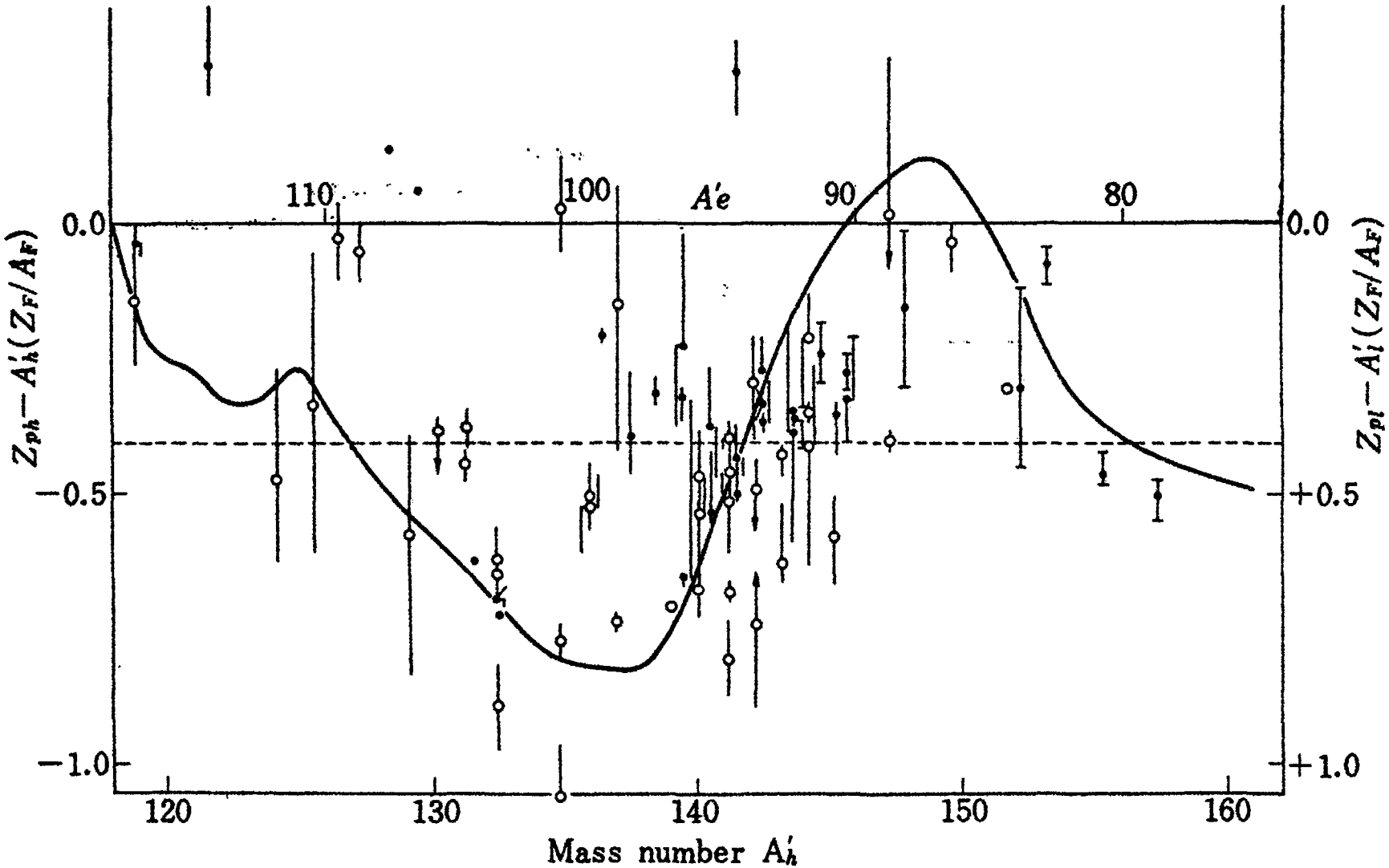

Fig. 3.3 Deviation of the most probable charge Z_p from the unchanged charge distribution Z_p^{UCD} (σ=0.55). This is provided for studying the dependence of empirical Z_p-values on the Gaussian width parameter σ in relation to the preceeding two figures. In this case the σ value is assumed to be o.55. The other discriptions are the same as Fig. 3.2.

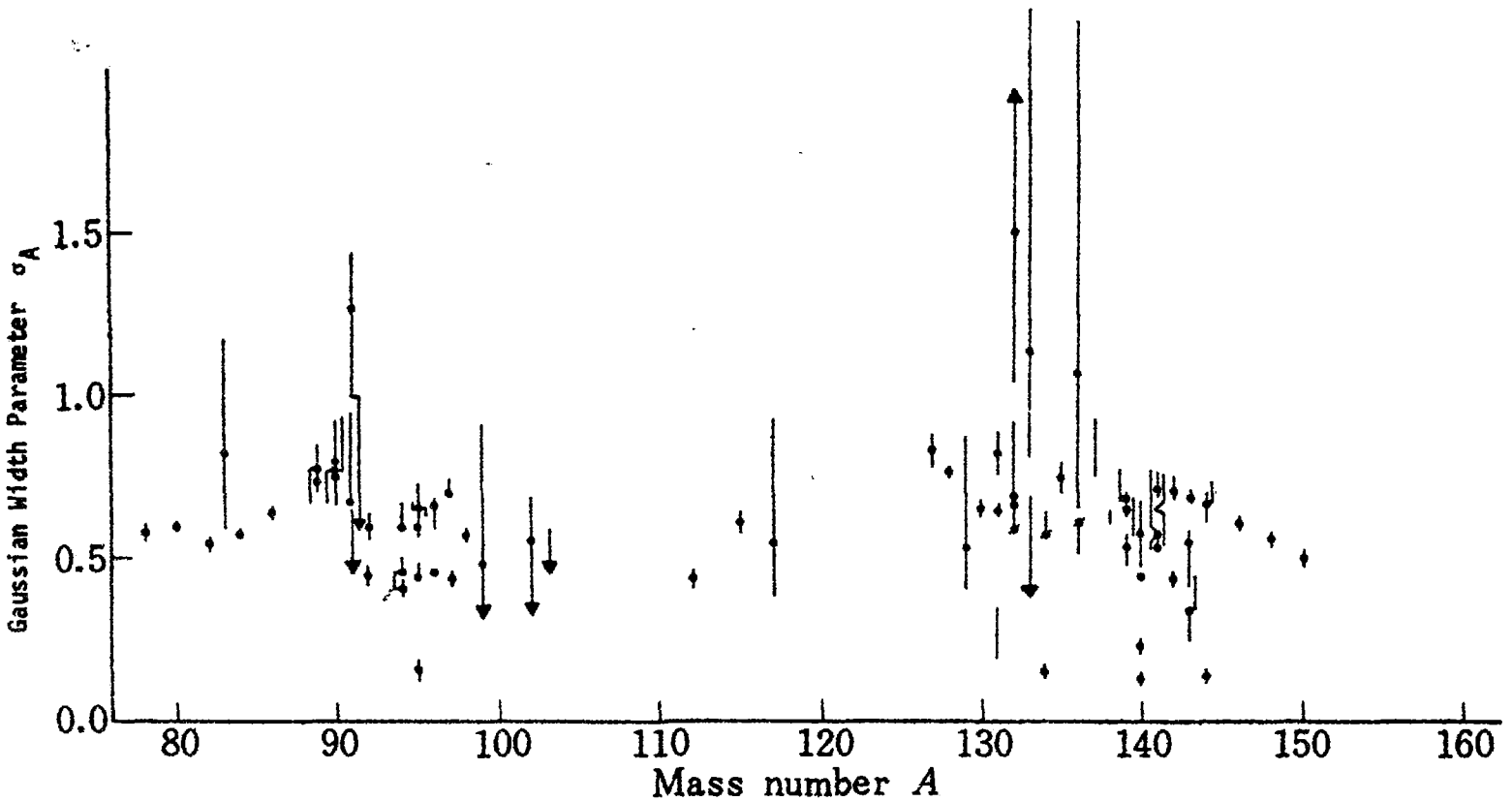

Fig. 3.4 Gaussian width parameter σ as a function of mass number A. Gaussian width parameter are derived from the observed fractional yields compiled by Wahl [3] using the estimated most probable charge Z_p shown by the solid line in Fig. 3.1. These semi-empirical σ-values are also shown in Fig. 3.7 for comparison with Crouch's [4].

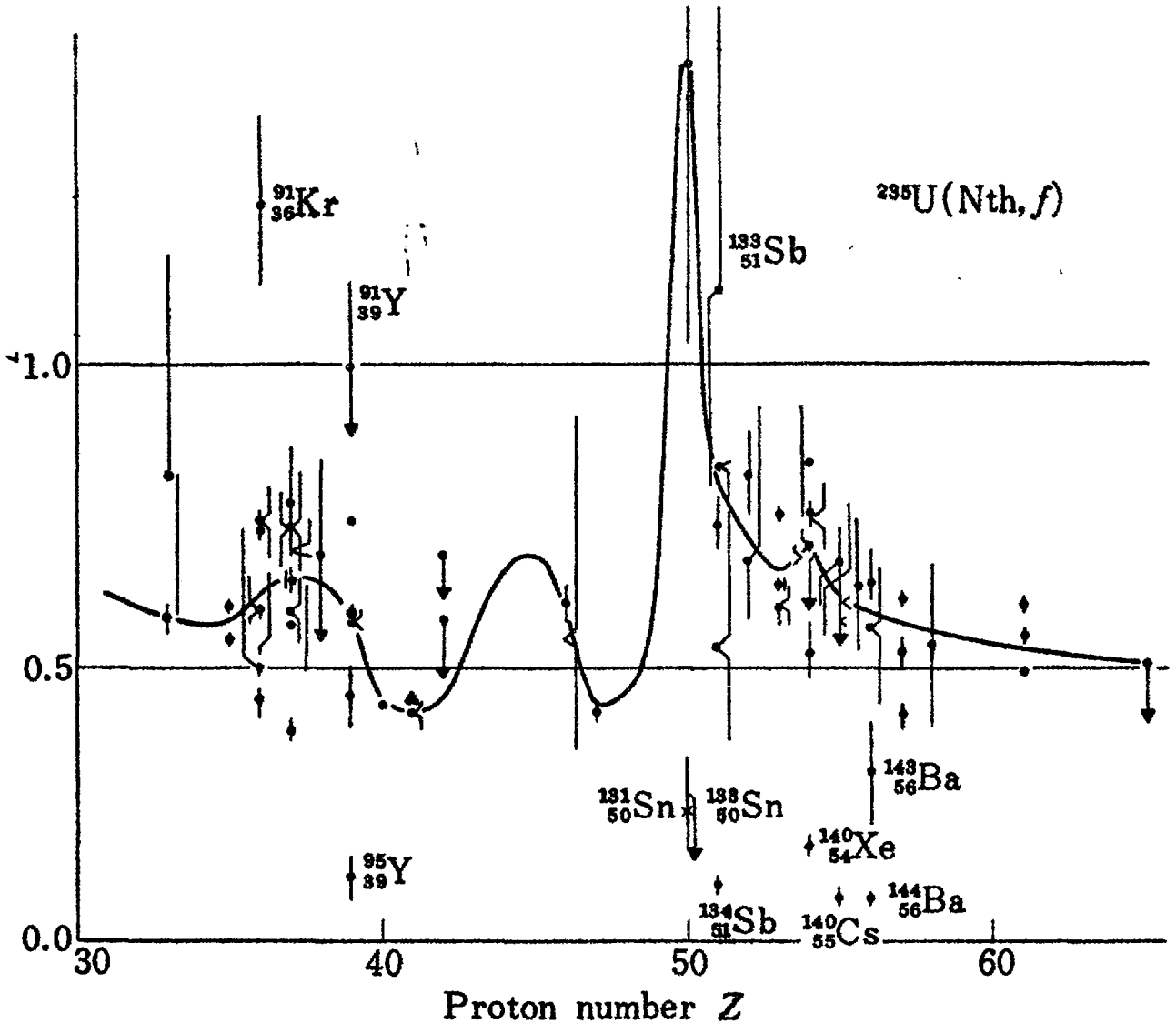

Fig. 3.5 Gaussian width parameter as a function of proton number Z. Semi-empirical Gaussian width parameter σ_A as a function of mass number A is plotted against the proton number Z. Solid line refers to the weighted mean of semi-empirical σ_z-values excluding the extream cases specified by chemical symbol with mass number and atomic number.

The magnitudes of Gaussian width parameters σ_Z's are shown in Table 3.3 together with σ_N's, and the Gaussian width parameter σ_A depending on the mass number A obtained by a combuiation of σ_z and σ_N is shown in Fig. 3.7.

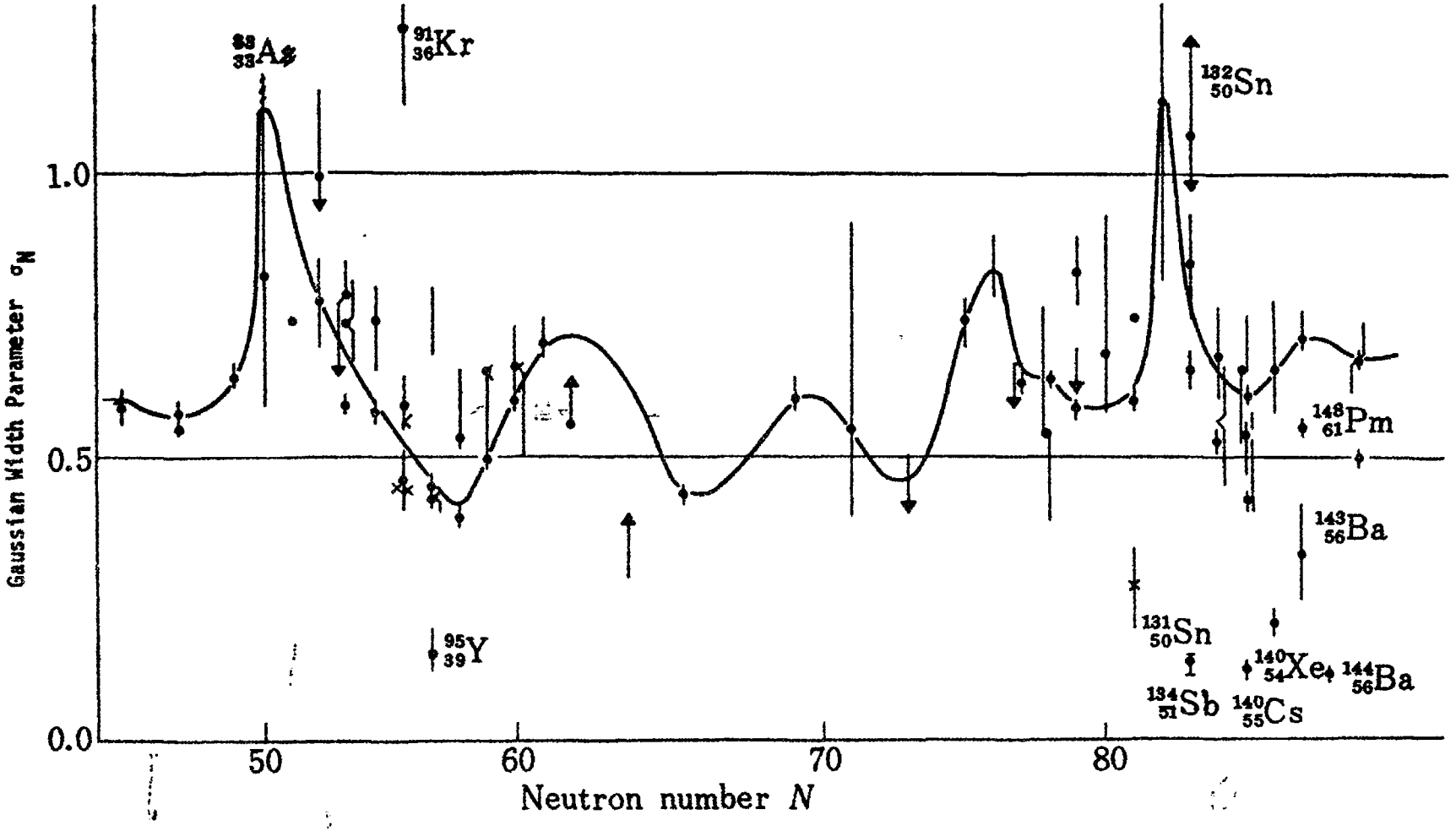

Fig. 3.6 Gaussian width parameter σ_N as a function of neutron number N. Semi-empirical Gaussian width parameter as a function of mass number A are plotted against the neutron number N. Solid line refers to the weighted mean of sem-semi-empirical σ_N-values excluding the extream cases specified by chemical symbols with mass number and atomic number.

The magnitudes of Gaussian width parameters σ_N's are shown in Table 3.3 together with σ_Z and σ_A.

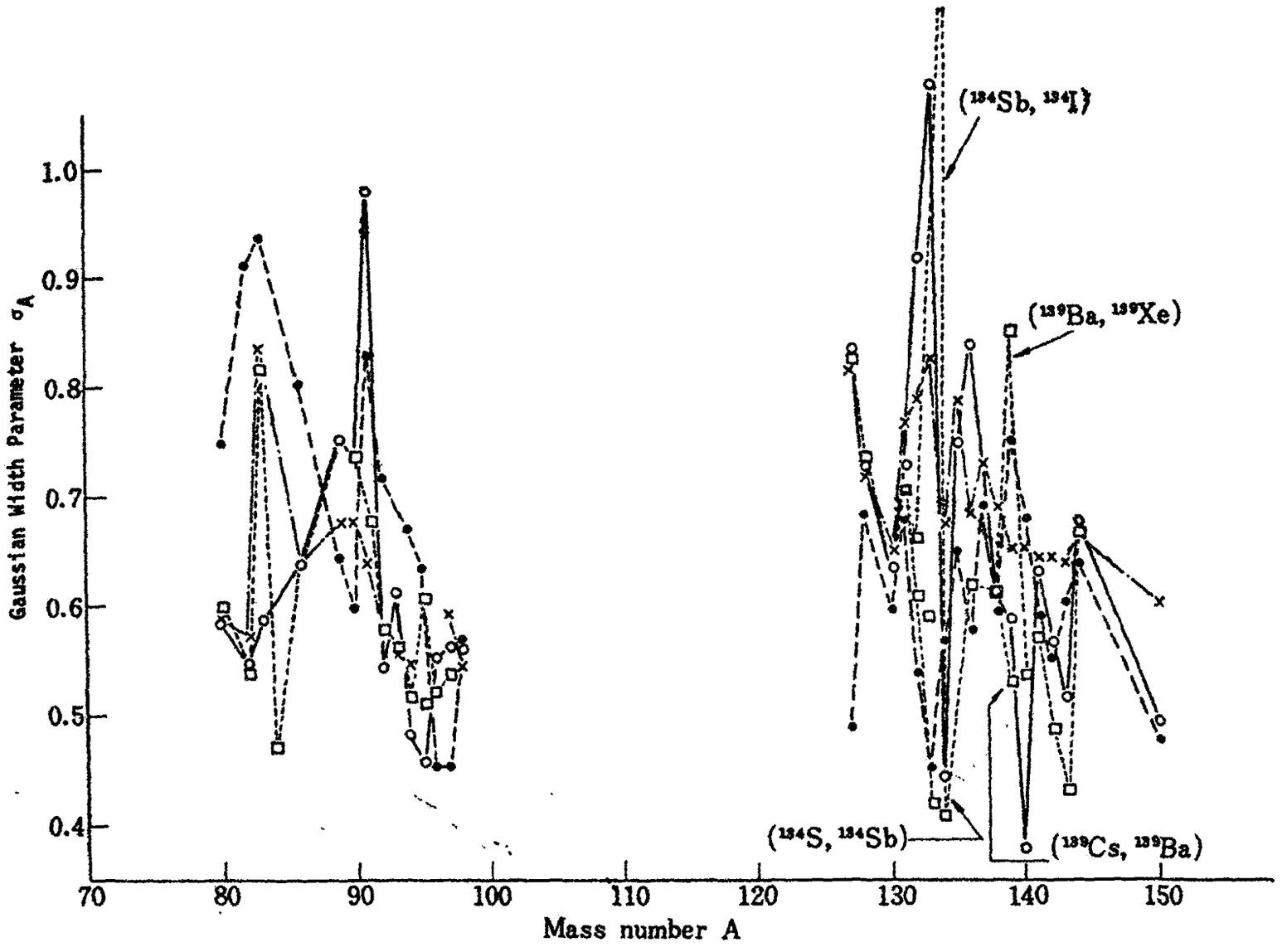

Fig. 3.7 Gaussian width parameter σ vs A. Four Gaussian width parameters obtained from the same observed fractional yields [3] by different procedures are compared with each other; o : by fitting Gaussian width parameter to the observed fractional yields using the calculated Z_p-values obtained from Garvey's mass table [1], ⊡ : by fitting two variables σ and Z_p to the same fractional yields, × : by combining σ_Z with σ_N; $\sigma_A = 1/2(\sigma_Z + \sigma_N)$, • : the recommendation by Crouch [4].

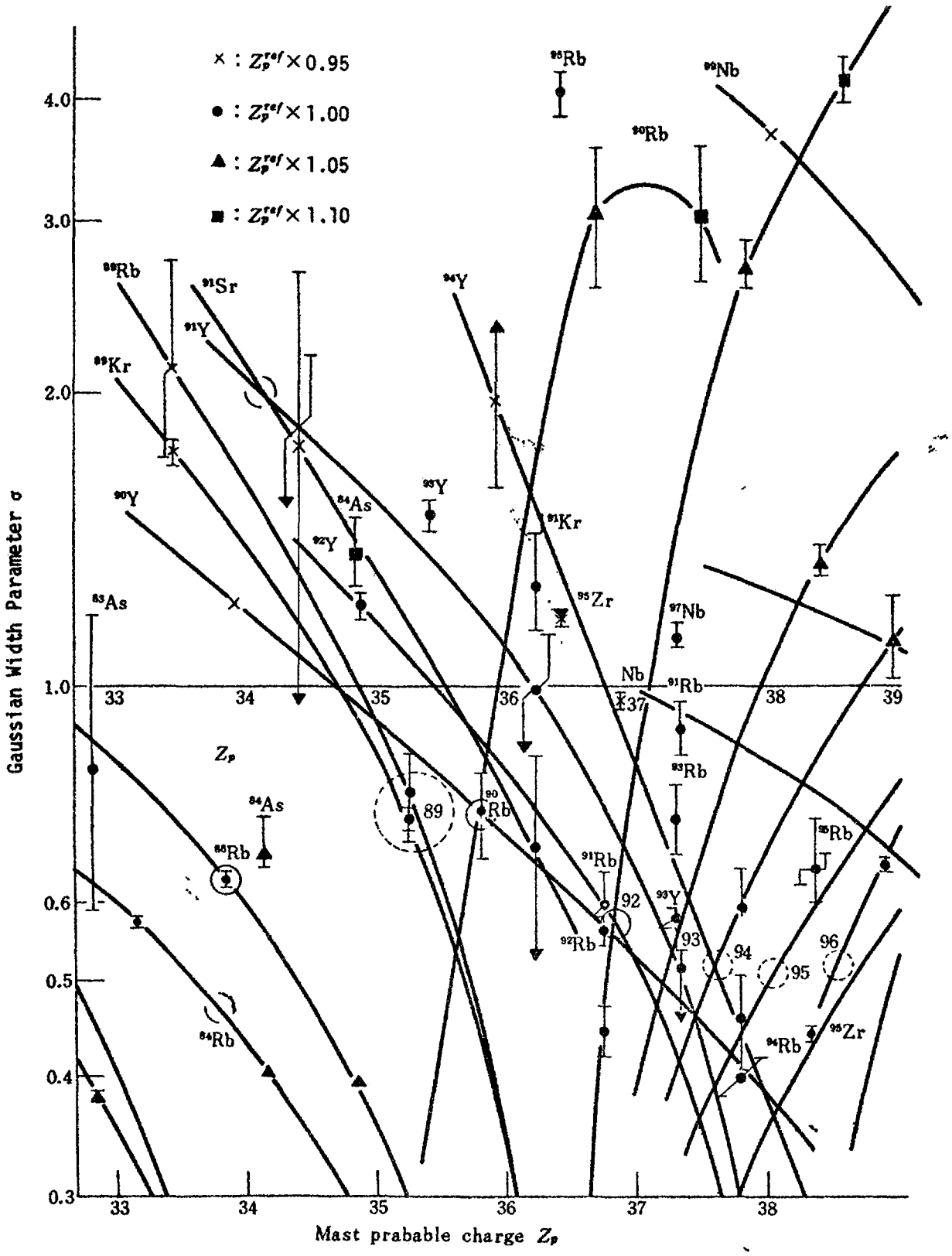

Fig. 3.8 Correlation between Z_p and σ. This is a part of whole Z_p-σ correlation map, and the reference Z_p denoted by Z_p^{ref} shown on the upper corner means the calculated most probable charge shown by the solid line in Fig. 3.1. Solid lines mean the correlation curves on which the observed fractional independent and/or cumulative yields compiled by Wahl [3] are theoretically predicted by using these Z_p and σ values for equ.(3.2) and (3.3). Larger open circles refer to the locations of the point (Z_p,σ) where more than two observed yields are simultanously satisfied.

The location of the point (Z_p,σ) mentioned above is summarized in Table 3.4 in comparison with the others.

Contributions to
Review Paper No. 11b

YIELDS IN FAST NEUTRON FISSION OF U-238 AND Th-232

M. Lammer

Nuclear Data Section, Division of Research & Labs.,
International Atomic Energy Agency, Vienna, Austria

(Revised)

Abstract: A critical discussion of the status of yields in fast neutron fission of U-238 and Th-232 is presented. After a brief survey of relevant measurements of these yield data and a discussion of the dependence on the neutron energy spectrum the experimental data are critically compared and the uncertainties assessed. Existing evaluations are discussed. Recommendations are given for suitable measurement techniques and further measurements and evaluation work required. Th-232 fission yields are re-evaluated.

1. INTRODUCTION

In the case of fast neutron fission yield data for Th-232 and U-238 there are as many different sets of recommended data as there are evaluations. This is due to difficulties in evaluation methods employed and preferences for certain measurements, as outlined in detail in an earlier publication [Lam 73]. Therefore this paper starts with a discussion of the publications of experimental data used in the evaluations in order to enable a critical comparison of available yield data. This will allow us to detect discrepancies and recommend further experimental work required. Th-232 yields are re-evaluated for the Panel and referred to as "present evaluation" in chapter 3.

2. U-238 FAST NEUTRON FISSION YIELDS

2.1. Experiments

Different methods for fission yield measurements have been discussed in detail in [Lam 73], particularly in the light of the possibilities the evaluator has to check and correct the original experimental data. In this context it should be borne in mind that radiochemical measurements cannot be corrected by an evaluator, if the decay data used in the original work are out of date. The only possibility is to check the nuclear data used.

2.1.1. Mathews and Tomlinson [Mat 72]

The authors report results on mass-spectrometric measurements of yields in the heavy mass peak. Information on experimental details included in the publication is sufficient to allow a check of the corrections applied.

The 3% contribution of Pu-239 fission should be taken into account in cases where differences in fission yield ratios between U-238 and Pu-239 fast fission approach or exceed 10%. So, for example, was the measured yield ratio Cs-137/Nd-145 = 1.385, whereas the same ratio for Pu-239 fast fission is about 2.2, or 1.6 times the measured ratio (using chain yields for Pu-239 fast fission as recommended by Crouch [Cro 73]. Thus a 3% contribution of Pu-239 fission (50 days irradiation) would result in a 2% increase in the above ratio. For a 30 day irradiation the increase is still about 1%. Such corrections should not be neglected for relative yields.

It is not clear whether I-133 has been considered for correcting the measured Xe-133 abundance for decay, which would be important for samples E and F. The change of the Xe-133 half-life from 5.27 days (at the time of the quoted half-life measurement, Xe-133m was not known and therefore the value is in error) to 5.29 ± 0.01 days [Ede 73] causes only little changes of the decay corrections (about 0.3% and 0.5% for samples E and F, respectively). The constancy of the Cs-133/Cs-137 ratio does not prove the absence of contamination, if the samples are prepared from the same material. As all values are within the quoted standard deviations it can be concluded that the chemical procedures and mass spectrometric analysis, as performed at different times, did not introduce noticeable contamination.

Other decay corrections introduce negligible uncertainties (Ba-140, Ce-144).

In the case of Ba, Ce and Sm reliable correction for contamination is not possible and therefore contamination may cause serious problems. Further measurements are required for clarification (see Section 2.3. below).

2.1.2. Other mass-spectrometric measurements

Rider et al. [Rid 67]: Nothing is said about irradiation conditions, purity of U-238 (including fissions), contamination corrections for Nd isotopes or gammaspectrometric measurements of Cs-137. Only relative yields are given.

Wanless and Thode [Wan 55] measured relative yields of stable Xe and Kr isotopes, including Kr-85. No information on the decay correction for Kr-85 is given.

Robin et al. [Rob 71] measured relative yields of Nd isotopes and the absolute yield of Nd-148. Details of the data analysis and corrections applied can be checked.

2.1.3. Gamma-spectrometric measurements of Larsen et al. [Lar 72, Lar 74]

Absolute yields of strong γ-emitters among fission products with half-lives from 1 - 100 days were measured using a Ge(Li) detector.

The preliminary publication [Lar 72] contains little information on the work. Most of the details can be found in the recent publication [Lar 74]. Half-lives and γ-ray data used can be checked, but decay corrections by the evaluator are not possible.

[Lar 74] contains the average of 2 measurements, including the one published in [Lar 72]. However, the earlier results [Lar 72] for Zr-97 and I-131 appear to be superseded by a later analysis of the data, the Te-132 does not appear in [Lar 74]. Therefrom these earlier results are shown in brackets in Table I for comparison.

2.1.4. Ratio measurements

Bunney et al. [Bun 58] measured R-values (see [Lam 73] and others for this technique).

Ciuffolotti [Ciu 68] and Dierckx et al. [Die 71] measured the Ba-140 yield relative to U-235 thermal fission with a NaI detector, thus avoiding errors due to detector calibration and γ-ray branching. It might be worth noting that in [Die 71] the U-235 reference yield was obtained from a Cd-shielded sample. This might be a potential source of error since the thermal fission yield value is used. However, so far no significant difference has been found between mass peak yields in thermal and epicadmium fission. Even the difference between thermal and fast fission yield is less than 2.5% [Lis 70, Lar 74].

2.1.5. Radiochemical measurements

Cuninghame et al. [Cun 72] quote all errors involved in their measurements separately, but do not give information on the decay data used. Although no check is possible, they should be more up-to-date than those used in earlier measurements.

The decay data used in the earlier measurements [Eng 51, Kel 54, Bon 60, Pet 60] are out of date, but no correction is possible. Corrections for wrong half-lives can be applied for long-lived fission products (Sr-90, Cs-137) if it can be assumed that the original decay correction introduced negligible error and thus the total half-life error appears in the deduction of the fission yield from the measured activity.

Other measurements are not considered here.

2.2. Neutron Spectrum

2.2.1. Fission cross-section of U-238

Since the fission cross section of U-238 is

0.001 b below 600 KeV
0.02 b at 1 MeV
0.3-0.6 b from 1.5-2 MeV and above,

the neutron spectrum above 1.5 MeV is significant if any changes in fission yield due to neutron spectrum occur. Differences in fast neutron spectra below 1 MeV can be neglected. More important than changes of fission yield with discrete neutron energy values would be studies of yield variation with neutron spectrum above 1.5-2 MeV. Borisova et al. (Yad.Fiz. 6 (1967) 454) measured yields of Ba-140, Cd-115, Ag-111 and As-77 relative to the yield of Mo-99 at 1.5, 2, 3, 3.9, 4 8, 13, 15, 16.4 and 17.7 MeV. The yield ratio Mo-99/Ba-140 is 1.03 at 1.5 MeV and varies slightly around 1.20 from 3 to 17.7 MeV. The ratio of Cd-115, Ag-111 and As-77 yields to that of Mo-99 increase rapidly from 1.5 to 13 MeV by a factor of 100 for Cd-115 and remain fairly constant above 15 MeV.

From these results it can be concluded that yields in the peak regions of the mass yield curve can be evaluated with some confidence for different fast reactor spectra. For yields in the valley region and at the wings of the peaks an evaluation of best values for all reactor spectra is presently not possible, unless a large uncertainty is allowed for, or the high energy tails of fast reactor neutron spectra are similar.

2.2.2. Neutron fluxes used in experiments

Mat 72: Thermal reactor neutrons, sample covered by 0.03 inch Cd. U-235 depleted to 100 ppm (0.01%).

Wan 55. Fast reactor (Los Alamos, USA), U-235 depleted to about 0.02%.

Rid 67· Thermal power reactor (VBWR, Vellecitos, USA), Cd-filter, depleted Uranium.

Rob 71: Fast reactor spectrum (MAPSODIE, France), U-235 depleted to 0.04%.

Lar 74: Fast reactor spectrum (ZPR-3, Argonne, USA), high isotopic purity (99.999+ %) of sample.

Dun 58: Spectrum similar to fission spectrum (Be bombarded with 12 MeV protons), Cd shielded. U-235 content 0.03%.

Ciu 68: 2 mm Cd shielded, surrounded by 1 mm Uranium converter: predominantly fission neutrons. U-235 depleted to 0.035%.

Die 71: Thermal reactor (Ispra-I, Italy), 0.1 mm Cd, natural and depleted Uranium, pure U-238 yield evaluated.

Cun 72· Fast reactor (DFR, Scotland), 0.4% U-235.

Eng 51: Cd shielded, surrounded by Uranium converter: predominantly fission neutrons. U-235 content ~0.04%.

Kel 54: Converter, fission spectrum with median neutron energy of 2.8 MeV.

Bon 60: Unmoderated fission neutrons and Uranium converter, Cd-covered.

Pet 60· Cd-covered, Uranium converter.

Any influence of U-235 or Pu-239 (built up during irradiation) should be largest in pile neutron spectra (Cd-shielded) and smallest in fission spectra.

2.3. Status of U-238 fast fission yields

2.3.1. Comparison of experimental data

Fission yields for which more than one measurement exist are compared in Table I. In the original contribution to review paper 11b, sent to J.G. Cuninghame, [Rob 71] was not included and neither was the normalization to Nd-148. Therefore the data in Table I are partially different to those shown in review paper 11b, Appendix 3. The normalization points, namely 6.14% for the Mo-99 yield, 5.94% for the Ba-140 yield, and 2.40% for the Nd-148 yield, should not be considered as evaluated values. Reasonable values have been chosen to allow a better comparison of renormalized data.

Except for the valley region largest discrepancies can be observed for the important fission products Zr-95 and Cs-137. Only the relative mass-spectrometric Nd yields and the Ba-140 yield show good agreement. Therefore it is recommended that the Ba-140 absolute yield should be used as a standard. Furthermore, since more than 20 years the half-life of Ba-140 is well known and has only changed from 12.80 days to 12.789±0.005 days [Ede 73]. The only objection would be that systematic differences have

been observed [Lar 74] between γ-spectrometric and mass-spectrometric measurements, which are still unresolved.

It is difficult to draw conclusions from the comparison of experimental data in Table I. The earlier measurements [Eng 51, Kel 54, Don 60, Pet 60] suffer from out-of-date corrections of raw data. For example, the Cs-137 yield of [Kel 54] decreases from 7.4% to 6.7% if a half-life of 30 years [Ede 73] is used instead of 33 years, if the error in the original decay correction is considered negligible (see section 2.1). It would be worth estimating the reliability of early measurements with respect to decay data by performing model calculations using most recent data in comparison with the data used in the original work (see 2.4.3). The two more recent measurements [Gun 72, Lar 74] can only be compared for a few fission products which is not very informative. The values of mass-spectrometric measurements depend on the normalization point chosen. The absolute Nd-148 yield (common to all mass-spectrometric measurements) of [Rob 71] has a large uncertainty (>8%).

The results of [Gun 72] and [Lar 74] agree in the case of Mo-99 and Ba-140 (for which all recent measurements agree within the error limits), but disagree for Zr-95 and Zr-97. The Zr-95 yield of [Lar 74] is favoured by earlier measurements and has much higher accuracy than that of [Gun 72]. The agreement between different measurements of the yields of Sr-89, Ru-103, Ru-106, Ag-111, Cd-115g and Eu-156 varies. Discrepancies in the cases of Ag-111 and Eu-156 may be due to differences in the neutron spectrum.

The situation in the heavy mass peak is very much confused by the results of [Nat 72]. In their measurements, relative element yields of Xe and Cs were linked isobarically via mass 133, those of Ba, Ce and Nd via masses 140 and 144. The yield ratio Cs-137/Nd-145 was obtained by isotope dilution mass spectrometry. It can be seen in Table I that the normalization of their relative yields at Ba-140 is favoured by the agreement with other measurements at masses 131, 132 and 140, but disagrees with the absolute Nd-148 yield of [Rob 71]. Moreover, the sum of yields in the heavy mass peak obtained in this way would only be about 95%. The normalization of these relative yields to the absolute yield of Nd-148 brings the sum of yields up to about 105% and results in disagreement with other measurements, particularly at mass 140. The severe discrepancy of the Cs-137 yield with other measurements remains. It is possible that the Ce-140 yield suffers from contamination (see section 2.1.1) but this does not resolve the discrepancy in the Cs-137 yield. Due to the large uncertainty of the absolute Nd-148 yield, the mass 144 yield is not reliable enough to perform the contamination correction proposed in section 2.4.1.

There is no possible explanation of the discrepancies between measured Cs-137 yields. It is possible that the isotope dilution ratio of [Nat 72] is in error. But raising the Cs-137 yield to the average of other measurements would simultaneously raise the Xe yields (linked via Xe-133 and Cs-133), resulting in severe disagreement with other measurements at masses 131 and 132. On the other hand it is very unlikely that all other Cs-137 yield measurements are in error.

A comparison of relative Nd yields suggests that the Nd-150 abundance measured by [Rid 67] is in error. This argument is supported by the general trend of the mass yield curve. The discrepancy cannot be explained.

Table I. Comparison of experimental yield data for U-238 fast fission

FP	Yield	St.	Ref.
Sr-89	3.12±0.19	absol.	Cun72
	4.4±0.4	absol.	Bon60
	3.4±0.3	Mo-99	Pet60
	2.8±0.3	Ba-140	Kel54
	3.2	Ba-140	Eng51
Zr-95	7.24±1.31	absol.	Cun72
	5.44±0.16	absol.	Lar74
	5.2±0.6	absol.	Bon60
	6.1±0.6	Mo-99	Pet60
	4.9±0.7	Ba-140	Kel54
	7.1	Ba-140	Eng51
Zr-97	6.00±0.37	absol.	Cun72
	(5.91±0.18)	absol.	Lar72
	5.32±0.16	absol.	Lar74
	5.2±0.6	absol.	Bon60
Mo-99	6.00±0.79	absol.	Cun72
	6.03±0.12	absol.	Lar74
	7.0±0.7	absol.	Bon60
	6.6±0.4	absol.	Pet60
	6.7±0.7	Ba-140	Kel54
	5.74	Ba-140	Eng51
Ru-103	6.29±0.22	absol.	Lar74
	3.9±0.5	absol.	Bon60
	6.6±1.0	Ba-140	Kel54
	7.2	Ba-140	Eng51
Ru-106	2.85±0.30	absol.	Bon60
	3.02±0.30	Ba-140	Kel54
	2.63	Ba-140	Eng51
Ag-111	.058±.011	absol.	Cun72
	.094±.012	absol.	Bon60
	.087±.008	Mo-99	Pet60
	.067±.006	Ba-140	Kel54
	.070	Ba-140	Eng51
Cd-115g	.033±.005	absol.	Cun72
	.046±.007	absol.	Bon60
	.039±.004	Mo-99	Pet60
	.033±.006	Ba-140	Kel54
I-131	(3.62±0.11)	absol.	Lar72
	3.05±0.12	absol.	Lar74
Xe-131	3.17	Ba-140	Mat72
	3.66	Nd-148	Mat72
Te-132	4.23±0.34	absol.	Cun72
	(5.27±0.32)	absol.	Lar72
	4.1±0.4	absol.	Bon60
	4.9±0.6	Ba-140	Kel54
Xe-132	4.64	Ba-140	Mat72
	5.36	Nd-148	Mat72
Cs-137	7.68±1.72	absol.	Cun72
	6.1±0.7	absol.	Bon60
	7.4±0.7	Ba-140	Kel54
	5.15	Ba-140	Mat72
	5.95	Nd-148	Mat72
	7.70	Nd-148	Rid67
	6.52	Nd	Rid67
Ba-140	6.03±0.42	absol.	Cun72
	5.92±0.18	absol.	Lar74
	5.8±0.5	absol.	Bon60
	6.7±0.5	absol.	Pet60
	6.03±0.19	U-235	Ciu68
	5.72±0.14	U-235	Die71
Ba-140) +Ce-140)	6.85	Nd-148	Mat72
Nd-143	4.40	Ba-140	Mat72
	5.22	Nd-148	Mat72
	5.21	Nd-148	Rob71
	5.38	Nd-148	Rid67

Table I, continued

FP	Yield	St.	Ref.
Ce-144 +Nd-144	3.55	R-value	Dun58
	3.91	R-value	Dun58
	5.1±0.5	Ba-140	Kel54
	4.56	Ba-140	Mat72
	5.27	Nd-148	Mat72
	5.34	Nd-148	Mid67
Nd-145	3.72	Ba-140	Mat72
	4.29	Nd-148	Mat72
	4.36	Nd-148	Mid67
	4.25	Nd-148	Rob71
Nd-146	3.36	Ba-140	Mat72
	3.88	Nd-148	Mat72
	3.94	Nd-148	Rob71
	3.93	Nd-148	Mid67
Nd-148	2.40±0.20	absol.	Rob71
	2.08	Ba-140	Mat72
Nd-150	1.47	Nd-148	Mat72
	1.45	Nd-148	Rob71
	1.06	Nd-148	Mid67
Eu-156	0.042±0.008	absol.	Cun72
	0.072	R-value	Dun58
	0.065	R-value	Dun58
	0.076±0.010	Ba-140	Kel54
	0.061	Ba-140	Thg51

FP = Fission product

Standard (St.):

absolute (absol.): number of fissions determined for each sample

Mo-99: renormalized to Mo-99 yield of 6.14 [Lar72].

Ba-140: renormalized to Ba-140 yield of 5.93 (unweighted average of [Cun72], [Lar74], [Ciu68] and [Die71]).

Nd-148: relative to Nd-148 yield of 2.40 [Rob71].

Nd: sum of Nd yields without Nd-150 of [Mid67] normalized to the sum of the same yields of [Mat72] (relative to Ba-140).

R-value: yields rel Mo-99 as ratio to U-235 thermal yields, renormalized here.

U-235:, measured relative U-235 thermal fission yield of Ba-140 (6.36% used here).

2.3.2. Uncertainties

Apart from the standards Mo-99 and Ba-140, used most frequently in relative fission yield measurements, I will discuss the uncertainty of fission yields important for burnup, namely Zr-95, Ru-103, Ru-106, Cs-133, Cs-137, Ba-140, Ce-144 and Nd isotopes, in more detail and make some general statements on the other mass yields. The mass-spectrometrically determined yields of [Hat 72] need further clarification. Presently, their measured isotopic abundancies can only be normalized to yield data obtained by other authors.

The absolute Ba-140 yield has been confirmed by several measurements using different methods. Its uncertainty is about 2%.

The 2% accuracy of the Mo-99 yield assigned by Larsen et al. seems reasonable. However, their value should be confirmed by further measurements of comparable accuracy. In view of the discrepancies among results an average value is uncertain to about 4-5%.

For the Zr-95 yield the 3% uncertainty of [Lar 74] is recommended. Fortuitously, this value is close to the weighted average of rather discrepant values with large uncertainties.

For Cs-137 it is difficult to find a best value at all. In view of the discrepancies also among recent measurements the uncertainty of such a yield is at least 20%. Consequently, the Cs-137 yield has the same uncertainty.

The Nd yields are presently no more accurate than the absolute yield of Nd-148 [Nob 71], namely 8-9%. This includes the yield of Ce-144, for which no other reliable measurement exists.

For Ru-103 the 3.5% uncertainty of [Lar 74] is acceptable, the uncertainty of the Ru-106 yield is about 10%.

Other yield data:

- Relative Xe yields [Wan 55] seem to fit reasonably at masses 131 [Lar 74] and 132 [Cun 72]. The uncertainty should be 5-8%.
- Only relative Sm yields exist [Hat 72]. If adjusted to fit the mass yield curve (Nd isotopes, measurements of [Dun 58]) the uncertainty is about 15%.
- Apart from those mentioned already, very few yields have been measured in the light mass peak (masses 77, 89, 90, 97, 105). Their uncertainties are about 6-8% (89, 97) and 20% (others).

It should be kept in mind that yields below about 0.2% (valley region and wings of the peaks) depend strongly on the neutron spectrum. They can be used for all neutron spectra only with about 30-50% uncertainty.

2.3.3. Existing evaluations

I have not studied the most recent evaluation [Cro 73a, Mee 72] in sufficient detail to enable an analysis of the treatment of individual data and the evaluation method employed. I have noticed, however, that only few corrections of experimental data have been applied. Generally, only relative yields have been adjusted to evaluated reference yields. For a discussion of evaluation methods see [Lam 73] and 2.4.3. below.

a) Meek and Rider [Mee 72]: From a check of some fission products it is not clear how individual data were treated and errors assigned, as can be illustrated by some examples of fission yields discussed also above:

> Only [Mob 71] measured the absolute yield of Nd-148. In [Mee 72] this reference appears twice in the list of experimental data, once as absolute value, the second time as relative value. The absolute value has been "adjusted", but I cannot see how this can be done. All relative measurements of Nd yields [Mid 67, Mob 71, Mat 64] ([Mat 64] is probably the same as [Mat 72]) have been normalized and converted to absolute values, but no information is available how this was done. Furthermore, the adjusted relative yields of Nd-148 (converted to absolute values) have smaller uncertainty than the absolute yield and were averaged with the latter value, although it is 15% higher than the others, as shown in [Mee 72]. Clearly, relative Nd yields with an accuracy of 1-2% are distorted by this averaging procedure.
>
> Similarly, it is not clear how the relative Xe yields of [Wan 55, Mat 64] have been converted to absolute yields. Nevertheless, they have higher weight at masses 131 and 132 than the absolute measurements of [Lar 72] (which are superseded by [Lar 74]).
>
> Consequently, I cannot agree with the uncertainties obtained in [Mee 72], for example 2-4% in the case of Xe and Nd yields. Since relative yields have to be normalized to a reference yield, they cannot be more accurate than the latter when converted to absolute values.
>
> I cannot see how the authors derive an uncertainty of 2-4% for the important Cs-137 yield from the tabulated original reference data. The highest accuracy of the data shown have those of [Lev 61] for monoenergetic neutrons of about 2-3 MeV, namely 5.1%. (Other experimental data have assigned uncertainties of 7.1%, 7.9%, 11% and more.) Also the error assigned to the mass 89 yield does not reflect the discrepancies. The errors quoted in [Mee 72] for the other mass yields discussed in section 2.3.2. appear to reasonably reflect the uncertainties of experimental data.

b) Crouch [Cro 73a]: In this evaluation the uncertainties assigned by authors are shown in the tables. Although I was informed that these uncertainties are not the same as those assigned by the evaluator and used for the recommended yield, I found in a check that the weighted averages correspond in 4 cases (Zr-95, Mo-99, Ba-140, Ce-144) to the errors shown in table 16 of [Cro 73a] and only for Cs-137 they do not. Errors assigned by authors are sometimes optimistic and do not take into account nuclear data uncertainties used for corrections. It will be discussed later that particularly wrong decay data used in the original work should be considered by the evaluator (see also the example of the Cs-137 yield in section 2.3.1.).

In [Cro 73a] the uncertainties of the average generally reflect well the uncertainties of experimental data and existing discrepancies. This is due to the fact that Crouch has used the larger error of weighted and simple average (together with the result of the weighted average). I have, however, a few comments:

- Although this procedure reflects fairly well the uncertainties of experimental data, the yield value itself obtained by the weighted average is determined by the uncertainties assigned by authors to their

experimental data. Thus it is still necessary for the evaluator to make his own judgement of all sources of error.

- Due to the nuclear data uncertainties in earlier measurements discrepancies may be observed among experimental results. Thus, if reliable recent measurements are opposed by discrepant data from earlier measurements or with large uncertainty [Cun 72], the yield and error of the weighted average or the most reliable measurement could be adapted. Among the fission products discussed here, the weighted and simple means of [Cro 73a] are, for Zr-95: 3% and 6%, for Ru-103: 3% and 13%. The higher uncertainties are adopted in [Cro 73a].

- [Cro 73a] does not include the experimental data of [Wan 55, Mat 72 (or Mat 64), Rid 67, Die 71]. Therefore some mass yields are missing and, particularly, the discrepancies among the Cs-137 yield data shown in table 16 of [Cro 73a] are not as large as those in Table I in this work.

- In cases where authors have not quoted uncertainties, Crouch has assigned errors common to all experiments of a certain type. However, I am of the opinion that errors should be assigned by the evaluator individually to experimental results, judging from other measurements under similar conditions. For (earlier) radiochemical measurements such a procedure would be more complicated as counting statistics may differ widely for the same nuclide. In this case the absolute error should be higher than the average of similar measurements.

  Principally, higher uncertainties should be assigned for measurements of low yield fission products. Otherwise the common error assigned during the evaluation may be lower than those from other experiments. The (low) yields of As-77 and Sb-127 in table 16 of [Cro 73a] are good examples where the 15% error assigned by Crouch is opposed by author-assigned errors of 25% and 23%, respectively, of other measurements of comparable reliability.

When comparing the two evaluations [Hee 72, Cro 73a] it should be kept in mind that more experimental data (particularly the mass-spectrometric measurements of [Rid 67, Mat 64] are included in [Hee 72] and that both use the superseded data of [Lar 72] for mass numbers 131 and 132.

2.4. Future work

2.4.1. Suitable techniques

The very low fission cross section of U-235 imposes several restrictions on suitable measurement techniques.

Mass-spectrometric measurements require longer irradiations (at least a few days) in order to accumulate a sufficient number of fission products. Particularly in Cd-shielded samples irradiated in a thermal reactor spectrum the buildup of Pu-239 due to resonance capture in U-238 may be significant together with the rather high resonance fission cross-section of Pu-239. This problem is much less serious for irradiations in fast reactor or fission neutron spectra.

In view of the low fission cross-section of U-238 and hence the low burnup, contamination problems are more serious than in other fission yield measurements (e.g. thermal yields). This affects particularly the elements

Rb, Sr, Cs, Ba and Ce which have either no isotope not occurring as fission product or the abundances of such isotopes are very low in the natural element. Experience has shown that contamination by Cs and Rb was rare in the past. However, Ba and Ce yields often showed discrepancies. I would propose to measure the Ba-140/Ce-144 yield ratio to about 1-2% accuracy, e.g. by γ-spectrometry [Deb 73]. Then measured relative Ce abundancies can be corrected for contamination using this ratio, rather than by the method employed by [Mat 72].

Corrections for contamination by natural Sm introduce great uncertainties in the yields of Sm-152 and Sm-154, which have highest abundance in the naturally occurring element. In addition, resonance capture in Pm-147 cannot be neglected after long irradiations in the case of Cd-shielded samples, and calculation of the amount of Sm-148 formed this way is rather uncertain. This difficulty could be circumvented using large samples irradiated less than 10 days. Because of the 11-day half-life of Nd-147 capture in Pm-147 can be kept negligible.

Contamination problems for radiochemical measurements are not serious as fast neutron capture cross-sections are very low. (As a rough estimate it can be shown: if in a fast reactor spectrum the neutron flux in the range from 100 to about 700 KeV is 10 times the flux of 1.5 - 3 MeV, then 1000 ppm Mo-98 would produce an amount of Mo-99 which would be of the order of 1% of the fission product.)

The determination of absolute yields with the aid of fission chambers or fission track detectors requires rather thin samples. The inelastic scattering cross-section of U-238 is about 2.5 b in the range of 1-3 MeV. Roughly half of that would be responsible for scattering 1.5 - 3 MeV neutrons below U-238 fission threshold. A reduction of the neutron flux in this energy range by less than 1% requires a sample thickness of ≤ 2 g/cm^2.

Due to these restrictions in sample size, absolute measurements of fission yields by radiochemical techniques can only be performed with good counting statistics for high activity fission products, since short irradiations are required to avoid uncertain decay corrections.

Relative yields can be determined radiochemically by β-counting of separated fission products from large samples with good counting statistics, using the predetermined yields of high activity fission products as reference.

Thin samples are always required for the determination of yields by gamma spectrometry without dissolution of the sample and separation of fission products. Although this method has fewer sources of error, it is applicable only for a restricted number of fission products.

A suitable method for chain yields is the measurement of R-values relative to the well-known U-235 thermal fission yields. One source of error, the detector calibration, can be avoided.

2.4.2. Further measurements required

Recommendations for further measurements depend on the accuracies required in application fields:

- For burnup determination ~5% accuracy is required for the FP mentioned in 2.3.2.

- Other application fields probably require an accuracy of 15-20%, depending on the significance of the FP. Certainly yields in the valley region and at the wings of the mass peaks are needed with lower accuracy.

Presently only the yields of Zr-95, Ru-103 and Ba-140 meet burnup requirements. Among these the Zr-95 and Ru-103 yield as well as that of the standard Mo-99 should be confirmed by other measurements, as discrepant but less reliable data exist.

Further measurements of the yields of Ru-106, Cs-133, Cs-137, Ce-144 and Nd isotopes are required. Relative Nd yields are sufficiently accurate, thus requiring only a redetermination of the Nd-148 yield, or alternatively a measurement of the absolute Ce-144 yield.

All the above-mentioned fission product yields can be determined by gamma spectrometry with sufficient accuracy [Deb 73, Lar 74]. The relative yields of Cs-133 and Nd isotopes can be normalized to one of these fission products. In addition, the ratio of Cs to Nd yields could be redetermined by isotope dilution mass spectrometry.

For other applications measured relative and absolute yields in the heavy mass peak together with the measurements recommended above should be sufficient. In the light mass peak yields for a number of mass chains are missing. These could be measured most conveniently and with sufficient accuracy by the K-value technique. Mass-spectrometric measurements are not required, since relative Kr yields are known [Wan 55].

The use of Ba-140 as reference yield is recommended until more reliable data for other fission products (Zr-95, Mo-99, Ce-144) exist. Further absolute yield measurements would be useful. The dependence of fission yields on neutron energy, particularly in the regions of low yields, should be investigated.

2.4.3. Evaluation work

Up to now all experimental yield data, ranging from Cd-shielded irradiations in thermal reactors over fast reactor spectra to fission spectrum and 3 MeV yields, have been evaluated together resulting in a recommended "fast" fission yield. In future these different types of measurements should be separated and the effect of neutron energy be studied, unless there will be evidence that certain yields do not depend on this effect.

A source of error is the use of superseded decay data in earlier measurements. Nuclear data like half-lives, β-branching ratios, endpoint and mean energies, intensities of conversion electrons, are required in radiochemical measurements for analysis of raw data, corrections for build-up and decay, corrections for other fission products present and for counting rate as well as for calculation of fission yields from measured activities. Although in earlier measurements no details on error analysis are given, nuclear data uncertainties were generally not included in the calculation of errors. In addition, earlier measurements suffer from errors due to superseded nuclear data which are not reflected by the uncertainties calculated for the results.

Such uncertainties should be estimated by the evaluator. In a very time-consuming evaluation these additional uncertainties could be estimated from model calculations, using the nuclear data and experimental conditions (irradiation and cooling times, samples) of the original work and comparing

the results with the calculations using presently adopted nuclear data. The results shoudl be used to estimate systematic errors and check the reliability of these data, as appropriate corrections are hardly possible.

If time does not permit this procedure, additional uncertainties should be assigned to experimental data individually, according to the evaluator's judgement of the nuclear data used and the experimental details described.

Furthermore, evaluators should try to resolve discrepansies in order to reduce the uncertainties of fission yield data and save experimental work. This requires a thorough check of details of experimental procedures and data analysis and justifies to seek pertinent information, which is not included in publications, directly from authors.

3. Th-232 FAST NEUTRON FISSION YIELDS

3.1. Experiments

The experiments discussed below and listed in Table II are those included in the evaluation presented in [Lam 73].

3.1.1. Iyer et al. [Iye 63]

Iyer et al. measured the most complete set of Th-232 fission yields. They measured R-values relative to U-235 thermal fission using Mo-99 as standard. By normalizing their relative yields in such a way that the sum of all fission yields is 200%, they obtained a value of 2.78% for Mo-99.

The table 1 in [Iye 63] contains two errors:

The Ba-139 yield for thermal neutron fission of U-235 should read 6.55% (instead of 5.55). The value 6.55 has been used to calculate the Th-232 yield of 6.64%.

The error quoted for the same yield, namely 6.64±0.033, is wrong, as can be calculated from the R-value. There the error is 5%, whereas the error of the yield is 0.5%. Therefore the value should read 6.64±0.33.

The errors quoted in [Iye 63] are standard deviations of the measured R-values and do not include uncertainties of U-235 yields, the Mo-99 reference yield and systematic errors. Inspite of the measurement of R-values, additional errors can be introduced for example by differences in decay curve analysis (between U-235 and Th-232 fission products), differences in decay corrections, etc. Furthermore, a 1.3% error (Cs-137, Zr-97) or 0.38% error (Ce-144) as standard deviation for 2 measurements has to be considered fortuitous, as long as errors for other high yield fission products are 5% in the average.

In the present evaluation all yields have been recalculated using the published R-values and the U-235 yields of [Lam 73]. The yields in Table II have been normalized arbitrarily to a Ba-140 yield of 8%.

3.1.2. Kennett and Thode [Ken 57]

The mass 85 yield has been calculated using a branching of 22% to Kr-85g. The originally measured yield of Kr-85g relative to Kr-86, corrected for decay, was 0.145. The authors quote 5.97±0.15% as measured

absolute yield of Kr-86. This is, however, the "unweighted average" of approximately, as the authors say, 5.8% (sample A) and 5.11% (sample B). Therefore it has not been used in the present evaluation, although it is the only measurement of an absolute yield for Th-232 fast fission.

In the present evaluation the relative yields have been normalized together with the mass-spectrometric measurements of [Har 68a] to the Cs-137 yield of [Iye 63], using the Xe Kr ratio of [Wen 57]. This Cs-137 yield might, however, be wrong (see 3.4.1.).

3.1.3. Harvey et al., mass-spectrometric measurements [Har 68a]

The same impurity problems arise for Cs-137 and Nd isotopes as stated for U-238 fast fission. Nd contamination should be detected by the abundance of Nd-142. However, nothing is said in the publication.

In the present evaluation the relative Xe and Kr yields have been normalized together with those of [Wen 57]. Relative Nd yields have been normalized at mass 143. The value of 6.64 is the average of [Iye 63, Har 68b] and [Bre 67] (with 1/2 weight).

3.1.4. Harvey et al., R-values [Har 68b]

In the present evaluation measured R-values have been adjusted using the U-235 yields of [Lam 73] with the exception of masses 131 and 132. Recent gamma-spectrometric measurements of U-235 yields relative Ce-144 [Deb 73] have confirmed the mass 131 relative yield quoted by Farrar et al. [Far 62]. The latter value had been obtained from an unpublished Xe-132/Xe-133 yield ratio and therefore not been used in [Lam 73]. Thus the new U-235 yields used are 2.93% for mass 131 and 4.36% for mass 132 (with a fractional cumulative yield of 0.996 for U-235 and 1.0 for Th-232).

The relative Th-232 yields have been normalized at mass 132 as obtained from the normalization of mass-spectrometric measurements.

3.1.5. Bresesti et al. [Bre 67]

Fission yields were measured with a NaI detector calibrated by a $4\pi\beta\gamma$ coincidence method. The internal standard was Ce-141.

The reported errors are standard deviations. The uncertainties due to $4\pi\beta\gamma$ calibration of the detector are not considered. In [Lam 73] the deviations of measured U-235 yields from recommended values were considered to be systematically due to this detector calibration. Therefore, the Th-232 yields were adjusted according to these deviations.

However, fission products have been chemically separated before gamma-spectrometric measurements and experimental conditions such as mounting of samples, etc., were not explicitly stated to be identical in the determinations of U-235 and Th-232 yields. Since a readjustment of measured values without detailed information from the authors is always critical and should not be done without good reasons, the original relative yields are used in the present comparison (Table II), although the two measurements could be considered as R-values.

At present the discrepancies among measured Th-232 yields are too large to make detailed studies of individual measurements worthwhile. Should a more thorough and detailed evaluation be attempted when further precise measurements become available, such information on experimental details, as mentioned above, should be sought from the authors.

The reported yields of Pm-149 and Pm-151 were corrected for U-235 reference yields, as these were used for detector calibration.

3.1.6. Kobayashi et al. [Kob 70]

These measurements in a fast neutron spectrum (close to a fission spectrum) are not yet published in the open literature. Ba-140 was used as standard and the quoted uncertainties are high: 10% for Zr-95, 12% for Te-132, 15% for Sr-91 and 23% for Xe-135. However, the agreement with other measurements (mass-spectrometric [Har 68, Rye 63]) is far better than the quoted uncertainties.

No experimental details are available. Therefore these measurements are mainly used as a check and only the yields of Sr-91 and Zr-95 are included in the average with low weight (see 3.3.3.).

3.1.7. Wyttenbach and von Gunten [Wyt 65]

The quoted errors are standard deviations resulting from 3-8 measurements. Systematic errors are not considered. Ru-103, Ag-111, Pd-112, I-131, Cs-137, Ba-140 and Ce-141 were measured gamma-spectrometrically using a calibrated counter and disintegration data from Nuclear Data Sheets. Sr-90, Ru-106 and Ce-144 were measured against calibrated IAEA standards in a gas flow proportional counter. Mo-99 was used as standard.

In the present evaluation it was assumed that Mo-99 was measured by both methods. Gamma-spectrometrically determined yields were corrected for differences in the emission probabilities of the most abundant gamma ray tabulated in Nuclear Data Sheets up to 1964 to those of the Seibersdorf computer library [Ede 73, Lam 73a]. The relative yields of Ru-106 and Ce-144 remained unchanged. That of Sr-90 was corrected for half-life. The corrected relative yields were normalized to 8% for Ba-140.

3.1.8. Turkevich and Niday [Tur 51]

At the time of these early measurements data on half-lives and beta rays (branching, energy, etc.) were not well known. However, a number of fission products (Sr-91, Zr-97, Mo-99, Ru-103, Rh-105, Ru-106, Pd-109, Ag-111, Pd-112 and Cs-137) were measured relative to U-235 fission yields with Sr-89 as standard.

The yields measured relative to U-235 have been readjusted in the present evaluation. The other yields reported in the article are not used.

3.1.9. Crook and Voight [Cro 63]

All details on measured values are given in the report. The raw data are reduced to counting rates at reference time. In some cases large discrepancies are obvious among individual saturation activities of the same fission product.

As experimental details are given, it was attempted to correct the measured yields for differences in half-lives used in the original work to those reported in [Ede 73]. This was done by calculating yields from the raw data as well as by calculating decay correction factors using the original half-life values and the new ones.

The severe discrepancies of the yields measured by Crook and Voight compared to those of other authors could not be improved by these correc-

tions. Table II shows the corrected data normalized to 8% yield for their internal standard Ba-140. Any other normalization either using the original or the corrected values, gave agreement with other authors for 3 relative yields out of 9 measured ones at the most. For this reason the data of Crook and Voight have not been used in the present evaluation.

3.2. Neutron spectrum

3.2.1. Fission cross-section of Th-232

The fission cross-section of Th-232 rises from zero at 1.1 MeV to0.11 b at 2 MeV, remains fairly constant from 3 MeV (0.13 b) to 6 MeV (0.15 b) and rises up to 0.3 b between 6 and 7 MeV. The cross-section is roughly similar to that of U-238 and all that has been said for U-238 is also valid for Th-232. The same arguments used for U-238 with respect to inelastic neutron cross-section and sample size can be used for Th-232.

3.2.2. Neutron flux used in experiments

Iye 63: Irradiation of bare samples in the core of "Apsara" reactor. Fast flux should be close to fission spectrum.

Ken 57: Samples in cylinder of natural Uranium should be close to fission spectrum.

Har 68a: Samples wrapped in 2 layers of 0.015 inch Cd. Pile neutrons.

Har 68b: Thermal flux reduced by B_2O_3 plug in addition to Cd. Th-232 containers to enhance fast flux of incoming pile neutrons.

Bre 67: Cd-wrapped samples irradiated in graphite reflector as well as close to core.

Kob 70: Fast reactor spectrum close to fission spectrum.

Wyt 65: Cd-wrapped samples at the side of core.

Tur 51 and Cro 63: pile neutrons.

The samples used were of very high purity, sufficient to make U fisfions negligible.

With the exception of [Ken 57], [Kob 70] and perhaps [Har 68b], essentially pile neutrons were used in all experiments. As stated for U-238, the dependence on the hard part of the incoming neutron spectrum might be significant at the wings of the mass peaks and in the valley region. Yields in the peak regions should be the same within a certain confidence limit. This should be further investigated. Work in this direction is in progress at Idaho. It might well be possible that, if desired, yields will have to be determined with high accurary for individual or prototype fast reactor spectra.

3.3. The present evaluation

The "present evaluation" is not a new evaluation, but only a modification of [Lam 73], which I consider as improvement. The general procedure remained the same and differences are discussed in 3.3.4.

3.3.1. General procedure

As no absolute Th-232 fast fission yields exist, except the very rough measurements of Kennett and Thode, the arbitrary normalization of relative yields is justified. As stated in the comments to U-238 fast yields, Ba-140 has generally been measured most accurately and was therefore chosen as standard wherever possible, even if this fission product was not used as standard in the original work. There may be an objection against this procedure as e.g. [Iye 63] used Mo-99 as internal standard for different samples which were not all analyzed for Ba-140. Furthermore, all reported yield values are averages of several determinations, including the yield of Ba-140, which would be different when normalized to the latter for each sample.

However, published standard deviations for individual fission products are generally small compared to the overall uncertainties, which indicates no systematic error due to the choice of the standard. The reference yields used in measurements vary: Mo-99, Ba-140, Ce-141, Te-132 and Sr-89 (see 3.1.). No fission product has been measured more frequently than Ba-140, and this normalization showed best agreement among experimental data. Besides, using the normalization points of the original measurements would cause only little changes (see below).

Relative experimental yields in Th-232 fast fission are shown in Table II. The data of [Iye 63] are used as starting point relative to 8% for the Ba-140 yield. Mass-spectrometric data [Ken 57, Har 68a] in the mass range 83 - 88 and 131 - 137 are normalized at mass 137. The data of [Har 68b] are normalized to the mass 132 yield obtained from [Ken 57]. Together with other measurements including Ba-140 [Bre 67, Kob 70, Wyt 65] normalization points for the data of [Tur 51] and relative Nd-yields [Har 68b] could be found.

Normalizing the data of [Wyt 65] at Mo-99 would have increased them by 1.5% relative to the data of [Iye 63]. The resulting average of the Ce-141 yield would be 7.15 and would increase the data of [Bre 67] by 2% if chosen as reference yield. This would cause changes of about 1-1.5% in some average yields.

Relative yields were averaged as explained in 3.3.3. The data obtained in this way are shown in the column headed 'average' of Table II. The final normalization as shown in the last column of Table II was obtained by making the sum of yields in the heavy mass peak total 100%, as there are less estimated yields than in the light mass peak.

3.3.2. Quoted uncertainties of experimental data

With the exception of [Tur 51] and, probably, [Kob 70] all authors quote standard deviations relative to the reference yield used. The average standard deviations for high yield fission products of more than two measurements are:

Iye 63:	3-5% (except Sr-91, 8%)
Ken 57:	0.5-1%
Har 68a:	0.5-2%
Har 68b:	1-2% (except I-131, 6%)
Bre 67:	2-5%
Kob 70.	10% and more
Wyt 65:	1-5% (average 3%)
(Tur 51:	10% minimum (standard Sr-89))
Cro 63:	6-8%

Table II. Th-232 fast yields: experimental data in the normalization used in the evaluation

Underlined: Normalization Point

Mass No.	Iye63	Ken57 Har68a	Har68b	Bre67	Kob70	Wyt65	Tur51	Cro63	average	final
72							(3.2-4)		3.2-4	3.4-4
73							(4.4-4)		4.4-4	4.6-4
77	9.8-3						(0.02)		.01	.01
83	1.87	1.78					(1.86)		1.80	1.90
84		3.26							3.26	3.44
85		3.54	3.55						3.54	3.74
86		5.38							5.38	5.69
87		5.69							5.69	6.01
88		6.00							6.00	6.34
89							6.08	(8.29)	6.08	6.43
90	7.13					6.63	(6.80)	(8.86)	6.88	7.27
91	6.51		6.60		6.2		6.55	(5.11)	6.55	6.92
93				7.24					7.24	7.65
95	5.10				5.2				5.12	5.41
97	4.03		3.60				4.61		3.80	4.02
99	2.63					2.59	2.47	(3.20)	2.60	2.74
103	.145					.146	.145		.145	.153
105	.0279						.061		.04	.04
106	.039					.057	.040		.039	.041
109	.038						.039		.038	.040
111	.046					.075	.035		.04	.04
112	.073					.083	.061		.06	.06
113	.055								.055	.058
115	.054						(.057)		.054	.057
117	.048								.048	.051
121	.053								.053	.056
123	.030								.030	.032
125	.032								.032	.034
127	.072								.072	.076
131	1.54	1.44	1.29			2.07	(1.17)		1.44	1.52
132		2.55	2.55		2.6		(2.35)		2.55	2.69
133		3.46	3.68						3.55	3.75
134		4.79							4.79	5.06

Table II (continued)

Mass No.	Iye63	Ken57 Har68a	Har68b	Bre67	Kob70	Wyt65	Tur51	Gro63	average	final
135		4.31	4.78		4.1				4.5	4.76
136		5.09							5.09	5.38
137	4.26	4.26				6.08	5.78		4.26	4.50
139	6.24		6.60						6.42	6.78
140	8.00			8.00	8.0	8.0	(6.06)	(8.0)	8.00	8.45
141	7.18			7.01		7.02	(8.80)	(7.45)	7.10	7.50
143	6.78	6.64	6.53	6.57				(7.77)	6.64	7.02
144	6.71			7.51		7.43	(6.94)	(8.55)	7.09	7.49
145		5.39							5.39	5.70
146		4.62							4.62	4.88
147	2.94			2.99				(3.24)	2.96	3.13
148		2.03							2.03	2.15
149	.823			1.39					1.39	1.47
150		1.02							1.02	1.08
151				.393					.393	.42
153				.198					.198	.21
156	.0025								.0025	.0026

It is evident that the measurements of [Iye 63, Bre 67 and Wyt 65] have about equal precision. As [Iye 63] measured R-values their results are considered more reliable than those of [Wyt 65] and [Bre 67]. An assignment of overall uncertainties was not attempted.

3.3.3. Selection of experimental data

In Table II those yields of [Tur 51] are shown in brackets which had not been measured relative to U-235. They are not used to obtain average yields except for masses nos. 72 and 73.

The following data were used to obtain the relative yields shown in the column headed "average" in Table II (see also discussion in 3.4.1.).

As-77:	[Iye 63]
mass 83:	[Ken 57] and with 1/2 weight [Iye 63]
masses 84 - 88:	mass spectrometric data [Ken 57, Har 68a]
Sr-90:	unweighted average of [Iye 63, Wyt 65], since the latter has much higher precision.
mass 91:	highest weight given to [Har 68b], lowest to [Kob 70]

Zr-95:	[Iye 63] weighted higher than [Kob 70]
Zr-97:	unweighted average of (equal precision) results of [Iye 63, Mar 68b]
Mo-99:	highest weight given to [Iye 63], lowest to [Tur 51], in view of the different reliability of the data.
masses 105 - 111:	about equal weight given to [Iye 63] and [Tur 51], since they show good agreement (except Rh-105, where only an approximate value is taken as average). The data of [Wyt 65] have not been used, as the situation of yields in the trough region needs further clarification.
mass 112:	[Iye 63] quote also a result for Ag-112 which would be 0.058 in the normalization shown in Table II. Only approximate value used as average.
masses 131, 132:	mass-spectrometric data.
masses 133, 135:	average of [Mar 68a] and [Mar 68b]. The ratio 133/132 has equal precision in both measurements. Therefore the normalization of mass-spectrometrically measured ratio 135/132 cannot be more precise (see also 3.4.1. for further discussion).
Cs-137:	the value of [Iye 63] was chosen as it agreed best with mass-spectrometric measurements, combined with I-131 yields of [Iye 63] and [Mar 68b] (overall agreement). This yield, however, needs further clarification (see 3.4.1.).
masses 139 to 144:	equal weight given to R-values, 1/2 weight to [Bre 67] and [Wyt 65].
Pm-149:	the yield of [Bre 67] fits better between mass-spectrometric data and has been preferred.

3.3.4. Differences between Table II and [Lam 73]

The evaluation presented in [Lam 73] was done for internal use at a time when new important measurements became available [Mar 68, Bre 67], but were not incorporated in evaluations. The normalization was done in one of several possible ways. Individual experiments were examined carefully and checked for reliability. However, no account was taken of the precision of individual yields within one experiment. Rather was the reliability judged from an experiment as a whole including the method used, and the specific fission products considered for taking an average since no overall errors were estimated by authors (cf. 3.3.2.).

The values presented in Table II should be considered as a slightly different way of normalizing and selecting experimental data, using the same evaluation principle. The influence of such differences may become evident from a comparison.

The differences between the procedure to obtain the two sets of data are:

- In [Lam 73] the readjustments of Ba-139 (see 3.1.1.) and Ce-144 yields of [Iye 63] was in error (assuming wrong U-235 reference yields used in the original work). This time only the R-values were used for corrections.

- U-235 reference yields for Ru-103, I-131 and Te-132 used now are 3.09% [Deb 73], 2.93% and 4.36%, respectively. In [Lam 73] the U-235 yields published there have been used. This affects the I-131 yield of [Iye 63] and all adjusted R-values of [Har 68b].

- Mass-spectrometric relative Kr, Xe and Cs yields were previously normalized to agree in the sum of mass 83, 131 and 137 yields.

- The data of [Bre 67] were readjusted for differences between measured and recommended U-235 yields in [Lam 73] and thus treated as R-values.

- The data of [Tur 51] were previously normalized at mass numbers 91 and 99, this time only at 91.

- In [Lam 73] the mass-spectrometric Xe-133/Xe-132 was averaged first with that obtained from the R-value [Har 68]; relative Cs-yields were normalized to this average value.

- The preference of data was:

  1) mass-spectrometric
  2) [Har 68b]
  3) [Iye 63] and [Bre 67]
  4) [Wyt 65] and [Tur 51]

  Other data were not used.
  Exceptions were Ce-141 (γ-spectrometric measurements preferred), Ce-144 ([Iye 63, Bre 67, Wyt 65] equal weight), mass 143 ([Har 68b, Iye 63, Bre 67] equal weight) and Ba-139 ([Iye 63, Har 68b] equal weight).

3.4. Status of Th-232 fast fission yields

3.4.1. Comparison of experimental data

A comparison of experimental data as displayed in Table II is of course influenced by the normalization chosen. The following comments have to be understood as "relative to the Ba-140 yield".

Apart from the valley region the most striking discrepancies occur at mass numbers 131 and 137. With the normalization chosen, the Cs-137 yield of [Wyt 65] is 43% higher than that of [Iye 63]. If the Xe-131 yield of [Ken 57] is chosen as reference, the I-131 yield reported in [Har 68b] is 10% lower, those of [Iye 63] and [Wyt 65] are higher by 7% and 44% respectively. All data sets that include a measurement of the mass 131 yield are normalized at this value in Table III for comparison. The most striking observation is the good agreement among the 137/131 yield ratios ([Iye 63] ~6% lower). Also in the valley region the values of [Iye 63] and [Wyt 65] are much closer whereas all other yields (including [Har 68b] exhibit severe disagreement.

It can be cloncluded that the discrepancies are in the mass 131 yield. The Cs-137 yield is either around relative yields of 4.3 or 6. Averaging these two values makes no sense. The reason for the preference of a Cs-137 yield of 4.26 in this evaluation is that it is confirmed by 4 measurements, 3 of which are completely independent ([Iye 63], mass-spectrometric, [Har 68b]; U-235 reference yields can be excluded as cause for the discrepancies). A normalization to the Cs-137 yield of [Wyt 65] would raise the mass spectrometric data [Ken 57, Har 68a] and those of [Har 68b] by 43% and cause severe

discrepancies of the latter with other data at mass numbers 91, 97, 139 and 143 (relative yields would exceed 9% except for Sr-97).

Table III. Experimental Th-232 yields relative mass no. 131

Mass No.	Iye63	Ken57 Har68a	Har68b	Wyt65	Mass No.	Iye63	Ken57 Har68a	Har68b	Wyt65
83	1.21	1.24			132		1.77	1.98	
90	4.63			3.20	133		2.40	2.85	
91	4.23		5.12		135		2.99	3.71	
97	2.62		2.79		137	2.77	2.96		2.94
99	1.71			1.25	139	4.05		5.12	
106	.0253			.0275	140	5.19			3.86
111	.030			.036	141	4.66			3.39
112	.047 (.038)			.040	143	4.40		5.06	
					144	4.36			3.59
131	1	1	1	1					

However, there are also severe arguments against the choice of the low Cs-137 yield

- The yields of [Wyt 65] could be corrected for γ-ray abundancies and the half-life used for Cs-137 is correct. There is no evidence for distrusting this measurement.

- There is evidence from recent work [Mud 73] that the higher value is correct.

- $\bar{\nu}$ in Th-232 fast fission varies from 2.1 - 2.3 in the range 1.4 to 3 MeV [Man 72]. $\bar{\nu}$ calculated according to [Lam 73, Wal 73] from the data shown in the last column of Table II is 1.55.

- There is no correspondence in the light mass peak to high and low yields in the heavy mass peak and vice versa, with the possible exception of the pair 90 - 140. This cannot be explained by variations in neutron emission.

In addition it has been observed that the Cs element yields measured mass-spectrometrically at McMaster University ([Har 68a] for Th-232) are systematically low [Lam 73b, Wal 73c] and the isobaric link (Xe/Cs)-133 is generally in conflict with other measurements [Lam 73, Lam 73b] (see also U-238 fast fission discussed in chapter 2).

I have attempted two different renormalizations in order to check their effect on $\bar{\nu}$. In the first one all data of [Ken 57, Har 68] were adjusted to 6.08 for Cs-137 and all high yields of [Har 68b] (see above) ignored. In the second one the mass-spectrometric data of [Har 68] for masses number 133, 135 and 137 were ignored, 1.54 for mass 131 was chosen as

reference point for [Ken 57, Har 68], and all data of [Har 68b] used as well as 6.08 for Cs-137. The resulting values for $\bar{\nu}$ are 2.79 and 1.96 respectively. However, there are too many factors of uncertainties and no clear reasons to favour the one or the other set of experimental data to allow any reliable conclusions.

When comparing experimental data in Table II, other discrepancies are also evident, e.g. at mass numbers 90, 97, valley region (105 - 112), 139, 149 and, most important, at 144. These depend, however, partially on the particular normalization chosen. Interesting is the good agreement among relative mass 140, 141 and 144 yields of [Bre 67] and [Wyt 65].

In order to check the influence of the choice of the reference yield and the normalization of relative yields to 100% in the heavy mass peak, I have performed another comparison of experimental data, using the reference yield of the original work wherever possible, and the absolute yield of Kr-86 (5.97% [Ken 57]) as starting point. The other data were adjusted in the following steps.

a) [Ken 57] Kr and Xe at Kr-86

b) [Har 68a] Kr-87, Kr-83 at Kr-86, Xe-133 at Xe-134
relative Cs yields not used

c) [Har 68b] R-value yields at mass 132 [Ken 57]

d) [Iye 63] at masses 83 and 131 [Ken 57] (original: 99)

e) [Wyt 65] at mass 99 [Iye 63]
[Tur 51] R-value yields at mass 99 [Iye 63] (original: 89)

f) [Bre 67] at mass 141 (average [Iye 63, Wyt 65])

g) [Har 68a] stable Nd yields at mass 143 (average [Har 68b, Iye 63, Bre 67]).

A simple average was taken, omitting discrepant data of [Iye 63] (masses 91, 131, 137, 139, 144), [Wyt 65] (mass 131) and [Tur 51] (mass 97) and the results presented in Table IV under "absolute" together with other evaluations.

This normalization reduces the discrepancies at masses 90 and 97, but increases the others. However, there is close agreement between the Cs-137 yields of [Tur 51] and [Wyt 65] and better agreement among all data at masses 141 and 143. The changes in the final yields are not very significant (cf. Table IV), except for the Cs-137 yield.

A common feature of all normalizations is that the sum of yields in the light mass peak (including interpolations) is less than that in the heavy mass peak. In the last absolute normalization the sum of yields in the light mass peak is 97.67, that in the heavy mass peak is 105.32. This and the fact that no high yields in the light mass peak correspond to those at masses 140 and 144 in the heavy mass peak suggest that the yields in the region 140 - 144 could be too high. Clarification by further measurements is necessary.

3.4.2. Discussion of evaluations

As discussed in the previous section the uncertainties of Th-232 fission yields depend significantly on a particular normalization chosen. Therefore we shall discuss evaluations and normalizations of other authors

and compare them (Table IV) before we draw any conclusions on the uncertainties of available data.

Crouch separated pile [Cro 73b] and fast [Cro 73a] neutron fission yields of Th-232, which he did not do for U-238. The criteria for the separation are not quite clear, as under "fast" [Cro 73a] the data of [Ken 57] (fission spectrum), [Har 68] and [Wyt 64], an earlier publication of [Wyt 65], (both pile neutrons) appear, whereas under "pile" [Wyt 65] is listed together with the other data (cf. section 3.2.2.). Furthermore, we have seen that the shape of the neutron spectrum above ~1.5 MeV is the essential criterium. In that region the spectrum of fission neutrons in a water moderated reactor is closer to a pure fission spectrum than the neutron spectrum of a fast reactor.

a) [Cro 73a], table 3, "fast" (the reference numbers are those quoted in [Cro 73a]): This evaluation includes the data of [Ken 57] (=ref. 241), [Har 68] (=ref. 369) and [Wyt 64] (=ref. 389, which is the same as [Wyt 65]). The reference yield chosen for Mo-99 is that obtained by [Iye 63] which is not included in this evaluation. It should be noted that the data quoted in this table for ref. 369 are those obtained in the final normalization by [Har 68], which include the data of [Ken 57], and [Iye 63]. The yields of stable Kr and Xe isotopes quoted for ref. 369 (=[Har 68]) are those of [Ken 57] in the normalization of [Har 68] and averaged with those of ref. 241 (=[Ken 57]) in table 3 of [Cro 73a]. On the other hand mass yields 91 and 97 [Har 68b] are not used. Furthermore, the data of refs. 241 and 369 were not found using a Mo-99 yield of 2.78%. Finally, it is not clear why a 10% uncertainty was assigned to the mass spectrometric data of [Ken 57, Har 68] and 5% uncertainty to the radiochemical yields of [Wyt 64] (cf. section 3.3.2.).

b) [Cro 73b], table V, "pile" (reference numbers are taken from this table): This evaluation includes the data of [Cro 63, Iye 63, Tur 51, Wyt 65, Dre 67] among others. It has been shown in section 3.3.2. that all authors, except [Tur 51], quote standard deviations of relative yields. In this evaluation the standard deviations quoted by authors were used for references 15 (=[Cro 63]), 228 (=[Iye 63]) and 326 (=[Tur 51], overall error), if they exceeded 5%. In the case of ref. 336 (=[Wyt 65]) the quoted standard deviations were used for Sr-90 and Ru-103, whereas for all other yields a common 15% error was assigned, which compares to a 5% uncertainty used for [Wyt 64] in [Cro 73a]. An error of 15% was also assigned to all data of refs. 348 (=[Nid 50]) and 367 (=[Bre 67]). To be consistent, either all relative measurements should have a common error when converted to absolute yields, or all errors should be assigned individually (e.g. by adding an estimated systematic to the statistical error in quadrature). [Nid 50] is an earlier publication of [Tur 51], but not the same data.

R-values have been corrected for U-235 reference yields and Mo-99 was chosen as reference yield (2.78% [Iye 63]) wherever possible. Since no final normalization was made, the averages are not strictly absolute yields. It is not clear from the experimental data shown how the high Ce-141 yield was obtained.

c) [Mee 72]: The general statements made in 2.3.3. on how the authors obtained their "updated" yields are also valid here. In particular, the reference yields used in a certain experiment are indicated in the table of original reference data, but the "updated" reference yield does not correspond to the average (or recommended) yield (see table V, mass numbers 141 [Bre 67] and 143 [Har 68a]; some of such errors are, however, corrected in the latest uptake [Mee 74]. This and the comparison of different normalizations in evaluations (table V) suggest that experimental data were adjusted to give

the best overall agreement irrespective of their original reference point. It is possible that the adjustment was changed during subsequent iterations of the computerized fit to give the smallest overall uncertainty.

Original and revised data were raised by ~3% in the light mass peak and lowered by ~4% in the heavy mass peak in order to make the sum of recommended yields 100% in each mass peak, thus causing a 7% change in originally measured relative yields in different mass peaks. On the other hand, this is consistent with the observation made in this work mentioned at the end of subsection 3.4.1.

The assignment of relative errors to experimental data appears to be reasonable. However, since all measurements are only relative (also in [Mee 72]) these errors are too small when data are converted to absolute yields. This is demonstrated by the change of yields in the light mass peak by 7% relative to those in the heavy mass peak, which is opposed by uncertainties as small as 2% (stable Kr and Xe yields cf. table IV).

It is not clear why the data of [Bre 67] are assigned much higher errors than others, as their quoted uncertainties are comparable to those of other authors (cf. section 3.3.2.). Those yields of [Tur 51] which were measured relative to U-235 should be assigned lower uncertainties, as those assigned by the authors [Tur 51] are overall errors including those of the reference yields. Also in [Mee 72] both sets of data [Wyt 64, Wyt 65] are used as well as [Nid 50, Tur 51].

[Mee 74] is an update of [Mee 72] published recently. It is included in tables IV and V, as a comparison with the previous evaluation [Mee 72] and others is interesting, but will not be discussed in detail.

In this new evaluation some normalizations of experimental data are changed considerably (cf. table V). Also the uncertainties of the data are increased, some even drastically (e.g. [Iye 63], Ba-140 and Ce-141 yields from ~4.7% to ~30%). It appears from a few checks of the new evaluation that for some yields "estimated" by evaluators (e.g. [Eng 65, Sid 72, Lam 73]) not only updated values were calculated, but they were even included in weighted averages. This should be further checked but in no case should they be mixed with experimental data. They should even be omitted from the tables.

In the new evaluation the duplication [Wyt 64, Wyt 65] is avoided.

3.4.3. Comparison of evaluations

Different normalizations made in this work are compared in Table IV to the evaluations discussed in the previous subsection. Differences in the general trends of yield values are due to the particular normalization chosen for each set of data, differences in individual relative yields are, in addition, due to the weights (including omissions) assigned by evaluators to experimental data.

The effect of the normalization should be such that the recommended yields in the light mass peak of [Mee 72, Mee 74] should generally be higher than others, as relative yields were increased by 3% to make the sum of yields 100%. "Absolute" yields of Lammer (table IV) should in both mass peaks be comparable to those of Crouch [Cro 73a, b], who used the Mo-99 yield as reference. Other yields evaluated by Lammer (see table IV) should be lower in the light mass peak, as they were obtained by making the sum of yields in the heavy mass peak 100% (see discussion in previous sections). In the heavy mass peak the "absolute" yields and those of [Cro 73] should generally be

Table IV. Comparison of evaluated Th-232 fast fission yields

Uncertainties are given in % in brackets

Mass no.	Lammer			Crouch		Meek and Rider	
	Table II	Lam 73	absol.	Cro 73b	Cro 73a	Mee 72	Mee 74
72	.00034		.00036	.000136(15)		.00027(16)	.00035(16)
73	.00046		.0005	.00035(50)		.00054(32)	.0005(23)
77	.01	.0102	.01	.011(24)		.0126(8)	.0126(8)
83	1.90	1.87	1.98	1.98(9)	2.03(7)	2.14(4)	2.04(2)
84	3.44	3.44	3.62		3.72(7)	3.91(4)	3.72(4)
85	3.74	4.02	3.93		3.95(7)	4.06(2)	3.82(2.8)
86	5.69	5.66	5.97		6.11(7)	6.25(2)	6.09(2.8)
87	6.01	5.99	6.31		6.57(10)	6.81(4)	6.48(4)
88	6.34	6.32	6.66		6.92(10)	7.18(4)	6.85(4)
89	6.43	6.72	6.77	6.96(5)		7.79(8)	7.83(8)
90	7.27	7.40	7.25	7.24(4)	6.99(5)	7.85(4)	7.96(6)
91	6.92	7.26	7.31	5.18(11)		7.33(4)	7.10(4)
93	7.65	7.21	7.41	7.86(15)		7.28(16)	7.75(8)
95	5.41	5.30	5.33	5.30(6)		5.64(8)	5.53(8)
97	4.02	3.96	4.10	4.65(9)		4.38(4)	4.12(2.8)
99	2.74	2.76	2.75	2.78 -	2.78 -	2.85(4)	3.02(6)
103	.153	.146	.155	.15(6)		.0164(4)	.167(6)
105	.04	.05	.07	.072(14)		.040(8)	.036(11)
106	.041	.041	.05	.043(10)		.053(4)	.045(11)
109	.040	.042	.04	.050(7)		.051(8)	.060(16)
111	.04	.045	.06	.054(14)		.078(8)	.085(8)
112	.06	.062	.07	.057(14)		.088(8)	.091(6)
113	.058	.06	.06	.045(7)		.072(8)	.061(23)
115	.057	.057	.06	.050(13)		.063(8)	.088(16)
117	.051	.049	.05	.048(11)		.070(16)	.059(16)
121	.056	.055	.05	.046(15)		.047(8)	.052(8)
123	.032	.031	.03	.027(15)		.044(8)	.036(16)
125	.034	.033	.03	.037(15)		.034(16)	.036(11)
127	.076	.089	.075	.17(15)		.078(4)	.096(8)
131	1.52	1.52	1.60	1.27(22)	1.87(11)	1.58(2)	1.45(2.8)
132	2.69	2.70	2.83	1.76(15)	2.82(7)	2.67(2)	2.66(2)
133	3.75	3.74	3.96		3.75(10)	3.85(4)	3.66(2.8)
134	5.06	5.06	5.32		5.48(7)	5.15(2)	4.87(2.8)
135	4.76	4.65	5.30		4.66(10)	5.07(4)	4.85(4)

Table IV (continued)

Mass no.	Lammer			Crouch		Meek and Rider	
	Table II	Lam 73	absol.	Cro 73b	Cro 73a	Mee 72	Mee 74
136	5.38	5.30	5.65		5.55(7)	5.20(4)	5.12(2.8)
137	4.50	4.44	6.45	4.76(9)	5.92(18)	5.28(4)	7.02(6)
139	6.73	7.38	7.32	7.60(10)	7.00(10)	6.50(4)	6.73(4)
140	8.45	8.31	8.48	7.59(7)	7.72(5)	7.81(4)	7.91(4)
141	7.40	7.28	7.48	7.60(6)	7.26(5)	7.29(4)	7.65(6)
143	7.02	7.12	7.22	6.81(4)	6.79(10)	6.87(4)	6.99(4)
144	7.49	7.66	7.95	7.10(4)	7.98(5)	7.50(4)	8.22(6)
145	5.70	5.78	5.86		5.52(10)	5.37(8)	5.67(4)
146	4.88	4.95	5.02		4.73(10)	4.60(8)	4.85(6)
147	3.13	2.97	3.00	2.96(6)		3.05(8)	3.27(6)
148	2.15	2.18	2.21		2.08(10)	2.02(8)	2.11(6)
149	1.47	1.44	1.48	1.22(30)		1.23(16)	.94(16)
150	1.08	1.09	1.10		1.04(10)	.99(8)	.34(16)
151	.42	.41	.42	.46(15)		.40(16)	.175(16)
153	.21	.21	.24	.22(15)		.19(16)	.032(16)
156	.0026	.0026	.0026	.0029(15)		.0025(16)	.0027(11)

higher than all others, for which the sum of yields is 100%. An inspection of Table IV shows that these general trends can only be observed approximately in the light mass peak. Whereas relative yields, which were originally measured mass-spectrometrically, agree in all evaluations, differences in preferred values at other mass numbers are large enough to influence the whole normalization, particularly in the heavy mass peak.

Table V compares how evaluators have adjusted experimental data. This Table is restricted to measurements discussed in section 3.1. and evaluations shown in Table IV. The mass numbers chosen are those for which several measured yields exist and which are essential for the normalizations obtained by evaluators. The most important observations can be summarized:

a) Comparison of normalizations.

In Meek and Riders evaluations [Mee 72, Mee 74] the data of [Tur 51] (and [Mid 50]) are much higher than in any of the others. The reason for this is not clear. A possible explanation is that the adopted yields to which the data were adjusted in the evaluations [Mee 72, Mee 74] are rather high (e.g. masses 83, 89, 90, 99, 144, see also discussion below) and/or the yields of [Tur 51] particularly low (e.g. masses 131, 140). In any case, the good agreement of the yields measured relative to U-235 thermal fission, which can be readjusted like R-values in evaluations, with other measurements is distorted in this normalization. This suggests that the "R-value type" data of [Tur 51] should be treated separatly from the others.

Table V. Comparison of different adjustments of experimental Th-232 fast yield data by evaluators

(Reference yields quoted by evaluators are underlined; "nu" and values shown in brackets were not used for obtaining the "final" value)

Mass no.	Eval.	a) Ken57	Har68a	Har68b	Iye63	Myt64	Myt65	Dre67	Mid50	Tur51	Cro63	Final
90	Mee73				7.97	7.41	7.39		7.88	7.30	8.73	7.85
	Cro73a					6.99						6.99
	Cro73b				?7.46		7.01		6.18	7.24	7.55	7.24
	Table II				7.53		7.01			(7.19)	(9.36)	7.27
	absolute				7.45		7.04			(7.57)	(9.39)	7.25
	Mee74				8.20		7.63		7.26	7.19	8.66	7.96
91	Mee72		7.14		7.00				7.62	8.38	(nu)	7.33
	Cro73a											-
	Cro73b				6.81				5.97	7.34	4.44	5.18
	Table II		6.97		6.88					6.92	(5.40)	6.92
	absolute		7.32		(6.81)					7.29	(5.42)	7.31
	Mee74		7.00		7.45				7.48	(nu)	(nu)	7.10
131	Mee72	1.49	1.29		1.51	2.11	2.10		(nu)	1.45		1.58
	Cro73a	1.62	1.56			2.13						1.87
	Cro73b				1.57		2.14		0.68	1.18		1.27
	Table II	1.52	(1.36)		(1.63)		(2.19)			(1.24)		1.52
	absolute	1.60	(1.43)		1.61		(2.20)			(1.30)		1.60
	Mee74	1.45	1.34		1.70		(nu)		(nu)	1.40		1.45
137	Mee72	4.83			4.40	6.50	6.50		7.24	7.08		5.28
	Cro73a	4.60				6.59						5.92
	Cro73a				4.50		6.59		6.07	6.44		4.76
	Table II	4.50			4.50		(6.42)			(6.11)		4.50
	absolute	(4.73)			(4.45)		6.46			6.44		6.45
	Mee74				(nu)		7.12		7.53	7.36		7.02
140	Mee72				8.23	7.63	7.62	7.97	6.86	6.93	7.07	7.81
	Cro73a					7.72						7.72
	Cro73b				8.38		7.73	8.67	5.67	6.14	6.94	7.59
	Table II				8.45		8.45	8.45		(6.40)	8.45	8.45
	absolute				8.36		8.49	8.54		(6.75)	8.48	8.48
	Mee74				9.04		8.35	8.65	7.15	7.22	7.67	7.91
141	Mee72				7.51	7.16	7.17	6.64	7.49	10.06	7.13	7.29
	Cro73a					7.26						7.26
	Cro73b				7.38		7.26	7.60	6.28	8.69	6.59	7.60
	Table II				7.59		7.42	7.41		(9.30)	(7.87)	7.50
	absolute				7.51		7.45	7.48		(9.80)	(7.90)	7.48
	Mee74				8.24		7.84	7.37	7.79	(nu)	7.49	7.65
143	Mee72	6.33	6.32		7.05			6.56			7.13	6.87
	Cro73a		6.79									6.79
	Cro73b				?7.02			7.12			6.59	6.81
	Table II	7.02	6.90		7.16			6.94			(8.21)	7.02
	absolute	7.22	7.25		7.09			7.31			(8.24)	7.22
	Mee74	6.86	(6.68)		7.78			7.15				6.99

Table V (continued)

Mass no.	Eval. a)	Ken57 Mar68a Mar68b	Mye63	Wyt64	Wyt65	Dre67	Mid50	Tur51	Cro63	Final
144	Mee72		7.01	7.88	7.88	7.50	7.74	7.93	7.80	7.50
	Cro73a			7.98						7.98
	Cro73b		6.98		7.98	8.14	6.49	6.93	7.15	7.10
	Table II		7.09		7.85	7.94		(7.33)	(9.03)	7.49
	absolute		(7.02)		7.89	8.01		(7.73)	(9.06)	7.95
	Mee74		7.69		8.62	8.16	8.05	8.26	8.19	8.22

a) [Mee 72, Mee 74] "updated" values are shown.

"Table II": The "final" values of Table II are shown in the last column. These were obtained by multiplying the "average" yields of Table II by the factor 1.056. In order to allow a better comparison with the other evaluations, all experimental data shown in Table II are multiplied by the same factor for this table.

It can generally be observed that the normalizations of Crouch and Lammer are rather similar and different from those of Meek and Rider. The data of [Wyt 65] are corrected for β- and γ-ray intensities in this work (Table II and "absolute") and therefore the adjusted values differ from those of other evaluators, but the agreement with other measurements is improved. The normalizations of the measurements of [Cro 63] differ considerably.

b) Comparison of recommended yields:

In the evaluations [Cro 73, Mee 72, Mee 74] recommended yields were obtained from weighted averages, as discussed in 3.4.2. In the present work the reliability of the data was judged from the experimental method employed and the overall agreement, generally a simple average was calculated and discrepant data omitted. These different methods are reflected by a comparison of adjusted experimental data and "final" yields in Table V. In the case of [Mee 74] the selection and averaging is not so obvious because additional data sets not shown in Table V were used, possible also estimates (see subsection 3.4.2.).

The high Sr-89 yields of [Mee 72, Mee 74] (see Table IV) are due to the normalization of the data of [Cro 63, Tur 51, Mid 50]. Higher values obtained in these evaluations for other yields in the light mass peak are due to their final normalization to make the sum of yields total 100%. The influence of the high weight given to the data of [Cro 63] by Crouch is reflected by the final mass 91 yield.

In the heavy mass peak mass spectrometric data were preferred in the evaluations "Table II", "absolute" and [Mee 74], in the latter this is done only effectively by assigning a much smaller error to these data.

Mass 131: The higher weight assigned to [Wyt 64] in [Cro 73a] is reflected by the average. In the case of [Cro 73b] the low average is due to the fact that Crouch has assigned a 15% error to the extremely low value of [Mid 50] (who quote no error) which is opposed to a 50% uncertainty for [Tur 51]

(as given by the authors). Similar observations can be made for Cs-137 except for the strong influence of the low yield measured by [Iye 63].

The high Ba-140 yield evaluated in this work is due to the correction of the [Wyt 65] measurements and the omission of other data. In the other evaluations the rather high weight given to the measurements of [Cro 63], which were discarded altogether in this work as being completely out of the range of other values, has a noticeable effect on the final value. The same is true for the Ce-141 yield (except [Cro 73b]: see 3.4.2.), and mass 143 in the case of [Cro 73b]. The final mass 143 yield obtained in [Mee 72, Mee 74] is determined by the mass-spectrometric data and it is not clear how they were adjusted in these evaluations.

The lower Ce-144 yield of [Cro 73b] is due to the high weight assigned to the R-value measurement of [Iye 63]. The comparison of individual data adjusted by [Cro 73b] and [Mee 74] is a good illustration how agreement among experimental data is influenced by the particular normalizations chosen.

3.4.4. Uncertainties

In [Lam 73] no uncertainties were assigned to individual yields, but a minimum of 5% was estimated to be due to the final normalization. The evaluation procedure outlined in 3.3. did not allow to calculate a variance of the mean obtained, as experimental data were not weighted by the reverse of the squares of their errors. Errors quoted by measures are generally standard deviations and lack of time did not allow to analyze experimental results in detail and estimate overall uncertainties as discussed in section 3.3. In addition it was felt that the absence of absolute yield measurements and the rather arbitrary adjustment of relative yields do not allow a reliable assignment of uncertainties to individual yields. These arguments have now been confirmed by the other new evaluations discussed above, as Table V shows. On the other hand, this comparison allows a better estimate of the uncertainty introduced by the normalization.

As in the case of U-238 fast fission we shall discuss the uncertainties of those yields in more detail that are either used in fuel analysis (burnup) or which are commonly used as reference yields. Since we are essentially dealing with relative yields we shall estimate their accuracy first and then add an error for conversion to absolute yields. Individual estimates are presented in Table VI.

Column P of Table VI lists the precision obtained in the measurements discussed in section 3.1. (see also 3.3.2.), expressed as 1 standard deviation. This is the average of the most accurate measurements generally (Iye 63, Bre 67, Wyt 65]. The precision is combined with an uncertainty of 2 - 4% to obtain the overall experimental accuracy, listed in column A of Table VI. This additional uncertainty accounts for calibration, corrections, nuclear data, etc., and is taken to be about 2% if mass spectrometry or an R-value or different independent methods are involved, and about 3 - 4% for more recent radiochemical measurements, but in no case was A allowed to be less than 3%. It has to be kept in mind that the accuracy A represents the capability of the experiments discussed but does not include a comparison of the actual results. The latter depends on how sets of measured relative yields are adjusted to one another. For this purpose the different adjustments as presented in Table V (and Table II) were used and standard deviations of the unweighted average calculated. These turned out to be similar for all evaluations and typical values are shown in column avg of Table VI, which should reflect the agreement among experimental data. Column "rel"

Table VI. Uncertainties (%) of Th-232 fast yields[a)]

Mass no.	relative P	A	avg	rel	eval	total
95	6	7	2	7	2.3	11
99	2	3	-	3	4	7
103	5	6	2	6	5	10
106	5	6	12	20	10	25
133	2	3	3(10)	3(15)	3	6-20
137	1(3)	3(5)	10	20(5)	16	9-25
140	1.5	3	0.6(7)	3(7)	4.4	7-12
143	2	4	3	4	2.1	8
144	3	5	4	5	5	9

a) All uncertainties are relative (%)

P .... experimental precision (1 standard deviation)
A .... experimental overall accuracy
avg .. standard deviation of a simple mean of experimental data
rel .. assigned overall uncertainty of relative yields
eval . average deviation of evaluated yields from the mean
total ... estimated total uncertainty of absolute yields

lists the estimated uncertainty of presently available relative yield data, which corresponds generally to the larger of errors "A" and "avg". There are a few exceptions:

- If a mass 133 yield is derived from the higher Cs-137 yield [Wyt 65, Tur 51] using relative mass-spectrometric Cs yields [Har 68], it disagrees with other mass 133 yields obtained relative to Xe-yields. The uncertainties due to this discrepancy are shown in brackets.

- The uncertainties shown for Cs-137 are derived from the inclusion of the mass-spectrometric measurements and that of [Iye 63]. If we exclude these low values, then the uncertainties shown in brackets (confirmed by [Mud 73]) would be applicable.

- In the case of mass 140 there was no agreement among evaluations. The lower uncertainty was derived from "absolute" in Table V, the higher (shown in bracktes) from [Cro 73b].

- If discrepancies exceed experimental errors by far, a standard deviation is no more a good estimate of the uncertainty. Therefore the uncertainty in column rel is increased and corresponds approximately to the average deviation of individual values from the mean.

The uncertainty due to the conversion of relative to absolute yields is unknown, but can be estimated in two different ways. Meek and Rider [Mee 72] and Lammer ('absolute') have tried to derive absolute yields from experimental data and have observed deviations of 3% and 4% respectively 3% and 5% in the sum of yields in the light and heavy mass peak from 100%. (Crouch has not compared the sum of his yields to 100% and in [Mee 74] the adjustments obtained finally in [Mee 72] were used.) From this we may conclude that the uncertainty due to the final normalization is about 3 - 5%. As another approach we may compare the final values of different evaluators. The average deviation of individual evaluated data from the mean (a standard deviation of the mean itself is meaningless in this case) is shown in column "eval" of Table VI. [Lam 73] was not used for this comparison, as the data are similar to those in Table II. These average deviations are about 2 - 5% in agreement with the first estimate of 3 - 5%, except for those mass numbers where discrepancies exist already among experimental data.

The uncertainty due to the final normalization has to be added to the uncertainty of relative yields as the normalization is not independent of relative yields and causes a shift in one direction. An average of 4% is added to each of the estimated uncertainties of relative yields and the estimated total uncertainty of absolute yields is shown in the last column of Table VI. A range is given if 2 uncertainties of relative yields were estimated.

Relative Nd yields have an accuracy of 1.4%, 3%, 1.4% and 8% for mass numbers 145, 146, 148 and 150 respectively [Mar 68a]. Absolute Nd yields depend on the accuracy of the mass 143 yield. Their overall uncertainties are 8% for masses 143, 145 and 148, 9% for Nd-146 and 11% for Nd-150 (errors combined quadratically in this case).

Other yields:

- Absolute yields of stable Kr and Xe have an accuracy of about 5% (from [Kon 57]), unstable Kr-87, 88 and Xe-133 (see also above) about 6% accordingly.

- Other absolute yields in the peak regions should have an accuracy of about 8 - 20%. It should be noted that discrepancies up to about a factor of 2 exist among measured mass 131 yields, but the mass-spectrometric data are considered more reliable by all evaluators in this case.

- Yields in the valley region are based mainly on R-value measurements. Here the U-235 reference yields have an uncertainty of ~10% for experimental data, and about 20 - 30% for interpolated yields (masses 113, 117, 119). Variation of these yields with neutron energy has to be checked.

- Yields at the light wing below mass 83 are scarce. Measured yields in the heavy wing at mass 148 and below show two different trends: [Rye 63] on the one hand and [Mar 68a, Bre 67] on the other hand. Although not very likely, these differences could be due to differences in the neutron spectrum. This effect should be further investigated.

Presently the accuracy of Th-232 fast fission yields is limited by the large uncertainty of the conversion of relative to absolute yields. Reliable measurements of absolute yields, particularly at reference points, with sufficiently high accuracy should reduce this uncertainty considerably.

Uncertainties of relative yields could be reduced and combined woth those of absolute yields in quadrature. Thus uncertainties of presently 7-9% could be reduced to about 3 - 4% without additional relative yield measurements.

3.5. Future work

3.5.1. Suitable techniques

These are essentially the same as mentioned for U-238 fast yields. In addition it might be stated that gamma-spectrometric techniques as used by [Wyt 65] and [Dre 67] are more suitable especially for measurements of Zr-95, Ru-103, Ru-106, Ce-141, Ce-144 and other fission products for which daughter products have to be taken into account or which involve decay curve analysis in β-spectrometry. Possible systematic errors in chemical separations are the same as in β-spectrometry.

3.5.2. Further measurements required

The recommendations for further measurements are similar to those for U-235 fast fission yields. First of all, measurements of absolute yields are needed. Suitable fission products are Sr-90, Zr-95, Mo-99, I-131, Cs-137, Ba-140, Ce-141 and Ce-144, or Nd-isotopes if mass-spectrometry is employed. These proposals include the redetermination of the ratio of yields in the light mass peak to those in the heavy mass peak and a check of yields in the mass range 140 - 144 relative to others.

A fairly large number of reasonably accurate measurements of relative yields already exists. It can be hoped that the proposed future measurements help to select among these data, resolve the inconsistencies and clarify the uncertainties associated presently with normalization points.

As for U-238, the change of yields with incident neutron energy or neutron spectrum should be studied.

3.5.3. Evaluation work

In this evaluation the data of [Pro 63] were corrected for half-life and those of [Wyt 65] for γ-ray abundance. Both corrections were not successful in resolving the most serious discrepancies, although in the case of [Wyt 65] the agreement with other data could be improved for some yields.

Evaluation work should aim at the proposal put forward in section 2.4.3. In particular, the causes of the discrepancies should be investigated, but further experimental work should be awaited in view of the unclear situation.

4. Final remarks

This contribution in its present form has been extended and revised in 1974. It therefore contains information not included in the original contribution sent to J.A. Cuninghame.

This original contribution was done rather hastily and therefore incomplete and unsatisfactory. It was followed by letters with further comments, corrections and additions (e.g. the inclusion of [Mob 71] in the U-238 survey and its consequences). Since the style was not suitable for publication, the whole contribution was revised to include all additional information and, as a consequence of more thorough work, normalizations and evalua-

tions are now studied in more detail. It will be noted by the reader that references published in 1974 are included for completeness, if they contain important information, whereas evaluations not dealt with in Review Paper 11b are omitted here. Therefore it should be noted that important information contained in this paper was not available at the time of preparation of Review Paper 11b (e.g. estimates of uncertainties, normalizations other than those in Table II, discussion of [Lee 72, Lee 74]).

Just now I became aware of a recent publication on absolute Th-232 fast fission yields (J.R. Deen, F.C. Draper Jr., Trans. Am. Nucl. Soc. 17 (Nov. 1973) 531). The results cause more confusion than adding to a clarification among the data discussed in chapter 3. I have a few reservations about the measurement method, but the description given is too brief. More detailed information on data used and corrections applied is necessary to allow more definite conclusions.

Great care is required in the design of future measurements, calibration and data analysis, if the results are to clarify the present situation in both Th-232 and U-238 fast fission yields. Also the discussion of whether discrepancies can be explained by different neutron spectra should be settled by a measurement of this effect for various mass numbers, neutron energies and neutron spectra in one experiment, or several coordinated experiments.

References

Bon 60 E.K. Bonyushkin et al, AEC-tr-4682 (1960)

Bre 67 L. Bresesti et al, J. inorg. nucl. Chem. 29 (1967) 1189

Bun 58 L.A. Bunney et al, 2nd Int. Conf. PUAE, Geneva 1958, Vol. 15, p. 449

Ciu 68 L. Ciufollotti, Energia Nucleare 15 (1968) 272

Cro 63 J.E. Crook and A.P. Voight, IS-558 (1963)

Cro 73a E.A.C. Crouch, U.K. Rep. AERE-R-7394 (1973)

Cro 73b E.A.C. Crouch, IAEA Symposium on Nuclear Data in Science and Technology, Paris, March 1973, proceedings Vol. I, p. 393

Cun 72 J.G. Cuninghame et al, AERE-6862 (Rev) (1972)

Deb 73 K. Debertin, private communication, May 1973 paper sumbitted to Radiochim. Acta.

Die 71 M. Dierckx et al, J. Nucl. Sn. 25 (1971) 85

Ede 73 O.J. Eder and H. Lammer, IAEA Symposium on Nuclear Data in Science and Technology, Paris, March 1973, proceedings Vol. I, p. 233

Eng 51 D.W. Engelkemeir et al, paper 318 in "Radiochemical Studies: The Fission Products" (C.D. Coryell, N. Sugarman, Eds.), N.N.E.S., Div. IV, Vol. 9, Part 4, Book 3, p. 1375
and: ANL-4927 (1952)

Eng 65 T.R. England, WAPD-TM-333, Add. no. 1 (Jan. 1965)

Far 62 H. Farrar and A.H. Tomlinson, Nucl. Phys. 34 (1962) 367

Fud 73 A.J. Fudge (Harwell, UK) during Panel discussion, results quoted as private communication in [Lee 74]

Har 68 J.W. Harvey et al, Can. J. Chem. 46 (1968) 2911
a) mass spectrometric measurements
b) Ge(Li) Q-values

Iye 63 R.H. Iyer et al, J. inorg. nucl. Chem. 25 (1963) 465

Kel 54 R.W. Keller et al, Phys. Rev. 94 (1954) 969

Ken 57 T.J. Kennett and H.G. Thode, Can. J. Phys. 35 (1957) 969

Kob 70 K. Kobayashi and I. Kimura, EANDC(J)-19L, p. 37
and annual reports KURRI-3 (1970) 84

Lam 73 H. Lammer and G.J. Eder, IAEA Symposium on Nuclear Data in Science and Technology, Paris, March 1973, proceedings Vol. I, p. 505

Lam 73a H. Lammer, contribution to Review Paper 12, these Panel proceedings

Lam 73b H. Lammer, informal contribution to Review Paper 11a (W.H. Walker), this Panel.

Lar 72 R.P. Larsen et al, Trans. Am. Nucl. Soc. 15 (1972) 483

Lar 74 R.P. Larsen et al, Nucl. Sci. Engg. 54 (1974) 263

Lev 61 H.B. Levy et al, Phys. Rev. 124 (1961) 544

Lis 70 F.L. Lisman et al, Nucl. Sci. Engg. 42 (1970) 191

Man 72 F. Manero and V. Konshin, At. En. Review 10 (1972) 637

Mat 64 C.K. Mathews, Ph.D. Thesis, McMaster University, Hamilton, Ontario, Canada

Mat 72 C.K. Mathews and R.H. Tomlinson, Can. J. Phys. 50 (1972) 3100

Mee 72 M.E. Meek and B.F. Rider, USAEC report NEDO-12154 (Jan. 1972)

Mee 74 M.E. Meek and B.F. Rider, NEDO-12154-1 (Jan. 1974)

Mid 50 J.B. Miday and A. Turkevich, AECD-2862 (1950),
see also App. B, loc. cit. ref. [Eng 51]

Pet 60 K.A. Petrzhak et al, AEC-tr-4696 (1960)

Rid 67 B.F. Rider et al, USAEC report GEAP-5505 (1967) 21

Rob 71 M. Robin et al, Proc. Int. Conf. on Chemical Nuclear Data, Canterbury (UK), 1971, p. 19

Sid 72 E.W. Sidebotham, UKAEA Rep. TRG-2143(R) (1972)

Tur 51 A. Turkevich and J.B. Miday, Phys. Rev. 84 (1951) 52

Wal 73 W.H. Walker
a) Review Paper 11a, this Panel
b) Proc. IAEA Symposium on Nuclear Data in Science and Technology, Paris, March 1973, Vol. I, p. 459
c) AECL-3037/Part II (1973)

Wan 55 R.K. Wanless and H.G. Thode, Can. J. Phys. 33 (1955) 541

Wyt 64 A. Wyttenbach et al, Radiochim. Acta 3 (1964) 118

Wyt 65 A. Wyttenbach and H.R. von Gunten, IAEA Symposium on Physics and Chemistry of Fission, Salzburg, 1965, Vol. 1, p. 414

COMPILATION OF FISSION PRODUCT YIELDS OF U-238 FOR 14 MeV NEUTRONS

S. Daróczy, P. Raics, S. Nagy
Institute of Exp. Phys. Kossuth Univ., Debrecen, Hungary

Abstract:

Measured cumulative yields from the 14-15 MeV neutron induced fission of U-238 have been collected, corrected and recommended values are proposed /also for masses without any published experimental data, by interpolation/. The available independent and fractional cumulative yields are presented too.

1. Present status of the U-238 14 MeV neutron fission yield compilations

There are some new careful compilations of fission product yields for various fissile nuclides, e.g. [1, 2, 3] , but the situation is quite different for the 14 MeV neutron fission of U-238.

Katcoff, 1960 [4] : Generally available recommendation containing the largest number of data up to now. The original data and errors have not been given. This compilation includes experimental data up to 1960.

Gunten, 1969 [5] : Only recommended values have been presented for a limited number of masses, without error quotation.

Meek and Rider, 1968 [6] : Not generally available compilation. It is known for us only from references.

Zysin et al, 1963 [7] and Greshilov et al, 1969 [8] : Only collections of measured data without recommendations.

2. Collection of experimental data

We did our best to collect 14 MeV neutron fission yields of U-238 published up to now, but are not sure whether we have not missed the one or other work. In particular, laboratory reports or preprints have not been available to us at all.

We have collected yield data measured in the neutron energy range of 14 - 15 MeV. The published neutron energies and their uncertainties /if they have been quoted/ are listed together with the references.

In addition to our recently published yields [Da73] we have taken some preliminary results of our new measurement [Da73a] in some critical cases.

3. Treatment of the measured yiels

All measured yields, for which a literature value was used for normalisation, were treated as relative ones.

All absolute measurements /employing fission chambers or flux monitor foils/ included a determination of either the Mo-99 yield or the Ba-140 yield or both. In order to take into account all absolute measurements, we have first evaluated the Mo-99:Ba-140 yield ratio by averaging all available data /Table I/. Using this ratio, we have then evaluated the absolute yields of Mo-99 and Ba 140 /Table II/. These absolute yields were used to normalise the other measurements wherever possible. These "new" cumulative yields have been converted into absolute chain yields according to Nethaway [Ne72] . The original measured and the "new" cumulative yields as well as the recommended chain yields for mass numbers between 66 and 172 are presented in Table III.

Table IV contains a collection of the measured independent and fractional cumulative yields without recommendations because generally single measurements are only available for each investigated fragment.

4. Comments to the Tables

Data which severely disagree with others or data that are considered as being unreliable are marked with a " + " sign in the tables and not included in the average. We have assumed that the errors quoted by authors correspond to one standard deviation (68.3 % confidence level).

Both the simple /A/ and the weighted averages /WA/ were calculated with their standard error in all possible cases as followes:

$$A = \frac{\sum_{i=1}^{N} Y_i}{N}, \qquad \Delta A = \left[\frac{\sum_{i=1}^{N}(Y_i - A)^2}{N\cdot(N-1)}\right]^{1/2}$$

$$WA = \frac{\sum_{i=1}^{N} Y_i/(\Delta Y_i)^2}{\sum_{i=1}^{N} 1/(\Delta Y_i)^2}, \qquad \Delta WA = \left[\frac{1}{\sum_{i=1}^{N} 1/(\Delta Y_i)^2}\right]^{1/2}$$

where Y_i and ΔY_i are the measured yields and their standard errors respectively. The same errors were accepted for the recommended chain yields although their physical meaning is very questionable. All errors are written after the values for the last figures, e.g. 0,625 12 means 0.625 ± 0.012. If the yields are less than 0.001 % an abbreviated normal format is used, e.g. /8.5 9/-5 stands for $/8.5 \pm 0.9/\cdot 10^{-5}$%.

Abbreviations used for the experimental methods:

a./ General methods

RC - measurement with radiochemical separation

MS - mass spectrometry /including also on-line methods/

DG - direct GeLi gamma spectrometry of the irradiated sample without any chemical separation or using recoil effect

DGR - as DG without GeLi efficiency calibration using the so called R-method /relative to the same fragment in the U-235 thermal neutron fission/.

b./ Detection techniques in the RC method

be - simple beta counting with end-window GM-tube or not mentioned clearly in the original paper

2be - beta counting with 2π gas flow proportional counter

4be - beta counting with 4π gas flow proportional counter

ga - NaI/Tl/ gamma spectrometry

Ge - GeLi gamma spectrometry.

c./ Absolutisation methods

FC - absolute counting of the fission events with a fission chamber

Al - neutron flux measured by the Al^{27}/n,alpha/ monitor reaction using literature cross sections for monitor and fission reactions

Cu - same as Al but using Cu^{65}/n,2n/ monitor reaction

R - R-method /see above/.

When the method was not mentioned clearly in the original article or the latter was not available for us the method is marked with " ? " sign.

Corrections on the measured yields were carried out using the following accepted data:

- the cross sections for the monitor reactions at different energies by the compilation of Kanda and Nakasima [9] ;
- the U-235 thermal neutron fission yields of Wahl [1] were used for the R-method,
- the U-238 fission cross sections at different neutron energies by Pitterle's new data [10].

In the choice of Pitterle's new U-238 neutron fission cross sections we have been influenced by their freshness although there are other references /[15], [Ne69,72], Pitterle's old curve, etc/ giving values higher by 4-7 %.

As original articles did not contain sufficient information on half-lives, beta or gamma ray energies and intensities, conversion coefficients etc. used in the data analysis, it was not possible to correct published yields using recent data.

No corrections have been applied for delayed neutrons.

4.1. Special comments to Table I

a./ All measurements containing both the Mo-99 and Ba-140 cumulative yields are listed.

b./ In columns 3 and 4 the original data are presented, while column 5 contains the ratios. The measurement of [Go68] was corrected for U-235 thermal fission reference yields using the recommended data of [1] which are accepted by us. The corrected values are given in columns 3 and 4 in brackets.

c./ In column 6 only the errors are changed in some cases. At the measurement of [Pr58] and [Ja64] the originally quoted errors seemed to be too small as to the applied technique. Because the original paper of [Am58] was not available for us and the values cited by [Br62] did not contain errors and the details of the experimental technique we accepted a 10 % relative error to each yield.

4.2. Special comments to Table II

a./ In this table there are absolute Mo-99 and Ba-140 yields. If both of these had been measured in a work only that one was taken into account which seemed to be more reliable.

b./ Column 4 contains the original absolute yields while in column 5 the corrected values and the revised errors are given. The reason for the error revision is similar to that mentioned in 4.1.c. In [Ga66] no data are given on the conversion of relative to absolute yields and therefore the yields could not be readjusted. Therefore the error was increased by a 10 % relative systematic error.

c./ Column 6 shows apart from measured absolute Mo-99 yields also Mo-99 yields converted from absolute Ba-140 yields with the aid of the accepted ratio of Table I. Both types of Mo-99 yields were used for calculating the average. The recommended absolute Ba-140 yield was obtained from the Mo-99 yield and the Mo-99:Ba-140 yield ratio of Table I.

d./ The errors of the recommended absolute yields contain also a 4 % relative systematical error because of the Al^{27}/n,alpha/ reaction cross section predominantly used for absolutisation.

4.3. Special comments to Table III

a./ In column 1 the mass number is underlined when measured yields have been available. If the measurements refer to a metastable /m/ or ground /g/ state or both /mg/ it is noted in column 2. In some cases there is no indication for m or g states in the papers although their presence is clear from the decay schemes [11], e.g. Br-84, Pd-111, Ag-111, Ag-115 in [Ja64] , Ag-113 in all works, Cd-115 in [Am58] and [Co70] , Xe-135 in all works. These cases are not indicated in column 2 except for Cd-115 and A=113 where the special note " 47Ag5h " refers to the 5.3 h half-life state.

Sometimes the authors' element notation for the measured yield did not seem to be quite adequate. These are revised by us : [Co70] notes Gd-156 instead of /io/ Eu-156, Sm-147 io Pr-147, Eu-153 io Sm-153 and La-140 io Ba-140; [Bl71] notes I-132 io Te-132, La-140 io Ba-140 and Ce-142 io La-142; [Go68] notes Y-91 io Sr-91 and I-132 io Te-132.

b./ Column 5 contains the original measured data /generally cumulative yields in % or relative values/. The R-measurement of [Go68] have been corrected for the accepted U-235 thermal fission yields with their error [1] and put into brackets. The normalisations refer to these data. [Bq72] published relative cumulative yields. Line noted with " chain " gives relative chain yields corrected by the author himself using measured fractional cumulative yields of [Wo65]. Our normalisation refers to these chain yields.

Column 6 and 7 contain data normalised to the recommended Mo-99 and Ba-140 absolute yields if these nuclides have been measured. In column 8 there is the average of these normalised yields or the only available one. If neither Mo-99 nor Ba-140 have been investigated in a work the normalisation was carried out to the recommended value of an appropriate mass number /noted with "=" /. [Fo65] have measured relatively few masses which did not give possibility for normalisation. Its original absolute yields were accepted with addition of a 10 % relative systematical error. As mentioned before /see 4.1./ there is no error quotation in [Am58] that is why a 10 % relative systematical error is added to its data. There is no other error revision in this table. If in an article an unreasonable small error was quoted the simple rather than the weighted average is accepted as recommendation at a given mass.

If the fractional cumulative yield of the measured element is not 100 % the average value in column 8 is put into brackets and the chain yield corrected by the Nethaway-method [Ne72] is given below it.

Column 9 gives the recommended chain yield in %. If this value is accepted from one experiment or from the average /A or WA/ of more, it is underlined. At mass numbers experimentally not investigated an exponential interpolation was made and is shown without error and underlining. If it is clear that the authors have measured the yield at a given mass for the m or g state only the recommended value is a lower limit for the chain yield and is denoted by a " " sign.

a./ At the mass number 102 none of the experimental data were accepted because of their unreliability. The situation is quite different for the mass number 129 : although all yields are very close together and seem to be reliable but they do not fit to the trend of the mass distribution curve in this region. It may be caused by the presence of an unknown metastable state. Interpolated yields are recommended for these two cases.

d./ All iodine yields of Br62 had been evaluated from a complex beta decay curve and some of them are far from the other authors' data. Therefore all these yields were omitted.

e./ Using 117.68 for the centre of the mass distribution, as obtained by [Ne69], we get the following sums of recommended chain yields:

for the light mass region from A=66 to A=117	
measured chain yields	64.52 %
interpolated	35.95 %
total	100.47 % ;
for the heavy mass region from A=118 to A=172	
measured chain yields	75.05 %
interpolated	21.48 %
total	96.53 % ;
for the entire mass region from A=66 to A=172	
measured chain yields	139.57 %
interpolated	57.43 %
total	197.00 % .

Taking into account the 4.5 % relative error of the absolutisation /see Table II/ the sum of the yields of the heavy and light fragments seems to be satisfactory. More accurate experimental yields and measurements for the interpolated masses would be necessary for renormalisation.

f./ The recommended chain yields versus mass number are shown on a lin - lin as well as on a log - lin plot.

4.4. Special comments to Table IV

a./ This table is only a collection of the experimental independent and fractional cumulative yields. Key for the abbreviations used :

IY - independent yield
FIY - fractional independent yield
FCY - fractional cumulative yield.

b./ Column 5, 6 and 7 contain the measured yields generally in per cent, data of [Bq72] are relative ones.

c./ An attempt was made by us also to calculate the measured yields using Nethaway's empirical rule [Ne72], Umezawa's proce-

dure generally recommended for medium energy fission [12] and a method based on Bocquet's experimental results [Bq72].

This last method applies an experimentally determined $|\Delta Z| = Z_p - Z_{UCD} = 0.32 \pm 0.10$ value [Bq72] generally accepted by us for the asymmetric region only and Wahl's charge dispersion of 0.56 ± 0.06 [1]. Z_{UCD} was calculated using an average value of 4.4 fission neutrons [13] from which 0.75 are prefission ones [14] in the U-238 14 MeV neutron fission. The post fission neutrons were assumed to be equally distributed between the complementary products.

Either Nethaway's method or that of mentioned at last gives practically the same results in good agreement with the measured yields. To distinguish between them is not possible because of the present status of the experiments. At the same time Umezawa's method generally does not give reasonable results for light fragments. It seems to be caused presumably by the low excitation of the compound nucleus in 14 MeV neutron bombardment.

Since all methods use roughly the same charge dispersion the difference between them arises mainly from their predicted Z_p values. That is why only these most probable charge values are given in column 8, 9 and 10.

5. General conclusions and remarks

a./ As it can be clearly seen the mass distribution has an appreciable structure in the heavy region. It is interesting to note that this structure is very similar to that of the thermal neutron induced fission of U-235 where pronounced maxima occur at masses 134, 138, and 142.

At the moment, evidence for structure at the light peak may neither be declared nor rejected because of the lack or the uncertainty of the experimental data for critical masses, e.g. 94, 96, 98, 100, 101, 102. The deviation from the smooth curve at masses 84 and 86 is quite remarkable and is due presumably to the 50 and 52 neutron numbers.

The structures mentioned above would not disappear even applying delayed neutron corrections.

The presence of the fragment shell effects in the mass distribution even at 20 MeV excitation energy is interesting

from the point of view of the nuclear fission theory. Therefore each measurement even in the peak regions are of great importance in the future.

On the basis of these considerations reflecting the measured yields /"mirror points"/ and smoothing the mass distribution is not quite correct.

b./ The average yields for the peaks /including masses 99, 100, 101, 133, 134, 135, 136/ is 5.85 ± 0.1 %, and that of the valley /including masses 115, 121/ is 0.83 ± 0.02 %. The peak-to-valley ratio is then 7.05 ± 0.21 being a little greater than 6.8 coming from a smoothed plot of the mass-yield curve [Ne72].

The lack of the experimental yields requires new measurements particularly in the symmetric region.

c./ The center of the mass distribution was calculated as

$$A_0 = \left(\sum_{A=66}^{132} Y_A \cdot A \right) \Big/ \left(\sum_{A=66}^{132} Y_A \right)$$

where Y_A is the recommended chain yield for the mass A /from Table III/. It gives A_0=116.97 . This value is less than the true one because of the difference between the light and heavy peak normalisations /see 4.3.e/. Applying an appropriate correction we have A_0=117.36 ± 0.15 . The average number of neutrons emitted per fission can be calculated from A_0, and is 4.3 ± 0.2 . Calculating the weighted center of the light and heavy peaks similar to that mentioned above /summing to-from 117.36 / we have $\bar{A}_L$ = 97.98 ± 0.10 and $\bar{A}_H$ = 136.62 ± 0.10 respectively. It gives 4.40 ± 0.15 for the average number of neutrons emitted per fission. These are in good agreement with each other as well as with the direct measurements [13].

It is interesting to note that our center value is lower than that of Nethaway's 117.68 ± 0.09 [Ne69] which have been calculated from the low yield fragments on the wings. This difference can be explained by the assumption that the neutron emission curve for 14 MeV neutron induced fission of U-238 has also a "saw-tooth" shape similar to that wellknown in the low energy fission.

d./ In the asymmetric regions Nethaway's method [Ne72] may be recommended to calculate the most probable charge, Z_p, for a given mass as well as the independent or fractional cumulative yields using Wahl's dispersion value of 0.56 ± 0.06 [1]. The unchanged charge distribution assumption may be applied for calculation in the symmetric region where the former value of the charge dispersion may also be used. It is a pity that there are no measured independent or fractional cumulative yields here.

e./ The full width at half maximum of the heavy and light peaks is about 5 % greater than that of the thermal neutron fission of U-235. This can be connected to the many-chance fission processes.

f./ The general requirement for the future is to make new measurements /rather than such compilations/ in the entire fragment mass region applying the full arsenal of the nuclear physicists' and radiochemists' fantasy and experimental methods.

References

[Te53] J.Terrel, W.E.Scott, J.S.Gilmore, C.D.Minkkinen, Phys.Rev., 92, 1091 /1953/; 14 MeV.

[Bo55] Е.К.Бонштин, Ю.С.Замятин, И.С.Кирин, Н.П.Мартынов, Е.А. Скворцов, В.Н.Ушатский, Нейтронная Физика (сб. статей под редакцией П.А.Крупчицкого), 224, ГОСАТОМИЗДАТ, Москва, 1961; 14.5 Мэв.

[Fo56] G.P.Ford, J.S.Gilmore, Ref.5. in Ref. [Wo65].

[Cu57] J.G.Cuninghame, J.Inorg.Nucl.Chem., 5, 1 /1957/; 14 MeV.

[Am58] D.P.Ames, J.W.Barnes, J.P.Balagna, A.A.Comstock, G.A.Cowan, P.B.Elkin, G.P.Ford, J.S.Gilmore, D.C.Hoffman, G.W.Knobeloch, E.J.Lang, M.A.Melnick, C.D.Minkkinen, B.D.Pollack, J.E. Sattizahn, C.W.Stanley, B.Waren, Ref.9. in Ref. [Br62].

[Pr58] А.Н.Протопопов, Г.М.Толмачев, В.Н.Ушатский, Р.В.Венедиктова, И.Т.Крисюк, Л.П.Родионова, Г.В.Яковлева, Атомная Энергия, 5, 130 (1958); 14.6 Мэв.

[Kr60] И.Т.Крисюк, Г.П.Лепнев, Н.Б.Платунова, Радиохимия, II, 743 (1960); 14 Мэв.

[St60] P.C.Stevenson, H.G.Hicks, J.C.Armstrong, S.R.Gunn, Phys.Rev., 117, 186 /1960/; 14 MeV.

[Ap62] А.Н.Апполонова, И.Т.Крисюк, В.Н.Ушатский, Радиохимия, IV, 587 (I962); I4 Мэв.

[Ap62a] А.Н.Апполонова, И.Т.Крисюк, В.Н.Ушатский, Радиохимия, IV, 7II (I962); I4 Мэв.

[Br62] K.M.Broom, Phys.Rev. 126, 627 /1962/; 14.7 ± 0.4 MeV.

[Ja64] R.H.James, G.R.Martin, D.J.Silvester, Radiochim.Acta, 3, 76 /1964/; 14.7 ± 0.2 MeV.

[Me64] M.P.Menon, P.K.Kuroda, J.Inorg.Nucl.Chem., 26, 401 /1964/; 14.7 ± 0.4 MeV.

[Fo65] G.P.Ford, R.B.Leachman, Phys.Rev., 137, B 826 /1965/; 14.1 ± 0.17 and 14.9 ± 0.25 MeV.

[Wo65] K.Wolfsberg, Phys.Rev., 137, B 929 /1965/; 14.6 ± 0.2 MeV.

[Ga66] R.Ganapathy, H.Ihochi, J.Inorg.Nucl.Chem., 28, 3o71 /1966/; 14.8 ± 0.2 MeV.

[Go68] D.J.Gorman, R.H.Tomlinson, Can.J.Chem., 46, 1663 /1968/; 14 MeV.

[Ne69] D.R.Nethaway, B.Mendoza, T.E.Voss, Phys.Rev., 182, 1251 /1969/; 14.8 ± 0.3 MeV.

[Pe69] К.А.Петр[illegible]к, В.Ф.Теплых, М.Г.Паньян, Бюллетень Центра по Ядерным [illegible]нным, Выпуск 6, 226 (I969), АТОМИЗДАТ; I4.7 Мэв.

[Co70] F.Communeau, Ref.9. in Ref. [Bl71].

[Ge70] L.H.Gevaert, R.E.Jervis, H.D.Sharma, Can.J.Chem., 48, 641 /1970/; 14.7 MeV.

[Bi71] O.Birgul, S.J.Lyle, R.Wellum, Radiochim.Acta, 16, 104 /1971/; 14.8 MeV.

[Bl71] J.Blachot, P.Cavalloni, C.Chauvin, Proc. of Int.Conf. on Chemical Nuclear Data, p. 13 of Vol. "Measurements and Applications" The Institution of Civil Engineers London, 1972; 14.8 MeV.

[Sw71] D.L.Swindle, R.J.Wright, T.E.Ward, P.K.Kuroda, J.Inorg.Nucl. Chem., 33, 651 /1971/; 14.8 ± 0.2 MeV.

[Al72] P.Alexander, Nucl.Phys., A198, 228 /1972/; 14 MeV.

[Bq72] J.P.Bocquet, R.Brissot, J.Crancon, A.Moussa, Nucl.Phys., A189, 556 /1972/; 14.5 MeV.

[Ne72] D.R.Nethaway, B.Mendoza, Phys.Rev., C6, 1827 /1972/; 14.8 ± 0.3 MeV.

[Pi72] A.L.Prindle, Ref.7. in Ref. [Ne72].

[Da73] S.Daróczy, E.Germán, P.Raics, S.Nagy, J.Csikai, Soviet National Conference on Neutron Physics, Kiev, May 28 - June 1, 1973; 14.4 ± 0.2 MeV.

[Da73a] S.Daróczy, S.Nagy, L.Kövér, P.Raics, J.Csikai, to be published; 14.4 ± 0.2 MeV.

[1] A.C.Wahl, A.E.Norris, R.A.Rouse, J.C.Williams, 2nd IAEA Symp. on Phys. and Chem. of Fission, 813 /1969/, IAEA, Vienna.

[2] A.E.Crouch, IAEA Symp. on Appl. of Nucl. Data in Science and Technology, Paris, 12-16 March 1973, IAEA/SM-170/94.

[3] M.Lammer, O.J.Eder, IAEA Symp. on Appl. of Nucl.Data in Science and Technology, Paris, 12-16 March 1973, IAEA/SM-170/13.

[4] S.Katcoff, Nucleonics, 18 /No.11./, 201 /1960/.

[5] H.R.Von Gunten, Actinides Rev., 1, 275 /1969/.

[6] M.E.Meek, B.F.Rider, Ref.22. in Ref.[3].

[7] Ю.А.Зысин, А.А.Лдов, Л.И.Сельченков, Выходы продуктов деления и их распределение по массам, ГОСАТОМИЗДАТ, Москва, 1963.

[8] А.А.Гремилов, В.М.Колобашкин, С.И.Дементьев, Продукты мгновенного деления U^{235}, U^{238}, Pu^{239} в интервале 0-1 ч., АТОМИЗДАТ, Москва, 1969.

[9] Y.Kanda, R.Nakasima, Proc. Conf. on Neutron Cross Section and Technology /Washington,D.C., March 4-7, 1968/, NBS Spec. Publ. 299., Vol.I., 193 /1968/.

[10] T.A.Pitterle, 2nd Int. Conf. on Nucl. Data for Reactors, Vol.II., 687, IAEA, Vienna, 1970.

[11] C.M.Lederer, J.M.Hollander, I.Perlman, Table of Isotopes, 6th Edition, J.Wiley and Sons, Inc., New York - London - Sidney, 1967; Nukldkarte, 3. Auflage, 1968.

[12] H.Umezawa, S.Baba, H.Baba, Nucl.Phys., A160, 65 /1971/.

[13] И.В.Гордеев, Д.А.Кардашев, А.В.Малышев, Ядернофизические константы, 377, ГОСАТОМИЗДАТ, Москва, 1963.

[14] W.G.Davey, Nucl.Sci.Eng., 44, 345 /1971/.

[15] BNL 325, 2nd ed., Supplement No.2., USAEC /1965/.

Table I. Mo-99 / Ba-140 cumulative yield ratios for 14 MeV neutron induced fission of U-238

Ref.	Method	Measured data			Accepted ratio
		Mo-99	Ba-140	Mo/Ba ratio	
1	2	3	4	5	6
Bo55	RCbe	6.5 5	4.9 4	1.327 150	1.327 150
Cu57	RC2be	5.58 28	4.41 22	1.265 90	1.265 90
Pr58	RCbe	1	0.80 4	1.250 63	1.250 89
Am58	?	5.7	4.6	1.239	1.239 190
Ja64	RC2be	1.315 47	0.949 28	1.386 64	1.386 80
Go68	DGR	1.000	0.825 90		
		/1.000/	/0.830 90/	1.205 130	1.205 130
Co70	?	5.50 66	4.92 70	1.118 208	1.118 208
Bl71	DG	5.8 8	5.1 3	1.137 171	1.137 171
Da73	DG	5.61 56	4.44 45	1.264 130	1.264 130
					A 1.243 28
					WA 1.277 39
				Recommended	1.277 39

Table II. Absolute cumulative yields of Mo-99 and Ba-140 for 14 MeV neutron induced fission of U-238

Nuclide	Ref.	Method	Meas. data %		Corr. data %		Transf. to Mo-99	
1	2	3	4		5		6	
Mo-99	Te53	RCbe FC	5.68	14	5.68	28	5.68	28
	Bo55	RCbe FC	6.5	5	6.5	5	6.5	5 +
	St60	RCga R	5.86	16	5.91	20	5.91	20
	Ga66	RC2be Al?	5.60	28	5.60	62	5.60	62
	Ge70	RCGe Cu	5.60	14	5.40	26	5.40	26
Ba-140	Br62	RC2be Al	4.3	4	4.00	37	5.11	47
	Ne69	RCgaGeAl	4.46	32	4.52	32	5.77	41
	Da73	DG Al	4.44	45	4.74	48	6.05	61
						A	5.65	12
						WA	5.69	12
Mo-99 recommended absolute yield %							5.69	26
Ba-140 recommended absolute yield %							4.46	20

Table III. Cumulative and chain yields for 14 MeV neutron induced fission of U-238

A	Element	Measurement			Normalised yield %			Recommended chain yield %
		ref.	method	data	to Mo-99	to Ba-140	accepted and corr.	
1	2	3	4	5	6	7	8	9
66	28-Ni	Ne69	RCbe	/8.5 9/-5		/8.5 9/-5	/8.5 9/-5	/8.5 9/-5
67	29-Cu	Ne69	RCbega	/1.4 4/-4		/1.4 4/-4	/1.4 4/-4	/1.4 4/-4
68								/2.7 /-4
69								/4.8 /-4
70								/8.8 /-4
71								0.0016
72	30-Zn	Ne69	RCbe	0.0030 4		0.0030 4	0.0030 4	0.0030 4
73	31-Ga	Sw71	RC2be	0.0053 10	0.0054 10		0.0054 10	0.0054 10
74								0.0082
75								0.013
76								0.019

1	2	3	4	5	6	7	8	9
77	32Ge/mg	Sw71	RC2be	0.030 5	0.030 5		0.030 5	0.030 4
	33-As	Sw71	RC2be	0.030 5	0.030 5		0.030 5	
							A 0.030	
							WA 0.030 4	
78	32-Ge	Sw71	RC2be	0.040 5	0.041 5		0.041 5	0.041 4
	33-As	Sw71	RC2be	0.041 10	0.042 10		0.042 10	
							A 0.042 1	
							WA 0.041 4	
79	33-As	Sw71	RC2be	0.18 3	0.18 3		0.18 3	0.18 3
80								0.25
81	34-Se	Sw71	RC2be	0.33 5	0.34 5		0.34 5	0.34 5
82								0.48
83	35-Br	Ja64	RC2be	0.138 10	0.597 43	0.649 47	0.623 45	0.683 28
	36-Kr	Go68	MS	0.423 4			0.719 35	
							A 0.671 48	
							WA 0.683 28	

1	2	3	4	5	6	7	8	9
84	35-Br	Ja64	RC2be	0.270 8	1.17 4	1.27 4	1.22 4	1.22 3
	36-Kr	Go68	MS	0.716 7			1.22 6	
							A 1.22	
							WA 1.22 3	
85	36Kr/mg	Go68	DGR	0.203 7				
				/0.198 9/	1.13 5	1.06 5	1.10 5	1.08 5
	36Kr/mg	B171	DG	0.94 15	0.92 15	0.82 13	0.87 14	
	36Kr/mg	Da73	DG	1.52 30	1.54 30	1.53 30	1.53 30	
							A 1.17 19	
							WA 1.08 5	
	36Kr/mg	Go68	MS	0.635 6			= 1.08 5	
86	36-Kr	Go68	MS	1			1.70 8	1.70 8
87	36-Kr	Bq72	MS	66 2				1.61 8
	chain			57 1			1.61 8	
88	36-Kr	B171	DG	1.35 10	1.32 10	1.18 9	1.25 9 +	1.75 9
	36-Kr	Bq72	MS	71 3				
	chain			62.0 1.5			1.75 9	

1	2	3	4	5	6	7	8	9
89	36-Kr	Co70	?	2.80 31	2.90 32	2.54 28	/2.72 30/	2.61 7
							2.80 31	
	36-Kr	Bq72	MS	98 1				
	chain			88 2			2.48 13	
	38-Sr	Bo55	RCbe	3.3 3	2.89 26	3.00 27	2.95 27	
	38-Sr	Cu57	RC2be	2.30 12	2.35 12	2.33 12	2.34 12	
	38-Sr	Pr58	RC be	0.55 3	3.13 17	3.07 17	3.10 17	
	38-Sr	Am58	?	3.0	2.99	2.91	2.95 30	
	38-Sr	Br62	RC2be	2.0 2		2.07 20	2.07 20 +	
							A 2.77 12	
							WA 2.61 7	
90	36-Kr	Bq72	MS	100 3				2.97 14
	chain			100 3			2.82 16	
	38-Sr	Br62	RC2be	3.4 3		3.53 31	3.53 31	
							A 3.18 35	
							WA 2.97 14	
91	38-Sr	Pr58	RCbe	0.65 5	3.70 28	3.62 28	3.66 28	3.55 12
	38-Sr	Br62	RC2be	2.6 3		2.70 31	2.70 31 +	
	38-Sr	Go68	DGR	0.666 43				
				/0.659 47/	3.75 27	3.54 25	3.65 26	

1	2	3	4	5	6	7	8	9
	38-Sr	Co70	?	4.0 6	4.14 62	3.63 54	3.89 58	
	38-Sr	Bl71	DG	3.61 22	3.54 22	3.16 19	3.35 21	
	38-Sr	Bi71	RCbe	3.60 28	3.61 28		3.61 28	
	38-Sr	Da73	DG	3.47 90	3.52 91	3.49 90	3.51 90	
	39-Y	Cu57	RC2be	2.78 14	2.83 14	2.81 14	2.82 14 +	
							A 3.61 7	
							WA 3.55 12	
	36-Kr	Bq72	MS	94 1				
	chain			126 4			= 3.55 12	
92	36-Kr	Bq72	MS	70 3			3.89 29	4.03 20
	chain			138 8				
	38-Sr	Bl71	DG	4.19 50	4.11 49	3.66 44	3.89 46	
	38-Sr	Da73	DG	3.56 40	3.61 41	3.58 40	3.60 41 +	
	38-Sr	Da73a	DG	4.31 34			4.31 34	
							A 4.03 14	
							WA 4.03 20	
93	36-Kr	Bq72	MS	30 2				4.41 26
	chain			159 13			4.48 42	
	39-Y	Ja64	RC2be	0.835 28	3.61 12	3.92 13	3.77 13 +	
	39-Y	Ne69	RCbe	4.4 4		4.4 4	4.4 4	
	39-Y	Co70	?	4.45 56	4,60 58	4.03 51	4.32 54	
							A 4.40 5	
							WA 4.41 26	

1	2	3	4	5	6	7	8	9
94								4.75
95	40-Zr	Bo55	RCbe	4.6 4	4.03 35	4.19 36	4.11 36 +	5.11 16
	40-Zr	Pr58	RCbe	0.93 4	5.29 23	5.18 22	5.24 23	
	40-Zr	Co70	?	5.38 92	5.57 96	4.88 83	5.23 90	
	40-Zr	B171	DG	5.0 2	4.91 20	4.37 17	4.64 19	
	40-Zr	Da73	DG	5.29 61	5.37 62	5.31 61	5.34 62	
							A 5.11 16	
							WA 4.92 14	
96								5.23
97	40-Zr	Bo55	RCbe	4.9 4	4.29 35	4.46 36	4.38 36 +	5.36 15
	40-Zr	Pr58	RCbe	1.02 5	5.80 28	5.69 28	5.75 28	
	40-Zr	Am58	?	4.8	4.79	4.65	4.72 47	
	40-Zr	Ja64	RC2be	1.213 67	5.25 29	5.70 31	5.48 30	
	40-Zr	Go68	DGR	0.959 62				
				/0.963 68/	5.48 39	5.17 37	5.33 38	
	40-Zr	Co70	?	5.40 93	5.59 96	4.90 84	5.25 90	
	40-Zr	B171	DG	5.38	5.28	4.70	4.99 50	
	40-Zr	Da73	DG	4.82 52	4.89 53	4.84 52	4.87 53	
							A 5.20 14	
							WA 5.36 15	

1	2	3	4	5	6	7	8	9
98								5.52
99	42-Mo	To53	RCbe	5.68	14			5.69 10
	42-Mo	Bo55	RCbe	6.5	5			
	42-Mo	Cu57	RC2be	5.58	28			
	42-Mo	Pr58	RCbe	1.				
	42-Mo	Am58	?	5.7				
	42-Mo	Sh60	RCbe	5.85	16			
	42-Mo	Ja64	RC2be	1.315	47			
	42-Mo	Ga66	RC2be	5.60	28			
	42-Mo	Ge68	DGR	1.000				
				/1.00	5/			
	42-Mo	Ge70	RC ?	5.60	14			
	42-Mo	Co70	?	5.50	66			
	42-Mo	Bl71	DG	5.8	8			
	42-Mo	Sw71	RC2be	5.6	5			
	42-Mo	Bi71	RCbe	5.68				
	42-Mo	Da73	DG	5.61	79			
100								5.79

1	2	3	4	5	6	7	8	9
101	42-Mo	Pr58	RCbe	0.99 4	5.63 23	5.52 22	5.58 23	5.90 18
	42-Mo	Ga66	RC2be	6.35 30	6.45 30		6.45 30	
							A 6.02 44	
							WA 5.90 18	
102	42-Mo	Pr58	RCbe	0.71 8	4.04 46	3.96 45	4.00 45 +	5.12
	42-Mo	Ga66	RC2be	2.85 30	2.90 30		2.90 30 +	
103	44-Ru	Bo55	RCbe	3.0 3	2.63 26	2.73 27	2.68 26 +	4.43 12
	44-Ru	Go68	DGR	0.936 120				
				/0.854 126/	4.86 71	4.59 67	4.73 69	
	44-Ru	Ge70	RC ?	4.44 15	4.51 15		4.51 15	
	44-Ru	B171	DG	4.64 40	4.55 39	4.06 35	4.31 37	
	44-Ru	Da73	DG	4.14 47	4.20 48	4.16 47	4.18 48	
							A 4.43 12	
							WA 4.47 13	
104								3.62

1	2	3	4	5	6	7	8	9
105	44-Ru	Pr58	RCbe	0.39 3	2.22 17	2.17 17	2.20 17 +	2.97 7
	44-Ru	Ja64	RC2be	0.539 33	2.33 14	2.53 16	2.43 15	
	44-Ru	Ge70	RC ?	3.00 10	3.05 10		3.05 10	
	44-Ru	Bl71	DG	3.79 40	3.72 39	3.31 35	3.52 37	
	44-Ru	Bi71	RCbe	3.70 42	3.71 42		3.71 42	
	44-Ru	Da73	DG	3.62 40	3.67 41	3.64 40	3.66 41	
	45-Rh	Bo55	RCbe	3.3 3	2.89 26	3.00 27	2.95 26	
	45-Rh	Am58	?	3.4	3.39	3.30	3.35 34	
							A 3.24 17	
							WA 2.97 7	
106	44-Ru	Bo55	RCbe	2.4 3	2.10 26	2.18 27	2.14 26	2.14 26
107	45-Rh	Bi71	RCbe	1.74 5	1.74 5		1.74 5	1.74 5
108								1.53
109	46-Pd	Ja64	RC2be	0.244 41	1.06 18	1.15 19	1.11 19	1.34 7
	46-Pd	Fo65	RCbe	1.14 5			1.14 11	
	46-Pd	Ge70	RCbe	1.54 15	1.56 15		1.56 15	

1	2	3	4	5	6	7	8	9
	46-Pd	Co70	?	1.19 29	1.23 30	1.08 26	1.16 28	
	46-Pd	Bi71	RCbe	1.56 12	1.56 12		1.56 12	
							A 1.31 10	
							WA 1.34 7	
110								1.12
111	46-Pd	Ja64	RC2be	0.132 16	0.571 69	0.620 75	0.596 72 +	0.953 24
	47-Ag	Bo55	RCbe	1.06 12	0.928 105	0.965 110	0.947 107	
	47-Ag	Cu57	RC2be	0.81 4	0.826 41	0.819 40	0.823 41	
	47-Ag	Pr58	RCbe	0.18 1	1.02 6	1.00 6	1.01 6	
	47-Ag	Am58	?	0.87	0.868	0.844	0.856 90	
	47-Ag	Br62	RC2be	0.6 1	1.12 5	0.622 104	0.622 104 +	
	47-Ag	Ja64	RC2be	0.199 33	0.861 143	0.935 155	0.898 149	
	47-Ag	Fo65	RCbe	1.08 4			1.08 11	
	47-Ag	Ge70	RC ?	1.10 5			1.12 5	
	48-Ag	Co70	?	0.97 11	1.00 11	0.879 100	0.940 103	
							A 0.959 37	
							WA 0.953 24	

1	2	3	4	5	6	7	8	9
112	46-Pd	Bo55	RCbe	0.7	0.613	0.637	0.625 70	0.985 33
	46-Pd	Ja64	RC2be	0.161 16	0.697 69	0.757 75	0.727 72	
	46-Pd	Fo65	RCbe	1.11 5			1.11 11	
	46-Pd	Ge70	RC ?	1.24 5	1.26 5		1.26 5	
	46-Pd	B171	DG	1.30 30	1.28 29	1.14 26	1.21 27	
						A	0.986 130	
						WA	0.985 33	
113	47Ag5h	Pr58	RCbe	0.16 1	0.910 60	0.892 56	0.901 59	≥0.877 29
	47Ag5h	Br62	RC2be	0.6 1		0.622 104	0.622 104	
	47Ag5h	Ja64	RC2be	0.177 12	0.766 52	0.832 56	0.799 54	
	47Ag5h	Fo65	RCbe	0.663 20			0.663 70	
	47Ag5h	Ge70	RC ?	0.88 5	0.894 51		0.894 51	
						A	0.776 58	
						WA	0.877 29	
114								0.85
115	47-Ag	Ja64	RC2be	0.130 10	0.563 43	0.611 47	0.587 45 +	0.814 58
	48Cd/m	Bo55	RCbe	0.06	0.053	0.055	0.054 10	
	48Cd/m	Cu57	RC2be	0.06 1	0.061 10	0.061 10	0.061 10	
						A	0.058 4	
						WA	0.058 7	

1	2	3	4	5	6	7	8	9
	48Cd/g	Bo55	RCbe	0.80 9	0.700 79	0.730 80	0.715 80	
	48Cd/g	Cu57	RC2be	0.58 3	0.591 31	0.587 30	0.589 30	
	48Cd/g	Pr58	RCbe	0.16 1	0.910 57	0.892 56	0.901 56	
	48Cd/g	Am58	?	0.71	0.709	0.688	0.699 70	
	48Cd/g	Ge70	RC ?	0.86 9	0.874 91		0.874 91	
	48Cd/g	Co70	?	0.96 12	0.993 124	0.870 109	0.932 116 +	
							A 0.756 58	
							WA 0.681 23	
116								0.82
117								0.83
118								0.83
119								0.84
120								0.84

1	2	3	4	5	6	7	8	9
121	50Sn/g	Am58	?	0.73	0.729	0.708	0.719 72	≥0.851 60
	50Sn/g	Ge70	RCbe	1.14 11	1.16 11		1.16 11	
							A 0.940 221	
							WA 0.851 60	
122								0.85
123								0.84
124								0.84
125	50Sn/g	Am58	?	0.83	0.829	0.805	0.817 82	≥0.839 59
	50Sn/g	Ge70	RCbe	0.850 85	0.864 86		0.864 86	
							A 0.841 24	
							WA 0.839 59	
126								1.08

1	2	3	4	5	6	7	8	9
127	51-Sb	Am58	?	1.43	1.43	1.39	1.41 14	1.40 6
	51-Sb	Bl71	DG	1.40 10	1.37 10	1.22 9	1.30 10	
	51-Sb	Bi71	RCbe	1.54 2	1.54 2		1.54 2	
	51-Sb	Da73	DG	1.31 33	1.33 33	1.32 33	1.33 33	
							A 1.40 6	
							WA 1.53 2	
128								1.82
129	51-Sb	Ja64	RC2be	0.240 2	1.04 1	1.13 1	1.09 1 +	/ ≥1.09 8 /
	51-Sb	Bi71	RCbe	1.69 2	1.07 2		1.07 2 +	2.35
	52Te/m	Bo55	RCbe	1.22 9	1.07 8	1.11 8	1.09 8	
130								3.00
131	53-I	Pr58	RCbe	0.91 5	5.18 28	5.07 28	5.13 28 +	3.90 10
	53-I	Br 62	RC2be	2.7 2		2.80 21	2.80 21 +	
	53-I	Ja64	RC2be	0.935 85	4.05 37	4.39 40	4.22 39	
	53-I	Go68	DGR	0.707 68				
				/0.699 70/	3.98 40	3.76 38	3.87 39	

1	2	3	4	5	6	7	8	9
	53-I	Bl71	DG	4.33 50	4.25 49	3.79 44	4.02 46	
	53-I	Bl71	RCbe	3.61 6	3.62 6		3.62 6	
	53-I	Da73	DG	3.75 48	3.80 49	3.77 48	3.79 49	
							A 3.90 10	
							WA 3.65 6	
	54-Xe	Go68	MS	0.618 2			= 3.90 10	
	54-Xe	Pe69	MS	18.64 55			= 3.90 10	
132	52-Te	Bo55	RCbe	4.4 3	3.85 26	4.00 27	3.93 27 +	4.72 10
	52-Te	Am58	?	4.7	4.69	4.56	4.63 46	
	52-Te	Go68	DGR	0.795 87				
				/0.786 88/	4.47 50	4.22 47	4.35 49	
	52-Te	Bl71	DG	4.91 30	4.82 29	4.29 26	4.56 27	
	52-Te	Da73	DG	4.20 43	4.26 44	4.22 43	4.24 43	
	53-I	Br62	RC2be	4.5 4		4.67 41	4.67 41 +	
	54-Xe	Go68	MS	0.760 4			4.80 13	
	54-Xe	Pe69	MS	23.06 50			4.82 22	
							A 4.57 10	
							WA 4.72 10	

1	2	3	4	5	6	7	8	9
133	53-I	Br62	RC2be	2.6 3		2.70 31	2.70 31 +	5.96 11
	53-I	Go68	DGR	1.10 9				
				/1.09 9/	6.21 52	5.86 49	6.04 50	
	53-I	B171	DG	6.53 40	6.41 39	5.71 35	6.06 37	
	53-I	Da73	DG	5.46 62	5.54 63	5.48 62	5.51 62	
	54-Xe	Ja64	RC2be	1.352 47	5.85 20	6.35 22	6.10 21	
	54-Xe	Go68	MS	0.935 1			5.90 15	
							A 5.92 11	
							WA 5.96 11	
134	53-I	Br62	RC2be	4.7 5		4.87 52	4.87 52 +	6.40 14
	53-I	Da73a	DG	6.21 67			6.21 67	
	54-Xe	Go68	MS	1.000			6.31 16	
	54-Xe	Pe69	MS	31.68 50			6.63 28	
							A 6.38 13	
							WA 6.40 14	
135	53-I	Br62	RC2be	5.0 5		5.19 52	/5.19 52/	5.65 28
							5.38 54 +	
	53-I	B171	DG	4.55 70	4.46 69	3.98 61	/4.22 65/	
							4.37 67 +	

1	2	3	4	5	6	7	8	9
	53-I	Da73	DG	4.29 50	4.35 51	4.31 50	/4.33 51/	
							4.49 53 +	
	54-Xe	Ja64	RC2be	1.136 39	4.92 17	5.34 18	5.13 18	
	54-Xe	Go68	DGR	1.11 6				
				/1.10 7/	6.26 40	5.91 38	6.09 39	
	54-Xe	Go68	MS	0.906 16			5.72 18	
	55-Cs	Go68	MS	1.00			= 5.72 18 +	
							A 5.65 28	
							WA 5.49 12	
136	54-Xe	Go68	MS	0.883 3			5.57 15	5.57 13
	54-Xe	Pe69	MS	26.63 60			5.57 25	
							A 5.57	
							WA 5.57 13	
137	54-Xe	Bq72	MS	100 2				4.72 26
	chain			100 2			4.65 30	
	55-Cs	Bo55	RCbe	6.6 6	5.78 53	6.01 55	5.90 54 +	
	55-Cs	Go68	MS	0.863 86			4.94 52	
							A 4.80 15	
							WA 4.72 26	

1	2	3	4	5	6	7	8	9
138	54-Xe	Bq72	MS	91 2				4.75 28
	chain			96 4			4.46 33	
	55-Cs	Da73a	DG	5.54 55			5.54 55	
							A 5.00 54	
							WA 4.75 28	
139	54-Xe	Bq72	MS	79 2				4.68 16
	chain			97 4			4.51 33	
	56-Ba	Ja64	RC2be	1.000	4.33 15	4.70 14	4.52 15	
	56-Ba	Go68	DGR	0.912 43				
				/0.904 50/	5.14 29	4.86 27	5.00 28	
							A 4.68 16	
							WA 4.61 12	
140	56-Ba	Bo55	RCbe	4.9 4				4.46 22
	56-Ba	Cu57	RC2be	4.41 22				
	56-Ba	Pr58	RCbe	0.80 4				
	56-Ba	Am58	?	4.6				
	56-Ba	Br62	RC2be	4.3 4				
	56-Ba	Ja64	RC2be	0.949 2				
	56-Ba	Me64	RCbe	4.3 4				

1	2	3	4	5	6	7	8	9
	56-Ba	Go68	DGR	0.825 90 /0.830 90/				
	56-Ba	Ne69	RCgaGe	4.46 18				
	56-Ba	Co70	?	4.92 70				
	56-Ba	Bl71	DG	5.1 3				
	56-Ba	Da73	DG	4.44 45				
	54-Xe	Bq72	MS	59 2				
	chain			96 4			=4.46 22	
141	54-Xe	Bq72	MS	27 1				4.22 23
	chain			92 9			4.27 49	
	58-Ce	Bo55	RCbe	5.8 6	5.08 53	5.28 55	5.18 54 +	
	58-Ce	Me64	RCbe	3.9 4		4.05 41	4.05 41	
	58-Ce	Co70	?	4.53 41	4.69 42	4.11 37	4.40 39	
	58-Ce	Da73	DG	4.04 66	4.10 67	4.06 66	4.08 66	
							A 4.20 8	
							WA 4.22 23	
142	57-La	Bl71	DG	3.90 50	3.83 49	3.41 44	3.62 64	4.20 31
	57-La	Da73a	DG	4.37 35			4.37 35	
							A 4.00 38	
							WA 4.20 31	

1	2	3	4	5	6	7	8	9
143	58-Ce	Cu57	RC2be	3.91 27	3.99 28	3.95 27	3.97 27	3.86 12
	58-Ce	Ja64	RC2be	0.713 142	3.09 61	3.35 67	3.22 64	
	58-Ce	Me64	RCbe	4.3 5		4.46 52	4.46 52	
	58-Ce	Go68	DGR	0.744 72				
				/0.769 74/	4.38 42	4.13 40	4.26 41	
	58-Ce	Co70	?	3.45 41	3.57 42	3.13 37	3.35 39	
	58-Ce	B171	DG	3.76 25	3.69 25	3.29 22	3.49 24	
	58-Ce	B171	RCbe	4.64 36	4.65 36		4.65 36	
	58-Ce	Da73	DG	3.05 37	3.09 38	3.06 37	3.08 38 +	
	58-Ce	Da73a	DG	3.73 35			3.73 35	
	59-Pr	Cu57	RC2be	3.16 16	3.22 16	3.20 16	3.21 16 +	
							A 3.89 19	
							WA 3.86 12	
144	58-Ce	Cu57	RC2be	2.68 16	2.73 17	2.71 16	2.72 16	3.04 31
	58-Ce	Am58	?	3.4	3.39	3.30	3.35 34	
	58-Ce	Me64	RCbe	4 2		4.15 2.10	4.15 2.10 +	
							A 3.04 31	
							WA 2.83 14	
145	59-Pr	B171	RCbe	3.11 16	3.12 16		3.12 16	3.12 16
146								2.58

1	2	3	4	5	6	7	8	9
147	60-Nd	Cu57	RC2be	1.99 10	2.03 10	2.01 10	2.02 10	2.15 9
	60-Nd	Ne69	RCgaGe	2.20 15		2.20 15	2.20 15	
	60-Nd	Da73	DG	2.78 64	2.82 65	2.79 64	2.81 64 +	
	61-Pm	Me64	RCbe	2.3 3		2.39 31	2.39 31	
	61-Pm	Co70	?	2.05 24	2.12 25	1.86 22	1.99 23	
							A 2.15 9	
							WA 2.08 8	
148								1.62
149								1.22
150								0.93
151								0.71
152								0.54
153	62-Sm	Cu57	RC2be	0.39 2	0.398 20	0.394 20	0.396 20	0.408 12
	62-Sm	Ne69	SCbega	0.42 4		0.42 4	0.42 4	
	62-Sm	Co70	?	0.334 49	0.346 51	0.303 44	0.325 48 +	
							A 0.408 12	
							WA 0.401 18	

1	2	3	4	5	6	7	8	9
154								0.27
155								0.18
156	63-Eu	Cu57	RC2be	0.13 1	0.13 1	0.13 1	0.13 1	0.12 1
	63-Eu	Am58	?	0.22	0.22	0.21	0.22 2 +	
	63-Eu	Fo65	RCbe	0.109 7			0.109 11	
	63-Eu	Co70	?	0.13 4	0.13 4	0.12 4	0.13 4	
							A 0.12 1	
							WA 0.12 1	
157								0.072
158								0.043
159	64-Gd	Ne69	RCbe	0.026 3		0.026 3	0.026 3	0.026 3
160								0.0145
161	65-Tb	Ne69	RC4be	0.0089 5		0.0089 5	0.0089 5 +	0.0085 4
	65-Tb	Ne72, P172	?	0.0085 4			0.0085 4	
162								0.0051

1	2	3	4	5	6	7	8	9
163								0.0029
164								0.0018
165								0.00105
166	66-Dy	Ne69	RC4be	/6.3 6/-4		/6.3 6/-4	/6.3 6/-4	/6.3 6/-4
167								/3.7 /-4
168								/2.2 /-4
169	68-Er	Ne69	RC4be	/1.29 9/-4		/1.29 9/-4	/1.29 9/-4	/1.29 9/-4
170								/7.1 /-5
171								/3.8 /-5
172	68-Er	Ne69	RC4be	/2.1 7/-5		/2.1 7/-5	/2.1 7/-5	/2.1 7/-5

Table IV. Independent and fractional cumulative yields for 14 MeV neutron induced fission of U-238

A	Element	Data of the measurement					Calculated Z_p		
		Ref.	Method	IY %	FIY %	FCY %	[Bq72]	[Ne72]	[12]
1	2	3	4	5	6	7	8	9	10
87	36-Kr	Bq72	MS	4.2 8			34.57	34.60	34.0
88	36-Kr	Bq72	MS	31.8 2.0			34.97	35.03	34.35
89	36-Kr	Bq72	MS	74.5 6.0			35.36	35.44	34.8
90	36-Kr	Bq72	MS	100 5			35.75	35.84	35.15
91	36-Kr	Wo65	RCbe			65 2	36.15	36.24	35.65
	36-Kr	Bq72	MS	108.3 2.0					
92	36-Kr	Wo65	RCbe			44 2	36.54	36.64	36.05
	36-Kr	Bq72	MS	88.2 4.0					
93	36-Kr	Wo65	RCbe			16.4 1.1	36.93	37.05	36.41
	36-Kr	Bq72	MS	39.0 2.5					
96	41-Nb	Ne72	RCGe	/1.07 9/ -4			38.12	38.25	37.6

1	2	3	4	5	6	7	8	9	10
133	54Xe/mg	Al72	RCGe		0.30 13		51.69	51.54	51.69
135	54Xe/mg	Al72	RCGe		5.6 3.7		52.48	52.45	52.41
136	55-Cs	Bo55	RCbe	0.034 4			52.87	52.87	52.77
	55-Cs	Fo56	?		0.0052 2				
	55-Cs	Pi72	?	0.0219 10					
137	54-Xe	Bq72	MS	100 3			53.26	53.28	53.13
138	53-I	Ap62a	RCbe			55.0	53.65	53.66	53.49
	54-Xe	Ap62a	RCbe		36.7				
	54-Xe	Wo65	RCbe			94 2			
	54-Xe	Bq72	MS	144 5					
	55-Cs	Ap62a	RCbe		8.3 5				
139	53-I	Ap62	RCbe			18.3	54.04	54.08	54.14
	54-Xe	Ap62	RCbe		47.5				
	54-Xe	Wo65	RCbe			80.5 6			
	54-Xe	Bq72	MS	160 5					
	55-Cs	Kr60	RCbe		28.6 1.5				
	56-Ba	Kr60	RCbe		5.6 1.3				

1	2	3	4	5	6	7	8	9	10
140	54-Xe	Wo65	RCbe			61.1 1.1	54.43	54.48	54.53
	54-Xe	Bq72	MS	152 5					
141	54-Xe	Wo65	RCbe			29 2	54.82	54.88	54.9
	54-Xe	Bq72	MS	77 5					
142	54-Xe	Bq72	MS	41 5.			55.21	55.28	55.3
160	65-Tb	Ne72	RCbe	/2.1 2/-5			62.25	62.36	62.25

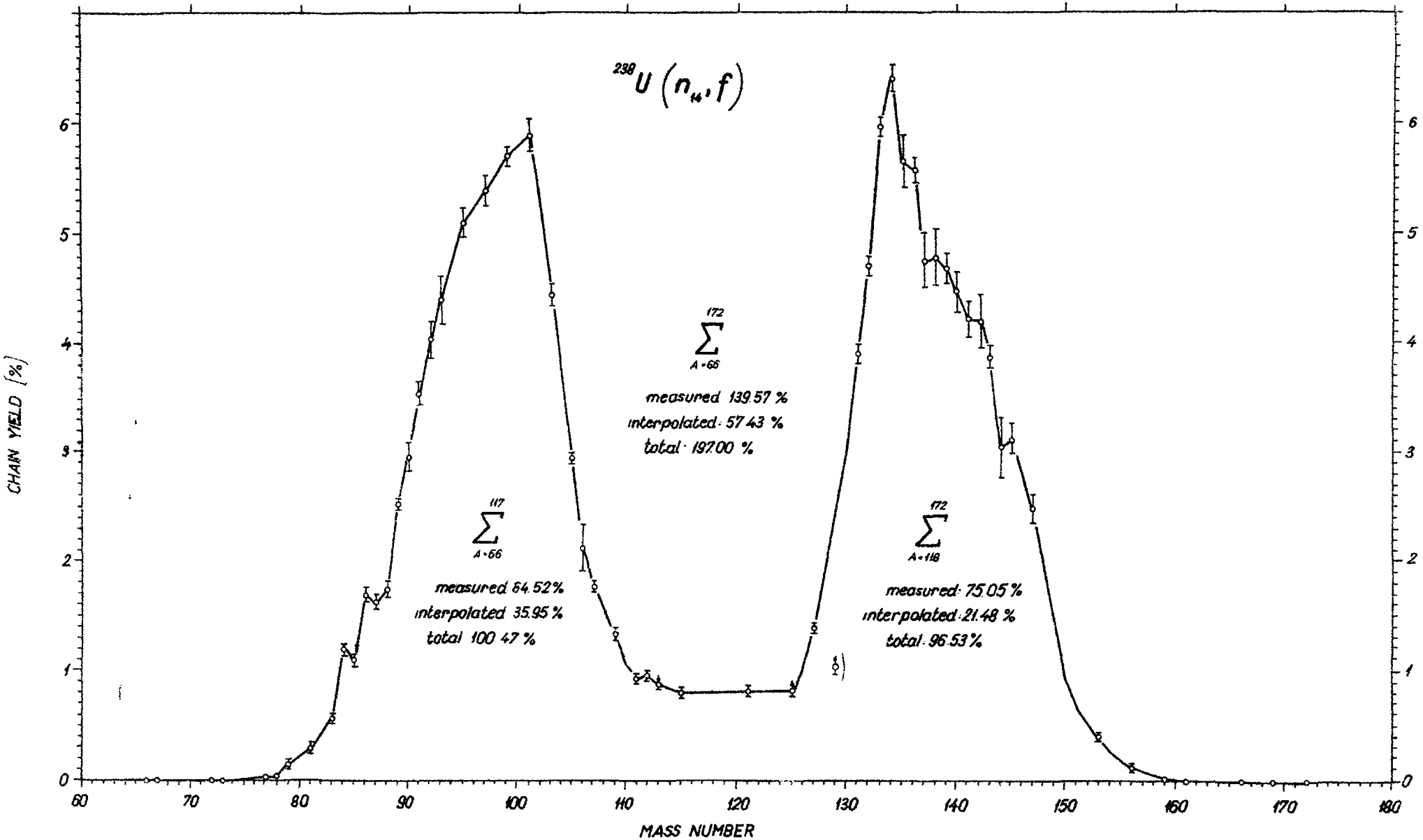
$^{238}U\,(n_{14},f)$
$\sum_{A=66}^{172}$
measured 139.57 %
interpolated 57.43 %
total 197.00 %
$\sum_{A=66}^{117}$
measured 64.52 %
interpolated 35.95 %
total 100.47 %
$\sum_{A=118}^{172}$
measured 75.05 %
interpolated 21.48 %
total 96.53 %
CHAIN YIELD (%)
MASS NUMBER
0
1
2
3
4
5
6
60
70
80
90
100
110
120
130
140
150
160
170
180

Contributions to
Review Paper No. 12

NEW MEASUREMENTS ON GAMMA-RAY EMISSION PROBABILITIES OF FISSION PRODUCT NUCLIDES IMPORTANT FOR NONDESTRUCTIVE FUEL ANALYSIS

K.Debertin, U.Schötzig, K.F.Walz, H.M.Weiß
Physikalisch-Technische Bundesanstalt, Braunschweig, Germany

Abstract:

Nuclear data of medium - and long-lived fission products are known with an accuracy generally sufficient in most application fields. An exception are γ-ray emission probabilities which have relative uncertainties of 3 % and more for a number of important cases. An attempt to reach an accuracy of 1 % for absolute γ-ray emission probabilities is described.

The Symposium on Applications of Nuclear Data in Science and Technology, 12-16 March 1973 in Paris, has shown up the status of existing experimental nuclear data of fission products [1]. The tables of Martin and Blichert-Toft [2], though now about four years old, still reveal the degree of uncertainty of nuclear data of the most important fission products. Half-lives of most medium- and long-lived fission products are known with an accuracy of 1 % or better. Only in the case of ^{95}Zr a discrepancy of 2.3 % exists between the results of Flynn et al. [3] and Debertin [4]. Gamma-ray energies are very well known whereas mean beta-ray energies, normally calculated from the maximum energies by means of semi-empirical formulae, have an uncertainty of 1 % to 2 %. The situation is worse for γ-ray emission probabilities (commonly called absolute γ-ray intensities). In Table 1 the emission probabilities of the most abundant γ-rays of fission products important in burn-up determination and safeguards techniques are listed as evaluated in reference [2]. The values given in the more recent tables of Tobias [5] deviate, if at all, only slightly from those in reference

[2] . Because of the scarcity of new experimental results the error limits of reference [2] are believed to be still valid. For 9 of the 18 lines of Table 1 the relative uncertainty is larger than 3 %.

Table 1: Emission probabilities of abundant γ-lines of important fission products according to reference 2

Fission product	Energy in keV	Emission probability in %
^{95}Zr	724.2	43.5 ± 0.5
	756.9	54.3 ± 0.5
^{95}Nb	765.8	99.80 ± 0.04
^{103}Ru	496.9	89 ± 1
	610.2	5.4 ± 0.4
^{106}Rh	511.8	20.6 ± 0.9
	622.1	9.94 ± 0.11
	1050.1	1.48 ± 0.04
^{137}Cs	661.6	84.6 ± 0.4
^{140}Ba	537.4	23.8 ± 1.2
^{140}La	328.8	21 ± 2
	487.0	45 ± 2
	1596.6	95.6 ± 0.3
^{141}Ce	145.4	49.0 ± 1.0
^{144}Ce	133.5	10.8 ± 0.5
^{144}Pr	696.5	1.51 ± 0.05
	1489.1	0.29 ± 0.02
	2185.7	0.74 ± 0.03

In the Physikalisch-Technische Bundesanstalt (PTB), Germany, a program for the determination of γ-ray emission probabilities with a relative measurement uncertainty of the order of 1 % has been started, A powerful tool for the measurement of r e l a t i v e γ-ray emission probabilities is a calibrated Ge(Li)-spectrometer

The efficiency calibration is usually done by means of standard sources of known activity. This method is applied in many laboratories, it suffers, however, from the fact that commonly only a small number of well-calibrated standards is available so that the efficiency for energies between the calibration points has to be interpolated. The dependence of efficiency on energy can not be represented by a simple analytical function, and errors introduced by the uncertainty of the interpolation may reach 2 % to 4 % in unfavourable cases. There are attempts to calculate the efficiency by means of Monte Carlo methods; we do not believe, however, that the error limits can thus be reduced. A better approach to this problem is an increase of the number of calibration points. In the Laboratory for Radioactive Standards of the PTB several precision measuring facilities are available to determine the activity of most γ-ray emitting radionuclides with half-lives greater than a few hours. In the energy region between 250 and 3000 keV we use about 15 nuclides as primary standards, the activity of which is determined with an uncertainty of 0.2 % to 0.5 % (68 % confidence limit). Only those γ-rays are accepted as calibration lines for which the absolute γ-ray emission probability is known to 0.5 % or better. A Ge(Li)-spectrometer calibrated in this way permits the measurement of relative γ-ray emission probabilities with an uncertainty of about 1 %. Details of measuring and evaluation procedures are outlined elsewhere [6].

In order to arrive at a b s o l u t e γ-ray emission probabilities the activity of the radionuclide source under investigation has to be known. Otherwise, additional informations are needed, e.g. branching ratios or conversion electron intensities, the errors of which propagate into the final result. A literature survey shows that this latter method of interconnecting several data to determine absolute γ-ray emission probabilities is common practice. This is avoided by determining the activity of the source by methods independent on the accurate decay scheme.

At present we are primarily concerned with fission products important for burn-up and safeguards techniques. Measurements on ^{95}Zr, $^{106}Ru/^{106}Rh$ and $^{144}Ce/^{144}Pr$ are finished [7] measurements on other fission products (^{103}Ru, ^{134}Cs, $^{140}Ba/^{140}La$) are in progress.

References

[1] IAEA-Symposium on Applications of Nuclear Data in Science and Technology, 12-16 March 1973, Paris; e.g. papers SM-170/12 and SM-170/63

[2] M.J. Martin, P.H. Blichert-Toft, Nuclear Data Tables A8, 1 (1970)

[3] K.F. Flynn, L.E. Glendenin, E.P. Steinberg, Nucl. Sci. Eng. 22, 416 (1965)

[4] K. Debertin, Z. f. Naturf. 26a, 596 (1971)

[5] A. Tobias, Report CEGB-RD/B/M 2453, Oct. 1972

[6] U. Schötzig, K. Debertin, H.M. Weiß, PTB-Mitteilungen 83, 307 (1973)

[7] K. Debertin, U. Schötzig, K.F. Walz, H.M. Weiß to be published

STANDARDS FOR CALIBRATION OF SEMICONDUCTOR DETECTORS

M. Lammer
Nuclear Data Section
Div.of Research & Labs.
Vienna, Austria

Abstract:

Energy scales and fundamental standards are defined for gamma ray energies. A consistent set of primary and secondary energy calibration lines is tabulated. A set of detector efficiency calibration standards is presented that is derived from level schemes of the standard nuclei. The survey is restricted to γ-rays up to about 3 MeV which is sufficient for fission product decay studies.

I. INTRODUCTION

In many application fields presently high resolution semiconductor detectors are used routine work, which have to be calibrated. In most practical application high precision values for gamma energy calibration lines are not needed due to limitations of detector resolution. However, it seems to be appropriate to make the user familiar with the definition and accuracy of primary and secondary standards and the limitations of accuracy that can be achieved. Similarly the role of standards in detector efficiency calibration is discussed. Since measurements of γ-ray energies and intensities of fission products are based on standards and evaluations based on measurements, "best" values of these data cannot be more accurate than those of the standards. Therefore this paper presents not only a set of calibration standards but may also help the user to judge the accuracies of fission product gamma ray data presented by evaluator.

II. GAMMA RAY ENERGY CALIBRATION STANDARDS

The survey given in the table is mainly based on the work of Greenwood et al. [1] and Helmer et al. [2] (up to 1.3 MeV). Measurements of these authors in the range of 1.3 - 3.6 MeV are in progress but yet unpublished.

For a more detailed discussion see [1,2,10]

II.1. Energy scales

Gamma ray energies are generally measured in one of two energy scales, the reference energies being

- the electron rest-mass energy, m_0c^2
- the wavelength of the $K\alpha_1$ X-ray from tungsten.

The work [1,2] is based on the most recent adjustment of fundamental constants by Taylor et al. [3], yielding a value for $m_o c^2$ of:

$$E(m_o c^2) = 511.0041 \pm 0.0016 \text{ keV } (\pm 3.1 \text{ ppm})$$

For crystal spectrograph measurements it is necessary to convert wavelength's measured in X-units into Å. It is agreed to fix the tungsten $K\alpha_1$ line at:

$$\lambda(W\ K\alpha_1) = 208.5770 \text{ XU}$$

There are several conflicting results for the conversion of XU to Å (see discussion by Marion [4]). The best agreement between the $WK\alpha_1$ and $m_o c^2$ based energy scales was reached (see ref. [1] for detailed discussion) using the following readjusted conversion factors:

$$\Lambda = 1.0020960 \text{ mÅ/XU } (\pm 5.3 \text{ ppm})$$
$$E = 12398.541 \pm 0.041 \text{ eV} \cdot \text{Å}$$

yielding the energy (eV) of the W $K\alpha_1$ line:

$$E(W\ K\alpha_1) = 59.31918 \pm 0.00035 \text{ keV } (\pm 5.9 \text{ ppm})$$

The most recent results of direct comparisons of the 412 keV Au-198 γ-ray by Murray et al [5,6] with $m_o c^2$ were adjusted by Greenwood et al. to the new value for $m_o c^2$. The result is:

Au-198: 411.794 ± 0.008 keV (± 19 ppm)

II.2. Standards and accuracies

Primary standards are defined as transition energies determined in a direct comparison with the W-$K\alpha_1$ line or the Au-198 412 keV γ-line.

Secondary standards are those calibrated against a primary standard.

It is evident that a measurement of a γ-ray energy is actually a measurement of the energy difference between the gamma line investigated and the standard used. Thus in such a measurement 3 types of errors are involved:

(1) The statistical error in the determination of the location of the γ-peak.

(2) The error in the measurement of the energy difference including the determination of the location of the reference peak and the nonlinearity of the scale.

(3) The uncertainty of energy value of the reference line.

Errors (1) and (2) combined yield the error of the measured energy difference, their composition with error (3) gives the absolute error of the measured γ-ray energy.

This has two consequences:

- The energy of any γ-line cannot be more accurate than that of the standard used. In particular: primary standards are less accurate than either the Au-198 412 keV γ-line or the W $K\alpha_1$ X-ray, and secondary standards cannot be more accurate than primary standards.

- The same is true for a (weighted or unweighted) average obtained in an evaluation. If in several high precision measurements errors (1) and (2) are considerable smaller than error (3), the average may have lower uncertainty than the standard originally used. Therefore in principle it is the energy differences together with the combined error of (1) and (2) that should be used in weighted averages, then the absolute value of the energy standard added and the combined error calculated by the evaluator.

II.3. Set of selected energy standards

Energy calibration standards are collected in table I. Only primary and secondary standards are included.

Below 1300 keV:

As Greenwood et al [1] and Helmer et al [2] have evaluated energy differences and have also adjusted other results of direct comparisons and included them in their set of recommended calibration energies, their values up to 1.3 MeV are preferred and reproduced here. Exceptions are the Th-228 d (Pb-212) 238.6keV γ-ray (adjusted to the new value for Au-198), the Th-228d (Tl-208) 510.7 keV γ-ray and the Ra-228d (Ac228) 911 keV γ-ray which are taken from Marion's evaluation [4].

Above 1300 keV:

The energy of the Co-60 1332 keV γ-ray is the unweighted average of the re-adjusted data of Murray et al [6] (as adjusted by Helmer et al [2]) and Gunnik et al [8] (adjusted here: difference between double escape peak at 310.5 keV and Ir-192 γ-lines at 308.4 and 316.5 keV. The uncertainty of ± 15 eV quoted by Gunnik et al [8] is based on the uncertainties of the Ir-192-lines adjacent to the double escape peak.

Helmer et al [7] and Gunnik et al [8] have pointed out that acceleration of photo electrons in the detector by the electric field causes a peak shift depending on the direction of the incoming γ-ray relative to the electric field and the γ-ray energy. This peak shift was determined to be ~10 eV for ~500keV photons [8] and ~200 - 300 eV for ~2 MeV photons [7,8]. The field effect on a positron is of opposite sign and exceeds that on the electron slightly (see[8]). Thus a comparison of double escape peaks with neighbouring full energy peaks may yield erroneous results. This can be avoided if gamma rays enter the detector perpendicule to the field. When using data from such measurements, attention has to be payed to this.

Further, it has been pointed out [7] that positrons annihilate with slightly bound electrons and the annihilation gammas have an energy slightly less than m_0c^2. This effect was determined [7] to be about 15 eV, which is the error of the 1.3 MeV Co-60 γ-ray measured by Gunnik et al. [8]. Therefore only the unweighted averages of the two measurements are taken:

1332.515 ± 0.015	[8]	
1332.491 ± 0.041	[6,2]	
1332.503 ± 0.030		Co-60

In this case the assigned error of the energy differences and also the uncertainty of the average exceed that of the standards used and thus the uncertainty is acceptable.

Table I: ENERGY CALIBRATION STANDARDS

Since Co-56 is a convenient standard, all γ-rays emitted in the decay of this nuclide are ..luded, although some are of lower accuracy than others of similar energy.

Note: d arter mass numbers mean: γ-rays from daughter products in secular equilibrium with the nuclides listed.

Nuclide	Energy (keV)	Nuclide	Energy (keV)
Ta-183	52.596 ± 0.001	Ce-141	145.440 ± 0.003
W($K\alpha_1$-X)	59.31918 ± 0.00035	Ta-182	152.434 ± 0.002
Am-241	59.537 ± 0.001	Ta-182	156.387 ± 0.002
Se-75	66.055 ± 0.009	Au-199	158.370 ± 0.003
Ta-182	67.750 ± 0.001	Os-185	162.854 ± 0.008
Sm(Gd)-153	69.676 ± 0.002	Ce-139	165.853 ± 0.007
Ba-133	80.998 ± 0.008	Ta-182	179.393 ± 0.003
Ta-183	82.919 ± 0.001	Fe-59	192.344 ± 0.006
Tm-170	84.254 ± 0.003	Ta-183	192.646 ± 0.005
Ta-182	84.680 ± 0.002	Ta-182	198.356 ± 0.004
Ta-183	84.712 ± 0.002	Se-75	198.596 ± 0.007
Cd-109	88.037 ± 0.005	Tc-95m	204.117 ± 0.005
Se-75	96.733 ± 0.002	Au-199	208.196 ± 0.005
Gd-153	97.432 ± 0.003	Lu-177	208.362 ± 0.010
Ta-183	99.080 ± 0.002	Ta-182	222.110 ± 0.003
Ta-182	100.105 ± 0.001	Ta-182	229.322 ± 0.006
Sm(Gd)-153	103.180 ± 0.002	Os-185	234.158 ± 0.010
Ta-183	107.932 ± 0.001	Th-228 d	238.623 ± 0.009
Lu-177	112.954 ± 0.003	Tc-95 m	253.066 ± 0.006
Ta-182	113.673 ± 0.002	Ta-182	264.072 ± 0.006
Ta-182	116.418 ± 0.002	Se-75	264.651 ± 0.008
Se-75	121.115 ± 0.003	Ba-133	276.397 ± 0.012
Co-57	122.063 ± 0.004	Hg-203	279.188 ± 0.006
Os-185	125 358 ± 0.004	Se-75	279.528 ± 0.008
Se-75	136.000 ± 0.005	Ta-183	291.724 ± 0.006
Co-57	136.473 ± 0.004	Ir-192	295.949 ± 0.006
Fe-59	142.648 ± 0.004	Tb-160	298.572 ± 0.006
Ta-183	144.127 ± 0.002	Ba-133	302.851 ± 0.015

Table I: (cont.)

Nuclide	Energy (keV)	Nuclide	Energy (keV)
Se-75	303.913 ± 0.007	Nb-94	702.627 ± 0.019
Ir-192	308.445 ± 0.007	Ag-110m	706.660 ± 0.018
Ir-192	316.497 ± 0.007	Os-185	717.424 ± 0.018
Cr-51	320.078 ± 0.008	Zr-95	724.184 ± 0.018
Ta-183	353.999 ± 0.004	Ag-110m	744.250 ± 0.018
Ba-133	356.005 ± 0.017	Zr-95	756.715 ± 0.019
Ta-183	365.615 ± 0.007	Ag-110m	763.929 ± 0.018
Ba-133	383.851 ± 0.020	Nb-95	765.786 ± 0.019
Sn-113	391.688 ± 0.010	Tc-95m	786.184 ± 0.017
Se-75	400.646 ± 0.009	Co-56	787.79 ± 0.06
Pb-203	401.315 ± 0.013	Co-58	810.757 ± 0.021
Au-198	411.794 ± 0.008	Ag-110m	818.006 ± 0.020
Ag-110 m	446.790 ± 0.018	Tc-95 m	820.608 ± 0.019
Ir-192	468.062 ± 0.010	Mn-54	834.827 ± 0.021
Be-7	477.593 ± 0.012	Tc-95m	835.132 ± 0.018
Ir-192	484.570 ± 0.011	Co-56	846.751 ± 0.019
Th-228d	510.721 ± 0.020	Nb-94	871.099 ± 0.018
$m_o c^2$	511.0041 ± 0.0016	Os-185	874.814 ± 0.019
Sr-85	513.996 ± 0.016	Tb-160	879.364 ± 0.018
Bi-207	569.689 ± 0.013	Os-185	880.272 ± 0.019
Tc-95m	582.068 ± 0.013	Ir-192	884.523 ± 0.018
Th-228d	583.174 ± 0.013	Ag-110m	884.662 ± 0.019
Ir-192	588.572 ± 0.012	Sc-46	889.258 ± 0.018
Os-185	592.066 ± 0.014	Y-88	898.021 ± 0.019
Ir-192	604.401 ± 0.012	Ra-228d	911.07 ± 0.07
Ir-192	612.450 ± 0.013	Ag-110m	937.468 ± 0.020
Ag-110m	620.305 ± 0.018	Tb-160	962.295 ± 0.020
Os-185	646.111 ± 0.017	Tb-160	966.151 ± 0.020
Ag-110m	657.631 ± 0.016	Co-56	977.46 ± 0.06
Cs-137	661.638 ± 0.019	Co-56	1037.86 ± 0.06
Au-198	675.871 ± 0.018	Tc-95m	1039.247 ± 0.022
Ag-110m	677.590 ± 0.020	Bi-207	1063.635 ± 0.024
Pb-203	680.495 ± 0.017	Au-198	1087.663 ± 0.024
Ag-110m	686.965 ± 0.020	Fe-59	1099.224 ± 0.025

Table I: (cont.)

Nuclide	Energy (keV)	Nuclide	Energy (keV)
Zn-65	1115.518 ± 0.025	Ag-110m	1504.983 ± 0.032
Sc-46	1120.516 ± 0.025	Ag-110m	1562.252 ± 0.033
Ta-182	1121.272 ± 0.026	La-140	1596.217 ± 0.040
Co-60	1173.208 ± 0.025	Sb-124	1691.028 ± 0.040
Co-56	1175.15 ± 0.08	Bi-207	1769.71 ± 0.13
Tb-160	1177.934 ± 0.024	Co-56	1771.53 ± 0.07
Ta-182	1189.022 ± 0.027	Y-88	1836.13 ± 0.04
Ta-182	1221.376 ± 0.027	Co-56	1963.93 ± 0.07
Ta-182	1230.989 ± 0.028	Co-56	2015.30 ± 0.06
Co-56	1238.31 ± 0.05	Co-56	2034.92 ± 0.07
Ta-182	1257.390 ± 0.028	Co-56	2113.36 ± 0.08
Tb-160	1271.850 ± 0.026	Ce-Pr-144	2185.32 ± 0.05
Ta-182	1273.703 ± 0.028	Co-56	2598.52 ± 0.06
Na-22	1274.511 ± 0.028	Th-228d	2614.611 ± 0.060
Ta-182	1289.126 ± 0.029	Na-24	2754.10 ± 0.07
Fe-59	1291.564 ± 0.028	Co-56	3009.80 ± 0.07
Co-60	1332.503 ± 0.030	Co-56	3202.20 ± 0.07
Co-56	1360.24 ± 0.06	Co-56	3253.56 ± 0.06
Na-24	1368.650 ± 0.050	Co-56	3273.18 ± 0.07
Ag-110m	1384.250 ± 0.028	Co-56	3451.24 ± 0.08
Ag-110m	1475.734 ± 0.032	Co-56	3548.21 ± 0.26
Ce-Pr-144	1489.14 ± 0.07		

Sources of other data:

Bi-207, 1770 keV: Marion [4]

Y-88, Na-24, Th-228 d: Heath [9]

Co-56: Kern [10]

Ag-110 m: weighted average of [2,7] and [10]; the weighting and the overall uncertainty was obtained as discussed above.

La-140, Sb-124: Gunnik [8], corrected for reference energies (table I). Reservations with respect to the precise energy values and the quoted uncertainties have been discussed above.

III. STANDARDS FOR DETECTOR EFFICIENCY CALIBRATION

The standards shown in table II are only primary standards. Primary standards are nuclides for which the values for absolute gamma ray branching can be calculated from the decay scheme with high confidence. Thus the selected values do not depend on a previous detector efficiency calibration. The values used depend only on:

- values for beta ray branching;
- internal conversion coefficients;
- in some cases on relative intensities of weaker γ-rays feeding or depopulating the same level, as the γ-ray listed; however, the uncertainty of the intensity of the weak gamma rays does not severely influence the uncertainty of the primary γ-ray.

It is common practice to obtain a detector efficiency curve by interpolating between and extrapolating beyond calibration points or by fitting a theoretical curve. While this is the only reasonable way to determine the detector efficiency and the assumption of a smooth curve is supported by theoretical considerations, it has to be born in mind that the detector efficiency is known only at, and close to, the calibration point with the accuracy of the standard used. This is not the case, however, for energy ranges not covered by standards, as, e.g., the range 136 keV - 265 keV or 900 keV - 1.2 MeV etc. in table II, where the value of the efficiency depends on how the curve was obtained. Therefore the uncertainty of the detector efficiency in this range has to be estimated, but must be larger than in the vicinity of calibration points.

It can be observed quite frequently that experimenters quote a common uncertainty for the whole efficiency curve. This uncertainty is often the same as, sometimes even better than (in the case of a fit), that of the standards used, neglecting the facts pointed out above. These observations have several important consequences:

a) Uncertainties quoted by measurers sometimes differ widely although experimental conditions were similar. Therefore the evaluator should check the calibration standards used, how the uncertainty of the efficiency curve was determined and whether the quoted errors of measured γ-ray intensities are reasonable. If necessary, he should assign errors according to his own judgement before taking an average.

Table II: STANDARDS FOR DETECTOR EFFICIENCY CALIBRATION

Nuclide	Energy(keV)	Intensity(%)	I_γ (%)	Ref.	Note	Parent
Am-241	59.537	35.3 ± 0.5	1.4	11	a	
Hg-203	74.6	12.8 ± 0.2	1.6	11	a	
Co-57	122.063	85.6 ± 0.2	0.23	11	b	
Co-57	136.473	10.6 ± 0.2	1.9	11	c	
Ni-56	158.3	98.7 ± 0.1	0.1	11	b	
Se-75	264.651	59.1 ± 0.2	0.34	11	b	
Hg-203	279.188	81.5 ± 0.2	0.25	11	b	
I-131	364.49	82.4 ± 0.5	0.61	11	a,b	
Au-198	411.794	95.53± 0.05	0.05	11	b	
Na-22	511.004	181.08± 0.04	0.022	11	b	
Sr-85	513.996	99.28± 0.01	0.01	11	b	
Sb-124	602.71	98.2 ± 0.1	0.1	11	b	
Cs-137	661.638	84.6 ± 0.4	0.47	11	b	
Nb-95	765.786	99.80± 0.04	0.04	11	b	Zr-95
Co-58	810.757	99.44± 0.02	0.02	11	b	
Mn-54	834.827	99.978±0.002	0.002	11	b	
Co-56	846.751	99.974±0.001	0.001	11	b	
Y-88	898.021	93.4 ± 0.7	0.75	11	a	
Co-60	1173.208	99.86± 0.02	0.02	e)	b	
Na-22	1274.511	99.95± 0.07	0.07	11	b	
Co-60	1332.503	99.986±0.001	0.001	e)	b	
Na-24	1368.650	100	-	11	b,d	
La-140	1596.20	95.6 ± 0.3	0.3	11	b	Ba-140
Y-88	1836.13	99.37± 0.02	0.02	11	b	
Na-24	2754.10	99.85± 0.02	0.02	11	b,d	

a ... The accuracy of the intensity is less than 0.5% of the value. However, there is no other more suitable standard in this energy range.

b ... High accuracy intensity value calculated from level scheme.

c ... Low accuracy, but reliable; as calculated from level scheme.

d ... Limited usefulness because of short half life and/or difficult to produce.

e ... β^- branch to 2505.7 keV level: 99.88 ± 0.02%; no β^- to ground state
1173 keV transition: I_T = 99.88 ± 0.02 %, $\alpha_T = 1.7 \times 10^{-4}$
ground state transitions: 2158 keV (I_γ = 0.0012 %) and 1332 keV
1332 keV transition: I_T = 99.9988 %, $^{\gamma}\alpha_T = 1.3 \times 10^{-4}$

b) In principle, a measurement of a gamma ray intensity is always relative to a standard. Similar to γ-ray energies, 3 types of errors are involved in such a measurement and the evaluator should proceed as proposed in II.2. However, the main difference is that an additional error is that of the activity of the standard at the time of measurement, which is composed of the errors of the determination of its activity at the time of preparation, the γ-ray absorption in the sample cover and the decay correction for the time elapsed between preparation of the standard and the time of measurement. in most practical cases this error exceeds that of the absolute γ-ray intensity if primary standards are used. However, the evaluator should take care that his recommended value, if determined with a calibrated detector and not deduced from a level scheme, is reasonably larger than the intensity of primary standards.

c) Consequently, even relative γ-ray intensities cannot be more accurate than the absolute intensities of standards listed in table II, if a calibrated γ-ray detector is employed.

d) Absolute γ-ray intensities measured close to a calibration point obtained from a standard can be corrected by an evaluator, if more accurate data for the standard are available. This is, however, hardly possible for measurements of γ-ray intensities in an energy range not covered by standards, as it is uncertain, how the efficiency curve was obtained, unless it is given numerically.

For the reasons given above a reliable set of primary standards as given in table II is recommended for use. However, in many practical applications it is more convenient to calibrate the detector with a standard source emitting a large number of prominent γ-rays. This has the advantage of being fast and covering a large range of the efficiency curve. Then the user has to bear in mind the limited accuracy of the data.

Since the activity of efficiency calibration sources has to be corrected for decay, pertinent half-life data are given in table III.

REFERENCES:

[1] R.C. Greenwood, R.G. Helmer, R.J. Gehrke, Nucl. Instr. Meth. 77 (1970) 141

[2] R.G. Helmer, R.C. Greenwood, R.J. Gehrke, Nuclear Instr. Meth. 96 (1971) 173

[3] B.N. Taylor, W.H. Parker, D.N. Langenberg, Rev. Mod. Phys. 41 (1969) 375

[4] J.B. Marion, Nuclear Data A4 (1968) 301

[5] G. Murray, R.L. Graham, J.S. Geiger, Nucl. Phys. 45 (1963) 177

[6] G. Murray, R.L. Graham, J.S. Geiger, Nucl. Phys. 63 (1965) 353

[7] R.G. Helmer, R.C. Greenwood, R.J. Gehrke, ANCR-1016 (1971) 403

[8] R. Gunnik, R.A. Meyer, J.B. Niday, R.P. Anderson, Nucl. Instr. Meth. 65 (1968) 26

[9] R.L. Heath, "Table of Isotopes", Handbook of Chemistry and Physics, 54th edition 1973-1974 (Chemical Rubber Co.), page B-248.

[10] J. Kern, IAEA Panel on Charged-Particle Induced Radiative Capture, Vienna, October 1972, Proceedings page 345.

[11] M.J. Martin, P.H. Blichert-Toft, Nuclear Data A8 (1970) 1

[12] J.F. Emery et al., Nucl. Sci. Engg. 48 (1972) 319

[13] M.J. Cabell, M. Wilkins, J. inorg. nucl. Chem. 32 (1970) 1409

[14] K.F. Walz, H.M. Weiss, Z. Naturf. 25a (1970) 921

[15] J.S. Merrit, J.G.V. Taylor, AECL-3512 (1969) 30

[16] S. Baba et al., J. inorg. nucl. Chem. 33 (1971) 589

[17] K. Debertin, Z. Naturf. 26a (1971) 596

[18] M. Lammer, "Evaluations performed for the SGAE fission product nuclear data file", Contribution to Review paper no. 12, this Panel.

Table III: HALF LIVES
(sorted by mass number)

Nuclide	Half-life [a]	Ref.	Nuclide	Half-life [a]	Ref.
Na-22	2.60 ± 0.01 a	11	Zr-95	63.98 ± 0.06 d	17
Na-24	15.030± 0.003 h	12	Nb-95	35.045± 0.005 d	15
Mn-54	312.5 ± 0.5 d	11	Sb-124	60.20 ± 0.02 d	11
Co-56	78.76 ± 0.12 d	12	I-131	8.040± 0.001 d	12
Ni-56	6.1 ± 0.1 d	11	Cs-137	30.17 ± 0.10 a	18
Co-57	269.8 ± 0.4 d	12	Ba-140	12.789± 0.006 d	16
Co-58	71.3 ± 0.2 d	11	La-140	40.27 ± 0.05 h	11
Co-60	5.272± 0.002 a	14	Au-198	2.6946± 0.0010 d	13
Se-75	120 ± 1 d	11	Hg-203	46.59 ± 0.05 d	11
Sr-85	64.5 ± 0.5 d	11	Am-241	433 ± 2 a	11
Y-88	107 ± 1 d	11			

a) Half life units: h = hours, d = days, a = years

EVALUATIONS PERFORMED FOR THE SGAE FISSION PRODUCT NUCLEAR DATA FILE

M. Lammer

Nuclear Data Section, Div. of Research and Laboratories

International Atomic Energy Agency
Vienna, Austria

Abstract:

A brief description of the SGAE fission product nuclear data file was given in [1] and recommended data tabulated without details. This paper discribes how the evaluation of half lives, γ-ray energies and absolute intensities and decay branching ratios was performed. References used for these data are listed and individual evaluations of half lives and branching ratios are tabulated together with the experimental data used.

1. INTRODUCTION

The investigations performed at SGAE are outlined in [1]. They are restricted to applications using fission products with half lives of one day and more, that can be measured gamma spectrometrically. In order to check the capability of predictions by computer calculations over a wide range of irradiation conditions, test samples of fissile material were irradiated for short times (~ hours). Therefore fission products with half lives of several hours that can be measured gamma-spectrometrically were also included recently.

No literature search for gamma rays was performed for fission products with half lives of less than 1 day. These data were taken from other surveys. The most recent update incorporates the data of Tobias [2].

The purpose of the gamma ray table is to enable calculation of fission product activities from measured gamma spectra. The table of gamma rays sorted by energy serves to facilitate the identification of measured gamma rays.

2. STATUS

Nuclear Data "Recent References" were scanned regularily up to issue 5/4 (April 1971). Pertinent data found in this journal series were incorporated into the evaluation if available. As the author left the SGAE to join the IAEA in October 1971, the regular literature scan and update of the library stopped. Occasionally new data were incorporated, only the half life data are fairly complete up to "Recent References" autumn 1972. For this paper new half life data found until end of 1973 are included in Appendix B.

Some new references found for gamma ray data are not yet evaluated and incorporated into the file.

3. UNCERTAINTIES

3.1. Weighted average

If experimental results (including errors) belong to the same distribution, then the quoted errors to be used for weighting should be proportional to the true errors. The standard deviation of the weighted mean can be calculated from:

$$\bar{S}_1 = \left(\sum \frac{1}{s_i^2}\right)^{-\frac{1}{2}} \qquad (1)$$

where s_i are errors of individual measurements.

As a consequence the deviations of the individual values (x_i) from the mean ($\bar{x}$) should have the same distribution as the s_i. This can be tested for a set of n data by:

$$\left(\frac{\sum \frac{(x_i - \bar{x})^2}{s_i^2}}{n-1} \right)^{\frac{1}{2}} = 1 \pm \left(\frac{2}{n-1}\right)^{\frac{1}{2}} \qquad (2)$$

In statistics (2) is called the Chi-quared test, if the distribution of the x_i is gaussian.

In this evaluation also an uncertainty $\bar{S}_2$ is calculated from (3):

$$\bar{S}_2 = \left(\frac{\sum \frac{(x_i - \bar{x})^2}{s_i^2}}{n-1} \right)^{\frac{1}{2}} \times \left(\sum \frac{1}{s_i^2}\right)^{-\frac{1}{2}} \qquad (3)$$

The larger value of $\bar{S}_1$ and $\bar{S}_2$ is taken as estimate of the uncertainty of the weighted average.

This is not strictly valid: The additional factor in (3) (compared to (1)) can be interpreted as the mean error of individual measurements leading to each $x_i \pm s_i$ used in the evaluation, assuming identical conditions and purely random errors. This is, however, not the case: Generally measurements suffer also from systematic errors. These systematic errors are only partially independent , sometimes not taken into account by experimenters or unknown, but in any case not common to all experiments and not random.

Therefore, if the left hand side of (2) is larger than 1, the weights used are not correct and, strictly speaking, should be changed accounting for systematic errors. However, in practice systematic errors are not known to the evaluator. The evaluator can reduce the weight of individual data by estimating systematic errors according to his own judgement or combine quoted errors with the common factor in equation (3). Then he runs the risk of treating very accurate results injustly. Or he calculates the weighted average and its uncertainty from equation (3). Then the uncertainty reflects discrepances reasonably, but the average itself may be wrong as some high precision data, which have undetected systematic errors, receive too high weight. Basically the latter approach is chosen in this evaluation as discussed in more detail below.

3.2. Unweighted average

The standard deviation of the unweighted average is calculated from the well known relation:

$$\bar{S}_1 = \left(\frac{\sum (x_i - \bar{x})^2}{n \cdot (n-1)} \right)^{\frac{1}{2}} \qquad (4)$$

The unweighted average is sometimes calculated in cases where some of the data are given without errors. If the uncertainty has to be estimated from an unweighted average, also $\bar{S}_2$ is calculated from:

$$\bar{S}_2 = \left(\sum_{i=1}^{m} \frac{1}{S_i^2} \right)^{-\frac{1}{2}} \cdot \left(\frac{m}{n} \right)^{\frac{1}{2}} \qquad (5)$$

m ..... number of data with quoted errors

n ..... total number of data used for unweighted average.

Again the larger value of $\bar{S}_1$ and $\bar{S}_2$ is used as uncertainty in order to avoid too small values caused by chance effects.

4. SELECTION OF VALUES

In some cases selected values were considered superior to others, or data were taken from other evaluations. These are the "recommended" data of half-lives and branching ratios for which individual evaluations are not reproduced and the references are given in appendix A. In the evaluation procedure data were omitted if they were either of low accuracy or if they disagreed drastically with a more consistent set of other data, rather than using equation (3).

Both, the selection of "superior" data and the omission of discrepant values might be considered somewhat problematic, as in many cases the experiments have not been studied in detail. However, if one value has much higher precision than others, these other data will have no influence on a weighted average. In the case of discrepancies it is often not possible to resolve them by studying publications of measurements. To take a weighted average is not a satisfactory solution. This can be supported by arguments of statistics and theory of error analysis, but this is beyond the scope of this paper. From a practical standpoint the following consideration is illustrative: It is not possible to clarify discrepancies by additional measurements, if all data are included in a weighted average. The addition of a new measurement will not improve the uncertainty to the level of experimental accuracy and the average will still not clearly be in favour of one group of results. A good example is the half-life of Cs-137 (see appendix B) where the successive addition of the data of Wal70, Eme72 and Die73 caused an oscillation of the average around 30 years and did not improve the uncertainty.

In this work the following criteria were adopted in the selection of preferred data:

- If data obtained in measurements employing different methods were found to be consistent, it can be assumed that a systematic error due to the method itself can be excluded, and inconsistent data were discarded.

- Data from laboratories that are known to produce reliable results and perform a thorough check of systematic errors were preferred.

- Criteria such as superior method or very thorough performance were adopted in some cases.

5. HALF-LIVES AND BRANCHING RATIOS

Half lives of several fission products evaluated in [3] are used in the SGAE file. If more recent experimental data not included in [3] became available, a new average was calculated using the results of earlier experiments as published in [3]. Half lives of other fission products were obtained from a literature search and evaluated. Sources of adopted values are listed in appendix A, detailed evaluations are reproduced in appendix B.

For each set of data a weighted and an unweighted (using equation (4) only) average is calculated. Final values are adopted from an inspection of the results, sometimes according to the criteria discussed in section 4. The calculated uncertainties were generally increased to account for observed discrepancies and to obtain a higher confidence level. Accordingly, if the result of one author was adopted, the quoted error was doubled if it corresponded to 1 standard deviation, but remained unchanged if it was given as an overall uncertainty or at least 2 standard deviations.

6. GAMMA-RAY DATA

As discussed in another contribution [4] to review paper 12 of this Panel, the uncertainties assigned by experimenters to measured gamma-ray intensities do not follow common criteria and have to be checked. Therefore the calculation of gamma ray intensities varies in this evaluation. Sometimes weighted averages are calculated using quoted uncertainties. In cases where the quoted uncertainties differed significantly among each other, the publications were checked more carefully (especially the spectra shown) and reasonable weights assigned accordingly. If data appeared to be equally accurate, unweighted averages were taken.

Often averages for intensities were calculated by different methods and the results were checked against the input data. Finally the method was chosen that best reflected the input data. Accuracies were not allowed to be higher than those of commonly used standards.

Absolute intensities were calculated in 3 different ways:

- the absolute intensity for one gamma ray was taken from other evaluations.

- Or it is calculated from results of direct measurements.

- Or they are calculated from the level scheme, generally from an intensity balance of all transitions feeding the ground state. In this case the fitted relative gamma ray intensities were used together with the beta transition to the ground state and, where necessary, with internal conversion coefficients supplemented by relative conversion electron intensities.

For the applications discussed in [1] gamma ray energies have to be known to $\pm$ 0.1 to 0.2 keV. This is generally satisfied by experimental and evaluated data. The evaluation of γ-ray energies is only a byproduct of the evaluation of intensities, using the same computer programme. A weighted average is calculated from selected data. In cases of very high accuracy the standards and energy scale used were also checked. As the uncertainties of γ-ray energies are insignificant for the applications described in [1], they were not evaluated as discussed in [4], but calculated according to equation (3). They should therefore not be used, if reliable uncertainties are required.

References:

[1] O.J. Eder, M. Lammer, IAEA Symposium on Nuclear Data in Science and Technology, Paris, March 1973, proceedings Vol. I, page 233.

[2] A. Tobias, CEGB (UK) report RD/B/M2669 (1973)

[3] M.J. Martin, P.H. Blichert-Toft, Nuclear Data A8 (1970) 1

[4] M. Lammer, "Standards for Calibration of Semiconductor Detectors", Contribution to review paper no. 12, this Panel.

Appendix A: SOURCES OF ADOPTED DECAY DATA

Half lives

AS-77	S. A. Reynolds, Nucl. Sci. Engg. 32 (1968) 46
Kr-85	[3] and D. Horen, Nucl. Data Sheets 5/2 (1971)
Sr-90	Weighted average of [3]
Sr-91	J.D. Knight et al., Nucl. Phys. A130 (1969) 433
Zr-95	K. Debertin, Z. Naturf. 26a (1971) 596
Nb-95m	[3]
Nb-95	J.S. Merritt and J.G.V. Taylor, AECL-3512, page 31 (1969)
Zr-97	KFK Chart of Nuclides (1968), estimated uncertainty
Ru-103	K. Debertin, Z. Naturf. 26 a (1971) 596
Rh-105	Y. Kobayashi, JAERI-1178 (1969) 21
Ru-106	weighted average of [3]
Pd-109	Nucl. Data B6/1 (1971)
Ag-110m	J.F. Emery et al., ORNL-4466 (1970) page 75
Ag-111	[3]
(Pd-Ag)-112	S. Raman and H.J. Kim, Nucl. Data Sheets 7/1 (1972)
Cd-115 g	S. Baba et al. J. inorg. nucl. Chem. 33 (1971) 589
Sn-121m	Nucl. Data Sheets 6/1 (1971)
Sn-121	From data shown by Erdal et al., J. inorg. Nucl. Chem. 30(1968) 1985
Sn-123	see Sn-121
Sb-124	[3]
Sn-125	see Sn-121
Te-125 m	[3]
Sb-126, Sb-127	E. Hagenbø, J. inorg. nucl. Chem. 29 (1967) 2515
Te-127m	G. Andersson et al. Ark. Fys. 28 (1965) 37
Te-131m	D.G. Sarantites et al, Phys.Rev. 138 (1965) B353 (30± 2 h)
(Te-I)-132	weighted average of [3]
Xe-133g	J.F. Emery et al, Nucl. Sci. Engg. 48 (1972) 319
(I-Xe)-135	R. Hawkings et al., Can.J. Phys. 49 (1971) 785
Cs-136, Ba-140	Baba, see Cd-115 g
La-140	[3]
Pr-142	Radiochim. Acta 9 (1968) 66
Ce-143	Lederer et al., Table of Isotopes (1967)
Ce-144	unweighted average of [3]
Pm-147	[3]

Pm-148m	R.S. Mowatt, W.H. Walker, Can.J.Phys. 49(1971) 108
Pm-148	M.J. Cabell, M. Wilkins, J.inorg. nucl. Chem. 32(1970) 1409
Pm-151	L.R. Bunney et al., J. inorg. nucl. Chem. 12 (1960) 228
Eu-154	Emery et al. (see Ag-110m)
Eu-157	W.R. Daniels and D.C. Hofmann, J. inorg. nucl. Chem. 28 (1966) 2424

For others see Appendix B.

Branching ratios:

Kr-85 → Kr-85	F.K. Wohn et al. Nucl. Phys. A152 (1970) 561
Mo-99 → Tc-99m	[3]
Ag-110m	Nuclear Data B 5/5 (1971) 494
Sb-125 → Te-125m	[3]
Sb-127 → Te-127m	B.R. Erdal et al. J.inorg. nucl. Chem. 31(1969) 2993
Te-127m → I-127	K.E.Apt et al., Nucl. Phys. A152(1970) 344
Sb-129 → Te-129m	Erdal et al. (see Sb-127)
I-131 → Xe-131m	[3]

For others see Appendix B

Gamma line table

Because of their considerable length, the gamma line table and individual evaluations cannot be reproduced here. References used for gamma ray data are shown and calculations of absolute intensities are indicated.

Abbreviations:

E	gamma ray energy (given numerically in KeV)
I_r	relative intensities
I_a	absolute intensities (or: I, if energy is given in brackets)
wa	weighted average
ua	unweighted average
avg	weighted and unweighted average
eval	evaluation or compilation, evaluated
equ	equilibrium
act	activity

trans ... transition
gs ..... ground state
IT ..... internal transition
br ..... branching ratio
α ..... conversion coefficient

Explanations:

If neither of wa, ua or avg is given, best values have been selected from an eye-inspection of experimental data.

Underlined references are preferred for several reasons:

E: The authors have made measurements of higher accuracy than the others shown or have made a careful calibration. Other measurements shown have sometimes comparable accuracy or/and are the only ones.

Ir: Contrary to E, accuracies are not so much different, at least for gammas of higher intensities. However, some authors (underlined) have measured with higher accuracy (using different detectors and methods) and better resolution (important for doublets, better enhancement of weak lines above background) and/or performed better calibration. Their data are preferred in cases of discrepancies, particularly for weak gamma rays. Other references listed are also used, those shown in brackets were often discarded.

Ge-77 eval Tob73

As-77 E: wa of Yth66, Ard68 and Sar69
I_r: wa of Yth66 and Ard68
I_a: I(239+250) = 2% (eval Art66)

Br-82 E: wa of Mer70 and Rei64
I_r: wa of Mer70, Ram70, Ram67 and Liu69
I_a: I(776.5+1426) = 100%

Kr-85m eval Tob73

Kr-85 E: Hel71 (from Sr-85 decay, see eval Lam73)
I_a: wa of Rid60, Gei61, Lyo61, Eas64, Den67, And66a and Nak66

Rb-86 E: wa of Har63, Mar65, Noo65 and Pie67
I_a: wa of Lyo54, Eme55, Cam60, Bra62, Gup65 and And66

Sr-89 eval Mar70

Sr-91 eval Tob73

Y-91 eval Mar70

Y-92 eval Tob73

Y-93 eval Tob73

Zr-95 E: Hel71 (see eval Lam73)
I_r: wa of Bru65, Bro67, Tsa66, Leg67b, Eme68, His68, Bra69 and Foi69
I_a: β^- to gs = 0.4±0.2%, β^- to Nb-95m = 0.84±0.26% (Appendix B)

Nb-95m E: wa of Leg67b, Bra69 and Foi69
I_a: from α_T (see Appendix B)

Nb-95 E: Hel71 (see eval Lam73)
I_a: eval Mar70

Zr-Nb-97 eval Tob73 (I calculated for equilibrium)

Mo-99 E: wa of Mai65,Eij68,Bas69 and Coo69
I_r: wa of Eij68 and Coo69
I_a: eval Mar70

Ru-103 E,I_r: wa of Kar64,Man68,Rae69,Zol69 and Pet 70
I_a: eval Mar70

Ru-105 eval Tob73

Rh-105 E: wa of Kar64,Pie65,Sch67 and Kaw70
I_r: wa of Pie65,Sch67,Kob67 and Odr69
I_a: I(319) wa of Sch67,Pie65 and Odr69

Ru-Rh-106 E: wa of Sch64,Rob65,For67,Rao67 and Str69
I_r: wa of For67,Rao67,Vrz67, Odr69 and Str69
I_a: Odr69

Pd-109 eval Tob73

Ag-110m in equilibrium with Ag-110g
E: wa of Hel71,Ker72, (see eval Lam73),Bra69a,eval Tob73
I_r: wa of Ber67,Leg67,Mor67,Bra69a and Aub69
I_a: in equ is 100 - 1.4%(β^- to gs) = I(658+1476) to gs (α_γ of Mor67)

Ag-111 eval Mar70

Pd-112 eval Tob73

Ag-112 eval Tob73

Cad-115m eval Tob73

Cad-115 in equ with In-115m: act (In) = 1.092×act(Cd)× %IT
E (Cd-115): wa of Gra66 and Bae67
E (In-115m): wa of Bae67 and Mur67
I_r: wa of Gra66 and Bae67
I_a: % IT (336) from Gr66, α_γ from Gra66 and Bae67

Sn-121m E: Sny68 Ia: uncertain, as % IT unknown

Sb-122 E: wa of Gfo69 and Spe69 (from I-122 decay)
I_r,I_a: Lag67 and data in N.D. sheets NRC-60-4-85

Sn-123 E: Aub66 and Bae68
I_a: Aub66

Sb-124 eval Mar70; E,Ir: Aue69 (with Ia: eval Mar70)

Sn-125 E,Ir: Wil67
I_a: 100-(β^- to gs [Wil67]) = sum of gammas to gs

Sb-Te-125 eval Mar70 (Te-125m in equ with Sb-125)

Sb-127 E,I_r: Rag67
I_a: from br to Te-127m and level scheme of Rag67

Te-127m E,I_r,I_a: from Apt70 (equ with Te-127g)

Te-129m equ with Te-129g
E,I_r: Dic69
I_a: from level scheme of Dic69

Te-131m equ with Te-131g
E,I_r: Bey67
I_a: from level scheme of Bey67

I-131 eval Mar70

Xe-131m E: eval Mar70
I_a: from br and ce/γ of eval Mar70 (in Mar 70, I_a is given for equ with I-131)

Te-I-132 in equ: act (I) = 1.026±0.001 * act (Te)
Te: eval Mar70
I: E: avg of Ham63, Boy65, Joh65, Ard66, Yth67, Car68, Hen69, Hen69a, Car70 and Qua70
I_r: wav of Car70, Ard67, Hen67 and Hen69 (Ard66, Yth67, Ard69 and Hen69a)
I_a: eval Mar70

I-133 eval Tob73

Xe-133m E: Fra69
I_a: eval Mar70

Xe-133 E: Gre70a, wa of Sie64, Mai65, Thu66, Hen67a, Bar68, Bos68, Don68 and Fra69
I_r: Ale68
I_a: eval Mar70

Cs-134 E: wa of Bro65, Leg67a and Rea67
I_r: wa of Bro65, Leg67a, Rae67, Abd68, Nag68 and Hof70
I_a: trans I(605 + 1168) = 100%, α_T (605) ≈ 0.006

I-135 eval Tob73

Xe-135 eval Tob73

Cs-136 E, I_a: Fra67 (Ia: I(818) = 100%)

Cs-137 E: Gei68 as eval by Hel71 (see also eval Lam73)
I_a: eval Mar70

Ba-140 E: Ker70
I_r: wa of Kal69 and Ker70
I_a: eval Mar70

La-140 E: wa of Bae66, Kar67, Bae68a, Gun68 and Ker70a
I_r: wa of Vrz66, Bae68a and Kal70 (Dzh66, Kar67)
I_a: eval Mar70

Ce-141 E: Gre70a (see eval Lam73)
I_a: eval Mar70

Ce-143 E, I_r: Gre68
I_a: from level scheme of Meg68

Ce-144 E: Gei60, avg of Ant70 and Fas70
I_r: wa of Ant70 and Fas70
I_a: wa of Gra58, Lyo58, Por59 and Sil61 for I(133)

Pr-144 E: wa of Ram68, Say68 and Fas70
I_r: wa of Por59, Mon61, Ram68, Say68 and Fas70
I_a: eval Mar70

Nd-147 E: wa of Hil67, Bae67a and Dou67
I_r: wa of Bae67a, Can67, Dou67 and Hil67
I_a: from Can67

Pm-147 E: Mow70 and Bel71
I_a: Mow70

Pm-148m E: wa of Har68 and Gre70
I_a: Gre70 (corrected for pure Pm-148m)

Pm-148 E: from Pm-148m
I_r: Gri69
I_a: Cab71 (I(1465))

Pm-149 E,I_a: McI66

Pm-151 eval Tob73

Sm-153 E: Gre70a (see eval Lam73), Rae70 and Ung69
I_a: Ung 69

Eu-154 E: of Mey68, Au69,Kel70,Rae70,Rei70 and Rie70
I_r: ua of Mei68,Aub69,Var69,Kel70 and Rie70
I_a: from Mey68 (more accurate than from level scheme using α)

Eu-155 E: wa of Rae70,Rei70 and Mey69
I_r: wa of Mey69,Ale68a and Rei70
I_a: I(60+86+105+146) = 100% - 13%(β^- to gs),α_T from α_K, α_L and multipolarity given by Mey69.

Eu-156 1) 89+199 KeV γs evaluated separately as severe discrepancies in intensity ratio 89/812 and 199/812 exist.
E: wa of Sch61 and Rae70
I_r: 199/89 wa of Ewa62 and Ale68a
89/812 :Ewa62 and Dzh66a

2) other gammas
E: ua of Ewa62 and Pee64,Dzh66a
I_r: strong lines and composite NaI peaks: avg of Cli61,Ewa62,Ewa64 Pee64,Dzh66a and Gri69
week lines and ratios for multiple peaks: avg of Dzh66a and Gri69

3) I_a: Dzh66a

Eu-157 eval Tob73

Tb-159 eval Tob73

References for gamma-ray data:

Abd68 A. Abdul-Malek and R.A. Naumann, Nucl.Phys. A 106 (1968) 225
Ale68 P. Alexander and J.P. Lau, Nucl.Phys. A 121 (1968) 612
Ale68a P. Alexander, Nucl.Phys. A 108 (1968) 145
And66 S. André and P. Depommier, Compt. Rend. B 262 (1966) 214
And66a H.J. Andrae et al, Z. Naturf. 21a (1966) 1987
Ant70 A. Antilla and M. Piiparinen, Z.Phys. 237 (1970) 126
Apt70 K.E. Apt et al, Nucl.Phys. A 152 (1970) 344
Ard66 G. Ardisson and F.X. Petit, Compt. Rend. C 263 (1966) 1408
Ard67 G. Ardisson, Compt. Rend. C 264 (1967) 1999
Ard68 G. Ardisson et al, Compt. Rend. B 267 (1968) 344
Ard69 G. Ardisson et al, Compt. Rend. B 268 (1969) 96
Art66 A. Artna, Nucl. Data B 1/4 (1966) 5
Aub66 R.L. Auble and W.H. Kelley, Nucl.Phys. 81 (1966) 442
Aub69 G. Aubin et al, Nucl.Instr.Meth. 76 (1969) 93
Bae66 H.W. Baer et al, Nucl.Phys. 86 (1966) 332
Bae67 A. Baecklin et al, Nucl.Phys. A 96 (1967) 539
Bae67a A. Baecklin and S.G. Malmskog, Ark.Fys. 34 (1967) 459

Bae68 P.A. Baedecker et al, Nucl.Phys. A 107 (1968) 449
Bae68a H.W. Baer et al, Nucl.Phys. A 113 (1968) 33
Bar68 J. Barette and S. Monero, Nucl.Instr.Meth. 63 (1968) 235
Bas69 E. Bashandy et al, Z.Naturf. 24a (1969) 1893
Bel71 R.A. Belt et al, Nucl.Phys. A 175 (1971) 129
Ber67 P. Van Bercham and F.C. Roehmer, Helvet.Phys.Acta 40 (1967) 809
Bey67 L.M. Beyer et al, Nucl.Phys. A 93 (1967) 436
Bos68 H.E. Bosch et al, Nucl.Phys. A 108 (1968) 209
Boy65 M.W. Boyd and J.H. Hamilton, Nucl.Phys. 72 (1965) 604
Bra62 H.W. Brandhorst, Jr. and J.W. Cobble, Phys.Rev. 125 (1962) 1323
Bra69 S.M. Brahmavar and J.H. Hamilton, Phys.Rev. 187 (1969) 1487
Bra69a S.M. Brahmavar et al, Nucl.Phys. A 125 (1969) 217
Bro65 R.A. Brown and G.T. Ewan, Nucl.Phys. 68 (1965) 325
Bro67 L. Broman and S. Boreving. Ark.Fys. 34 (1967) 259
Bru65 D. Brune et al, Nukleonik 7 (1965) 484
Cab71 M.J. Cabell and M. Wilkins, J.Inorg.Nucl.Chem. 33 (1971) 1957
Cam60 P.J. Campion et al, J.Appl.Rad.Isot. 8 (1960) 8
Can67 M.J. Canty and R.D. Connor, Nucl.Phys. A 104 (1967) 35
Car68 H.K. Carter and J.H. Hamilton, Nucl.Phys. A 115 (1968) 417
Car70 H.K. Carter et al, Phys.Rev. C 1 (1970) 649
Cli61 I.E. Cline and R.L. Heath, Nucl.Phys. 22 (1961) 598
Coo69 W.B. Cook et al, Nucl.Phys. A 139 (1969) 277
Den67 B. Denecke et al, Nucl.Sci.Engg. 28 (1967) 305
Dic69 W.C. Dickinson et al, Nucl.Phys. A 123 (1969) 481
Don68 D.P. Donnelly et al, Phys.Rev. 173 (1968) 1192
Dou67 P.W. Dougan and B. Erlandsson, Z.Phys. 207 (1967) 108
Dzh66 B.S. Dzhelepov et al, Izv. A.N.SSSR, Ser. Fiz 30 (1966) 403
Dzh66a B.S. Dzhelepov et al, Izv. A.N.SSSR, Ser. Fiz 30 (1966) 394
Eas64 T.A. Eastwood et al, Can.J.Phys. 42 (1964) 218
Eij68 C.W.E. Van Eijk et al, Nucl.Phys. A 121 (1968) 440
Eme55 E.W. Emery and N. Veall, Proc.Phys.Soc. (London) A 68 (1955) 346
Eme68 J.F. Emery, ORNL-4196(1968) 66
Ewa62 G.T. Ewan et al, Nucl.Phys. A 29 (1962) 153
Ewa64 G.T. Ewan and A.J. Tavendale, Can.J.Phys. 42 (1964) 2286
Fas70 J.L. Fasching et al, Phys.Rev. C 1 (1970) 1126
Foi69 C. Foin et al, Nucl.Phys. A 123 (1969) 513
For67 H. Forest et al, Compt. Rend. B 264 (1967) 1614
Fra67 J. Frana et al, Czech.J.Phys. B 17 (1967) 1048
Fra69 K. Fransson and P. Erman, Ark.Fys. 39 (1969) 7
Gei60 J.S. Geiger et al, Nucl.Phys. 16 (1960) 1
Gei61 K.W. Geiger et al, Nucleonics 19/1 (1961) 97
Gei68 J. S. Geiger, AECL-3166 (1968) 28
Gfo69 D. Gfoeller et al, Z.Phys. 227 (1969) 45
Gra58 R.L. Graham et al, Can.J.Phys. 36 (1958) 1084
Gra66 G. Graeffe et al, Phys.Rev. 149 (1966) 886
Gre68 P.R. Gregory, Can.J.Phys. 46 (1968) 2797
Gre70 W.M. Greenberg and H.J. Fischbeck, Z.Phys. 233 (1970) 391
Gre70a R.C. Greenwood et al, Nucl.Instr.Meth. 72 (1970) 141
Gri69 Z. Gritchenko et al, Yad.Fiz. 10 (1969) 929
Gun68 R. Gunnik et al, Nucl.Instr.Meth. 65 (1968) 26
Gup65 V.C. Gupta et al, Nucl.Phys. 73 (1965) 413

Ham63 J.H. Hamilton, Physica 29 (1963) 885
Har63 J.W. Harpster et al, Nucl.Phys.47 (1963) 443
Har68 B. Harmatz and T.H. Handley, Nucl.Phys. A 121 (1968) 481
Hel71 R.G. Helmer et al, Nucl.Instr.Meth. 96 (1971) 173 and ANCR-1016 (Oct 1971) 403
Hen67 R. Henck et al, Nucl.Phys. A 93 (1967) 601
Hen67a H.J. Hennecke et al, Phys.Rev. 159 (1967) 655
Hen69 R. Henck and A. Gizon, Compt. Rend. B 269 (1969) 337
Hen69a R. Henck, priv. comm. to Car70, (1969)
Hil67 J.C. Hill and M.L. Wiedenbeck, Nucl.Phys. A 98 (1967) 599
His68 J.E. Hiscott, AERE-R 5342 (1968)
Hof70 S. Hofmann et al, Z.Phys. 230 (1970) 37
Joh65 N.R. Johnson et al, Nucl.Phys. 72 (1965) 617
Kal69 V.G. Kallinikov and Kh.L. Ravn, Izv.A.N.SSSR,Ser.Fiz.33 (1969) 2068
Kal70 V.G. Kallinikov et al, Izv.A.N.SSSR,Ser.Fiz.34 (1970) 916
Kar64 S.E. Karlsson et al, Ark.Fys.27 (1964) 61
Kar67 S.E. Karlsson et al, Nucl.Phys. A 100 (1967) 113
Kaw70 H. Kawakami and K. Hisatake, Nucl.Phys. A 149 (1970) 523
Kel70 G.E. Keller and E.F. Zganjar, Nucl.Phys. A 153 (1970) 647
Ker70 J. Kern and G. Mauron, Helvet.Phys.Acta 43 (1970) 272
Ker70a J. Kern, Nucl.Instr.Meth. 79 (1970) 233
Ker72 J. Kern, IAEA Panel on"Charged-Particle Induced Radiative Capture", Vienna, Oct. 1972, Proceedings p. 345
Kob67 Y. Kobayashi, J.Inorg.Nucl.Chem. 29 (1967) 1376
Lag67 J.M. Lagrange et al, Ann.Phys. (Paris) 2 (1967) 141
Lam73 M. Lammer, contribution to Review Paper 12, this Panel: "Standards for Calibration of Semiconductor Detectors"
Leg67 J. Legrand and J.P. Boulanger, Compt. Rend. B 265 (1967) 697
Leg67a J. Legrand and J.P. Boulanger, Compt. Rend. B 265 (1967) 782
Leg67b J. Legrand et al, CEA-R-3285 (1967)
Liu69 E. Liukkonen, Nucl.Phys. A 138 (1969) 163
Lyo54 W.S. Lyon and J.E. Strain, Phys.Rev. 95 (1954) 1500
Lyo58 W.S. Lyon, Nucl.Sci.Engg. 4 (1958) 703
Lyo61 W.S. Lyon, Nucl.Sci.Engg. 9 (1968) 148
Mai65 B.P.K. Maier, Z.Phys. 184 (1965) 143
Man68 J.C. Manthurutil et al, Phys.Rev. 165 (1968) 1363
Mar65 K.W. Marlow, Nucl.Phys. 61 (1965) 13
Mar70 M.J. Martin and P.H. Blichert-Toft, Nucl.Data A 8 (1970) 1
McI66 L.D. McIsaac and R.G. Helmer, Phys.Rev. 150 (1966) 1033
Meg68 D.G. Megli et al, Nucl.Phys. A 107 (1968) 117
Mer70 G.F. Meredith and R.A. Meyer, Nucl.Phys. A 142 (1970) 513
Mey68 R.A. Meyer, Phys.Rev. 170 (1968) 1089
Mey69 R.A. Meyer and J.W.T. Meadows, Nucl.Phys. A 132 (1969) 177
Mon61 J.E. Monahan et al, Phys.Rev. 123 (1961) 1373
Mor67 J.A. Moragues et al, Nucl.Phys. A 99 (1967) 652
Mow70 R.S. Mowatt and J.S. Merritt, Can.J.Phys. 48 (1970) 453
Mur67 E.L. Murri et al, Phys.Rev. 155 (1967) 1263
Nag68 T.S. Nagpal, Can.J.Phys. 46 (1968) 2579
Nak61 I.E. Nakhutin et al, Sovj.Phys. JETP 12 (1961) 687
Noo65 B. Van Nooijen et al, Nucl.Phys. 63 (1965) 241
Odr69 P. Odru, Radiochim.Acta 12 (1969) 64
Pee64 N.F. Peek et al, Phys.Rev. B 136 (1964) 330
Pet70 H. Petterson et al, Z.Phys. 233 (1970) 260

Pie65 W.R. Pierson, Phys.Rev. B 140 (1965) 1516
Pie67 W.R. Pierson and K. Rengan, Phys.Rev. 159 (1967) 939
Por59 F.T. Porter and P.P. Day, Phys.Rev. 114 (1959) 1286
Qua70 S.M. Quaim, Nucl.Phys. A 154 (1970) 145
Rae67 D.E. Raeside et al, Nucl.Phys. A 93 (1967) 54
Rae69 D.E. Raeside et al, Nucl.Phys. A 134 (1969) 347
Rae70 D.E. Raeside, Nucl.Instr.Meth. 87 (1970) 7
Rag67 R.C. Ragani et al, Nucl.Phys. A 99 (1967) 547
Ram67 S. Raman, Nucl.Phys. A 90 (1967) 508
Ram68 S. Raman, Nucl.Phys. A 107 (1968) 402
Ram70 S. Raman, Phys.Rev. C 2 (1970) 2176
Rao67 P.V. Rao and R.W. Fink, Nucl.Phys. A 103 (1967) 385
Rei64 J.J. Reidy, TID-21826 (1964)
Rei70 J.D. Reierson et al, Nucl.Phys. A 153 (1970) 109
Rid60 B.F. Rider and J.P. Peterson, Jr., GEAP-3496 (1960) (revised Feb 1961)
Rie70 L.L. Riedinger et al, Phys.Rev. C 2 (1970) 2358
Rob65 R.L. Robinson et al, Nucl.Phys. 74 (1965) 281
Sar69 D.G. Sarantites and B.R. Erdal, Phys.Rev. 177 (1969) 1631
Say68 A.R. Sayres and C.C. Trail, Nucl.Phys. A 113 (1968) 521
Sch61 O.W.B. Schult, Z.Naturf. 16a (1961) 927
Sch64 W. Scheuer et al, Nucl.Phys. 54 (1964) 221
Sch67 S.O. Schriber and M.W. Johns, Nucl.Phys. A 96 (1967) 337
Sie64 K. Siegbahn et al, Nucl.Instr.Meth. 27 (1964) 173
Sil61 A.N. Silantev and B.S. Kusnetsov, Izv.A.N.SSSR,Ser.Fiz. 25 (1961) 1186
Sny68 R.E. Snyder and G.B. Beard, Nucl.Phys. A 113 (1968) 581
Spe69 E.H. Spejewsky, Phys.Rev. 186 (1969) 1270
Str69 K.D. Strutz et al, Z.Phys. 221 (1969) 231
Thu66 J.E. Thun et al, Nucl.Phys. 88 (1966) 289
Tob73 A. Tobias, C.E.G.B. (UK) report RD/B/M2669 (June 1973)
Tsa66 R. Tsaletka and Y. Vrzal, JINR-P-2739 (1966)
Ung69 J. Ungrin and M.W. Johns, Nucl.Phys. A 127 (1969) 353
Var69 L. Varnell et al, Nucl.Phys. A 127 (1969) 270
Vrz66 Y. Vrzal et al, JINR-P6-2986 (1966)
Vrz67 Y. Vrzal et al, Izv.A.N.SSSR,Ser.Fiz. 31 (1967) 696
Wil67 J.F. Wild and W.B. Walters, Nucl.Phys. A 103 (1967) 601
Yth66 C. Ythier et al, Physica 32 (1966) 1351
Yth67 C. Ythier et al, Compt. Rend. B 264 (1967) 84
Zol69 W.H. Zoller, Nucl.Phys. A 130 (1969) 293

APPENDIX B: BASIC DATA AND ADOPTED VALUES

The presentation of basic half-life data and adopted values follows essentially that of Martin and Blichert-Toft [3]. Some of the evaluations shown in Appendix B have been updated since the publication of [1]. This is indicated by a remark to the adopted value.

Abbreviations:

Headings: Ref = reference, $T^1/2$ = half -life
No = number of $T^1/2$ followed decay (d ' = complete decay)

Averages: wa = weighted average, ua = unweighted average

Production: p = proton, n = neutron, f = fission,
chem ..... radiochemical separation
ms ..... mass-spectrometry

Method: ew-pc ..... end-window proportional counter
gf-pc ..... gas flow proportional counter
GM ..... Geiger-Müller counter
hp-γ-ic .... high pressure 4π gamma ionization chamber
ic ..... ionization chamber
pc ..... proportional counter
p-scin ..... plastic scintillator
well- ..... well type crystal scintillator
N ..... number of atoms determined
st ..... standard

Half lives

Br-82

Ref	$T^1/2$ (hours)
Mer62	35.344 ± .013
Rey68	35.34 ± .03
Col73	35.28 ± .01
	35.31 ± .02 wa, 35.32 ± 0.02 ua
adopted	35.31 ± .04

others: 36.0 ± 0.1 [Ber50], 35.87 ± 0.05 [Cob50], 35.7 ± 0.3 [Sin51], 35.10 ± 0.13 [Win51], 35.55 ± 0.15 [Wya61]

Rb-86

Ref	T½ (days)	No	Production	Method
Eme55	18.66 ± .03	4	Rb(n,γ) chem	
Nid55	18.64 ± .04	9	FP, chem	
Wri57	18.68 ± .07	5	Rb(n,γ) chem	GM
Bab71	18.61 ± .04	19	U-238(p,f) chem	gf-pc
Eme72	*18.82 ± .11	2	Rb(n,γ) chem	NaI
all	18.650 ± .019 wa,	18.682 ± 0.036 ua		
*omitted	18.645 ± .020 wa,	18.648 ± 0.015 ua		
adopted	18.65 ± .03			

Sr-89

Ref	T½ (days)	No	Production	Method
Her55	50.5 ± .2	8	U(n,f), chem	
Her55	50.5 ± .2		Sr-88(n,γ), Y(n,p)Sr(n,γ)	
Osm59	50.36 ± .18	2.6	Sr-88(n,γ) chem	GM
Ans65	50.52 ± .03	5.1	Sr-88(n,γ)	pc
Bab71	50.55 ± .09	12	U-238(p,f) chem	gf-pc
	50.518 ± .028 wa,	50.486 ± .033 ua		
adopted	50.52 ± .05			
others:	51 ± 1 [Kje 56], 53.6 ± .4 [Sat 62], 52.7 ± .5 [Fly 65]			

Y-91

Ref	T½ (days)	No	Production	Method
Bun54	58.5 ± 1.0	1	U(n,f) chem	NaI, p-scin
Her56	58.3 ± 0.3		U(n,f)	
Wya61	59.1 ± 0.2	2	U(n,f) chem	2π -pc
Hof63	58.8 ± 0.2	6.6	U(n,f) chem	gf-pc
Mar65	59.0 ± 0.6		Pu-239(n,f) chem	4π -pc
Bab71	58.51 ± 0.06	11	U-238(p,f)	gf-pc
	58.58 ± 0.08 wa,	58.70 ± 0.13 ua		
adopted	58.51 ± 0.12			

Mo-99

Ref	T½ (hours)	No	Production	Method
Sei47	66.0 ± 0.1	8	U(n,f) chem	ic
Gun57	66.00 ± 0.15	8	U(n,f)+Mo(n,γ) chem	gf-pc
Pro58	*67.2 ± 0.2		U(n,f) chem	GM
New61	65.6 ± 0.2	11	U(n,f) chem	pc
Cro65	*66.7 ± 0.1	11	Mo-98(n,γ) chem	Well-NaI
Bal67	65.93 ± 0.24	8	Mo(n,γ)	ew-pc
Bal67	65.95 ± 0.04	9	Mo(n,γ)	scin
Rey68	*66.69 ± 0.06	3-5	U(n,f)+Mo(n,γ) chem	hp-γ-ic
Bab71	*66.5 ± 0.2	33	U-238(p,f) chem	gf-pc
Eme72	66.02 ± 0.01	5.4	U(n,f) chem	well-scin
all	66.04 ± 0.05 wa,		66.26 ± 0.15 ua	
*omitted	66.015 ± 0.012 wa,		65.92 ± 0.07 ua	
adopted	66.0 ± 0.1			

The lower values are adopted, because the higher ones may be in error due to possible contamination with induced activities or fission products /Eme72/. No clarification is possible without careful investigations of all sources of error.

Cd-115m

Ref	T½ (days)	No	Production	Method
Wah59	44.2 ± 0.5		U-235(n,f)	gf-pc
Bab71	44.8 ± 0.3	d	U-238(p,f)	gf-pc
	44.6 ± 0.3 wa,		44.5 ± 0.3 ua	
adopted	44.6 ± 0.5			

Sb-122

Ref	T½ (hours)	No	Production	Method
Hag67	64.34 ± 0.06		U(p,f) chem	
Bor68	67.7 ± 1.2		Sb(n,2n) chem	2π gf-pc
Eme72	65.14 ± 0.14	7.4	Sb(n,γ) chem	NaI
	64.47 ± 0.23 wa,		65.4 ± 1.0 ua	
adopted	65.1 ± 0.3	(supersedes T½ given in /1_7/)		

Sb-125

Ref	$T_{1/2}$ (years)	No	Production	Method
Kle60	2.69 ± 0.05			
Kle60	*2.53 ± 0.05			
Wya61	2.78 ± 0.04	1	Sn-125(β^-) chem	ic
Fly65	2.71 ± 0.02	3	chem	pc
Law66	2.81 ± 0.05	2	Sn-125(β^-) chem	pc

*omitted 2.73 ± 0.02 wa, 2.75 ± 0.03 ua
adopted 2.75 ± 0.04

Te-129m

Ref	$T_{1/2}$ (days)	No	Production	Method
And65	34.1 ± 0.2		La+19GeV p,chem,ms	NaI
Bor70	33.2 ± 0.5			β^-counting
Bab71	33.52 ± 0.12	12	U-238(p,f) chem	gf-pc
Eme72	34.1 ± 0.2	5.2	Te-128(n,γ) chem	ew-pc

33.74 ± 0.17 wa, 33.73 ± 0.22 ua
adopted 33.7 ± 0.3 (supersedes $T_{1/2}$ given in [1])

I-131

Ref	$T_{1/2}$ (days)	No	Production	Method
Sin51a	8.02 ± 0.03	8		ic,GM
Bar53	8.05 ± 0.01	6	U(n,f) chem	pc
Loc53	8.06 ± 0.02	6		electroscope
Pap53	8.02 ± 0.04	4	U(n,f) chem	GM
Sel53	8.075 ± 0.022	5		electroscope
Bur58	8.054 ± 0.010	6		scin
Kee58	8.067 ± 0.010	10		ic
Lag68	8.073 ± 0.008		$Te^{131}(\beta^-)$ chem	ic,pc,scin
Rey68	8.070 ± 0.009	4	U(n,f) chem	hp-γ-ic
Zol71	7.969 ± 0.014	<3		
Eme72	8.048 ± 0.016	6.2	U(n,f) chem	NaI
Eme72	8.040 ± 0.001	>10	U(n,f) chem	well-scin

8.041 ± 0.002 wa, 8.046 ± 0.009 ua
adopted 8.04 ± 0.01 (supersedes $T_{1/2}$ given in [1])

Instead of omitting several values (e.g. [Zol71] suspect possible contamination in their sample), the measurement of [Eme72] is adopted with increased uncertainty.

Xe-131m

Ref	T½ (days)	No	Production	Method
Ber52	12.0 ± 0.3	2	I-131(β⁻) chem,ms	scin
And65	11.8 ± 0.1		La+19 GeV p,U(n,f);chem,ms	scin
Kna66	11.94 ± 0.04		I-131(β⁻) chem	scin
Eme72	12.00 ± 0.02	> 10	U(n,f) chem	well-scin
	11.98 ± 0.02 wa,		11.94 ± 0.05 ua	
adopted	11.98 ± 0.05			

I-133

Ref	T½ (hours)	No	Production	Method
Kat51	20.8 ± 0.2			
Pap53	21.5 ± 0.2			
Wah55	20.9 ± 0.3			
And65	20.3 ± 0.3			
Eic66	20.8 ± 0.2			
Rey68	20.9 ± 0.1	14	U(n,f) chem	GM
	20.92 ± 0.12 wa,		20.87 ± 0.16 ua	
adopted	20.9 ± 0.2			

omitting [Pap53] and [And65] gives essentially the same result

Xe-133m

Ref	T½ (hours)	No	Production	Method
Ber51	55.2 ± 1.9			
Ber52	56.4 ± 1.9			
Erm61	54.24 ± 0.40			
Ale68	52.6 ± 0.7	< 7	Te-130(α,n)	Ge(Li)
	53.95 ± 0.49 wa,		54.6 ± 0.8 ua	
adopted	53 ± 1		(supersedes value given in [1])	

Cs-134

2.062 ± 0.005 years [Die73] supersedes value given in [1]

Cs-137

Because of possible systematic differences, the measurements are subdivided into 3 groups according to the method applied. Cs-137 is produced from fission in all cases.

Ref	T½ (years)	measurement years	Method
1) Specific activity (sa):			
Wil55	*26.6 ± 0.4		N:ms, 4π β
Bro55	30.0 ± 0.4		N:ms, 4π - pc
Mos58	*28.6 ± 1.0		N:ms, 4π β
Gla61	*29 ± 1		N:ms, 4π β
Coo62	29.40 ± 0.18		N:ms, 4π β
Fle62	30.1 ± 0.7		N:ms, liquid scin
Lew65	30.72 ± 0.10		N:ms, absolute γ well
Fly65a	30.9 ± 0.7		N:ms, 4π - pc
2) Ba-growth(Ba), ms:			
Far61	30.4 ± 0.4	0.14	
Rid63	29.2 ± 0.3	0.27	
Lew65	29.78 ± 0.14	9.5	
3) Cs-decay(Cs), experiments in order of time followed decay			
Gor63	29.68 ± 0.05	3	ic, electrometer
Wal70	29.901 ± 0.045	3.3	4π γ - ic, Ra-226 st
Fly65a	*31.4 ± 0.9	6.6	2π - pc
Lew65	30.55 ± 1.55	9.5	ms
Fly65a	29.3 ± 0.6	10.2	2π - pc
Har70	30.64 ± 0.43	10	internal gf - pc
Eme72	30.18 ± 0.10	10.5	hp-γ-ic
Die73	30.174 ± 0.013[a]	11	ms
without omissions: all	30.13 ± 0.05 wa,	29.82 ± 0.24 ua	
* omitted : all	30.13 ± 0.04 wa,	30.06 ± 0.14 ua	
Sa	30.39 ± 0.28 wa,	30.22 ± 0.27 ua	
Ba	29.74 ± 0.21 wa,	29.79 ± 0.35 ua	
Cs	30.13 ± 0.05 wa,	30.06 ± 0.18 ua	
Sa,Ba (9.5y) and Cs (≥10y):	30.176 ± 0.031 wa,	30.16 ± 0.16 ua	
adopted	30.17 ± 0.10	(supersedes value given in [1])	

For comparison: Without [Eme72] and [Die73] the following averages were obtained (as adopted in [1])

29.94 ± 0.08 wa, 30.06 ± 0.12 ua (adopted: 30.0 ± 0.2)

[a] [Die73] quote ± 0.034 at the 99% confidence level. The error shown here corresponds to 1 standard deviation (also shown in [Die73]).

There is no obvious reason to distrust the careful measurement of [Wal70]. However, fluctuations in the half life obtained during the first 3-4 years of decay have been observed [Rey67,Die73]. Therefore the longer decay times have been preferred, supported by unweighted averages and the most recent and careful measurements of [Eme72,Die73].

Ce-141

Ref	T½ (days)	No	Production	Method
Fre50	32.5 ± 0.2		Ce(n,γ)	ic
Ans65	32.55 ± 0.01	5	Ce-140(n,γ)	ic
OBr67	32.38 ± 0.02	8	La-139(n,γ),(n,γ)β⁻ and La-139(n,γ)(β⁻)(n,γ)	well -NaI
Bab71	32.6 ± 0.2	18	U-238(p,f)	gf-pc
Deb71	32.51 ± 0.06			Ge(Li)
Eme72	32.45 ± 0.13	3.1	Ce-140(n,γ)chem	ew-pc
	32.516 ± 0.030 wa, 32.50 ± 0.03 ua			
adopted:	32.50 ± 0.05			
others:	33.11 ± 0.23 [Wal49], 32 ± 2 [Wil60]			

Pr-143

Ref	T½ (days)	No	Production	Method
Poo48	13.5 ± 0.1		Ce(d,n)	ic
Fel49	13.7 ± 0.1			GM
Pep57	13.59 ± 0.04		Pr(n,γ)	gf-pc
Hof63	13.585 ± 0.035[a]	8.5	U(n,f)	gf-pc
Ish65	13.55 ± 0.02	10	U(n,f)	gf-pc
Bab71	13.57 ± 0.02	10	U-238(p,f)	gf-pc
	13.567 ± 0.012 wa, 13.583 ± 0.027 ua			
adopted:	13.57 ± 0.02	(supersedes value given in [1])		
others:	13.8 [Bal51], 13.95 [Mar56], 13.6 [Roy56], 13.76 ± 0.05 [Wri57].			

a) average of 2 measurements and 1σ error shown here

Nd-147

Ref	T½ (days)	No	Production	Method
Wri57	11.06 ± 0.04		U(n,f)chem	ic
Hof63	11.015 ± 0.003[b]	22	U-235(n,f)	gf-pc
Bab71	10.98 ± 0.01	41	U-238(p,f)	gf-pc
	11.012 ± 0.007 wa, 11.018 ± 0.023 ua			
adopted:	11.01 ± 0.02	(supersedes value shown in [1])		
others:	11.0 ± 0.3 [Mar51], 11.6 ± 0.3 [Kon51], 11.1 ± 0.5 [Emm51], 11.9 ± 0.3 [Rut52], 11.14 ± 0.06 [Als60], 11.5 ± 0.5 [Wil60]			

b) weighted average of 2 measurements and 1σ error shown here

Pm-149

Ref	T½ (hours)	No	Production	Method
Bun60	53.09 ± 0.09		Nd-148(n,γ)	4π β-pc
Hof63	53.07 ± 0.10	29	U-235(n,f)	gf-pc
McI66	53.08 ± 0.10	2.2	Nd-148(n,γ)	4π β-pc
Bab71	53.08 ± 0.10	13	U-238(p,f)	pc+absorber
	53.08 ± 0.05 wa,	53.080 ± 0.004 ua		
adopted:	53.08 ± 0.05	(errors are estimated overall uncertainties)		
others:	52.8 ± 0.3 [Art60]			

Sm-151

Ref	T½ (years)	Method (production: fission product in all cases)
Kar52	*73 $^{+25}_{-14}$	ms, change in Sm abundance after 3.8 years
Mel55	93	ms, change in Sm abundance after 7 years
Far62	98	ms, change in Sm abundance after 15 years, same sample as [Mel55]
Fly65	87 ± 9	2π gf-pc, decay followed 10 years
Rey68	93 ± 8	N:ms, specific activity, liquid scin, error estimated
* omitted	92.8±2.3 ua	(no wa as no errors assigned by [Mel55,Far62])
adopted	93 ± 5	
others:	122 [Ing50]	

Sm-153 (sorted by increasing value of halflife)

Ref	T½ (hours)	No	Production	Method
Bab71	*46.44 ± 0.08	13	U-238(p,f)	gf-pc
Hof63	*46.5 ± 0.3		U(n,f)	gf-pc
Chu70	46.75 ± 0.09			
Rey68	46.8 ± 0.1	2.1	Sm(n,γ)	CM
Lee54	47.0 ± 0.3		Sm-152(n,γ)	β-spectrometer
Cor58	47.1 ± 0.1		Sm-152(n,γ)	β-spectrometer, NaI
Cab62	47.1 ± 0.1	9	Sm-152(n,γ)	4π β-pc
all	46.79 ± 0.11 wa,	46.81 ± 0.10 ua		
*omitted	46.93 ± 0.07 wa,	46.95 ± 0.07 ua		
adopted	46.8 ± 0.2			
others:	46.5 ± 1.0 [Rut52], 46.16 ± 0.09 [Gre61]			

Eu-155

adopted: 4.96 ± 0.02 years [Eme72] (uncertainty = 2σ)
supersedes value given in [1]

others: 1.811 ± 0.002 [Pie59], 4.65 ± 0.20 [Mow70], 4.9 ± 0.1 [Bar69]

Eu-156

Ref	$T_{1/2}$ (days)	No	Production	Method
Car65	12.21 ± 0.24		U-238(α,f), 46MeV α	ew-pc
Dan66	15.11 ± 0.05	41	U-235(n,f),U-238(α,f), 25MeV α	gf-pc
		7	Gd-158(d,α), 14MeV d	
Bab71	15.17 ± 0.03	26	U-238(p,f)	gf-pc
	15.15 ± 0.03 wa,	15.16 ± 0.03 ua		
adopted	15.16 ± 0.03	(errors shown are overall uncertainties)		

Branching Ratios

(abbreviations as in Appendix A; gamma rays)

Zr-95→Nb-95m

Nb-95m IT : α_T = 2.92 ± 0.20([3] and $\alpha_T = \alpha_K + \alpha_L + 1.3\alpha_M$, M4 theory)

Ref	Branching (%)	obtained from
Bra69	0.72 ± 0.10	I_γ(rel Zr-95 757KeV)=0.34±0.03→I_γ(abs) = 0.185±0.02, α_T
Foi69	1.29 ± 0.43	I_γ(rel Zr-95 757KeV)=0.6±0.2→I_γ(abs) = 0.33±0.10, α_T
Eme68	1.00 ± 0.28	Zr-95 γ's: wa of 3 measurements: I_γ(abs) = 98.4±0.2, I(β⁻ to gs)=0.4±0.2
Eme68	1.35 ± 0.30	direct measurement of branching, error estimated
	0.83 ± 0.12 wa,	1.09 ± 0.15 ua
adopted	0.83 ± 0.20	(supersedes value given in [1])

Te-129m: IT

	% IT	Reference
	68	G. Andersson et al. Ark.Fys.22(1962) 349
	64 ± 7	S.H. Devare et al., Phys.Rev.134B(1964) 705
a)	72	G. Berzins et al., Nucl.Phys.A93(1967) 456
a)	63.4 ± 7	W.C. Dickinson et al., Nucl.Phys.A123(1969) 481
	64 ± 7	adopted

a) deduced values

For discussion see Dickinson et al.

I-133→Xe-133m

1) P. Alexander and J.P. Lau, Nucl. Phys. A121 (1968) 612
Population ratio Xe-133 m/Xe-133 in I-133 decay was found to be 0.029 ± 0.001

Thus: the branching I-133 → Xe-133 m is:

2.8 ± 0.1 %

2) R.N. Saxena and H.D. Sharma, Nucl. Phys. A171 (1971) 593
The intensity of the 510.4 keV gamma ray relative to that of the 529.5 keV gamma ray in the decay of I-133 was found to be 1.6%, populating the 233.5 keV level of Xe-133 m. The absolute intensity of the 529.5 keV gamma ray was deduced to be 87.4%. Thus the gamma branching to Xe-133 m (via 510 keV gamma) is 1.4%.

E. Eichler et al., Phys. Rev. 146 (1966)B899, found the direct beta feeding of the metastable state to be ~1.4%.

The total (gamma + beta) branching to I-133→Xe-133 m is then

2.8%

References for Appendix B:

Ale68 P. Alexander and J.P. Lau, Nucl.Phys. A 121 (1968) 612
Als60 J. Alstad and A.C. Pappas, J.inorg.nucl.Chem. 15 (1960) 222
And65 G. Andersson et al, Ark. Fysik 28 (1965) 37
Ans65 S.C. Anspach et al, NP-15663 (1965)
Art60 A. Artna and M.E. Law, Can.J.Phys. 38 (1960) 1577
Bab71 S. Baba et al, J.inorg.nucl. Chem. 33 (1971) 589
Bal51 N.E. Ballou et al, in "Radiochemical Studies: The Fission Products" N.N.E.S. Div IV, Vol. 9, p. 1181 (McGraw-Hill, New York, 1951)
Bal67 M.N. Baldwin, Nucl.Sci.Engg. 30 (1967) 144
Bar53 R.M. Bartholomew et al, Can.J.Chem. 31 (1953) 120
Bar69 D. Barr (Los Alamos,USA)1969, quoted in Nucl.Phys. A 132(1969)177
Ber50 E. Berne, Phys. Rev. 77 (1950) 568
Ber51 I. Bergstroem, Phys. Rev. 81 (1951) 638
Ber52 I. Bergstroem, Ark. Fys. 5 (1952) 191
Bor68 M. Bormann, Nucl.Phys. A 115 (1968) 309
Bor70 M. Bormann et al. Nucl.Phys. A 157 (1970) 481
Bra69 S.M. Brahmavar and J.H. Hamilton, Phys.Rev.187(1969)1487
Bro55 F. Brown et al, J.inorg.nucl.Chem. 1 (1955) 241
Bun60 L.R. Bunney et al, J.inorg.nucl.Chem. 12 (1960) 228
Bur58 L. Burkinshaw, Phys. in Med.Biol. 2 (1958) 255
Cab62 M.J. Cabell, J.inorg.nucl.Chem. 24 (1962) 749
Car65 C.L. Carnaham and L.R. Bunney, USNRDL-TR-868(1965)
Chu70 Y.Y. Chu et al, Phys. Rev. C1 (1970) 1826
Cob50 J.W. Cobble and R.W. Attenberry, Phys. Rev. 80 (1950) 917
Col73 K.E. Collins et al, Radiochem.Radioanal.Lett.13(1973) 169
Coo62 H.D. Cook, Gatlinburg Conf. on Analytical Chemistry in Nuclear Reactor Technology(1962) and WAPD-BT-30(1964) 31
Cor58 J.M.Cork et al, Phys.Rev. 110 (1958) 526
Cro65 P. Crowther and J.S. Eldridge, Nucl. Phys. 66 (1965) 472
Den66 W.R. Daniels and D.C. Hoffmann, J.inorg.nucl.Chem.28(1966)2424
Deb71 K. Debertin, Z.Naturf. 26a (1971) 596
Die73 L.A. Dietz and C.F. Pachucki, J.inorg.nucl.Chem. 35 (1973)1769
Eic66 E. Eichler, Phys.Rev. 146 (1966) 899
Eme55 E.W. Emery et al, Nature 175 (1955) 34
Eme68 J.F. Emery, ORNL-4196 (1968) 66
Eme72 J.F. Emery et al, Nucl.Sci.Engg. 48 (1972) 319
Emm51 W.S. Emmerich and J.D. Kurbatov, Phys.Rev. 83 (1951) 40
Far61 H. Farrar et al. Can.J.Chem. 39 (1961) 681
Far62 H. Farrar and R.H. Tomlinson, Nucl.Phys. 34 (1962) 367
Fel49 L. Feldmann et al, Phys.Rev. 76 (1949) 1888
Fle62 D.G. Fleishman et al, Atomnaya Energ. 13 (1962) 592, engl.: Sovj.J.Atom.En. 13 (1962) 1224
Fly65 K.F. Flynn et al, Nucl.Sci.Engg. 22 (1965) 416
Fly65a K.F. Flynn et al, J.inorg.nucl.Chem. 27 (1965) 21
Foi69 C. Foin et al, Nucl.Phys. A 123 (1969) 513
Fre50 M.S. Freedman and D.W. Engelkemeir, Phys.Rev. 79 (1950) 897
Gla61 M.P. Glazunov et al, Atomnaya En. 10 (1961) 622
Gor63 S.G. Gorbics et al, Nucleonics 21/1 (1963) 63
Gre61 R.E. Green and W.H. Walker, Can.J.Phys. 39 (1961) 1216
Gun57 S.R. Gunn et al, Phys.Rev. 107 (1957) 1642
Hag67 E.Hagenbø, J.inorg.nucl.Chem. 29 (1967) 2515
Har70 G. Harbottle, Radiochim. Acta 13 (1970) 132
Her55 G. Herrmann and F. Strassmann, Z.Naturf. 10a (1955) 146

Her56 G. Herrmann et al, Z. Naturf. 11a (1956) 946
Hof63 D.C. Hoffmann, J.inorg.nucl. Chem. 25 (1963) 1196
Ing.50 M.G. Inghram et al, Phys.Rev. 79 (1950) 271
Ish65 T. Ishimori and Y. Kobayashi, J.nucl.Sci.Technol. 2 (1965) 181
Kar52 D.G. Karraker et al, Phys.Rev. 87 (1952) 390
Kat51 S. Katcoff et al, Phys.Rev. 91 (1951) 1458
Kee58 J.P. Keene et al, Phys.in Med.Biol. 2 (1958) 360
Kje56 A. Kjelberg and A.C. Pappas, Nucl.Phys. 1 (1956) 322
Kle60 E.H. Kleer and A.F. Voigt, J.inorg.nucl.Chem. 16 (1960) 8
Kna66 K. Knauf et al, Z.Phys. 197 (1966) 101
Kon51 E. Kondaiah, Phys.Rev. 81 (1951) 1056
Lag68 F. Lagoutine et al, Int.J.Appl.Rad.Isot. 19 (1968) 475
Law66 F.O. Lawrence et al, J.inorg.nucl.Chem. 28 (1966) 2477
Lee54 M.R. Lee and R. Katz, Phys.Rev. 93 (1954) 155
Lew65 R.E. Lewis et al, Trans.Am.Nucl.Soc. 8 (1965) 79
Loc53 E.E. Lockett and R.H. Thomas, Nucleonics 11/3 (1953) 14
Mar51 J.A. Marinsky and L.E. Glendenin, ref.loc.cit. /Bal51/ p. 1229
Mar56 D.W. Martin et al, Phys.Rev. 101 (1956) 182
Mar65 D.A. Marsden and L. Yaffe, Can.J.Chem. 43 (1965) 249
McI66 L.D. McIsaak and R.G. Helmer, Phys.Rev. 150(1966) 1033
Mel55 E.A. Melaika et al, Can.J.Chem. 33 (1955) 830
Mer62 J.S. Merritt and J.G.V. Taylor, Can.J.Phys. 40 (1962) 1044
Mos58 Y. Moses and H. Cook, TID-7568, pt 2 (1958) 192
Mow70 R.S. Mowatt and W.H. Walker, Can.J.Phys. 48 (1970) 1933
New61 R.D. Newman, Ref. 61Nel5 in /1/ (priv. comm. 1961)
Nid55 J.B. Niday, Phys.Rev. 98 (1955) 42
OBr67 H.A. O'Brien Jr. and J.S. Eldridge, Nucleonics 25/2 (1967)41
Osm59 R.G. Osmond and M.J. Owers, J.inorg.nucl.Chem. 9 (1959) 96
Pap53 A.C. Pappas, MIT-Techn.Rep. 63 (1953) p. 97 and AECU-2806(1953)
Pep57 D.F. Peppard et al, J.inorg.nucl.Chem. 5 (1957) 141
Pie59 A. Pierroux et al, Bull.Soc.Roy.Sci. Liège 28 (1959) 180
and Nucl.Sci.Abstr. 16 (1962) No. 1053
Poo48 M.L. Pool and N.L. Krisberg, Phys.Rev.73 (1948) 1035
Pro58 A.N. Protopopov et al, Atomn.En.5(1958)130,
engl. J.Nucl.En.10A (1959) 80
Rey67 S.A. Reynolds and E.I. Wyatt, ORNL-4039(1967) 59
Rey68 S.A. Reynolds et al, Nucl.Sci.Engg. 32 (1968) 46
Rid63 B.F. Rider et al, Nucl.Sci.Engg. 15 (1963) 284
Roy56 L.P. Roy and L. Yaffe, Can.J.Chem. 34 (1956) 1023
Rut52 W.C. Rutledge et al, Phys. Rev. 86 (1952) 775
Sat62 A.R. Sattler, Nucl. Phys. 36 (1962) 648
Sei47 J.A. Seiler, ANL-4000 (1947) 119
Sel53 H.H Seliger et al, Phys. Rev. 90 (1953) 443
Sin51 W.K. Sinclair and A.F. Holloway, Nature 167(1951)365
Sin51a W.K. Sinclair and E.W. Emery , Brit.J.Radiology 23 (1951) 576
Wah55 A.C. Wahl, Phys. Rev. 99 (1955) 730
Wah59 A.C. Wahl, J.inorg.nucl.Chem. 10 (1959) 3
Wal49 D. Walker, Proc. Phys. Soc. London 62 (1949) 799
Wal70 K.F. Walz and H.M. Weiss, Z.Naturf. 25a (1970) 921
Wil55 D.M. Wiles and R.H. Tomlinson, Phys. Rev. 99 (1955) 188
Wil60 R.G. Wille and R.W. Fink, Phys. Rev. 118 (1960) 242
Win51 F.P.W. Winteringham, Nature 167 (1951) 155
Wri57 H.W. Wright et al, Nucl.Sci.Engg. 2 (1957) 427
Wya61 E.I. Wyatt et al, Nucl.Sci.Engg. 11 (1961) 74
Zol71 W.H. Zoller et al, Phys. Rev. C 3 (1971) 1699

Contributions to
Review Paper No. 13

M.Z. Tarasko, B.P. Maksyutenko
A New Approach to Finding the Distribution of
Delayed Neutron Precursors

Published in Yad.Fiz. 17 (1973) 1149,
English: Sovj.J.Nucl.Phys. 17 (1973) 598

DELAYED NEUTRON SPECTROMETRY

S. Shalev *, G. Rudstam

The Swedish Research Councils' Laboratory

Studsvik, Nyköping, Sweden

ABSTRACT

A number of delayed neutron precursors have been isolated by mass-separation. The delayed neutron energy spectra were measured using a high resolution ^{3}He neutron spectrometer, and preliminary results are given for ^{87}Br, ^{88}Br, ^{136}Te, ^{137}I, ^{138}I and ^{139}I.

---

* Permanent address: Department of Nuclear Engineering
Technion - Israel Institute of Technology
Haifa, Israel.

An intensive investigation is currently being carried out of delayed neutron emission from mass-separated precursors. The OSIRIS isotope-separator-on-line facility[1]) is used to extract fission products from a sample of ^{235}U located near the core of the 1 MW R2-0 reactor, and useful intensities can be obtained for elements ranging from zinc to strontium (Z = 30-38) and from silver to barium (Z = 47-56).

A ^{3}He neutron spectrometer has been developed with exceptionally good energy resolution, ranging from 16 keV to 35 keV FWHM for neutrons with energy up to 1 MeV. For each mass investigated the ion beam is allowed to impinge on an aluminized mylar tape located close to the neutron spectrometer. The tape is moved continuously at a rate adjusted to optimize the neutron counting rate while removing long-lived daughter products. A 1 mm thick lead shield is used to reduce the effect of β-particles and low energy gamma rays. Data are accumulated in sequentially-routed sections of a 4096 channel analyzer or an on-line PDP-9 computer.

Figures 1 - 6 show the pulse-height spectra obtained for the precursors ^{87}Br, ^{88}Br, ^{136}Te, ^{137}I, ^{138}I and ^{139}I. The spectra have not been corrected for spectrometer response function or detection efficiency and the solid line passing through the experimental points is intended only as a guide to the eye. For the cases ^{87}Br and ^{138}I a simple correction has been made for gamma-ray pile-up at low energies, and the corrected spectrum is shown as a dashed line.

The spectra for ^{87}Br, ^{136}Te and ^{137}I are remarkable for their discreteness and detailed structure. All three cases represent the emission of a single neutron outside a closed shell, i.e. :

$$(Z-1,N+2) \xrightarrow{\beta} (Z,N+1) \xrightarrow{n} (Z,N)$$

where N = 50 or 82. Hence the neutron binding energies[2]) are exceptionally low (5.46, 4.02 and 4.45 MeV respectively) with correspondingly low level-densities.

Delayed neutron emission following β-decay from ^{139}I represents the emission of an odd neutron, leaving a neutron pair outside a closed shell :

$$(Z-1,N+4) \xrightarrow{\beta} (Z,N+3) \xrightarrow{n} (Z,N+2).$$

This is also a quite stable configuration, and the binding energy is unusually low (3.89 MeV). Some structure appears in the spectrum, but unfortunately the statistical errors are quite large.

The spectra for ^{88}Br and ^{138}I appear to consist of a continuous component with some additional structure. The final nucleus is left with a single neutron outside a closed shell :

$$(Z-1,N+3) \xrightarrow{\beta} (Z,N+2) \xrightarrow{n} (Z,N+1)$$

and neutron emission involves the breaking of a pair. The binding energies are relatively high (7.15 and 5.86 MeV respectively).

These spectra provide not only interesting information on level densities[3]) and emission probabilities, but the synthesis of delayed neutron spectra for individual groups becomes possible. For instance, group I consists almost entirely of ^{87}Br, while group II is mainly ^{88}Br, ^{136}Te and ^{137}I. Further delayed neutron spectra, together with detailed discussion and analysis, will be published elsewhere.

We gratefully acknowledge the expert assistance of O.C. Jonsson in the experimental work, and operation of the isotope separator by L. Jacobsson.

References

1) S. Borg, I. Bergström, G.B. Holm, B. Rydberg, L.E. De Geer, G. Rudstam, B. Grapengiesser, E. Lund and L. Westgaard, Nucl. Instr. Methods 91 (1971) 109.

2) G.T. Garvey, W.J. Grace, R.L. Jaffe, I. Talmi and I. Kelson, Rev. Mod. Phys. 41 (1969) S1.

3) S. Shalev and G. Rudstam, Phys. Rev. Letters 28 (1972) 687.

Figure 1.

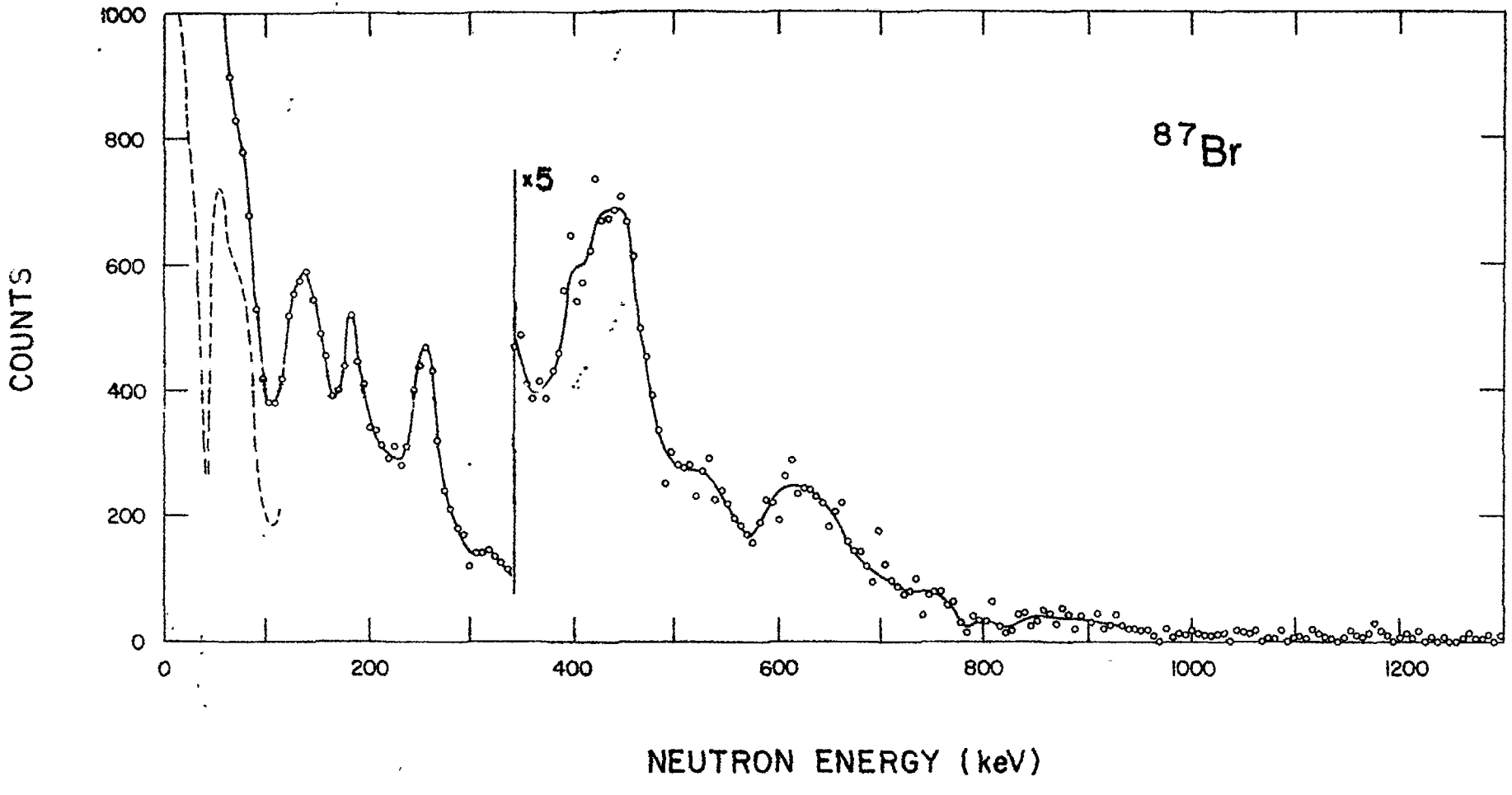
1000
800
600
400
200
0
COUNTS
x5
87Br
0
200
400
600
800
1000
1200
NEUTRON ENERGY (keV)

Figure 2.

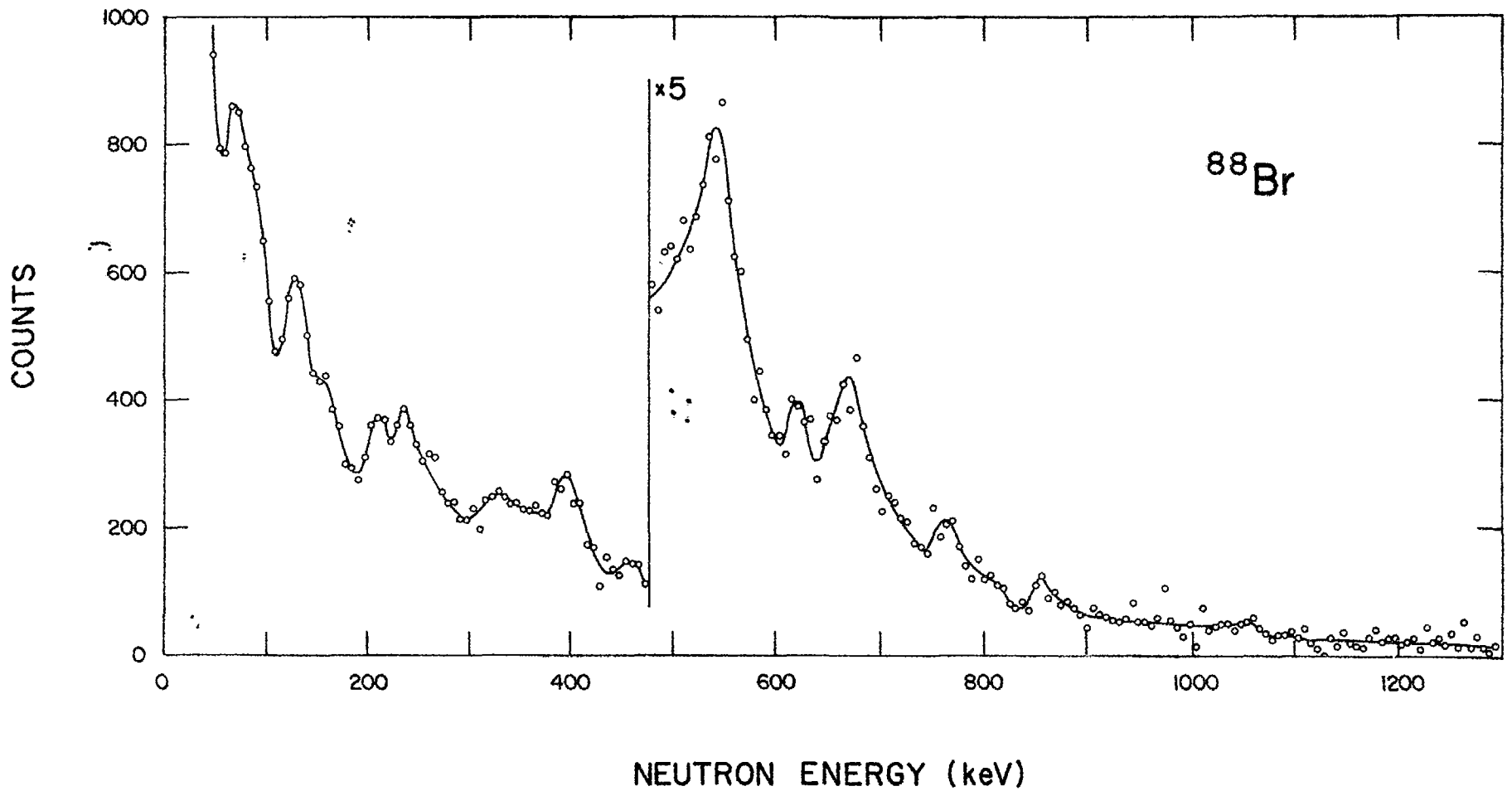
1000
800
600
400
200
0
COUNTS
×5
88Br
0
200
400
600
800
1000
1200
NEUTRON ENERGY (keV)

Figure 3.

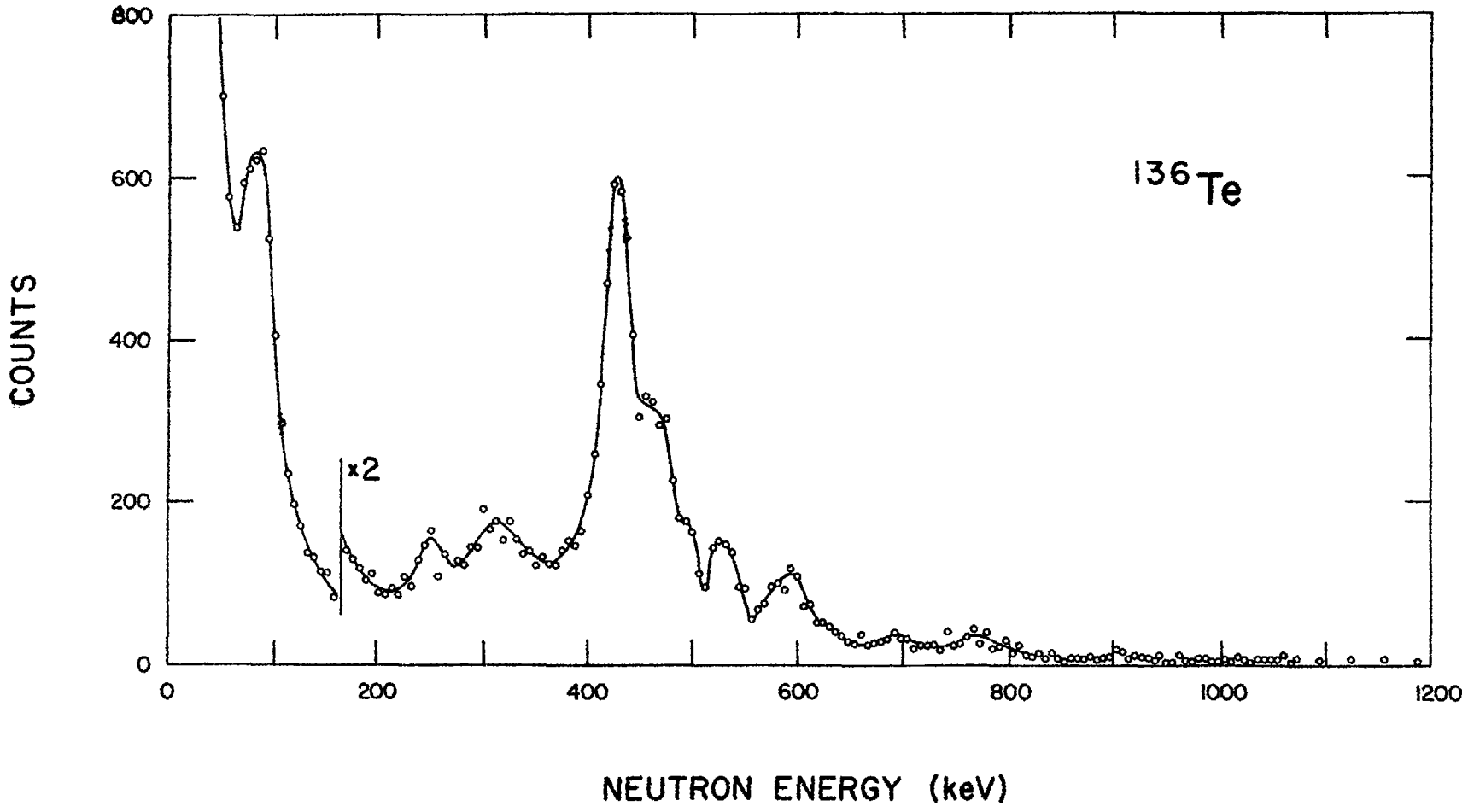
800
600
400
200
0
COUNTS
×2
136Te
0
200
400
600
800
1000
1200
NEUTRON ENERGY (keV)

Figure 4.

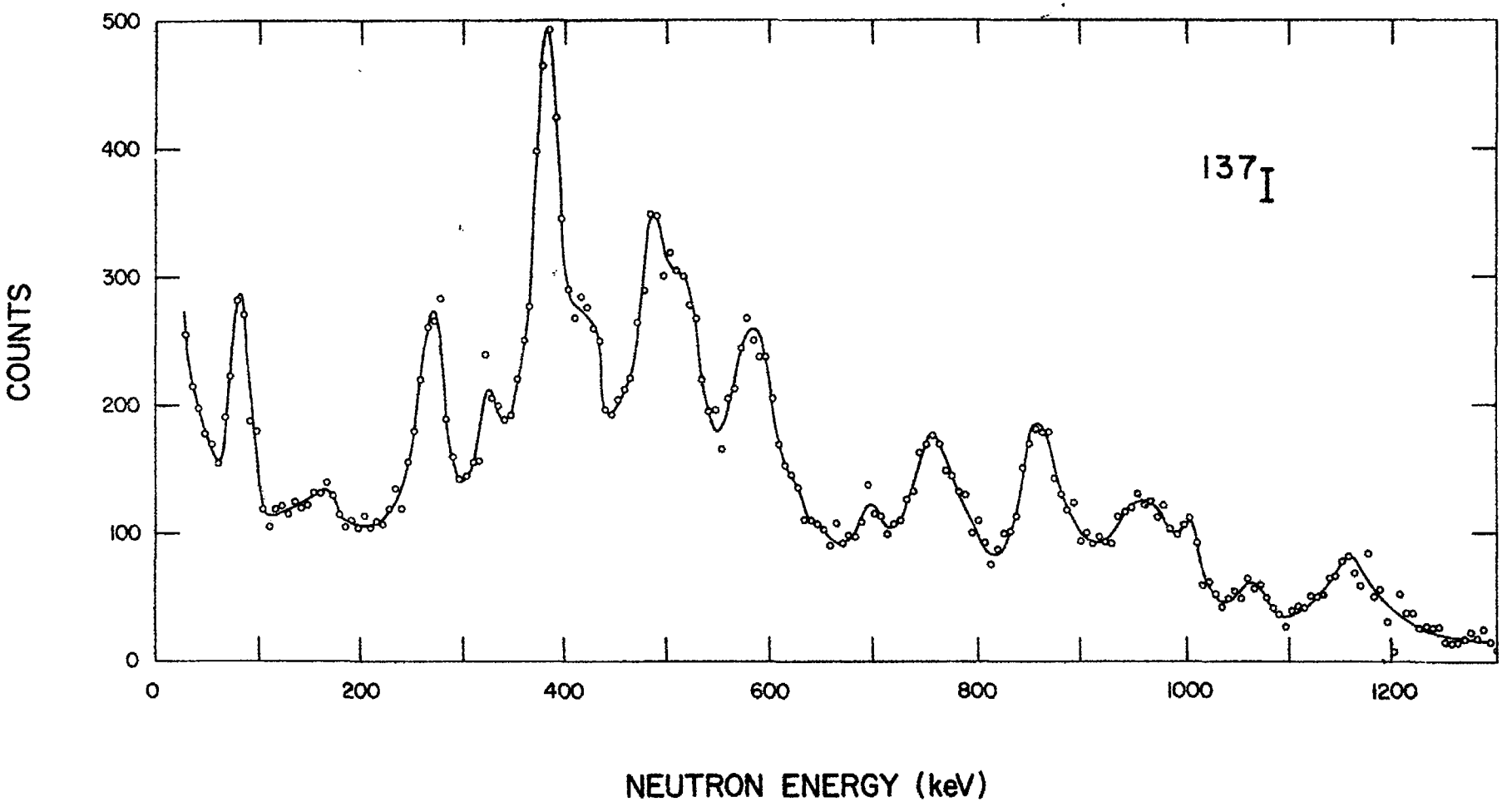
500
400
300
200
100
0
COUNTS
137I
0
200
400
600
800
1000
1200
NEUTRON ENERGY (keV)

Figure 5.

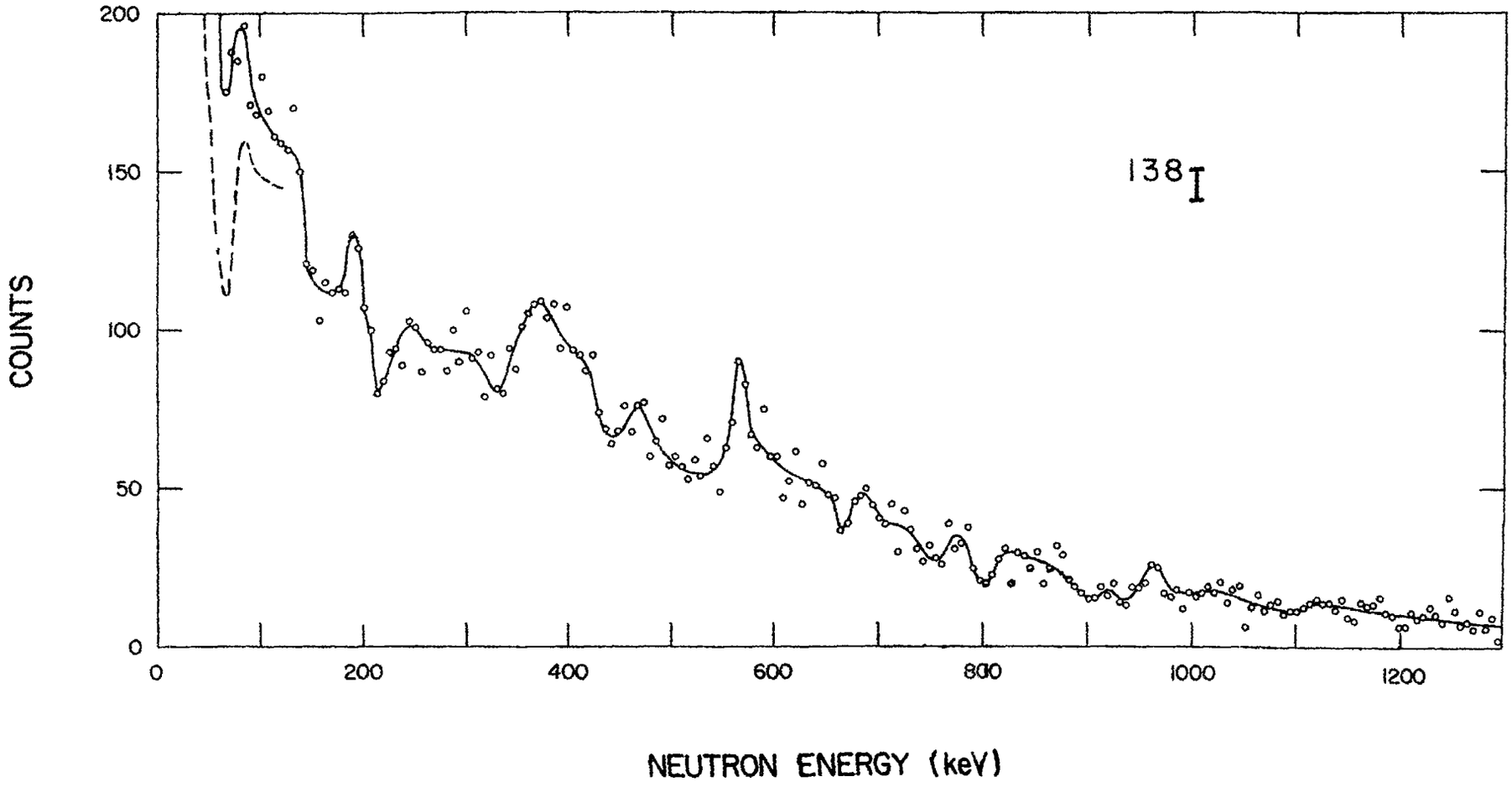
200
150
100
50
0
COUNTS
138I
0
200
400
600
800
1000
1200
NEUTRON ENERGY (keV)

Figure 6.

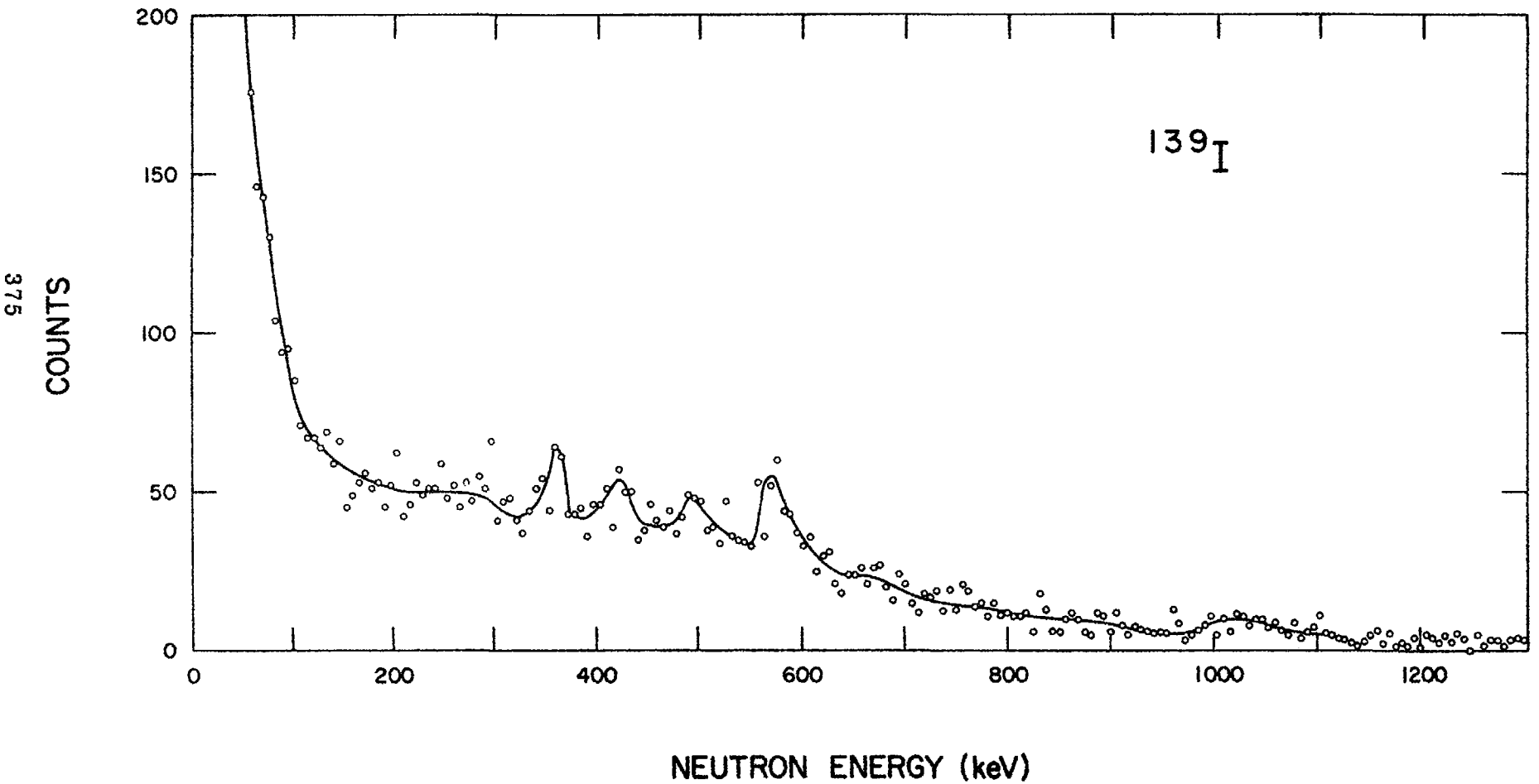
200
150
100
50
0
COUNTS
375
^{139}I
0
200
400
600
800
1000
1200
NEUTRON ENERGY (keV)

DELAYED NEUTRONS FROM FISSION: PRESENT STATUS OF MEASUREMENTS OF YIELDS, GROUP HALF-LIVES AND ABUNDANCES, AND SPECTRA*

A. E. Evans

Nuclear Analysis Research Group
University of California
Los Alamos Scientific Laboratory
Los Alamos, New Mexico 87544

ABSTRACT

The present status of measurements of delayed-neutron yields from fission, half-lives and relative abundances of delayed-neutron groups from fission, and spectra of delayed neutrons from fission is reviewed. Available data indicate that absolute delayed-neutron yields from fission of ^{233}U, ^{235}U, and ^{239}Pu are known to within ± 7% while a 10% uncertainty exists in the delayed-neutron yield from fission of ^{232}Th, and a 17% discrepancy exists in the case of ^{238}U. The dependence of the delayed-neutron yield upon the energy of neutron-causing fission has been studied and is qualitatively understood. The question of incident-neutron energy dependence of relative delayed-neutron group abundancies and half-lives is not well resolved. Recent measurements of delayed-neutron spectra indicate that these are of a complex, discrete energy nature.

*Work performed under the auspices of the U. S. Atomic Energy Commission.

I. INTRODUCTION

Delayed-neutron data are significant in the study of nuclear structure physics,[1,2] in the development of techniques for the non-destructive assay of fissionable materials,[3,4] and in the design of fast reactor systems.[5,6,7] The effect of present uncertainties in delayed-neutron data on Fast Reactor Calculations is pointed out by Saphier and Yiftah[8] who indicate that very large errors in predicting the dynamic behavior of large fast reactors result from present uncertainties in delayed-neutron yields and delayed-neutron spectra. Of particular interest is the effect of these uncertainties on the Fast Flux Test Reactor (FFTF) project.[9] In reference 9, the urgency for precise measurement (± 2%) of delayed-neutron yields and for accompanying improvement in the measurement of delayed-neutron spectra are cited.

II. ABSOLUTE DELAYED-NEUTRON YIELDS

The status of delayed-neutron yield measurements was reviewed in 1964 by Keepin.[10] The theory and systematics of delayed-neutron emission are discussed by Keepin,[10] Amiel,[1] Jahnsen et al.,[11] and Amiel.[2]

The absolute total delayed-neutron yield, i.e., the total number of delayed neutrons generated per fission, was measured by Keepin et al. in 1957.[12] The authors of this work measured absolute delayed-neutron yields from fast fission of ^{235}U, ^{233}U, ^{238}U, ^{239}Pu, ^{240}Pu, and ^{232}Th, and from thermal fission of ^{235}U, ^{233}U, and ^{239}Pu. The authors reported results with probable errors (probable error = 0.6745 σ) of ~5%. The fast fission results are shown in Table I.

An independent check of the delayed-neutron yields from fast fission of ^{233}U, ^{235}U, and ^{239}Pu comes from a measurement of the mass increment between delayed and prompt critical for the bare metal assemblies "Godiva" (^{235}U), "Jezebel" (^{239}Pu), and "Skidoo" (^{233}U). Using the latest calculated values of effec-

Table I. Comparison of revised delayed-neutron yield data of Masters et al.[16] and of Krick and Evans[20] for fission induced by neutrons of various energies with fast-fission yield data of Keepin.[12]

Element	Absolute Delayed Neutrons per Fission (Author, Neutron Energy)			
	Keepin et al. Fission Spectrum	Krick and Evans Averaged 0.1-1.8 MeV	Masters et al. 3.1-MeV Neutrons	Masters et al. 14.9-MeV Neutrons
^{232}Th	0.0496 ± 0.0035	-----	0.057 ± 0.005	0.030 ± 0.0020
^{233}U	0.0070 ± 0.0006	0.0075 ± 0.0006	0.0074 ± 0.0006	0.0041 ± 0.0003
^{235}U	0.0165 ± 0.0007	0.0163 ± 0.0013	0.0172 ± 0.0013	0.0091 ± 0.0004
^{238}U	0.0412 ± 0.0025	-----	0.0484 ± 0.0036	0.0283 ± 0.0013
^{239}Pu	0.0063 ± 0.0005	0.0062 ± 0.0005	0.0066 ± 0.0005	0.0041 ± 0.0002
^{242}Pu	-----	0.015 ± 0.005[a]	-----	-----

[a]Averaged 0.7 to 1.3 MeV

tive delayed-neutron fraction* for these assemblies,[13] one can derive as the delayed-neutron yield in neutrons/fission for ^{235}U, ^{239}Pu, and ^{233}U, respectively, 0.0163, 0.0064, and 0.0072, with a precision of ~2-3% (1 σ). However, the authors of this work have expressed uncertainty as to bias in this method of measuring delayed-neutron effective fractions.[14]

Another set of absolute delayed-neutron yield data is available from the work of Smith et al.[15]

In 1967, Masters et al.,[16] in preparation for application of delayed-neutron phenomena to the nondestructive assay of fissionable material, measured the absolute delayed-neutron yields from fission by 3.1- and 14.9-MeV neutrons of ^{239}Pu, ^{233}U, ^{235}U, ^{238}U, and ^{232}Th. These authors showed that the delayed-neutron yield for fission due to 14.9-MeV neutrons is some 40% lower than the yield due to 3.1-MeV neutrons, in agreement with theoretical predictions but in opposition to the results obtained by earlier workers,[17-19] who observed an increase in delayed-neutron yield. Also of note in the work of Masters et al. was the fact that measurement of absolute delayed-neutron yields at 3.1 MeV averaged some 10% higher than the delayed-neutron yields from fission-spectrum neutrons as measured by Keepin et al.[12]

Following this experiment, Krick and Evans[20] studied in detail the dependence of delayed-neutron yields upon the energy of the neutron causing fission. For neutron energies from 0.1 to 1.8 MeV, yields from ^{233}U, ^{235}U, and ^{239}Pu were obtained, and yields from ^{233}U, ^{235}U, and ^{238}U were obtained for neutrons of energies between 4.0 and 6.7 MeV. The delayed-neutron yield from ^{242}Pu was obtained for neutron energies from 0.7 to 1.3 MeV. Krick and Evans found that for all isotopes studied, delayed-neutron yields were independent of incident neutron energy from 0.1 to around 4 or 5 MeV, then fell off in a ~2-MeV interval to near the yield values

*The delayed-neutron fraction β is the ratio of delayed neutrons emitted from fission to total neutrons (promt and delayed) emitted from fission.

at 14.9 MeV as measured by Masters et al. Absolute yields in the energy-independent region agreed in general with those obtained by Masters et al. for 3.1-MeV fission. However, the Masters and Krick values are not entirely independent, since fission-monitoring foils and the isotopic neutron source used to calibrate the delayed-neutron detectors were common to both experimental programs. It was also unfortunate that an independent absolute value for the delayed-neutron yield from ^{238}U, for which the Keepin and Masters values are in disagreement by 20%, was not obtained. The Krick data for this isotope were normalized to the Masters delayed-neutron yield value at 3.1 MeV.

The $^{238}PuLi$ source used in the recent LASL measurements has been recalibrated by the National Bureau of Standards. The value given was $(3.74 \pm 0.05) \times 10^5$ neutrons/sec on March 1. 1972. The old LASL value was 4.01×10^5 neutrons/sec on December 8, 1968. Using a half-life for ^{238}Pu of 88.0 ± 2.0 years, the old value becomes $(3.91 \pm 0.20) \times 10^5$ neutrons/sec on March 1, 1970. This implies that delayed-neutron yield values reported by Masters et al.[16] and by Krick and Evans[20] should be multiplied by 0.956 and the uncertainties can be reduced somewhat. Recalibration of fission-chamber foils resulted in an upward correction of 3.35% for the delayed-neutron yield from fission of ^{238}U, so that the total correction factor applied to the yield from this isotope is 0.988. The corrected values[21] are shown in Table I. The recent LASL data are now in good agreement ($\leq \pm 5\%$) with the work of Keepin et al.,[12] except in the case of ^{238}U, in which case the 17% disagreement between the two delayed-neutron yield values is unacceptable.

Among more recent developments, Conant and Palmedo[22] have measured the delayed-neutron fractions from thermal fission of ^{235}U, ^{239}Pu, and ^{233}U. If one uses the current values of total neutron yield from fission ($\bar{\nu}$)[10] to convert delayed-neutron fractions to absolute delayed-neutron yields, one obtains values similar to those reported by Keepin.[12] Cox and Whiting[23] have made measurements of the energy dependence of the delayed-neutron yield from fission of ^{232}Th, ^{235}U, and ^{238}U, which are in essential agreement with the results of Krick and Evans.

A new compilation and evaluation of delayed-neutron data has just been completed by Tomlinson.[24] Tomlinson reports unpublished measurements by D. A. Clifford and H. N. McTaggert (AWRE, Aldermaston) of delayed-neutron yields from fission of ^{235}U and ^{238}U induced by fission-spectrum neutrons which support the higher yield for ^{238}U.

One need note that, in order to compare the delayed-neutron yields for fission caused by 0.1 to 1.8 or 3.1-MeV neutrons with yields from fission by fission-spectrum neutrons, it is necessary to take into account the dependence of the delayed-neutron yield upon the energy of the neutron-causing fission. In terms of this dependence, the delayed-neutron yield for fission by fission-spectrum neutrons is given by

$$Y_f = \frac{\int_0^\infty Y(E)\sigma_f(E)\Phi_f(E)dE}{\int_0^\infty \sigma_f(E)\Phi_f(E)dE}$$

where Y(E) is the delayed-neutron yield from fission caused by neutrons of energy E,[20] $\sigma_f(E)$ is the cross section for fission by neutrons of energy E, and $\Phi_f(E)$ is the flux of neutrons of energy E in the fission spectrum. For unmoderated fission-spectrum neutrons, it is found that Y_f is about 2 to 3% lower than Y(E) for $0.1 \leq E < 4$ MeV. Consideration of this fact in general improves the agreement between the data taken with monoenergetic neutrons and those taken with fission-spectrum neutrons.

III. DELAYED-NEUTRON DECAY: PERIODS AND ABUNDANCES, PRECURSORS

The most comprehensive study to date of the decay properties of delayed neutrons is that of Keepin et al.[12] These authors resolved delayed-neutron decay curves into six half lives: approximately 55, 22, 5.5, 2.1, 0.5, and 0.2 seconds in length. Data were obtained for fast fission of ^{233}U, ^{235}U, ^{238}U, ^{239}Pu, ^{240}Pu, and ^{232}Th, and for thermal fission of ^{233}U, ^{235}U, and ^{239}Pu. The group half lives, which are themselves each composites of the decay of several delayed-

neutron precursors vary slightly from isotope to isotope and between thermal and fast fission. There are marked differences between isotopes, however, in the relative populations of the various decay groups. The energy dependence between thermal and fission-spectrum-induced fission of the group abundances is not significant.

The energy dependence of the relative group abundances in delayed-neutron decay was studied by Maksiutenko,[25] whose data indicate little change in group abundances from thermal to 15-MeV fission. East and Keepin,[4] however, do note some differences in the delayed-neutron decay curves from 14.9-MeV fission as compared to those from fission induced by thermal or fission-spectrum neutrons. East et al.[26,27] have measured delayed-neutron groups and abundances from fission of ^{235}U, ^{233}U, and ^{238}U, ^{239}Pu, ^{242}Pu, and ^{232}Th.

Thermal fission delayed-neutron parameters for ^{241}Pu have been published by Cox.[28] Cox was unable to resolve the shortest (0.2-sec) decay group since his technique involved mechanical transfer of the sample. Fast fission group abundance data are available from the work of Smith et al.[15] Again, the shortest lived decay group was not resolved.

Delayed neutrons are emitted when short half-lived fission products decay into neutron-emitting excited states of daughter nuclei. There are dozens of fission products, only some of which have been identified, which contribute to this process. Such fission products are known as precursors. The study of individual precursors has been going on for some time[1,2,10,11,29] and promises to yield much information of value to nuclear structure physics and reactor technology. Of some importance to reactor technology is the identification of delayed-neutron precursors which are volatile and hence may escape from some reactor systems in a time comparable to their half lives, thus reducing the control effectiveness of the delayed neutrons which they emit.

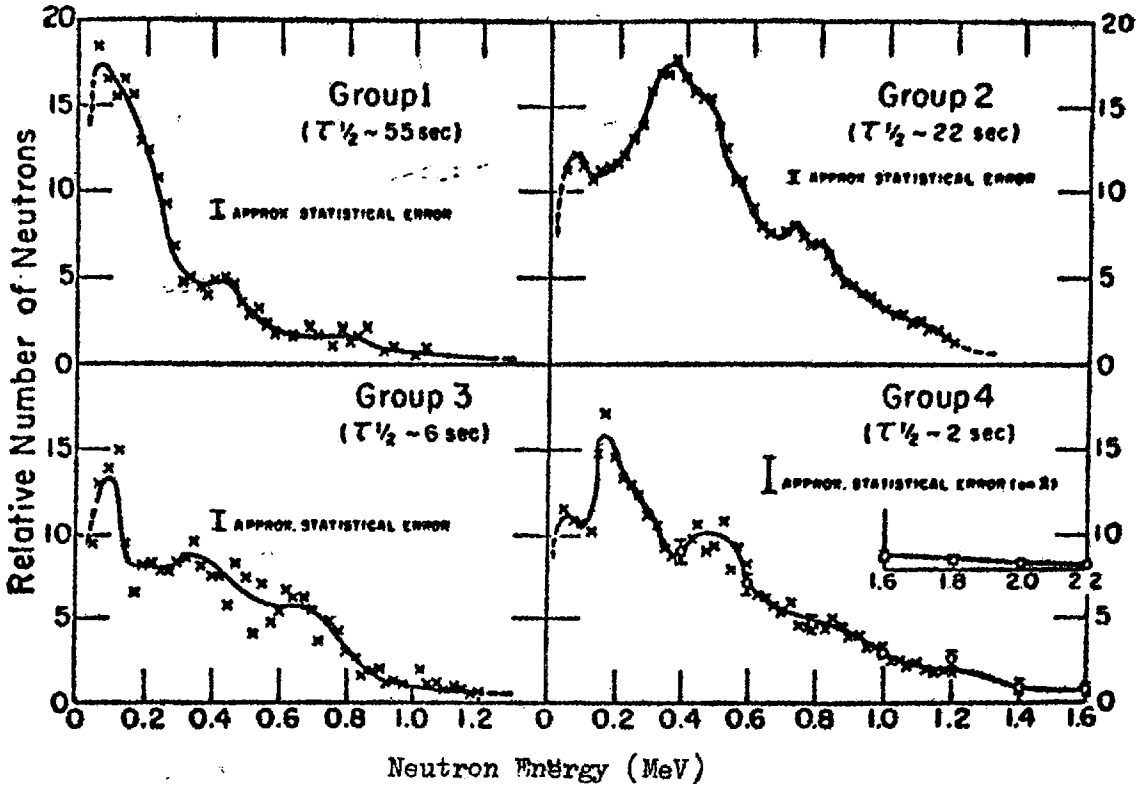

(A)

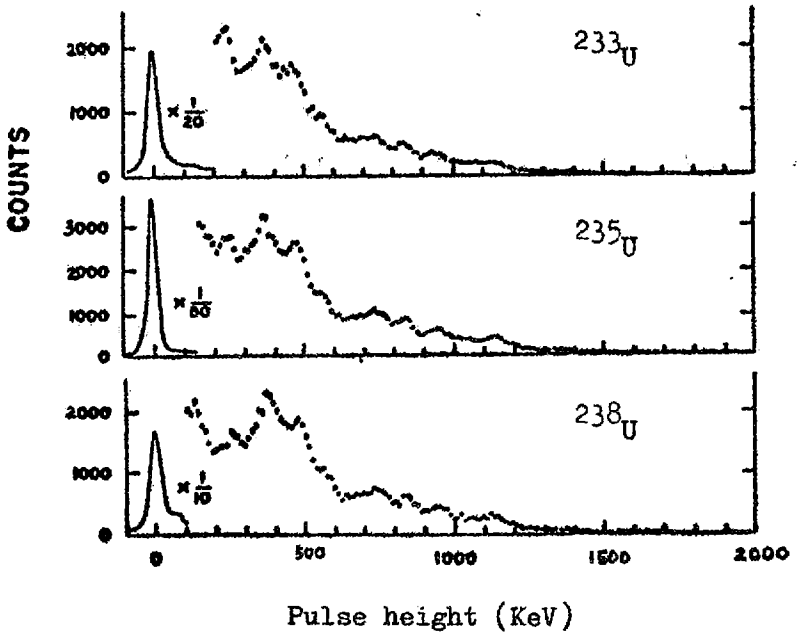

(B)

Fig. 1(A) Delayed-neutron spectra from thermal fission of ^{235}U, as measured by Batchelor and Mc K. Hyder (Ref. 30).

Fig. 1(B) Gross delayed-neutron spectra of Cuttler and Shalev for thermal fission of isotopes of uranium (Ref. 32,33).

IV. DELAYED-NEUTRON SPECTRA

The most definitive published information on the delayed-neutron spectra is found in the work of Batchelor and Hyder[30] who used a ^{3}He fast neutron spectrometer to measure the spectra of delayed neutrons from the four longest lived delayed-neutron groups resulting from the thermal fission of ^{235}U. Errors on these spectra are estimated at from $^{+6}_{-15}$% at zero energy to ± 8% at 1 MeV. Spectra obtained by these workers, shown in Figure 1, are not adequate for present-day needs of fast reactor design.[6, 9]

Shalev and co-workers, using a high-efficiency ^{3}He spectrometer tube developed especially for delayed-neutron spectrometry,[31] have measured spectra of delayed neutrons from thermal fission of isotopes of uranium[32, 33] as well as from ^{232}Th and ^{239}Pu.[33] Using a reactor neutron beam and sample-shuffling system, they were able to study spectra of the two longest half-lived groups. Their spectra, which have energy resolutions of the order of 70 keV for 1-MeV neutrons, show many discrete neutron-energy peaks, in accord with the accepted theory of delayed-neutron emission.[10, 11] This group has also measured delayed-neutron spectra from separated precursors.[34]

Chulick et al.[35] have measured energy spectra of delayed neutrons from spontaneous fission of ^{252}Cf, using a moving mylar tape to catch fission products from the sample and transfer them to a remote neutron-counting site. The spectrometer was a time-of-flight system using the β decay of the precursors as a "start" timing signal for the neutron flight. They used pulse-shape discrimination techniques to suppress the gamma background which plagued earlier efforts[36] to apply the time-of-flight technique to the measurement of delayed-neutron spectra from thermally-induced fission of ^{235}U.

Woodruff[37] has measured the spectra of delayed neutrons from fission using porton-recoil proportional counter tubes. He finds considerable structure and also a much larger fraction of

neutrons of energies less than 100 keV than had been observed by previous authors.

REFERENCES

1. S. Amiel, "Delayed Neutrons and Photoneutrons from Fission Products," Physics and Chemistry of Fission, Vol. 2, International Atomic Energy Agency (1965).

2. S. Amiel, "Delayed Neutrons in Fission," Proceedings of the Second IAEA Symposium on the Physics and Chemistry of Fission held by the International Atomic Energy Agency in Vienna 28 July - 1 August, 1969, IAEA, Vienna (1969), p. 569.

3. G. R. Keepin, R. H. Augustson, and R. B. Walton, "Los Alamos Scientific Laboratory Safeguards Research and Development Program," in Proceedings of the AEC Symposium on Safeguards Research and Development, Los Alamos Scientific Laboratory, October 27-29, 1969, Report WASH-1147, p. 110.

4. L. V. East and G. R. Keepin, "Fundamental Fission Signatures and Their Applications to Nuclear Safeguards," Proceedings of the Second IAEA Symposium on the Physics and Chemistry of Fission, IAEA, Vienna, 28 July - 1 August, 1969, p. 647.

5. G. R. Keepin, "Physics of Nuclear Kinetics," Chapters 6-10, Addison-Wesley Publishing Co., Inc., Reading, Massachusetts (1965).

6. G. R. Keepin, "Delayed Fission Neutron Data in Reactor Physics and Design," Delayed Fission Neutrons: Proceedings of a Panel held in Vienna, 24-27 April, 1967, IAEA, Vienna, 1968, p. 3.

7. S. Yiftah and D. Saphier, "The Importance of Exact Delayed Neutron Data in Fast Reactor Dynamic Behavior," Delayed Fission Neutrons: Proceedings of a Panel held in Vienna, 24-27 April, 1967, IAEA, Vienna, 1968, p. 23.

8. D. Saphier and S. Yiftah, "The Effect of Errors in the Delayed-Neutron Data on Fast Reactor Static and Dynamic Calculations," Nuclear Science and Eng. 42, 272 (1970).

9. S. Ramchandran and K. R. Birney, "Impact of the New LASL Delayed-Neutron Data on FTR Design," Proceedings National Topical Meeting on New Developments in Reactor Physics and Shielding, September 12-15, 1972, Report CONF-720901, USAEC (1972) p. 660.

10. G. R. Keepin, "Physics of Nuclear Kinetics," Chapter 4, Addison-Wesley Publishing Co., Inc., Reading, Massachusetts (1965).

11. T. Jahnsen, A. C. Pappas, and T. Tunaal, "Delayed Neutron Emission Theory and Precursor Systematics," Delayed Fission Neutrons: Proceedings of a Panel held in Vienna, 24-47 April, 1967, IAEA, Vienna, 1968, p. 35.

12. G. R. Keepin, T. F. Wimmett, and R. K. Zeigler, "Delayed Neutrons from Fissionable Isotopes of Uranium, Plutonium, and Thorium," Phys. Rev. 107, 1044 (1957) and J. Nuclear Energy 6, 1 (1957).

13. Gordon E. Hansen, Los Alamos Scientific Laboratory internal memorandum N-2-8182, June 3, 1968 (unpublished).

14. Gordon E. Hansen, private communication.

15. Smith, Rose, McVicar, and Thorne, J. Nuclear Energy I, 4, 133 (1957).

16. C. F. Masters, M. M. Thorpe, and D. B. Smith, "The Measurement of Absolute Delayed-Neutron Yields from 3.1 and 14.9-MeV Fission," Nucl. Sci. and Eng. 36, 202 (1969).

17. V. I. Shpakov, K. A. Petrzhak, M. A. Bak, S. S. Kovolenko, and O. I. Kostochkin, Atomnaya Energiya 11, 539 (1961).

18. B. P. Maksiutenko, Atomnaya Energiya 15, 321 (1963).

19. W. I. McGarry, R. J. Omohundro, and G. E. Holloway, Bull. Am. Phys. Soc. Ser II 5, 33 (1960).

20. M. S. Krick and A. E. Evans, "The Measurement of Total Delayed-Neutron Yields as a Function of the Energy of the Neutron Inducing Fission," Nucl. Sci. and Eng. 47, 311 (1972).

21. A. E. Evans, M. M. Thorpe, and M. S. Krick, Nucl. Sci. and Eng. 50, 80 (1973).

22. J. F. Conant and P. F. Palmedo, "Measurement of the Delayed Neutron Fractions for Thermal Fission of ^{235}U, ^{239}Pu, and ^{233}U," Nucl. Sci. and Eng. 44, 173 (1971).

23. S. A. Cox and E. E. D. Whiting, "Energy Dependence of the Delayed-Neutron Yield from Neutron-Induced Fission of ^{232}Th, ^{235}U, and ^{238}U," ANL 7610, p. 45, Argonne National Laboratory (1970).

24. L. Tomlinson, "Delayed Neutrons From Fission," United Kingdom Atomic Energy Authority Research Group Report AERE-R6993 (1972).

25. B. P. Maksiutenko, J. Exptl. Theoret. Phys. (USSR) 35, 814 (1958).

26. L. V. East, R. H. Augustson, and H. O. Menlove, "Delayed Neutron Abundances and Half Lives from 14.7-MeV Fission," Los Alamos Scientific Laboratory report LA-4605-MS (1970) p. 15.

27. R. H. Augustson, L. V. East, and H. O. Menlove, "Delayed Neutron Abundances and Half Lives from 14.7-MeV Fission," Los Alamos Scientific Laboratory report LA-4368-MS (1969) p. 12.

28. S. A. Cox, Phys. Rev. 123, 1735 (1961).

29. W. L. Talbert, Jr., A. B. Tucker, and G. M. Day, "Delayed Neutron Emission in the Decays of Short-Lived Separated Isotopes of Gaseous Fission Products," Phys. Rev. 177, 1805 (1969).

30. R. Batchelor and H. R. McK. Hyder, "The Energy of Delayed Neutrons from Fission," J. Nuclear Energy 3, 7 (1956).

31. S. Shalev, Progress Report No. 4, TNSD-R/412, Technion, Haifa (1970).

32. S. Shalev and J. Cuttler, "Energy of Delayed Neutrons from Uranium," Trans. Am. Nucl. Soc. 14, 1, 373 (1971).

33. S. Shalev, Final Report on IAEA Research Contract No. 611/R1/R13 (1971).

34. S. Shalev and G. Rudstam, "The ^{137}I Delayed-Neutron Energy Spectrum," Trans. Am. Nucl. Soc. 14, 1, 373 (1971).

35. E. T. Chulick, P. L. Reeder, C. E. Bemis, Jr. and E. Eichler, "Energy Spectrum of Delayed Neutrons from the Spontaneous Fission of ^{252}Cf," Nuclear Physics A168, 250 (1971).

36. N. G. Chrysochoides, A. J. Nicolitsas, N. N. Papadopoulos, C. C. Zikides, and C. A. Mitsonias, "Work in Greece on Delayed Neutrons," Delayed Fission Neutrons: Proceedings of a Panel held in Vienna, 24-27 April, 1967, IAEA, Vienna, 1968, p. 213.

37. G. L. Woodruff, USAEC report RLO-2225-T17-4 (July 1972); also W. R. Sloan and G. L. Woodruff, Trans. ANS 15, 202, 942 (Nov. 1972).